ISSN 1948-0210 (online)

World Journal of *Stem Cells*

Monthly Volume 17 Number 2 February 26, 2025

Published by Baishideng Publishing Group Inc

World Journal of Stem Cells

Contents

Monthly Volume 17 Number 2 February 26, 2025

REVIEW

MINIREVIEWS

ORIGINAL ARTICLE

Retrospective Study

Basic Study

LETTER TO THE EDITOR

World Journal of Stem Cells

Monthly Volume 17 Number 2 February 26, 2025

Contents

NAME OF JOURNAL
World Journal of Stem Cells

ISSN
ISSN 1948-0210 (online)

LAUNCH DATE
December 31, 2009

FREQUENCY
Monthly

EDITORS-IN-CHIEF
Shengwen Calvin Li, Carlo Ventura

EDITORIAL BOARD MEMBERS
https://www.wjgnet.com/1948-0210/editorialboard.htm

PUBLICATION DATE
February 26, 2025

INSTRUCTIONS TO AUTHORS
https://www.wjgnet.com/bpg/gerinfo/204

GUIDELINES FOR ETHICS DOCUMENTS
https://www.wjgnet.com/bpg/GerInfo/287

GUIDELINES FOR NON-NATIVE SPEAKERS OF ENGLISH
https://www.wjgnet.com/bpg/gerinfo/240

PUBLICATION ETHICS
https://www.wjgnet.com/bpg/GerInfo/288

PUBLICATION MISCONDUCT
https://www.wjgnet.com/bpg/gerinfo/208

ARTICLE PROCESSING CHARGE
https://www.wjgnet.com/bpg/gerinfo/242

STEPS FOR SUBMITTING MANUSCRIPTS
https://www.wjgnet.com/bpg/GerInfo/239

ONLINE SUBMISSION
https://www.f6publishing.com

E-mail: office@baishideng.com https://www.wjgnet.com

World Journal of Stem Cells

Submit a Manuscript: https://www.f6publishing.com

World J Stem Cells 2025 February 26; 17(2): 98693

DOI: 10.4252/wjsc.v17.i2.98693

ISSN 1948-0210 (online)

REVIEW

Stem cell therapy: A promising therapeutic approach for skeletal muscle atrophy

Ying-Jie Wang, Ze-Hao Chen, Yun-Tian Shen, Ke-Xin Wang, Yi-Min Han, Chen Zhang, Xiao-Ming Yang, Bing-Qian Chen

Specialty type: Cell and tissue engineering

Provenance and peer review: Unsolicited article; Externally peer reviewed.

Peer-review model: Single blind

Peer-review report's classification

Scientific Quality: Grade B, Grade B, Grade B, Grade B

Novelty: Grade B, Grade B, Grade B, Grade B

Creativity or Innovation: Grade B, Grade B, Grade B, Grade B

Scientific Significance: Grade A, Grade B, Grade B, Grade C

P-Reviewer: Chen JL; Qiu JY; Zhang S

Received: July 4, 2024

Revised: December 9, 2024

Accepted: January 23, 2025

Published online: February 26, 2025

Processing time: 234 Days and 22.4 Hours

Ying-Jie Wang, Ze-Hao Chen, Yun-Tian Shen, Ke-Xin Wang, Chen Zhang, Key Laboratory of Neuroregeneration of Jiangsu and Ministry of Education, Nantong University, Nantong 226000, Jiangsu Province, China

Yi-Min Han, Medical College, Nantong University, Nantong 226000, Jiangsu Province, China

Xiao-Ming Yang, Co-Innovation Center of Neuroregeneration, Jiangsu Clinical Medicine Center of Tissue Engineering and Nerve Injury Repair, Nantong University, Nantong 226000, Jiangsu Province, China

Xiao-Ming Yang, Research and Development Center for E-Learning, Ministry of Education, Beijing 100816, China

Bing-Qian Chen, Department of Orthopaedics, Changshu Hospital Affiliated to Soochow University, Changshu 215500, Jiangsu Province, China

Co-first authors: Ying-Jie Wang and Ze-Hao Chen.

Corresponding author: Bing-Qian Chen, MD, Professor, Department of Orthopaedics, Changshu Hospital Affiliated to Soochow University, No. 1 Shuyuan Street, Changshu 215500, Jiangsu Province, China. cbq0433@suda.edu.cn

Abstract

Skeletal muscle atrophy results from disruptions in the growth and metabolism of striated muscle, leading to a reduction or loss of muscle fibers. This condition not only significantly impacts patients' quality of life but also imposes substantial socioeconomic burdens. The complex molecular mechanisms driving skeletal muscle atrophy contribute to the absence of effective treatment options. Recent advances in stem cell therapy have positioned it as a promising approach for addressing this condition. This article reviews the molecular mechanisms of muscle atrophy and outlines current therapeutic strategies, focusing on mesenchymal stem cells, induced pluripotent stem cells, and their derivatives. Additionally, the challenges these stem cells face in clinical applications are discussed. A deeper understanding of the regenerative potential of various stem cells could pave the way for breakthroughs in the prevention and treatment of muscle atrophy.

Key Words: Stem cell; Muscle atrophy; Therapy; Mesenchymal stem cells; Induced pluripotent stem cells; Exosome

Core Tip: Muscle atrophy can exert a considerable influence on the quality of life of patients. The intricate molecular mechanisms of muscle atrophy give rise to a scarcity of effective treatment options. Recent advancements in stem cell therapy imply that it is a promising solution to this problem. This review summarizes the molecular mechanisms of muscle atrophy, presents current treatment strategies with a focus on mesenchymal stem cells, induced pluripotent stem cells, and their derivatives. Finally, it discusses the challenges encountered in the clinical application of these stem cells.

Citation: Wang YJ, Chen ZH, Shen YT, Wang KX, Han YM, Zhang C, Yang XM, Chen BQ. Stem cell therapy: A promising therapeutic approach for skeletal muscle atrophy. *World J Stem Cells* 2025; 17(2): 98693
URL: https://www.wjgnet.com/1948-0210/full/v17/i2/98693.htm
DOI: https://dx.doi.org/10.4252/wjsc.v17.i2.98693

INTRODUCTION

Muscle atrophy occurs in various physiological or pathological circumstances, including aging, disuse, dystrophy, amyotrophic lateral sclerosis (ALS), and systemic diseases such as cancer, sepsis, diabetes, chronic kidney disease and chronic obstructive pulmonary disease (Figure 1)[1-4]. Skeletal muscle atrophy causes a progressive decrease in the body's response to various stresses and chronic diseases, leading to a reduced quality of life and imposing a heavy socioeconomic burden, thus adversely impacting the prognosis of related diseases[5]. As such, the prevention and management of skeletal muscle atrophy has garnered increasing attention from researchers. Despite ongoing efforts, the pathogenesis of skeletal muscle atrophy remains incompletely understood, and aside from rehabilitation, no effective treatment options fully restore muscle function. However, with advancing research into therapeutic strategies for muscle atrophy, stem cell-based approaches have shown promising potential for preventing and treating atrophy-related disorders. The transplantation or injection of various stem cells has demonstrated efficacy in mitigating muscle atrophy and has become an integral part of the treatment strategy[6,7]. Additionally, exosomes derived from stem cells have been shown to modulate the balance between protein synthesis and degradation, further promoting muscle repair. This review explores the potential of stem cell-based therapies and their derivatives in treating muscle atrophy, offering promising prospects for clinical application.

MOLECULAR MECHANISM OF MUSCLE ATROPHY

Skeletal muscle atrophy refers to the reduction or loss of muscle fibers due to nutritional disorders or diseases, leading to decreased muscle mass. Muscle mass is primarily regulated by the balance between protein synthesis and degradation under normal physiological conditions. Disruptions in the body's microenvironment can result in an imbalance in skeletal muscle homeostasis, contributing to atrophy[8,9]. Recent findings suggest that skeletal muscle atrophy is linked to reduced protein synthesis and increased proteolysis, driven by factors such as inflammation, oxidative stress, autophagy, and apoptosis[10-12]. The key mechanisms of proteolysis include the ubiquitin-proteasome system, the autophagy-lysosome pathway, caspase-mediated proteolysis, and calpain-mediated proteolysis (Figure 2)[11,13,14]. Muscle RING-Finger protein 1 (MuRF-1) and Muscle Atrophy F-box protein are strongly associated with muscle protein degradation and serve as reliable biomarkers for this process. Moreover, the insulin-like growth factor/protein kinase B (Akt)/mechanistic target of rapamycin signaling pathway, which is critical for protein synthesis in skeletal muscle, is a major regulator of muscle atrophy[15].

Studies indicate that various triggering factors, including oxidative stress and inflammation either promote proteolytic processes or inhibit protein synthesis pathways, thereby leading to skeletal muscle atrophy[9,16-18]. Our previous research proposed a novel framework for understanding denervation-induced muscle atrophy, which involves four stages: Oxidative stress, inflammation, atrophy, and atrophic fibrosis[19]. Denervated skeletal muscles lose their contractile function, resulting in reduced blood flow to the affected muscles. This, in turn, induces a hypoxic environment that produces excess reactive oxygen species (ROS). The excessive ROS causes oxidative stress damage, triggering the release of inflammatory factors and activating inflammatory pathways, which cascade into a sustained inflammatory response. This response further accelerates muscle atrophy through reduced protein synthesis and enhanced proteolysis, ultimately leading to muscle atrophy and fibrosis[20]. Long-term oxidative stress injury and inflammation alter the microenvironment of skeletal muscle cells[21,22]. In particular, various inflammatory cytokines activate multiple signaling pathways *in vivo*, including nuclear factor-κB, Janus kinase/signal transducer and activator of transcription (JAK/STAT), and mitogen activated protein kinase (MAPK)/p38 pathway, leading to enhanced protein proteolysis and reduced protein synthesis in skeletal muscle[11,23,24]. In addition, denervation-induced muscular atrophy is likewise

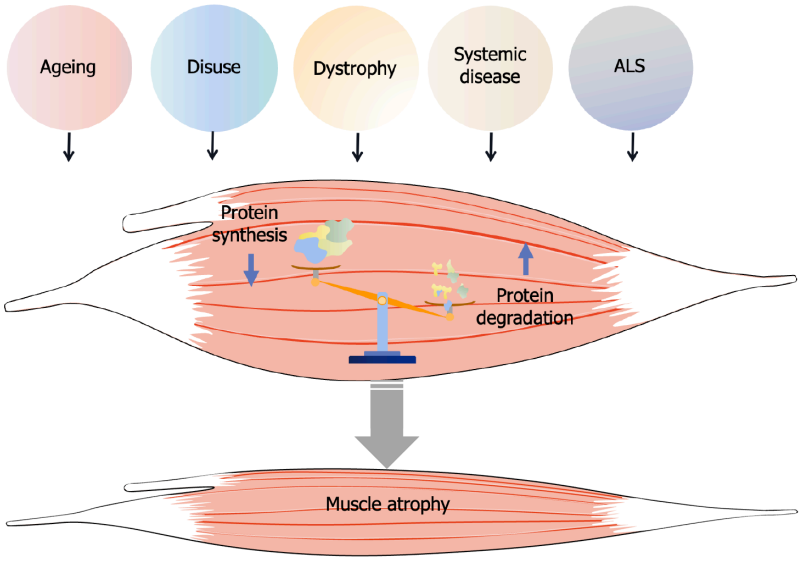

Figure 1 Different causes of muscular atrophy. ALS: Amyotrophic lateral sclerosis.

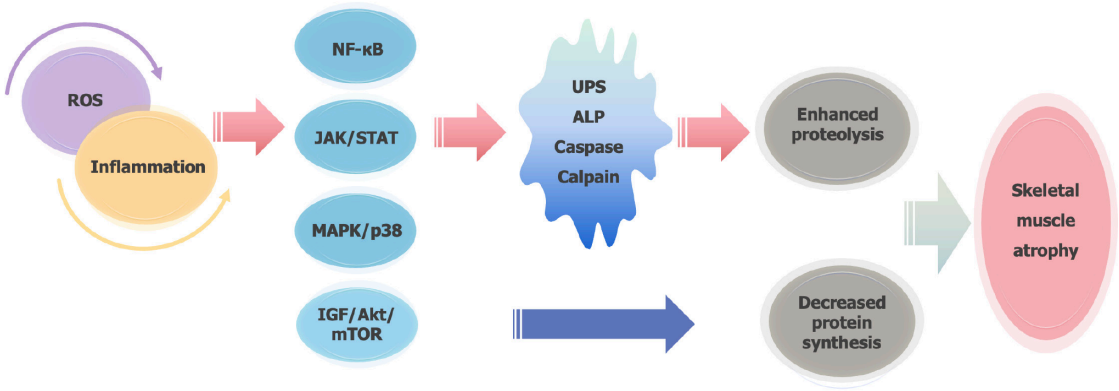

Figure 2 The mechanism underlying muscle atrophy. ROS: Reactive oxygen species; NF-κB: Nuclear factor-κB; JAK: Janus kinase; STAT: Signal transducer and activator of transcription; MAPK: Mitogen activated protein kinase; IGF: Insulin-like growth factor; Akt: Protein kinase B; mTOR: Mechanistic target of rapamycin; UPS: Ubiquitin-proteasome system; ALP: Autophagy-lysosome pathway.

associated with the diminished availability of neurotrophic factors and lowered levels of activity[25]. In conclusion, the complex molecular mechanisms of muscle atrophy have not been well understood, and still needed to be further investigated to provide potential therapeutic strategies for muscle atrophy.

CURRENT STATUS OF MUSCLE ATROPHY TREATMENT

Skeletal muscle atrophy is characterized by a significant reduction in muscle mass, resulting from the disruption of the dynamic equilibrium between protein synthesis and degradation. Given this imbalance, a series of unfavorable changes occur in muscle function and structure. As muscle tissue plays a crucial role in movement, energy metabolism, storage, circulation, and protection[26,27]. Therefore, muscle atrophy can have a significant impact on quality of life. Consequently, the prevention and treatment of muscle atrophy are critical. At present, rehabilitation therapy is the major clinical treatment for muscle atrophy, and the muscle strength is partially restored with the assistance of various rehabilitation exercises. However, rehabilitation exercises require patients to meet certain basic conditions[28]. For example, patients who have been bedridden for long time or have mobility problems due to fractures or nerve deficits are unable to undergo rehabilitation[7]. In addition, rehabilitation exercises need to be conducted according to strict standards, otherwise secondary injuries are likely to occur. Therefore, massage or acupuncture is mostly used to prevent disuse muscular atrophy in the patients who are unable to undergo rehabilitation[29,30]. Although rehabilitation therapy has minimal side effects and no obvious sequelae, it is not very effective in treating muscle atrophy in certain populations[31-33]. So that pursuing more effective treatment measures may be beneficial in patients with several of muscular disorders.

Current therapies focus on how to promote protein synthesis, inhibit protein degradation and facilitate muscle regeneration to prevent or reduce muscle atrophy[7,34]. To date, numerous experiments have shown that anti-inflam-

matory and antioxidant drugs effectively alleviate the progression of muscle atrophy and significantly improve muscle mass and function[17,35,36]. While the exact molecular mechanisms remain to be fully elucidated, treatment with these drugs has been shown to induce significant changes in blood flow, mitochondrial activity, and apoptosis[17]. Scavenging accumulated ROS, improving autophagy and protecting mitochondria can alleviate skeletal muscle atrophy[37-39]. Transforming growth factor-β1 (TGF-β1) is an essential regulator of skeletal muscle several physio-pathologic proceedings, such as myogenesis, regeneration, and muscle atrophy. Injection of TGF-β1 into mice tibialis anterior induced muscle atrophy, leading to decreased fiber diameter, increased MuRF-1 levels and ROS contents. The antioxidant activity of N-acetyl-L-cysteine is used to inhibit the production of ROS in the target muscle, thereby reducing TGF-β-induced muscle atrophy[37]. Other drugs with potent antioxidant properties, such as astaxanthin, nobiletin, pyrroloquinoline quinone, isoquercitrin, and salidroside, have been shown to significantly reduce ROS levels in muscle[7,40,41]. Consequently, the mitochondrial function is stabilized and enhanced, which further reduces apoptosis caused by oxidative stress and abnormalities in mitochondria, and finally inhibits the progression of muscle atrophy[18,36,39,42]. Overall, inhibiting inflammation and reducing ROS accumulation may influence protein synthesis and degradation through multiple pathways, thereby suppressing skeletal muscle atrophy. However, most of these anti-inflammatory and antioxidant drugs have been primarily tested in pre-clinical studies, and their efficacy and safety in human applications remain to be thoroughly investigated. In recent years, stem cell therapies with superior biological properties have emerged as promising treatments for muscle atrophy. Furthermore, stem cell-based interventions have shown substantial benefits in animal models, indicating their potential for future clinical applications.

STEM CELLS AND ITS DERIVATIVES THERAPHY

Stem cell transplantation offers a promising approach for treating various diseases due to the unique self-renewal capability of stem cells and their ability to differentiate into multiple lineages, including osteocytes, neurons, chondrocytes, hepatocytes, and adipocytes. This therapeutic strategy has also been applied to enhance the regenerative capacity of skeletal muscle following injury or degradation due to diseases such as muscular dystrophy[43,44]. In hereditary muscular dystrophies, such as facioscapulohumeral muscular dystrophy (FSHD), stem cell therapy has demonstrated significant improvements over non-transplanted controls, notably by reducing fibrosis and enhancing contractile-specific force[45]. Additionally, hematopoietic stem cells have also been discovered to alleviate muscle atrophy caused by Friedreich's ataxia and Pompe disease[46,47]. Transplantation of bone marrow mesenchymal stem cells (BMSCs) or injection of their secretory vesicles significantly improves symptoms of muscle atrophy with effective control of inflammation[48]. Due to their excellent properties such as proliferation and directed differentiation, stem cells have considerable promise for therapy of muscle atrophy. Some clinical trials have indicated that stem cell therapy is capable of addressing certain intractable hereditary motor neuron (MN) diseases, such as ALS and spinal muscular atrophy muscular atrophy[49-53]. Herein, we summarized the potential role of mesenchymal stem cells (MSCs), induced pluripotent stem cells (iPSCs), and stem cell derivatives as the basis for the treatment of skeletal muscle atrophy.

MSCs in the treatment of muscle atrophy

MSCs is one of the most promising multipotent stem cell types widely used in regenerative medicine. MSCs can be isolated from a variety of tissues, such as adipose tissue, bone marrow, cranial neural crest, umbilical cords, and allogeneic placenta[16,54-56]. Despite cells from different tissues showing similar surface markers, they exhibited substantial differences in cell abundance, proliferation capacity, immune regulation, and differentiation capacity[57]. It has been reported that several MSCs including BMSCs, adipose-derived stem cells (ADSCs) and umbilical cord-derived MSCs (UC-MSCs) are effective in promoting skeletal muscle regeneration in acute and chronic diseases[58-61].

BMSCs in the treatment of muscle atrophy: The application of MSCs has become an established treatment for muscle diseases[62]. MSC injection has been shown to significantly improve muscle mass parameters, including mean fiber diameter, muscle mass, and myonuclear count in the extensor digitorum longus of rats following denervation[63]. ALS, a severe and progressive neurodegenerative disease characterized by the degeneration and loss of MNs, leads to muscle atrophy and loss of motor control[2]. Intrathecal transplantation of BMSCs in ALS mouse models significantly alleviated disease symptoms, delayed disease progression, and improved motor outcomes[64,65]. Studies have demonstrated that BMSCs possess regenerative potential for skeletal muscle[63,66]. Notably, BMSC transplantation increases the number of muscle stem cells and significantly reduces muscle fibrosis. In rats with acute muscle injury, intramuscular BMSC injection downregulated the protein levels of inflammatory cytokines such as interleukin-1β (IL-1β), IL-6, and tumor necrosis factor-α (TNF-α), thereby promoting muscle healing. Following BMSC transplantation, damaged muscle fibers were regenerated, and impaired blood vessels were largely restored. Furthermore, fibrosis progression in injured muscles was inhibited through the suppression of TGF-β1 downstream signaling[67]. Allogeneic BMSCs, when directly injected into acutely injured rat muscle, promoted myofibrogenesis and accelerated functional muscle recovery[68]. MSCs also enhance myotube differentiation, with co-cultures of muscle stem cells and BMSCs showing significant improvements in myotube formation[69]. BMSCs have shown therapeutic potential for dystrophic muscular atrophy as well[70]. In the mdx mouse model of Duchenne muscular dystrophy, peritoneal cavity transplantation of BMSCs significantly alleviated pathological malnutrition in the diaphragm, substantially extending lifespan[66]. Recent studies indicate that hypoxic preconditioning increases the production and secretion of stromal cell-derived factor-1 (SDF-1) and vascular endothelial growth factor in BMSCs. Transplanting hypoxic pretreated BMSCs into injured muscles improves the formation of new blood vessels and enhance muscle repair ability[71]. Thus, BMSCs have demonstrated considerable promise as a

therapeutic approach for preventing muscle atrophy and promoting regeneration (Figure 3).

ADSCs in the treatment of muscle atrophy: A study has highlighted that both allogeneic BMSCs and ADSCs exhibit significant regenerative effects in treating skeletal muscle lacerations in rats, with ADSCs showing superior outcomes [72]. Local injection of ADSCs improves muscle strength and resistance to fatigue, primarily by regulating inflammation and gene products involved in regenerative processes. One study suggested that transplantation of a Matrigel 3D matrix containing TGFβ antibody-pretreated ADSCs into the injured gastrocnemius muscle of mice resulted in improved muscle mass and structure, reduced fibrosis, ameliorated the inflammatory microenvironment, and promoted skeletal muscle regeneration[73]. ADSCs can alleviate immune responses and support muscle reconstruction, with cytokine therapy further enhancing these effects. Preconditioning ADSCs with IL-4, SDF-1, or IL-11 overexpression further boosts their regenerative potential in damaged muscle tissue[74,75]. Recently, a novel approach involving the tethering of nanoparticles releasing TNF-α on the surface of ADSCs to stimulate their secretory activity has been shown to enhance perfusion, walking ability, and muscle mass recovery in ischemic hindlimb mice, providing a more efficient method for clinical stem cell therapy compared to previous pre-treatment strategies[76]. ADSCs have also demonstrated significant therapeutic potential in ALS, where they protect neurons and improve motor function by increasing neurotrophic factor expression[77,78]. These findings underscore the potential of ADSCs in treating muscle-wasting diseases (Figure 4).

UC-MSCs in the treatment of muscle atrophy: UC-MSCs are gaining traction as a promising clinical tool due to their noninvasive collection and superior proliferation capacity, alongside lower immunogenicity compared to other MSCs like BMSCs[79]. As early as 2016, Kim *et al*[80] demonstrated that conditioned medium from UC-MSCs protects muscle cells from hindlimb suspension-induced atrophy. The injection of UC-MSCs activated the expression of muscle-specific markers such as desmin and skeletal muscle actin in satellite cells, stimulating myoblast proliferation and regulating the phosphatidylinositol 3-kinase (PI3K)/Akt pathway by downregulating MuRF-1 and Muscle Atrophy F-box protein[80]. In senescence-accelerated mouse prone 10 mice, UC-MSC injection inhibited apoptosis and inflammation while improving mitochondrial biogenesis *via* the AMP-activated protein kinase (AMPK)/peroxisome proliferator-activated receptor gamma coactivator 1-alpha axis, thereby alleviating sarcopenia-related skeletal muscle atrophy[81]. Muscle atrophy is also associated with chronic metabolic and endocrine diseases such as obesity, hyperthyroidism, and type 2 diabetes mellitus[82,83]. A recent study evaluating the effects of human UC-MSCs (hUC-MSCs) on obesity- and diabetes-induced muscle atrophy found that exosomes derived from hUC-MSCs alleviated muscle atrophy symptoms by enhancing AMPK/UNC-51-like kinases 1 (ULK1)-mediated autophagy[84]. Therefore, UC-MSCs represent a promising therapeutic option for muscle atrophy prevention and regeneration (Figure 5).

In summary, MSCs from various sources offer effective strategies for mitigating muscle atrophy symptoms and maintaining muscle homeostasis by regulating local inflammation, promoting muscle regeneration, and protecting nerve innervation. These findings demonstrate the significant therapeutic potential of MSCs in treating muscle atrophy.

iPSCs in the treatment of muscle atrophy

Pluripotent stem cells (PSCs), including embryonic stem cells (ESCs) and iPSCs, are actively explored for applications in regenerative medicine, drug screening, and disease modeling[85]. ESCs, derived from early embryos at the blastocyst stage, are pluripotent and capable of differentiating into all cell types within an organism[86]. However, due to ethical concerns, challenges in generating high-purity lineage-specific cell lines, and the potential risk of tumorigenesis, ESCs are seldom used in direct disease treatment and are primarily employed in the *in vitro* cultivation of tissues and organs[87]. In contrast, iPSCs offer distinct advantages, sharing key properties with ESCs, such as differentiation potential, electrophysiological characteristics, biochemistry, and telomerase activity[88]. Compared to muscle cells or MSCs directly transplanted into patients, iPSCs are more abundant, can be easily isolated and purified using specific markers, and demonstrate robust differentiation capabilities[89-91]. Furthermore, iPSCs mitigate the risk of immune rejection, as they avoid allogeneic transplantation issues[92,93].

Differentiation of human iPSCs into myoblasts presents a promising approach for both autologous and allogeneic therapies in the treatment of muscle atrophy[91,94,95]. Human PSC-derived myogenic progenitor cells (MPCs), generated using both transgene-free and transgene-dependent protocols, have demonstrated potential in skeletal muscle engraftment[95]. Using a fluorescent reporter system, studies have shown that these MPCs promote myofiber regeneration in both local injury models and mdx mice[96]. PSC-derived PAX7$^+$ MPCs represent a compelling strategy for muscle regeneration, enabling large-scale production of human myogenic progenitors[97]. Furthermore, under optimized 3D culture conditions, PSC-derived PAX7$^+$ MPCs are capable of regenerating functional skeletal muscle[98]. In immunocompromised NSG mice, iSKM bundles derived from these cells were shown to survive, gradually vascularize, and maintain muscle function when implanted into the hind-limb muscles. Recent studies have directed human PSCs toward the differentiation of embryonic muscle progenitors, which subsequently developed into primary and secondary embryonic muscle, eventually forming three-dimensional muscle structures[99]. These tissue-engineered muscles exhibited high levels of maturation and function that closely resemble normal human muscle. After skeletal muscle atrophy, recovery is limited, even with sufficient blood supply and appropriate rest. In most cases, fibroblasts proliferate to repair damaged muscle tissue, leading to muscle mass reduction and impaired mobility. FSHD, a genetically dominant progressive myopathy characterized by muscle fibrosis, atrophy, and fat replacement, is one such condition. In an FSHD mouse model, the transplantation of MPCs derived from PSCs significantly improved muscle contractility compared to non-transplanted controls[45]. Moreover, the transplantation of human iPSC-derived MNs has shown potential in treating neuromuscular atrophy in mice with sciatic nerve injury[100]. Regeneration of neuromuscular junctions is vital for functional recovery in denervated muscles affected by trauma or MN diseases. P75$^+$ neural stem cells derived from human iPSCs have been shown to enhance the secretion of soluble factors that promote neuromuscular regeneration.

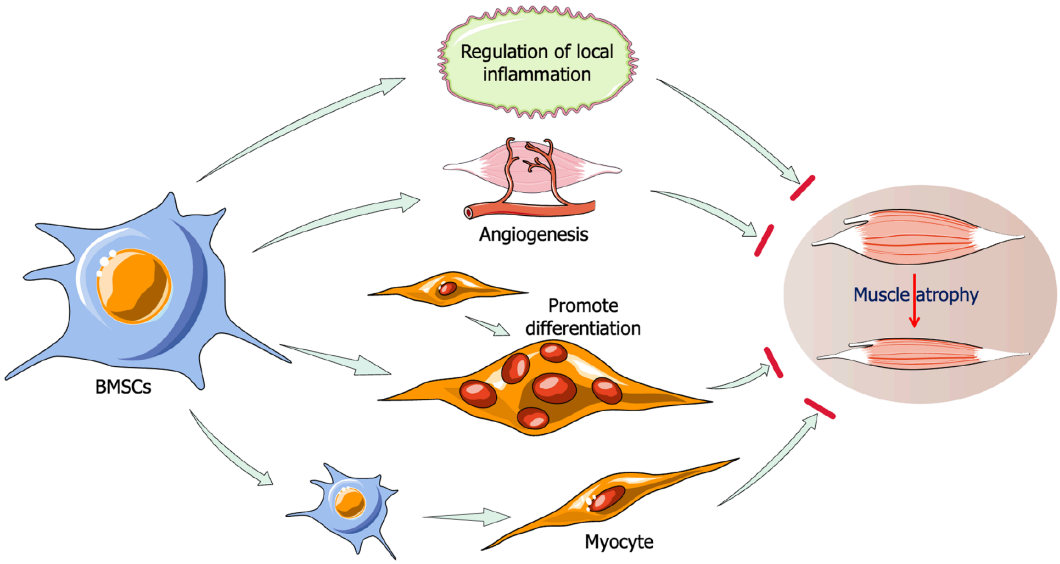

Figure 3 The potential role of bone marrow mesenchymal stem cells for the treatment of skeletal muscle atrophy. BMSCs: Bone marrow mesenchymal stem cells.

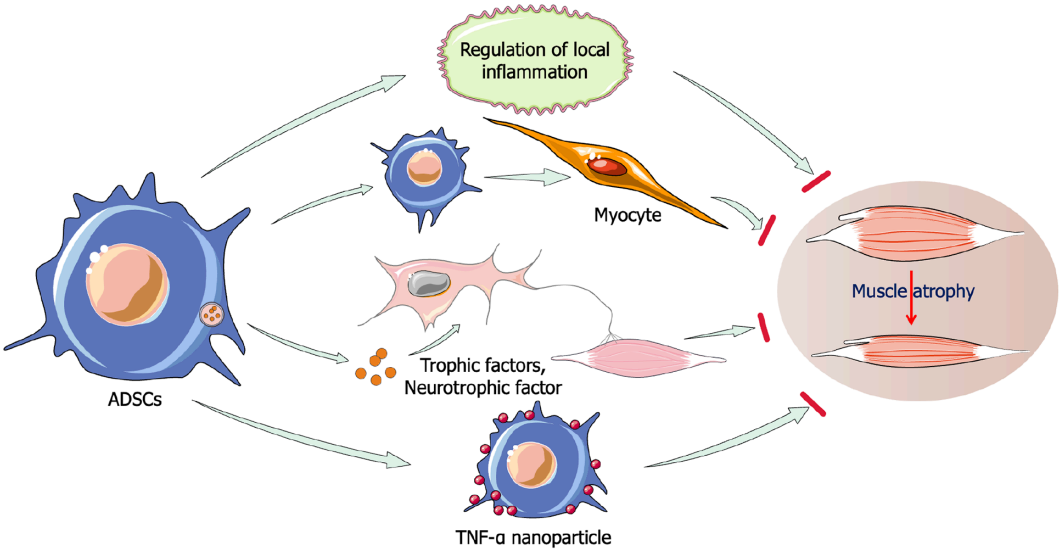

Figure 4 The potential role of adipose-derived stem cells for the treatment of skeletal muscle atrophy. ADSCs: Adipose-derived stem cells; TNF: Tumor necrosis factor.

When injected into denervated gastrocnemius muscle, these NCSC spheres significantly improved neuromuscular function recovery[101]. iPSCs also show promise in treating ALS. In an ALS mouse model, transplantation of neural stem cells derived from iPSCs improved the microenvironment by secreting growth factors and immunomodulatory molecules, which likely contributed to the reconstruction of neural circuits and restoration of motor control in ALS-affected muscles[102,103]. Therefore, iPSCs have the potential to treat muscle atrophy and provide a new technical idea for personalized treatment of dystrophic muscular atrophy in the future (Figure 6). The available results have shown that this method is feasible and has the potential for application and development in clinical practice.

Exosomes derived from stem cells in the treatment of muscle atrophy

The regenerative potential of MSCs stems not only from their direct transplantation into target tissues and subsequent differentiation but also from their secretions, particularly exosomes, which activate the regenerative capacity of resident cells. Exosomes contain various bioactive components, including growth factors, cytokines, mRNAs, signaling lipids, and regulatory microRNAs[104]. Although MSCs from different tissues and donors secrete distinct protein profiles, their actions *in vitro* can vary; they are nonetheless capable of regulating apoptosis in dystrophic myogenic cells and promoting cell migration and proliferation[105]. Skeletal muscle regeneration is closely linked to the biological factors secreted by exosomes, which exert significant bioactive effects on damaged muscle tissue[106,107]. Increasing evidence suggests that exosomes derived from stem cells offer promising therapeutic potential for muscle regeneration (Table 1).

Table 1 The potential role of mesenchymal stem cell-derived exosomes in the treatment of skeletal muscle atrophy

Resouce	Mechanism	Function	Ref.
UC-MSCs	Releasing circHIPK3, while circHIPK3 down-regulates miR-421, leading to increased expression of FOXO3a, thereby inhibiting IL-1β and IL-18	Accelerate repair of ischemic muscle injury in mice	[108]
	hUC-MSCs or hUC-MSC-derived exosomes induce the activation of AMPK/ULK1 signal and enhancement of autophagy	Alleviate muscle atrophy induced by diabetes and obesity in mice	[84]
	Down-regulating IL-6 and IL-1β, up-regulating IL-10, and regulating inflammation of injured nerves	Promote the recovery of motor function and regeneration of axons, alleviated denervated gastrocnemius atrophy in rats	[109]
	Regulating the miR-132-3p/FoxO3 axis	Improve age-related muscle atrophy in a mouse model	[110]
ADSCs	Promoting peripheral nerve regeneration *via* optimizing SC function	Alleviate denervated muscle atrophy in rats	[111]
	Inhibiting inflammation, enhancing proliferation of muscle satellite cells, resisting cell senescence and promoting angiogenesis	Maintain muscle homeostasis, promote muscle regeneration in a mouse model of cardiotoxin-induced injury	[112,113]
	Preventing the atrophy, fatty infiltration, inflammation, and vascularization of muscles	Decrease atrophy and degeneration associated with torn rotator cuffs, and improve muscle regeneration in rats	[114]
	Improving motor performance; protecting lumbar motoneurons, neuromuscular junction, and muscle, decreasing glial cells activation	Protect neuromuscular junction and muscle in SOD1 (G93A) murine model	[115]
BMSCs	Promoting M2 macrophages polarization, reducing the production of inflammatory cytokines, upregulating anti-inflammatory factors expression	Attenuate muscle injury and promote muscle healing in mice with hit injury	[116]
	Foxo1 expression was inhibited by up-regulating the miR486-5p/Foxo1 axis	Inhibit dexamethasone-induced muscle atrophy in mice	[117]
	M2 macrophage polarization is regulated by NF-κB pathway to reduce inflammatory pain, and myeloid axon regeneration is enhanced by MEK/ERK pathway	Improve denervated muscle atrophy and further promote functional recovery in rats	[106,107]

UC-MSCs: Umbilical cord-derived mesenchymal stromal cells; FOXO3a: Forkhead box O3a; IL: Interleukin; hUC-MSCs: Human umbilical cord-derived mesenchymal stromal cells; AMPK: AMP-activated protein kinase; ULK1: UNC-51-like kinases 1; ADSCs: Adipose-derived stem cells; SC: Schwann cell; BMSCs: Bone marrow mesenchymal stem cells; NF-κB: Nuclear factor-κB; MEK: Mitogen-activated protein kinase; ERK: Extracellular signal-regulated kinase.

Exosomes secreted by hUC-MSCs (hUC-MSC-Exos) have been confirmed to be effective against muscle injury. In a mouse model of ischemic induced skeletal muscle injury, purified hUC-MSC-Exos accelerates skeletal muscle regeneration by releasing circHIPK3[108]. This led to the downregulation of miR-421, resulting in Forkhead box O3a (FOXO3a) expression, inhibition of pyroptosis, and decreased release of IL-1β and IL-18[108]. Similarly, Song *et al*[84] reported that hUC-MSC-Exos alleviated diabetes-associated muscle atrophy by enhancing autophagy through the AMPK/ULK1 axis. In a rat sciatic nerve defect model, hUC-MSC-Exos promoted nerve regeneration and attenuated gastrocnemius muscle atrophy by modulating inflammation - downregulating IL-1β and IL-6, upregulating IL-10[109]. A recent study suggest that hUC-MSC-Exos may improve age-related and dexamethasone-induced muscle atrophy in a mouse model by regulating the miR-132-3p/FoxO3 axis[110]. These studies suggest that the application of exosomes derived from UC-MSCs have great potential for muscle atrophy.

The protective effect of exosomes secreted by human ADSCs on denervated muscle atrophy has been confirmed in rat studies, where exosomes secreted by human ADSCs significantly promoted nerve regeneration and alleviated muscle atrophy following sciatic nerve dissection[111]. Exosomes secreted by ADSCs (ADSC-Exos) enhanced Schwann cell proliferation, migration, and myelination, while also stimulating the release of neurotrophic factors through the upregulation of key genes. Furthermore, ADSC-Exos contributed to muscle homeostasis by inhibiting inflammation, promoting muscle satellite cell proliferation, resisting cellular senescence, and stimulating angiogenesis[112-114]. ADSC-Exos play a critical role in skeletal muscle regeneration at various stages by modulating key signaling pathways, including MAPK, Wnt, PI3K/Akt, and JAK/STAT[113]. For example, catenin derived from ADSC-Exos activates the classical Wnt pathway, supporting myogenic maintenance of satellite cells, while also coordinating their self-renewal and migration *via* the non-classical Wnt pathway[115]. In the early stages of muscle regeneration, ADSC-Exos activate MAPK/extracellular signal-regulated kinase 1/2 and MAPK/JNK pathways, promoting myoblast proliferation and preventing premature differentiation[116]. At later stages, the p38/MK2 and MEF2 pathways drive myogenic differentiation by enhancing MyoD transcriptional activity[117], while the MAPK/extracellular signal-regulated kinase 5 pathway facilitates multinucleated myotube formation. Additionally, ADSC-Exos influence the PI3K/Akt pathway to upregulate protein synthesis and

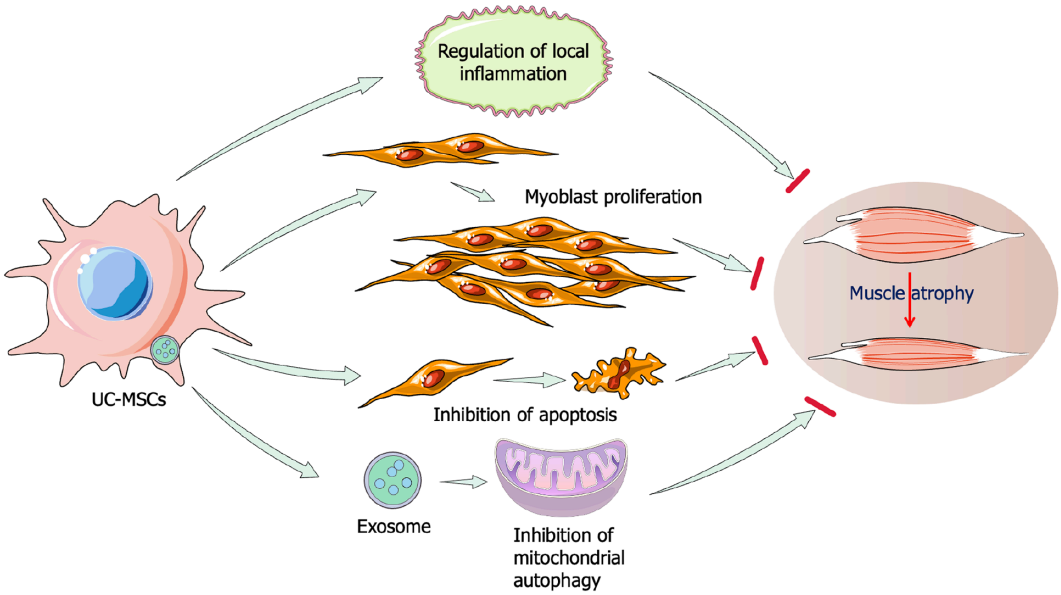

Figure 5 The potential role of umbilical cord-derived mesenchymal stromal cells for the treatment of skeletal muscle atrophy. UC-MSCs: Umbilical cord-derived mesenchymal stromal cells.

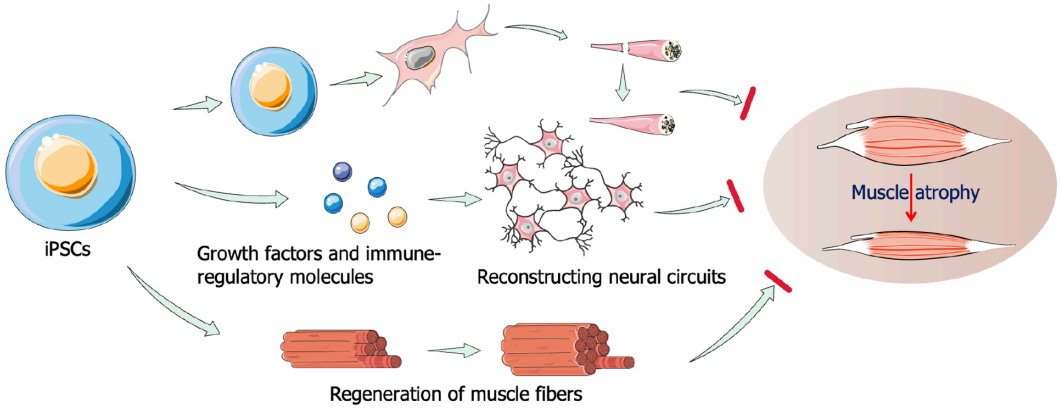

Figure 6 The potential role of induced pluripotent stem cells for the treatment of skeletal muscle atrophy. iPSCs: Induced pluripotent stem cells.

suppress protein degradation, counteracting muscle atrophy. However, the potential inhibitory effect of PI3K/Akt on autophagy *via* mechanistic target of rapamycin and FOXO suggests that its role in muscle regeneration may not be entirely beneficial[118]. Moreover, ADSC-Exos regulate the JAK1/STAT1/3 pathway to prevent premature differentiation of myoblasts, while JAK2/STAT2/3 and JAK3/STAT1/3 pathways promote myogenic differentiation. ADSC-Exos have also been shown to reduce muscle-related protein degeneration and muscle atrophy while enhancing regeneration and biomechanical properties in torn rotator cuff muscles in rats[119]. Additionally, repeated administration of ADSC-Exos reduced glial cell activation, protected muscles, MNs, and neuromuscular junctions, and improved motor performance in SOD1-G93A mice[120]. Proteomic analysis of ADSC-Exos revealed their influence on ALS-related pathways, including oxidative stress response, cell apoptosis, cell adhesion, and PI3K/Akt signaling[121]. In conclusion, extensive evidence highlights the significant potential of ADSC-Exos in the treatment of muscle diseases.

Exosomes secreted by BMSCs (BMSC-Exos) have shown therapeutic potential for muscle injury and atrophy. Intramuscular injection of BMSC-Exos reduces inflammation following muscle contusion in mice, mitigates muscle fibrosis, promotes regeneration, and enhances muscle biomechanical properties[122]. A study also demonstrated that BMSC-Exos counteract dexamethasone-induced muscle atrophy through the miR486-5p/Foxo1 pathway[123]. Recently, a BMSC-Exos-loaded electroconductive nerve dressing has been developed for treating diabetic peripheral nerve injury. Implantation of the BMSC-Exos-loaded electroconductive nerve dressing complex around damaged sciatic nerves enhances myelinated axon regeneration, ameliorates gastrocnemius muscle atrophy, and promotes functional recovery in diabetic rats[107]. Furthermore, supplementation with exosomes secreted by iPSCs in acellular nerve grafts through optimized chemical extraction processes has been shown to repair long-distance peripheral nerve defects, accelerating motor recovery and reversing denervated muscle atrophy[124]. Skin-derived precursors (SKPs), pluripotent cells derived from the dermis, are another promising stem cell source. Artificial nerve grafts incorporating SKP-derived Schwann cells can alleviate denervation-induced muscle atrophy[125]. In our recent study, direct intramuscular injection of SKP-SC-

extracellular vesicles alleviated blood flow reduction, oxidative stress, and inflammation in target muscles, thus reducing skeletal muscle atrophy caused by denervation[126]. Overall, stem cell-derived exosomes mitigate inflammation, reduce fibrosis, accelerate muscle regeneration, and promote functional recovery[122,127]. In conclusion, stem cell-derived exosomes present substantial promise for clinical applications, with exosomes secreted by MSCs offering a potential alternative to whole-cell regenerative therapies.

CHALLENGES OF STEM CELL THERAPY

Despite the considerable promise of stem cells in treating muscle atrophy and related diseases, challenges surrounding their source and biological characteristics, particularly ethical concerns related to the use of human ESCs, remain significant. Furthermore, other types of stem cells present notable limitations that impede the advancement of stem cell therapies. The potential risks of immune rejection and tumor formation after transplantation are significant issues worthy of attention. The approaches to mitigate these risks include strategies such as immunosuppression, immune matching, and stem cell genetic engineering. However, each strategy confronts its own unique challenges and may have varying degrees of impact on patient safety[128].

MSCs are widely utilized in medicine due to their pluripotency, broad tissue origins, and minimal ethical concerns. While MSC-based therapies offer advantages over conventional treatments in clinical trials, their therapeutic outcomes often fall short of expectations. Key challenges, including stem cell homing, immune modulation, and other factors, need to be addressed for successful MSC application. Under various conditions, such as ischemia or injury, MSCs - whether autologous or exogenous - migrate directionally from the vascular endothelium to the affected tissues, where they colonize and survive[129,130]. The activation of MSCs occurs in response to elevated inflammatory factors like IL-1 and TNF-α, which generate a concentration gradient of ligands around the target tissue, promoting MSC migration towards ischemic and hypoxic regions[131,132]. SDF-1 and its receptor C-X-C motif chemokine receptor 4 are the most extensively studied cytokines involved in cell homing[126]. SDF-1 is upregulated at injury sites, acting on MSC migration in a dose-dependent manner, thus enhancing BMSC homing for tissue repair[133,134]. However, maintaining MSCs at specific target sites, such as muscles, remains a significant challenge. MSCs secrete paracrine factors capable of tissue remodeling and repair, act as drug carriers, and modulate immune responses[135-138]. MSCs can detect injury sites and elicit stronger immune responses in low-immune states, while inhibiting immune cell function when inflammation is excessive in the damaged area[139]. They exhibit dual, opposing functions - pro-inflammatory or anti-inflammatory - depending on the inflammatory factors present in the local environment[66,140]. The key to optimizing their therapeutic effects lies in understanding how to modulate or exploit the immune-inducing properties of MSCs. Additionally, factors contributing to suboptimal therapeutic outcomes include the age of MSC donors, variations in cell isolation and culture protocols, the method of administration, and individual differences among recipients[141-143]. Long-term culture impairs the differentiation potential of MSCs, and the same cell batch may exhibit heterogeneous differentiation, which can skew experimental results. Moreover, various biological and experimental factors introduce safety risks in clinical and basic research applications of stem cells, such as tumor formation, infection, necrosis from tissue blockage due to stem cell homing[144], and other exogenous risks[145,146]. Although MSCs have good therapeutic effects in animal models of muscle diseases, biosafety evaluation standards for stem cell experiments and therapy are lacking. The heterogeneity of MSCs is one of the factors contributing to the variation in treatment outcomes, which presents challenges in determining the optimal stem cell therapy protocol, dosage, and timing[57]. These issues necessitate further research and clinical practice for resolution.

There was no unified and effective differentiation method for iPSCs to differentiate into muscle precursor cells, and their purification protocols are also inconsistent[95,147]. For transgene-free protocols, due to discrepancy in purification and transplantation times among the protocols, none of previously reported optimal purification strategies have been reproducibly validated. For transgene-dependent protocols, a risk factor that may not be ignored is the induced expression of proto-oncogenes introduced *via* viral vectors or existing in the host cells. It remains unclear whether other unknown genes are involved in the reprogramming process or if genetic and epigenetic changes occur during this process [148]. Consequently, several challenges remain before iPSCs can be reliably applied in clinical settings.

In the current social, scientific and ethical context, the use of stem cell derivatives as a cell-free therapy is rapidly emerging as an alternative with additional advantages. It can avoid safety issues related to the use of living cells, ethical issues related to the origin of the cells, and immunocompatibility issues. MSC-derived exosomes, which are characterized by low-immunogenicity, high biocompatibility, safety and low toxicity, provide a new approach to deliver therapeutic agents to target cells, which is the best alternative to stem cell therapy[149-151]. Although exosomes are generally considered to have great clinical therapeutic value, there are still many drawbacks such as extremely low concentration of active ingredients, poor specificity, and difficulty in traceability, which restrict the clinical use of exosomes. It is also worthy of note that cell-free therapeutic products might take a considerable amount of time for administration and could result in drug resistance as well as some adverse reactions[152].

It is crucial to prove the safety and efficacy of stem cells and their derived exosomes therapy through clinical trials. Evaluating long-term efficacy means tracking changes in cell survival, integration, and treatment response over time, and identifying any adverse events or delayed complications. This requires establishing standardized methods and guidelines [128]. Also, currently, there's no clear consensus or standard about the administration route, dose, and treatment time [57]. These require the establishment of standardized methods and guidelines. Of course, in addition to the ethical controversy related to the use of ESCs mentioned earlier, issues such as informed consent from patients, the experimental nature of the treatment, and fair access to emerging therapies should also be considered in the consideration of stem cell clinical use. Solving these multifaceted challenges requires not only the efforts of researchers and clinicians, but also

coordinated efforts with regulatory agencies and ethics committees, which will be key to realizing the potential of stem cell therapy for muscle atrophy.

CONCLUSION

The rapid advancements in stem cell research have opened new avenues for treating previously incurable diseases. Numerous clinical trials have demonstrated promising outcomes in addressing cardiovascular, neurological, and immune disorders[151,153-155]. This review systematically analyzes the therapeutic application of stem cells including BMSCs, ADSCs, UCMSCs, and iPSCs in skeletal muscle atrophy due to various causes. In addition, we also summarize the advantages of existing therapeutic strategies and further research development directions in order to mitigate or eliminate therapeutic deficiencies and establish a relatively sound therapeutic evaluation system. Cell-free therapies based on stem cell derivatives have better prospects compared to conventional cell transplantation therapy[156,157]. A full understanding of the capabilities of different types of stem cells, especially their derivatives, in muscle repair and regeneration would be a breakthrough in the treatment of muscle atrophy.

ACKNOWLEDGEMENTS

We would like to thank all the professionals who contributed to the discussion and elaboration of this review.

FOOTNOTES

Author contributions: Wang YJ and Chen ZH contributed equally to write the paper and are co-first authors of this manuscript; Shen YT modified the manuscript; Wang KX, Han YM, Zhang C, and Yang XM provided data; Chen BQ designed the review and were responsible for the final proofreading; and all authors have read and approve the final manuscript.

Supported by Suzhou Science and Technology Development Planning Project, No. SYW2024048; National Natural Science Foundation of China, No. 81901933; and Major Natural Science Research Projects in Universities of Jiangsu Province, No. 24KJA310007.

Conflict-of-interest statement: All the authors report no relevant conflicts of interest for this article.

Country of origin: China

ORCID number: Yun-Tian Shen 0000-0002-5145-4761; Bing-Qian Chen 0000-0002-4012-3481.

S-Editor: Wang JJ
L-Editor: A
P-Editor: Zhang XD

REFERENCES

1 **Sartori R**, Romanello V, Sandri M. Mechanisms of muscle atrophy and hypertrophy: implications in health and disease. *Nat Commun* 2021; **12**: 330 [PMID: 33436614 DOI: 10.1038/s41467-020-20123-1]
2 **Wang K**, Liu Q, Tang M, Qi G, Qiu C, Huang Y, Yu W, Wang W, Sun H, Ni X, Shen Y, Fang X. Chronic kidney disease-induced muscle atrophy: Molecular mechanisms and promising therapies. *Biochem Pharmacol* 2023; **208**: 115407 [PMID: 36596414 DOI: 10.1016/j.bcp.2022.115407]
3 **Shen Y**, Li M, Wang K, Qi G, Liu H, Wang W, Ji Y, Chang M, Deng C, Xu F, Shen M, Sun H. Diabetic Muscular Atrophy: Molecular Mechanisms and Promising Therapies. *Front Endocrinol (Lausanne)* 2022; **13**: 917113 [PMID: 35846289 DOI: 10.3389/fendo.2022.917113]
4 **Chang M**, Cai Y, Gao Z, Chen X, Liu B, Zhang C, Yu W, Cao Q, Shen Y, Yao X, Chen X, Sun H. Duchenne muscular dystrophy: pathogenesis and promising therapies. *J Neurol* 2023; **270**: 3733-3749 [PMID: 37258941 DOI: 10.1007/s00415-023-11796-x]
5 **Yin L**, Li N, Jia W, Wang N, Liang M, Yang X, Du G. Skeletal muscle atrophy: From mechanisms to treatments. *Pharmacol Res* 2021; **172**: 105807 [PMID: 34389456 DOI: 10.1016/j.phrs.2021.105807]
6 **Qazi TH**, Duda GN, Ort MJ, Perka C, Geissler S, Winkler T. Cell therapy to improve regeneration of skeletal muscle injuries. *J Cachexia Sarcopenia Muscle* 2019; **10**: 501-516 [PMID: 30843380 DOI: 10.1002/jcsm.12416]
7 **Huang L**, Li M, Deng C, Qiu J, Wang K, Chang M, Zhou S, Gu Y, Shen Y, Wang W, Huang Z, Sun H. Potential Therapeutic Strategies for Skeletal Muscle Atrophy. *Antioxidants (Basel)* 2022; **12**: 44 [PMID: 36670909 DOI: 10.3390/antiox12010044]
8 **You Z**, Huang X, Xiang Y, Dai J, Jiang J, Xu J. Molecular feature of neutrophils in immune microenvironment of muscle atrophy. *J Cell Mol*

Med 2022; **26**: 4658-4665 [PMID: 35899367 DOI: 10.1111/jcmm.17495]
9 **Sun H**, Sun J, Li M, Qian L, Zhang L, Huang Z, Shen Y, Law BY, Liu L, Gu X. Transcriptome Analysis of Immune Receptor Activation and Energy Metabolism Reduction as the Underlying Mechanisms in Interleukin-6-Induced Skeletal Muscle Atrophy. *Front Immunol* 2021; **12**: 730070 [PMID: 34552592 DOI: 10.3389/fimmu.2021.730070]
10 **Zhang H**, Qi G, Wang K, Yang J, Shen Y, Yang X, Chen X, Yao X, Gu X, Qi L, Zhou C, Sun H. Oxidative stress: Roles in skeletal muscle atrophy. *Biochem Pharmacol* 2023; **214**: 115664 [PMID: 37331636 DOI: 10.1016/j.bcp.2023.115664]
11 **Ji Y**, Li M, Chang M, Liu R, Qiu J, Wang K, Deng C, Shen Y, Zhu J, Wang W, Xu L, Sun H. Inflammation: Roles in Skeletal Muscle Atrophy. *Antioxidants (Basel)* 2022; **11**: 1686 [PMID: 36139760 DOI: 10.3390/antiox11091686]
12 **Liang W**, Xu F, Li L, Peng C, Sun H, Qiu J, Sun J. Epigenetic control of skeletal muscle atrophy. *Cell Mol Biol Lett* 2024; **29**: 99 [PMID: 38978023 DOI: 10.1186/s11658-024-00618-1]
13 **Huang Z**, Zhong L, Zhu J, Xu H, Ma W, Zhang L, Shen Y, Law BY, Ding F, Gu X, Sun H. Inhibition of IL-6/JAK/STAT3 pathway rescues denervation-induced skeletal muscle atrophy. *Ann Transl Med* 2020; **8**: 1681 [PMID: 33490193 DOI: 10.21037/atm-20-7269]
14 **He Q**, Qiu J, Dai M, Fang Q, Sun X, Gong Y, Ding F, Sun H. MicroRNA-351 inhibits denervation-induced muscle atrophy by targeting TRAF6. *Exp Ther Med* 2016; **12**: 4029-4034 [PMID: 28101181 DOI: 10.3892/etm.2016.3856]
15 **Ito N**, Ruegg UT, Takeda S. ATP-Induced Increase in Intracellular Calcium Levels and Subsequent Activation of mTOR as Regulators of Skeletal Muscle Hypertrophy. *Int J Mol Sci* 2018; **19**: 2804 [PMID: 30231482 DOI: 10.3390/ijms19092804]
16 **Yan Y**, Li M, Lin J, Ji Y, Wang K, Yan D, Shen Y, Wang W, Huang Z, Jiang H, Sun H, Qi L. Adenosine monophosphate activated protein kinase contributes to skeletal muscle health through the control of mitochondrial function. *Front Pharmacol* 2022; **13**: 947387 [PMID: 36339617 DOI: 10.3389/fphar.2022.947387]
17 **Zhang L**, Li M, Wang W, Yu W, Liu H, Wang K, Chang M, Deng C, Ji Y, Shen Y, Qi L, Sun H. Celecoxib alleviates denervation-induced muscle atrophy by suppressing inflammation and oxidative stress and improving microcirculation. *Biochem Pharmacol* 2022; **203**: 115186 [PMID: 35882305 DOI: 10.1016/j.bcp.2022.115186]
18 **Shen Y**, Zhang Q, Huang Z, Zhu J, Qiu J, Ma W, Yang X, Ding F, Sun H. Isoquercitrin Delays Denervated Soleus Muscle Atrophy by Inhibiting Oxidative Stress and Inflammation. *Front Physiol* 2020; **11**: 988 [PMID: 32903465 DOI: 10.3389/fphys.2020.00988]
19 **Shen Y**, Zhang R, Xu L, Wan Q, Zhu J, Gu J, Huang Z, Ma W, Shen M, Ding F, Sun H. Microarray Analysis of Gene Expression Provides New Insights Into Denervation-Induced Skeletal Muscle Atrophy. *Front Physiol* 2019; **10**: 1298 [PMID: 31681010 DOI: 10.3389/fphys.2019.01298]
20 **Wan Q**, Zhang L, Huang Z, Zhang H, Gu J, Xu H, Yang X, Shen Y, Law BY, Zhu J, Sun H. Aspirin alleviates denervation-induced muscle atrophy *via* regulating the Sirt1/PGC-1α axis and STAT3 signaling. *Ann Transl Med* 2020; **8**: 1524 [PMID: 33313269 DOI: 10.21037/atm-20-5460]
21 **Sun J**, Yang H, Yang X, Chen X, Xu H, Shen Y, Ding F, Gu X, Zhu J, Sun H. Global alternative splicing landscape of skeletal muscle atrophy induced by hindlimb unloading. *Ann Transl Med* 2021; **9**: 643 [PMID: 33987341 DOI: 10.21037/atm-20-5388]
22 **Ma W**, Cai Y, Shen Y, Chen X, Zhang L, Ji Y, Chen Z, Zhu J, Yang X, Sun H. HDAC4 Knockdown Alleviates Denervation-Induced Muscle Atrophy by Inhibiting Myogenin-Dependent Atrogene Activation. *Front Cell Neurosci* 2021; **15**: 663384 [PMID: 34276308 DOI: 10.3389/fncel.2021.663384]
23 **Liang Z**, Zhang T, Liu H, Li Z, Peng L, Wang C, Wang T. Inflammaging: The ground for sarcopenia? *Exp Gerontol* 2022; **168**: 111931 [PMID: 35985553 DOI: 10.1016/j.exger.2022.111931]
24 **Irazoki A**, Martinez-Vicente M, Aparicio P, Aris C, Alibakhshi E, Rubio-Valera M, Castellanos J, Lores L, Palacín M, Gumà A, Zorzano A, Sebastián D. Coordination of mitochondrial and lysosomal homeostasis mitigates inflammation and muscle atrophy during aging. *Aging Cell* 2022; **21**: e13583 [PMID: 35263007 DOI: 10.1111/acel.13583]
25 **Chu XL**, Song XZ, Li Q, Li YR, He F, Gu XS, Ming D. Basic mechanisms of peripheral nerve injury and treatment *via* electrical stimulation. *Neural Regen Res* 2022; **17**: 2185-2193 [PMID: 35259827 DOI: 10.4103/1673-5374.335823]
26 **Grgic J**, Schoenfeld BJ, Mikulic P. Effects of plyometric vs. resistance training on skeletal muscle hypertrophy: A review. *J Sport Health Sci* 2021; **10**: 530-536 [PMID: 32579911 DOI: 10.1016/j.jshs.2020.06.010]
27 **Chen X**, Ji Y, Liu R, Zhu X, Wang K, Yang X, Liu B, Gao Z, Huang Y, Shen Y, Liu H, Sun H. Mitochondrial dysfunction: roles in skeletal muscle atrophy. *J Transl Med* 2023; **21**: 503 [PMID: 37495991 DOI: 10.1186/s12967-023-04369-z]
28 **Howard EE**, Pasiakos SM, Fussell MA, Rodriguez NR. Skeletal Muscle Disuse Atrophy and the Rehabilitative Role of Protein in Recovery from Musculoskeletal Injury. *Adv Nutr* 2020; **11**: 989-1001 [PMID: 32167129 DOI: 10.1093/advances/nmaa015]
29 **Lawrence MM**, Van Pelt DW, Confides AL, Hunt ER, Hettinger ZR, Laurin JL, Reid JJ, Peelor FF 3rd, Butterfield TA, Dupont-Versteegden EE, Miller BF. Massage as a mechanotherapy promotes skeletal muscle protein and ribosomal turnover but does not mitigate muscle atrophy during disuse in adult rats. *Acta Physiol (Oxf)* 2020; **229**: e13460 [PMID: 32125770 DOI: 10.1111/apha.13460]
30 **Su Z**, Hu L, Cheng J, Klein JD, Hassounah F, Cai H, Li M, Wang H, Wang XH. Acupuncture plus low-frequency electrical stimulation (Acu-LFES) attenuates denervation-induced muscle atrophy. *J Appl Physiol (1985)* 2016; **120**: 426-436 [PMID: 26679610 DOI: 10.1152/japplphysiol.00175.2015]
31 **Lv T**, Mo Y, Yu T, Zhang Y, Shao S, Luo Y, Shen Y, Lu M, Wong SG. An Investigation into the Rehabilitative Mechanism of Tuina in the Treatment of Sciatic Nerve Injury. *Evid Based Complement Alternat Med* 2020; **2020**: 5859298 [PMID: 32724326 DOI: 10.1155/2020/5859298]
32 **Peng S**, Tian Y, Chang W, Yang Y, Li S, Ni J, Zhu W. Current state of research on acupuncture for the treatment of amyotrophic lateral sclerosis: A scoping review. *Front Neurol* 2022; **13**: 1019156 [PMID: 36408510 DOI: 10.3389/fneur.2022.1019156]
33 **Rahiminezhad E**, Sadeghi M, Ahmadinejad M, Mirzadi Gohari SI, Dehghan M. A randomized controlled clinical trial of the effects of range of motion exercises and massage on muscle strength in critically ill patients. *BMC Sports Sci Med Rehabil* 2022; **14**: 96 [PMID: 35619171 DOI: 10.1186/s13102-022-00489-z]
34 **Huang Z**, Zhu J, Ma W, Sun H. Strategies and potential therapeutic agents to counter skeletal muscle atrophy. *Biotarget* 2018; **2**: 8 [DOI: 10.21037/biotarget.2018.05.02]
35 **Qiu J**, Fang Q, Xu T, Wu C, Xu L, Wang L, Yang X, Yu S, Zhang Q, Ding F, Sun H. Mechanistic Role of Reactive Oxygen Species and Therapeutic Potential of Antioxidants in Denervation- or Fasting-Induced Skeletal Muscle Atrophy. *Front Physiol* 2018; **9**: 215 [PMID: 29593571 DOI: 10.3389/fphys.2018.00215]
36 **Xu T**, Yang X, Wu C, Qiu J, Fang Q, Wang L, Yu S, Sun H. Pyrroloquinoline quinone attenuates cachexia-induced muscle atrophy *via* suppression of reactive oxygen species. *J Thorac Dis* 2018; **10**: 2752-2759 [PMID: 29997937 DOI: 10.21037/jtd.2018.04.112]

37 **Abrigo J**, Rivera JC, Simon F, Cabrera D, Cabello-Verrugio C. Transforming growth factor type beta (TGF-β) requires reactive oxygen species to induce skeletal muscle atrophy. *Cell Signal* 2016; **28**: 366-376 [PMID: 26825874 DOI: 10.1016/j.cellsig.2016.01.010]

38 **Scalabrin M**, Engman V, Maccannell A, Critchlow A, Roberts LD, Yuldasheva N, Bowen TS. Temporal analysis of skeletal muscle remodeling post hindlimb ischemia reveals intricate autophagy regulation. *Am J Physiol Cell Physiol* 2022; **323**: C1601-C1610 [PMID: 36252128 DOI: 10.1152/ajpcell.00174.2022]

39 **Wang HH**, Sun YN, Qu TQ, Sang XQ, Zhou LM, Li YX, Ren FZ. Nobiletin Prevents D-Galactose-Induced C2C12 Cell Aging by Improving Mitochondrial Function. *Int J Mol Sci* 2022; **23**: 11963 [PMID: 36233264 DOI: 10.3390/ijms231911963]

40 **Huang Z**, Fang Q, Ma W, Zhang Q, Qiu J, Gu X, Yang H, Sun H. Skeletal Muscle Atrophy Was Alleviated by Salidroside Through Suppressing Oxidative Stress and Inflammation During Denervation. *Front Pharmacol* 2019; **10**: 997 [PMID: 31616291 DOI: 10.3389/fphar.2019.00997]

41 **Wu C**, Tang L, Ni X, Xu T, Fang Q, Xu L, Ma W, Yang X, Sun H. Salidroside Attenuates Denervation-Induced Skeletal Muscle Atrophy Through Negative Regulation of Pro-inflammatory Cytokine. *Front Physiol* 2019; **10**: 665 [PMID: 31293430 DOI: 10.3389/fphys.2019.00665]

42 **Yang X**, Ji Y, Wang W, Zhang L, Chen Z, Yu M, Shen Y, Ding F, Gu X, Sun H. Amyotrophic Lateral Sclerosis: Molecular Mechanisms, Biomarkers, and Therapeutic Strategies. *Antioxidants (Basel)* 2021; **10**: 1012 [PMID: 34202494 DOI: 10.3390/antiox10071012]

43 **Salles J**, Chanet A, Guillet C, Vaes AM, Brouwer-Brolsma EM, Rocher C, Giraudet C, Patrac V, Meugnier E, Montaurier C, Denis P, Le Bacquer O, Blot A, Jourdan M, Luiking Y, Furber M, Van Dijk M, Tardif N, Yves Boirie Y, Walrand S. Vitamin D status modulates mitochondrial oxidative capacities in skeletal muscle: role in sarcopenia. *Commun Biol* 2022; **5**: 1288 [PMID: 36434267 DOI: 10.1038/s42003-022-04246-3]

44 **Saeki S**, Tokutake K, Takasu M, Kurimoto S, Asami Y, Onaka K, Saeki M, Hirata H. Functional Reconstruction of Denervated Muscle by Xenotransplantation of Neural Cells from Porcine to Rat. *Int J Mol Sci* 2022; **23**: 8773 [PMID: 35955906 DOI: 10.3390/ijms23158773]

45 **Azzag K**, Bosnakovski D, Tungtur S, Salama P, Kyba M, Perlingeiro RCR. Transplantation of PSC-derived myogenic progenitors counteracts disease phenotypes in FSHD mice. *NPJ Regen Med* 2022; **7**: 43 [PMID: 36056021 DOI: 10.1038/s41536-022-00249-0]

46 **Rocca CJ**, Goodman SM, Dulin JN, Haquang JH, Gertsman I, Blondelle J, Smith JLM, Heyser CJ, Cherqui S. Transplantation of wild-type mouse hematopoietic stem and progenitor cells ameliorates deficits in a mouse model of Friedreich's ataxia. *Sci Transl Med* 2017; **9**: eaaj2347 [PMID: 29070698 DOI: 10.1126/scitranslmed.aaj2347]

47 **Yoon JK**, Schindler JW, Loperfido M, Baricordi C, DeAndrade MP, Jacobs ME, Treleaven C, Plasschaert RN, Yan A, Barese CN, Dogan Y, Chen VP, Fiorini C, Hull F, Barbarossa L, Unnisa Z, Ivanov D, Kutner RH, Guda S, Oborski C, Maiwald T, Michaud V, Rothe M, Schambach A, Pfeifer R, Mason C, Biasco L, van Til NP. Preclinical lentiviral hematopoietic stem cell gene therapy corrects Pompe disease-related muscle and neurological manifestations. *Mol Ther* 2024; **32**: 3847-3864 [PMID: 39295144 DOI: 10.1016/j.ymthe.2024.09.024]

48 **Kono Y**, Kajita H, Okada T, Nakagawa R, Fujita T, Konishi S. Mesenchymal Stem Cells Promote IL-6 Secretion and Suppress the Gene Expression of Proinflammatory Cytokines in Contractile C2C12 Myotubes. *Biol Pharm Bull* 2022; **45**: 962-967 [PMID: 35786604 DOI: 10.1248/bpb.b22-00118]

49 **Reis ALG**, Maximino JR, Lage LAPC, Gomes HR, Pereira J, Brofman PRS, Senegaglia AC, Rebelatto CLK, Daga DR, Paiva WS, Chadi G. Proteomic analysis of cerebrospinal fluid of amyotrophic lateral sclerosis patients in the presence of autologous bone marrow derived mesenchymal stem cells. *Stem Cell Res Ther* 2024; **15**: 301 [PMID: 39278909 DOI: 10.1186/s13287-024-03820-2]

50 **Berry JD**, Cudkowicz ME, Windebank AJ, Staff NP, Owegi M, Nicholson K, McKenna-Yasek D, Levy YS, Abramov N, Kaspi H, Mehra M, Aricha R, Gothelf Y, Brown RH. NurOwn, phase 2, randomized, clinical trial in patients with ALS: Safety, clinical, and biomarker results. *Neurology* 2019; **93**: e2294-e2305 [PMID: 31740545 DOI: 10.1212/WNL.0000000000008620]

51 **Forotti G**, Nizzardo M, Bucchia M, Ramirez A, Trombetta E, Gatti S, Bresolin N, Comi GP, Corti S. CSF transplantation of a specific iPSC-derived neural stem cell subpopulation ameliorates the disease phenotype in a mouse model of spinal muscular atrophy with respiratory distress type 1. *Exp Neurol* 2019; **321**: 113041 [PMID: 31445043 DOI: 10.1016/j.expneurol.2019.113041]

52 **Mohseni R**, Hamidieh AA, Shoae-Hassani A, Ghahvechi-Akbari M, Majma A, Mohammadi M, Nikougoftar M, Shervin-Badv R, Ai J, Montazerlotfelahi H, Ashrafi MR. An open-label phase 1 clinical trial of the allogeneic side population adipose-derived mesenchymal stem cells in SMA type 1 patients. *Neurol Sci* 2022; **43**: 399-410 [PMID: 34032944 DOI: 10.1007/s10072-021-05291-2]

53 **Yeo CJJ**, Tizzano EF, Darras BT. Challenges and opportunities in spinal muscular atrophy therapeutics. *Lancet Neurol* 2024; **23**: 205-218 [PMID: 38267192 DOI: 10.1016/S1474-4422(23)00419-2]

54 **Meesuk L**, Suwanprateeb J, Thammarakcharoen F, Tantrawatpan C, Kheolamai P, Palang I, Tantikanlayaporn D, Manochantr S. Osteogenic differentiation and proliferation potentials of human bone marrow and umbilical cord-derived mesenchymal stem cells on the 3D-printed hydroxyapatite scaffolds. *Sci Rep* 2022; **12**: 19509 [PMID: 36376498 DOI: 10.1038/s41598-022-24160-2]

55 **Oguma Y**, Kuroda Y, Wakao S, Kushida Y, Dezawa M. Single-cell RNA sequencing reveals different signatures of mesenchymal stromal cell pluripotent-like and multipotent populations. *iScience* 2022; **25**: 105395 [PMID: 36339265 DOI: 10.1016/j.isci.2022.105395]

56 **Tsai YC**, Cheng TS, Liao HJ, Chuang MH, Chen HT, Chen CH, Zhang KL, Chang CH, Lin PC, Huang CF. Mesenchymal Stem Cell Secreted-Extracellular Vesicles are Involved in Chondrocyte Production and Reduce Adipogenesis during Stem Cell Differentiation. *Tissue Eng Regen Med* 2022; **19**: 1295-1310 [PMID: 36346531 DOI: 10.1007/s13770-022-00490-0]

57 **Li J**, Wu Z, Zhao L, Liu Y, Su Y, Gong X, Liu F, Zhang L. The heterogeneity of mesenchymal stem cells: an important issue to be addressed in cell therapy. *Stem Cell Res Ther* 2023; **14**: 381 [PMID: 38124129 DOI: 10.1186/s13287-023-03587-y]

58 **Abrigo J**, Rivera JC, Aravena J, Cabrera D, Simon F, Ezquer F, Ezquer M, Cabello-Verrugio C. High Fat Diet-Induced Skeletal Muscle Wasting Is Decreased by Mesenchymal Stem Cells Administration: Implications on Oxidative Stress, Ubiquitin Proteasome Pathway Activation, and Myonuclear Apoptosis. *Oxid Med Cell Longev* 2016; **2016**: 9047821 [PMID: 27579157 DOI: 10.1155/2016/9047821]

59 **Li TS**, Shi H, Wang L, Yan C. Effect of Bone Marrow Mesenchymal Stem Cells on Satellite Cell Proliferation and Apoptosis in Immobilization-Induced Muscle Atrophy in Rats. *Med Sci Monit* 2016; **22**: 4651-4660 [PMID: 27898654 DOI: 10.12659/msm.898137]

60 **Schilling BK**, Schusterman MA 2nd, Kim DY, Repko AJ, Klett KC, Christ GJ, Marra KG. Adipose-derived stem cells delay muscle atrophy after peripheral nerve injury in the rodent model. *Muscle Nerve* 2019; **59**: 603-610 [PMID: 30681163 DOI: 10.1002/mus.26432]

61 **Artioli GG**, De Oliveira Silvestre JG, Guilherme JP, Baptista IL, Ramos GV, Da Silva WJ, Miyabara EH, Moriscot AS. Embryonic stem cells improve skeletal muscle recovery after extreme atrophy in mice. *Muscle Nerve* 2015; **51**: 346-352 [PMID: 24934406 DOI: 10.1002/mus.24320]

62 **Li WY**, Zhu GY, Yue WJ, Sun GD, Zhu XF, Wang Y. KLF7 overexpression in bone marrow stromal stem cells graft transplantation promotes sciatic nerve regeneration. *J Neural Eng* 2019; **16**: 056011 [PMID: 31296795 DOI: 10.1088/1741-2552/ab3188]

63 **Mierzejewski B**, Michalska Z, Jackowski D, Streminska W, Janczyk-Ilach K, Koblowska M, Iwanicka-Nowicka R, Gromadka A, Ciemerych

MA, Brzoska E. The miR151 and miR5100 Transfected Bone Marrow Stromal Cells Increase Myoblast Fusion in IGFBP2 Dependent Manner. *Stem Cell Rev Rep* 2022; **18**: 2164-2178 [PMID: 35190967 DOI: 10.1007/s12015-022-10350-y]

64 **de Munter JPJM**, Mey J, Strekalova T, Kramer BW, Wolters EC. Why do anti-inflammatory signals of bone marrow-derived stromal cells improve neurodegenerative conditions where anti-inflammatory drugs fail? *J Neural Transm (Vienna)* 2020; **127**: 715-727 [PMID: 32253536 DOI: 10.1007/s00702-020-02173-3]

65 **Sykova E**, Cizkova D, Kubinova S. Mesenchymal Stem Cells in Treatment of Spinal Cord Injury and Amyotrophic Lateral Sclerosis. *Front Cell Dev Biol* 2021; **9**: 695900 [PMID: 34295897 DOI: 10.3389/fcell.2021.695900]

66 **Świerczek-Lasek B**, Tolak L, Bijoch L, Stefaniuk M, Szpak P, Kalaszczynska I, Streminska W, Ciemerych MA, Archacka K. Comparison of Muscle Regeneration after BMSC-Conditioned Medium, Syngeneic, or Allogeneic BMSC Injection. *Cells* 2022; **11**: 2843 [PMID: 36139418 DOI: 10.3390/cells11182843]

67 **Helal MAM**, Shaheen NEM, Abu Zahra FA. Immunomodulatory capacity of the local mesenchymal stem cells transplantation after severe skeletal muscle injury in female rats. *Immunopharmacol Immunotoxicol* 2016; **38**: 414-422 [PMID: 27560658 DOI: 10.1080/08923973.2016.1222617]

68 **Andrade BM**, Baldanza MR, Ribeiro KC, Porto A, Peçanha R, Fortes FS, Zapata-Sudo G, Campos-de-Carvalho AC, Goldenberg RC, Werneck-de-Castro JP. Bone marrow mesenchymal cells improve muscle function in a skeletal muscle re-injury model. *PLoS One* 2015; **10**: e0127561 [PMID: 26039243 DOI: 10.1371/journal.pone.0127561]

69 **Maeda Y**, Yonemochi Y, Nakajyo Y, Hidaka H, Ikeda T, Ando Y. CXCL12 and osteopontin from bone marrow-derived mesenchymal stromal cells improve muscle regeneration. *Sci Rep* 2017; **7**: 3305 [PMID: 28607396 DOI: 10.1038/s41598-017-02928-1]

70 **Klimczak A**, Kozlowska U, Kurpisz M. Muscle Stem/Progenitor Cells and Mesenchymal Stem Cells of Bone Marrow Origin for Skeletal Muscle Regeneration in Muscular Dystrophies. *Arch Immunol Ther Exp (Warsz)* 2018; **66**: 341-354 [PMID: 29536116 DOI: 10.1007/s00005-018-0509-7]

71 **Archacka K**, Grabowska I, Mierzejewski B, Graffstein J, Górzyńska A, Krawczyk M, Różycka AM, Kalaszczyńska I, Muras G, Stremińska W, Jańczyk-Ilach K, Walczak P, Janowski M, Ciemerych MA, Brzoska E. Hypoxia preconditioned bone marrow-derived mesenchymal stromal/stem cells enhance myoblast fusion and skeletal muscle regeneration. *Stem Cell Res Ther* 2021; **12**: 448 [PMID: 34372911 DOI: 10.1186/s13287-021-02530-3]

72 **Moussa MH**, Hamam GG, Abd Elaziz AE, Rahoma MA, Abd El Samad AA, El-Waseef DAA, Hegazy MA. Comparative Study on Bone Marrow-Versus Adipose-Derived Stem Cells on Regeneration and Re-Innervation of Skeletal Muscle Injury in Wistar Rats. *Tissue Eng Regen Med* 2020; **17**: 887-900 [PMID: 33030680 DOI: 10.1007/s13770-020-00288-y]

73 **Grabowska I**, Zimowska M, Maciejewska K, Jablonska Z, Bazga A, Ozieblo M, Streminska W, Bem J, Brzoska E, Ciemerych MA. Adipose Tissue-Derived Stromal Cells in Matrigel Impacts the Regeneration of Severely Damaged Skeletal Muscles. *Int J Mol Sci* 2019; **20**: 3313 [PMID: 31284492 DOI: 10.3390/ijms20133313]

74 **Archacka K**, Bem J, Brzoska E, Czerwinska AM, Grabowska I, Kasprzycka P, Hoinkis D, Siennicka K, Pojda Z, Bernas P, Binkowski R, Jastrzebska K, Kupiec A, Malesza M, Michalczewska E, Soszynska M, Ilach K, Streminska W, Ciemerych MA. Beneficial Effect of IL-4 and SDF-1 on Myogenic Potential of Mouse and Human Adipose Tissue-Derived Stromal Cells. *Cells* 2020; **9**: 1479 [PMID: 32560483 DOI: 10.3390/cells9061479]

75 **Yang W**, Zhang S, Ou T, Jiang H, Jia D, Qi Z, Zou Y, Qian J, Sun A, Ge J. Interleukin-11 regulates the fate of adipose-derived mesenchymal stem cells *via* STAT3 signalling pathways. *Cell Prolif* 2020; **53**: e12771 [PMID: 32270546 DOI: 10.1111/cpr.12771]

76 **Leong J**, Hong YT, Wu YF, Ko E, Dvoretskiy S, Teo JY, Kim BS, Kim K, Jeon H, Boppart M, Yang YY, Kong H. Surface Tethering of Inflammation-Modulatory Nanostimulators to Stem Cells for Ischemic Muscle Repair. *ACS Nano* 2020; **14**: 5298-5313 [PMID: 32243129 DOI: 10.1021/acsnano.9b04926]

77 **Ciervo Y**, Gatto N, Allen C, Grierson A, Ferraiuolo L, Mead RJ, Shaw PJ. Adipose-derived stem cells protect motor neurons and reduce glial activation in both in vitro and in vivo models of ALS. *Mol Ther Methods Clin Dev* 2021; **21**: 413-433 [PMID: 33869658 DOI: 10.1016/j.omtm.2021.03.017]

78 **Wang X**, Zhang Y, Jin T, Botchway BOA, Fan R, Wang L, Liu X. Adipose-Derived Mesenchymal Stem Cells Combined With Extracellular Vesicles May Improve Amyotrophic Lateral Sclerosis. *Front Aging Neurosci* 2022; **14**: 830346 [PMID: 35663577 DOI: 10.3389/fnagi.2022.830346]

79 **Xie Q**, Liu R, Jiang J, Peng J, Yang C, Zhang W, Wang S, Song J. What is the impact of human umbilical cord mesenchymal stem cell transplantation on clinical treatment? *Stem Cell Res Ther* 2020; **11**: 519 [PMID: 33261658 DOI: 10.1186/s13287-020-02011-z]

80 **Kim MJ**, Kim ZH, Kim SM, Choi YS. Conditioned medium derived from umbilical cord mesenchymal stem cells regenerates atrophied muscles. *Tissue Cell* 2016; **48**: 533-543 [PMID: 27457384 DOI: 10.1016/j.tice.2016.06.010]

81 **Piao L**, Huang Z, Inoue A, Kuzuya M, Cheng XW. Human umbilical cord-derived mesenchymal stromal cells ameliorate aging-associated skeletal muscle atrophy and dysfunction by modulating apoptosis and mitochondrial damage in SAMP10 mice. *Stem Cell Res Ther* 2022; **13**: 226 [PMID: 35659361 DOI: 10.1186/s13287-022-02895-z]

82 **Cohen S**, Nathan JA, Goldberg AL. Muscle wasting in disease: molecular mechanisms and promising therapies. *Nat Rev Drug Discov* 2015; **14**: 58-74 [PMID: 25549588 DOI: 10.1038/nrd4467]

83 **Colleluori G**, Aguirre L, Phadnis U, Fowler K, Armamento-Villareal R, Sun Z, Brunetti L, Hyoung Park J, Kaipparettu BA, Putluri N, Auetumrongsawat V, Yarasheski K, Qualls C, Villareal DT. Aerobic Plus Resistance Exercise in Obese Older Adults Improves Muscle Protein Synthesis and Preserves Myocellular Quality Despite Weight Loss. *Cell Metab* 2019; **30**: 261-273.e6 [PMID: 31279675 DOI: 10.1016/j.cmet.2019.06.008]

84 **Song J**, Liu J, Cui C, Hu H, Zang N, Yang M, Yang J, Zou Y, Li J, Wang L, He Q, Guo X, Zhao R, Yan F, Liu F, Hou X, Sun Z, Chen L. Mesenchymal stromal cells ameliorate diabetes-induced muscle atrophy through exosomes by enhancing AMPK/ULK1-mediated autophagy. *J Cachexia Sarcopenia Muscle* 2023; **14**: 915-929 [PMID: 36708027 DOI: 10.1002/jcsm.13177]

85 **Nishimura K**, Fukuda A, Hisatake K. Mechanisms of the Metabolic Shift during Somatic Cell Reprogramming. *Int J Mol Sci* 2019; **20**: 2254 [PMID: 31067778 DOI: 10.3390/ijms20092254]

86 **Genet M**, Torres-Padilla ME. The molecular and cellular features of 2-cell-like cells: a reference guide. *Development* 2020; **147**: dev189688 [PMID: 32847823 DOI: 10.1242/dev.189688]

87 **Liu B**, Li M, Zhang L, Chen Z, Lu P. Motor neuron replacement therapy for amyotrophic lateral sclerosis. *Neural Regen Res* 2022; **17**: 1633-1639 [PMID: 35017408 DOI: 10.4103/1673-5374.332123]

88 **Mora C**, Serzanti M, Consiglio A, Memo M, Dell'Era P. Clinical potentials of human pluripotent stem cells. *Cell Biol Toxicol* 2017; **33**: 351-

360 [PMID: 28176010 DOI: 10.1007/s10565-017-9384-y]
89 **Novelli G**, Spitalieri P, Murdocca M, Centanini E, Sangiuolo F. Organoid factory: The recent role of the human induced pluripotent stem cells (hiPSCs) in precision medicine. *Front Cell Dev Biol* 2022; **10**: 1059579 [PMID: 36699015 DOI: 10.3389/fcell.2022.1059579]
90 **Zhang L**, Ma XJ, Fei YY, Han HT, Xu J, Cheng L, Li X. Stem cell therapy in liver regeneration: Focus on mesenchymal stem cells and induced pluripotent stem cells. *Pharmacol Ther* 2022; **232**: 108004 [PMID: 34597754 DOI: 10.1016/j.pharmthera.2021.108004]
91 **Iberite F**, Gruppioni E, Ricotti L. Skeletal muscle differentiation of human iPSCs meets bioengineering strategies: perspectives and challenges. *NPJ Regen Med* 2022; **7**: 23 [PMID: 35393412 DOI: 10.1038/s41536-022-00216-9]
92 **Ohuchi K**, Funato M, Kato Z, Seki J, Kawase C, Tamai Y, Ono Y, Nagahara Y, Noda Y, Kameyama T, Ando S, Tsuruma K, Shimazawa M, Hara H, Kaneko H. Established Stem Cell Model of Spinal Muscular Atrophy Is Applicable in the Evaluation of the Efficacy of Thyrotropin-Releasing Hormone Analog. *Stem Cells Transl Med* 2016; **5**: 152-163 [PMID: 26683872 DOI: 10.5966/sctm.2015-0059]
93 **Deuse T**, Hu X, Gravina A, Wang D, Tediashvili G, De C, Thayer WO, Wahl A, Garcia JV, Reichenspurner H, Davis MM, Lanier LL, Schrepfer S. Hypoimmunogenic derivatives of induced pluripotent stem cells evade immune rejection in fully immunocompetent allogeneic recipients. *Nat Biotechnol* 2019; **37**: 252-258 [PMID: 30778232 DOI: 10.1038/s41587-019-0016-3]
94 **Pinton L**, Khedr M, Lionello VM, Sarcar S, Maffioletti SM, Dastidar S, Negroni E, Choi S, Khokhar N, Bigot A, Counsell JR, Bernardo AS, Zammit PS, Tedesco FS. 3D human induced pluripotent stem cell-derived bioengineered skeletal muscles for tissue, disease and therapy modeling. *Nat Protoc* 2023; **18**: 1337-1376 [PMID: 36792780 DOI: 10.1038/s41596-022-00790-8]
95 **Kim H**, Perlingeiro RCR. Generation of human myogenic progenitors from pluripotent stem cells for in vivo regeneration. *Cell Mol Life Sci* 2022; **79**: 406 [PMID: 35802202 DOI: 10.1007/s00018-022-04434-8]
96 **Sun C**, Kannan S, Choi IY, Lim H, Zhang H, Chen GS, Zhang N, Park SH, Serra C, Iyer SR, Lloyd TE, Kwon C, Lovering RM, Lim SB, Andersen P, Wagner KR, Lee G. Human pluripotent stem cell-derived myogenic progenitors undergo maturation to quiescent satellite cells upon engraftment. *Cell Stem Cell* 2022; **29**: 610-619.e5 [PMID: 35395188 DOI: 10.1016/j.stem.2022.03.004]
97 **Kim H**, Selvaraj S, Kiley J, Azzag K, Garay BI, Perlingeiro RCR. Genomic Safe Harbor Expression of PAX7 for the Generation of Engraftable Myogenic Progenitors. *Stem Cell Reports* 2021; **16**: 10-19 [PMID: 33275879 DOI: 10.1016/j.stemcr.2020.11.001]
98 **Rao L**, Qian Y, Khodabukus A, Ribar T, Bursac N. Engineering human pluripotent stem cells into a functional skeletal muscle tissue. *Nat Commun* 2018; **9**: 126 [PMID: 29317646 DOI: 10.1038/s41467-017-02636-4]
99 **Shahriyari M**, Islam MR, Sakib SM, Rinn M, Rika A, Krüger D, Kaurani L, Gisa V, Winterhoff M, Anandakumar H, Shomroni O, Schmidt M, Salinas G, Unger A, Linke WA, Zschüntzsch J, Schmidt J, Bassel-Duby R, Olson EN, Fischer A, Zimmermann WH, Tiburcy M. Engineered skeletal muscle recapitulates human muscle development, regeneration and dystrophy. *J Cachexia Sarcopenia Muscle* 2022; **13**: 3106-3121 [PMID: 36254806 DOI: 10.1002/jcsm.13094]
100 **Pepper JP**, Wang TV, Hennes V, Sun SY, Ichida JK. Human Induced Pluripotent Stem Cell-Derived Motor Neuron Transplant for Neuromuscular Atrophy in a Mouse Model of Sciatic Nerve Injury. *JAMA Facial Plast Surg* 2017; **19**: 197-205 [PMID: 27978547 DOI: 10.1001/jamafacial.2016.1544]
101 **Adami R**, Bottai D. NSC Physiological Features in Spinal Muscular Atrophy: SMN Deficiency Effects on Neurogenesis. *Int J Mol Sci* 2022; **23**: 15209 [PMID: 36499528 DOI: 10.3390/ijms232315209]
102 **Abati E**, Bresolin N, Comi GP, Corti S. Preconditioning and Cellular Engineering to Increase the Survival of Transplanted Neural Stem Cells for Motor Neuron Disease Therapy. *Mol Neurobiol* 2019; **56**: 3356-3367 [PMID: 30120734 DOI: 10.1007/s12035-018-1305-4]
103 **Forostyak S**, Forostyak O, Kwok JCF, Romanyuk N, Rehorova M, Kriska J, Dayanithi G, Raha-Chowdhury R, Jendelova P, Anderova M, Fawcett JW, Sykova E. Transplantation of Neural Precursors Derived from Induced Pluripotent Cells Preserve Perineuronal Nets and Stimulate Neural Plasticity in ALS Rats. *Int J Mol Sci* 2020; **21**: 9593 [PMID: 33339362 DOI: 10.3390/ijms21249593]
104 **Wang W**, Li M, Chen Z, Xu L, Chang M, Wang K, Deng C, Gu Y, Zhou S, Shen Y, Tao F, Sun H. Biogenesis and function of extracellular vesicles in pathophysiological processes of skeletal muscle atrophy. *Biochem Pharmacol* 2022; **198**: 114954 [PMID: 35167807 DOI: 10.1016/j.bcp.2022.114954]
105 **Assoni A**, Coatti G, Valadares MC, Beccari M, Gomes J, Pelatti M, Mitne-Neto M, Carvalho VM, Zatz M. Different Donors Mesenchymal Stromal Cells Secretomes Reveal Heterogeneous Profile of Relevance for Therapeutic Use. *Stem Cells Dev* 2017; **26**: 206-214 [PMID: 27762666 DOI: 10.1089/scd.2016.0218]
106 **Youssef El Baradie KB**, Hamrick MW. Therapeutic application of extracellular vesicles for musculoskeletal repair & regeneration. *Connect Tissue Res* 2021; **62**: 99-114 [PMID: 32602385 DOI: 10.1080/03008207.2020.1781102]
107 **Yang Q**, Su S, Liu S, Yang S, Xu J, Zhong Y, Yang Y, Tian L, Tan Z, Wang J, Yu Z, Shi Z, Liang F. Exosomes-loaded electroconductive nerve dressing for nerve regeneration and pain relief against diabetic peripheral nerve injury. *Bioact Mater* 2023; **26**: 194-215 [PMID: 36923267 DOI: 10.1016/j.bioactmat.2023.02.024]
108 **Yan B**, Zhang Y, Liang C, Liu B, Ding F, Wang Y, Zhu B, Zhao R, Yu XY, Li Y. Stem cell-derived exosomes prevent pyroptosis and repair ischemic muscle injury through a novel exosome/circHIPK3/ FOXO3a pathway. *Theranostics* 2020; **10**: 6728-6742 [PMID: 32550900 DOI: 10.7150/thno.42259]
109 **Ma Y**, Dong L, Zhou D, Li L, Zhang W, Zhen Y, Wang T, Su J, Chen D, Mao C, Wang X. Extracellular vesicles from human umbilical cord mesenchymal stem cells improve nerve regeneration after sciatic nerve transection in rats. *J Cell Mol Med* 2019; **23**: 2822-2835 [PMID: 30772948 DOI: 10.1111/jcmm.14190]
110 **Ma H**, Jing Y, Zeng J, Ge J, Sun S, Cui R, Qian C, Qu S, Sheng H. Human umbilical cord mesenchymal stem cell-derived exosomes ameliorate muscle atrophy *via* the miR-132-3p/FoxO3 axis. *J Orthop Translat* 2024; **49**: 23-36 [PMID: 39420945 DOI: 10.1016/j.jot.2024.08.005]
111 **Chen J**, Ren S, Duscher D, Kang Y, Liu Y, Wang C, Yuan M, Guo G, Xiong H, Zhan P, Wang Y, Machens HG, Chen Z. Exosomes from human adipose-derived stem cells promote sciatic nerve regeneration *via* optimizing Schwann cell function. *J Cell Physiol* 2019; **234**: 23097-23110 [PMID: 31124125 DOI: 10.1002/jcp.28873]
112 **Mellows B**, Mitchell R, Antonioli M, Kretz O, Chambers D, Zeuner MT, Denecke B, Musante L, Ramachandra DL, Debacq-Chainiaux F, Holthofer H, Joch B, Ray S, Widera D, David AL, Huber TB, Dengjel J, De Coppi P, Patel K. Protein and Molecular Characterization of a Clinically Compliant Amniotic Fluid Stem Cell-Derived Extracellular Vesicle Fraction Capable of Accelerating Muscle Regeneration Through Enhancement of Angiogenesis. *Stem Cells Dev* 2017; **26**: 1316-1333 [PMID: 28679310 DOI: 10.1089/scd.2017.0089]
113 **Zhu A**, Liu N, Shang Y, Zhen Y, An Y. Signaling pathways of adipose stem cell-derived exosomes promoting muscle regeneration. *Chin Med J (Engl)* 2022; **135**: 2525-2534 [PMID: 36583914 DOI: 10.1097/CM9.0000000000002404]
114 **Lo Sicco C**, Reverberi D, Balbi C, Ulivi V, Principi E, Pascucci L, Becherini P, Bosco MC, Varesio L, Franzin C, Pozzobon M, Cancedda R,

Tasso R. Mesenchymal Stem Cell-Derived Extracellular Vesicles as Mediators of Anti-Inflammatory Effects: Endorsement of Macrophage Polarization. *Stem Cells Transl Med* 2017; **6**: 1018-1028 [PMID: 28186708 DOI: 10.1002/sctm.16-0363]

115 **Figeac N**, Zammit PS. Coordinated action of Axin1 and Axin2 suppresses β-catenin to regulate muscle stem cell function. *Cell Signal* 2015; **27**: 1652-1665 [PMID: 25866367 DOI: 10.1016/j.cellsig.2015.03.025]

116 **Gan L**, Zheng L, Yao L, Lei L, Huang Y, Zeng Z, Fang N. Exosomes from adipose-derived mesenchymal stem cells improve liver fibrosis by regulating the miR-20a-5p/TGFBR2 axis to affect the p38 MAPK/NF-κB pathway. *Cytokine* 2023; **172**: 156386 [PMID: 37852157 DOI: 10.1016/j.cyto.2023.156386]

117 **Fan W**, Gao XK, Rao XS, Shi YP, Liu XC, Wang FY, Liu YF, Cong XX, He MY, Xu SB, Shen WL, Shen Y, Yan SG, Luo Y, Low BC, Ouyang H, Bao Z, Zheng LL, Zhou YT. Hsp70 Interacts with Mitogen-Activated Protein Kinase (MAPK)-Activated Protein Kinase 2 To Regulate p38MAPK Stability and Myoblast Differentiation during Skeletal Muscle Regeneration. *Mol Cell Biol* 2018; **38**: e00211-18 [PMID: 30275345 DOI: 10.1128/MCB.00211-18]

118 **Nowosad A**, Jeannot P, Callot C, Creff J, Perchey RT, Joffre C, Codogno P, Manenti S, Besson A. p27 controls Ragulator and mTOR activity in amino acid-deprived cells to regulate the autophagy-lysosomal pathway and coordinate cell cycle and cell growth. *Nat Cell Biol* 2020; **22**: 1076-1090 [PMID: 32807902 DOI: 10.1038/s41556-020-0554-4]

119 **Wang C**, Song W, Chen B, Liu X, He Y. Exosomes Isolated From Adipose-Derived Stem Cells: A New Cell-Free Approach to Prevent the Muscle Degeneration Associated With Torn Rotator Cuffs. *Am J Sports Med* 2019; **47**: 3247-3255 [PMID: 31560856 DOI: 10.1177/0363546519876323]

120 **Bonafede R**, Turano E, Scambi I, Busato A, Bontempi P, Virla F, Schiaffino L, Marzola P, Bonetti B, Mariotti R. ASC-Exosomes Ameliorate the Disease Progression in SOD1(G93A) Murine Model Underlining Their Potential Therapeutic Use in Human ALS. *Int J Mol Sci* 2020; **21**: 3651 [PMID: 32455791 DOI: 10.3390/ijms21103651]

121 **Bonafede R**, Brandi J, Manfredi M, Scambi I, Schiaffino L, Merigo F, Turano E, Bonetti B, Marengo E, Cecconi D, Mariotti R. The Anti-Apoptotic Effect of ASC-Exosomes in an In Vitro ALS Model and Their Proteomic Analysis. *Cells* 2019; **8**: 1087 [PMID: 31540100 DOI: 10.3390/cells8091087]

122 **Luo Z**, Lin J, Sun Y, Wang C, Chen J. Bone Marrow Stromal Cell-Derived Exosomes Promote Muscle Healing Following Contusion Through Macrophage Polarization. *Stem Cells Dev* 2021; **30**: 135-148 [PMID: 33323007 DOI: 10.1089/scd.2020.0167]

123 **Li Z**, Liu C, Li S, Li T, Li Y, Wang N, Bao X, Xue P, Liu S. BMSC-Derived Exosomes Inhibit Dexamethasone-Induced Muscle Atrophy *via* the miR-486-5p/FoxO1 Axis. *Front Endocrinol (Lausanne)* 2021; **12**: 681267 [PMID: 34659106 DOI: 10.3389/fendo.2021.681267]

124 **Pan J**, Zhao M, Yi X, Tao J, Li S, Jiang Z, Cheng B, Yuan H, Zhang F. Acellular nerve grafts supplemented with induced pluripotent stem cell-derived exosomes promote peripheral nerve reconstruction and motor function recovery. *Bioact Mater* 2022; **15**: 272-287 [PMID: 35356813 DOI: 10.1016/j.bioactmat.2021.12.004]

125 **Yu M**, Gu G, Cong M, Du M, Wang W, Shen M, Zhang Q, Shi H, Gu X, Ding F. Repair of peripheral nerve defects by nerve grafts incorporated with extracellular vesicles from skin-derived precursor Schwann cells. *Acta Biomater* 2021; **134**: 190-203 [PMID: 34289422 DOI: 10.1016/j.actbio.2021.07.026]

126 **Wang W**, Shen D, Zhang L, Ji Y, Xu L, Chen Z, Shen Y, Gong L, Zhang Q, Shen M, Gu X, Sun H. SKP-SC-EVs Mitigate Denervated Muscle Atrophy by Inhibiting Oxidative Stress and Inflammation and Improving Microcirculation. *Antioxidants (Basel)* 2021; **11**: 66 [PMID: 35052570 DOI: 10.3390/antiox11010066]

127 **Iyer SR**, Scheiber AL, Yarowsky P, Henn RF 3rd, Otsuru S, Lovering RM. Exosomes Isolated From Platelet-Rich Plasma and Mesenchymal Stem Cells Promote Recovery of Function After Muscle Injury. *Am J Sports Med* 2020; **48**: 2277-2286 [PMID: 32543878 DOI: 10.1177/0363546520926462]

128 **Pan Y**, Li L, Cao N, Liao J, Chen H, Zhang M. Advanced nano delivery system for stem cell therapy for Alzheimer's disease. *Biomaterials* 2025; **314**: 122852 [PMID: 39357149 DOI: 10.1016/j.biomaterials.2024.122852]

129 **Bronckaers A**, Hilkens P, Martens W, Gervois P, Ratajczak J, Struys T, Lambrichts I. Mesenchymal stem/stromal cells as a pharmacological and therapeutic approach to accelerate angiogenesis. *Pharmacol Ther* 2014; **143**: 181-196 [PMID: 24594234 DOI: 10.1016/j.pharmthera.2014.02.013]

130 **Ullah M**, Liu DD, Thakor AS. Mesenchymal Stromal Cell Homing: Mechanisms and Strategies for Improvement. *iScience* 2019; **15**: 421-438 [PMID: 31121468 DOI: 10.1016/j.isci.2019.05.004]

131 **Goodman SB**, Lin T. Modifying MSC Phenotype to Facilitate Bone Healing: Biological Approaches. *Front Bioeng Biotechnol* 2020; **8**: 641 [PMID: 32671040 DOI: 10.3389/fbioe.2020.00641]

132 **Dabrowska S**, Andrzejewska A, Lukomska B, Janowski M. Neuroinflammation as a target for treatment of stroke using mesenchymal stem cells and extracellular vesicles. *J Neuroinflammation* 2019; **16**: 178 [PMID: 31514749 DOI: 10.1186/s12974-019-1571-8]

133 **Zhang F**, Leong W, Su K, Fang Y, Wang DA. A transduced living hyaline cartilage graft releasing transgenic stromal cell-derived factor-1 inducing endogenous stem cell homing in vivo. *Tissue Eng Part A* 2013; **19**: 1091-1099 [PMID: 23167782 DOI: 10.1089/ten.TEA.2012.0441]

134 **Chen L**, Li Y, Chen W, Han N, Li K, Guo R, Liu Z, Xiao Y. Enhanced recruitment and hematopoietic reconstitution of bone marrow-derived mesenchymal stem cells in bone marrow failure by the SDF-1/CXCR4. *J Tissue Eng Regen Med* 2020; **14**: 1250-1260 [PMID: 32633015 DOI: 10.1002/term.3096]

135 **Al-Kharboosh R**, ReFaey K, Lara-Velazquez M, Grewal SS, Imitola J, Quiñones-Hinojosa A. Inflammatory Mediators in Glioma Microenvironment Play a Dual Role in Gliomagenesis and Mesenchymal Stem Cell Homing: Implication for Cellular Therapy. *Mayo Clin Proc Innov Qual Outcomes* 2020; **4**: 443-459 [PMID: 32793872 DOI: 10.1016/j.mayocpiqo.2020.04.006]

136 **Ogay V**, Sekenova A, Li Y, Issabekova A, Saparov A. The Therapeutic Potential of Mesenchymal Stem Cells in the Treatment of Atherosclerosis. *Curr Stem Cell Res Ther* 2021; **16**: 897-913 [PMID: 33511957 DOI: 10.2174/1574888X16999210128193549]

137 **Sarsenova M**, Issabekova A, Abisheva S, Rutskaya-Moroshan K, Ogay V, Saparov A. Mesenchymal Stem Cell-Based Therapy for Rheumatoid Arthritis. *Int J Mol Sci* 2021; **22**: 11592 [PMID: 34769021 DOI: 10.3390/ijms222111592]

138 **Szydlak R**. Biological, chemical and mechanical factors regulating migration and homing of mesenchymal stem cells. *World J Stem Cells* 2021; **13**: 619-631 [PMID: 34249231 DOI: 10.4252/wjsc.v13.i6.619]

139 **Jovic D**, Yu Y, Wang D, Wang K, Li H, Xu F, Liu C, Liu J, Luo Y. A Brief Overview of Global Trends in MSC-Based Cell Therapy. *Stem Cell Rev Rep* 2022; **18**: 1525-1545 [PMID: 35344199 DOI: 10.1007/s12015-022-10369-1]

140 **Shi Y**, Wang Y, Li Q, Liu K, Hou J, Shao C, Wang Y. Immunoregulatory mechanisms of mesenchymal stem and stromal cells in inflammatory diseases. *Nat Rev Nephrol* 2018; **14**: 493-507 [PMID: 29895977 DOI: 10.1038/s41581-018-0023-5]

141 **Pezzi A**, Amorin B, Laureano Á, Valim V, Dahmer A, Zambonato B, Sehn F, Wilke I, Bruschi L, Silva MALD, Filippi-Chiela E, Silla L.

Effects Of Hypoxia in Long-Term In Vitro Expansion of Human Bone Marrow Derived Mesenchymal Stem Cells. *J Cell Biochem* 2017; **118**: 3072-3079 [PMID: 28240374 DOI: 10.1002/jcb.25953]

142 **Siegel G**, Kluba T, Hermanutz-Klein U, Bieback K, Northoff H, Schäfer R. Phenotype, donor age and gender affect function of human bone marrow-derived mesenchymal stromal cells. *BMC Med* 2013; **11**: 146 [PMID: 23758701 DOI: 10.1186/1741-7015-11-146]

143 **Stubbendorff M**, Deuse T, Hua X, Phan TT, Bieback K, Atkinson K, Eiermann TH, Velden J, Schröder C, Reichenspurner H, Robbins RC, Volk HD, Schrepfer S. Immunological properties of extraembryonic human mesenchymal stromal cells derived from gestational tissue. *Stem Cells Dev* 2013; **22**: 2619-2629 [PMID: 23711207 DOI: 10.1089/scd.2013.0043]

144 **Zhuang X**, Hu X, Zhang S, Li X, Yuan X, Wu Y. Mesenchymal Stem Cell-Based Therapy as a New Approach for the Treatment of Systemic Sclerosis. *Clin Rev Allergy Immunol* 2023; **64**: 284-320 [PMID: 35031958 DOI: 10.1007/s12016-021-08892-z]

145 **Drela K**, Stanaszek L, Nowakowski A, Kuczynska Z, Lukomska B. Experimental Strategies of Mesenchymal Stem Cell Propagation: Adverse Events and Potential Risk of Functional Changes. *Stem Cells Int* 2019; **2019**: 7012692 [PMID: 30956673 DOI: 10.1155/2019/7012692]

146 **Yang YK**, Ogando CR, Wang See C, Chang TY, Barabino GA. Changes in phenotype and differentiation potential of human mesenchymal stem cells aging in vitro. *Stem Cell Res Ther* 2018; **9**: 131 [PMID: 29751774 DOI: 10.1186/s13287-018-0876-3]

147 **Al Tanoury Z**, Rao J, Tassy O, Gobert B, Gapon S, Garnier JM, Wagner E, Hick A, Hall A, Gussoni E, Pourquié O. Differentiation of the human PAX7-positive myogenic precursors/satellite cell lineage in vitro. *Development* 2020; **147**: dev187344 [PMID: 32541004 DOI: 10.1242/dev.187344]

148 **Shamsian A**, Sahebnasagh R, Norouzy A, Hussein SH, Ghahremani MH, Azizi Z. Cancer cells as a new source of induced pluripotent stem cells. *Stem Cell Res Ther* 2022; **13**: 459 [PMID: 36064437 DOI: 10.1186/s13287-022-03145-y]

149 **Xiong J**, Hu H, Guo R, Wang H, Jiang H. Mesenchymal Stem Cell Exosomes as a New Strategy for the Treatment of Diabetes Complications. *Front Endocrinol (Lausanne)* 2021; **12**: 646233 [PMID: 33995278 DOI: 10.3389/fendo.2021.646233]

150 **Rezaie J**, Nejati V, Mahmoodi M, Ahmadi M. Mesenchymal stem cells derived extracellular vesicles: A promising nanomedicine for drug delivery system. *Biochem Pharmacol* 2022; **203**: 115167 [PMID: 35820499 DOI: 10.1016/j.bcp.2022.115167]

151 **Li Y**, Kamei Y, Kambe M, Ebisawa K, Oishi M, Takanari K. Peripheral Nerve Regeneration Using Different Germ Layer-Derived Adult Stem Cells in the Past Decade. *Behav Neurol* 2021; **2021**: 5586523 [PMID: 34539934 DOI: 10.1155/2021/5586523]

152 **Shan Y**, Zhang M, Tao E, Wang J, Wei N, Lu Y, Liu Q, Hao K, Zhou F, Wang G. Pharmacokinetic characteristics of mesenchymal stem cells in translational challenges. *Signal Transduct Target Ther* 2024; **9**: 242 [PMID: 39271680 DOI: 10.1038/s41392-024-01936-8]

153 **Winkler T**, Perka C, von Roth P, Agres AN, Plage H, Preininger B, Pumberger M, Geissler S, Hagai EL, Ofir R, Pinzur L, Eyal E, Stoltenburg-Didinger G, Meisel C, Consentius C, Streitz M, Reinke P, Duda GN, Volk HD. Immunomodulatory placental-expanded, mesenchymal stromal cells improve muscle function following hip arthroplasty. *J Cachexia Sarcopenia Muscle* 2018; **9**: 880-897 [PMID: 30230266 DOI: 10.1002/jcsm.12316]

154 **Jiang L**, Mee T, Zhou X, Jia X. Augmenting Peripheral Nerve Regeneration with Adipose-Derived Stem Cells. *Stem Cell Rev Rep* 2022; **18**: 544-558 [PMID: 34417730 DOI: 10.1007/s12015-021-10236-5]

155 **Kolagar TA**, Farzaneh M, Nikkar N, Khoshnam SE. Human Pluripotent Stem Cells in Neurodegenerative Diseases: Potentials, Advances and Limitations. *Curr Stem Cell Res Ther* 2020; **15**: 102-110 [PMID: 31441732 DOI: 10.2174/1574888X14666190823142911]

156 **Tan F**, Li X, Wang Z, Li J, Shahzad K, Zheng J. Clinical applications of stem cell-derived exosomes. *Signal Transduct Target Ther* 2024; **9**: 17 [PMID: 38212307 DOI: 10.1038/s41392-023-01704-0]

157 **Luo W**, Zhang H, Wan R, Cai Y, Liu Y, Wu Y, Yang Y, Chen J, Zhang D, Luo Z, Shang X. Biomaterials-Based Technologies in Skeletal Muscle Tissue Engineering. *Adv Healthc Mater* 2024; **13**: e2304196 [PMID: 38712598 DOI: 10.1002/adhm.202304196]

World Journal of Stem Cells

Submit a Manuscript: https://www.f6publishing.com

World J Stem Cells 2025 February 26; 17(2): 99331

DOI: 10.4252/wjsc.v17.i2.99331

ISSN 1948-0210 (online)

MINIREVIEWS

Induced pluripotent stem cell-derived mesenchymal stem cells for modeling and treating metabolic associated fatty liver disease and metabolic associated steatohepatitis: Challenges and opportunities

Bárbara Silva, José Bragança

Specialty type: Cell and tissue engineering

Provenance and peer review: Invited article; Externally peer reviewed.

Peer-review model: Single blind

Peer-review report's classification
Scientific Quality: Grade A, Grade B
Novelty: Grade A
Creativity or Innovation: Grade A
Scientific Significance: Grade A

P-Reviewer: Li SC; Yu CL

Received: July 19, 2024
Revised: November 21, 2024
Accepted: January 14, 2025
Published online: February 26, 2025
Processing time: 219 Days and 11.9 Hours

Bárbara Silva, Algarve Biomedical Center-Research Institute, University of Algarve, Faro 8005-139, Portugal

Bárbara Silva, José Bragança, Algarve Biomedical Center, University of Algarve, Faro 8005-139, Portugal

Bárbara Silva, José Bragança, Faculty of Medicine and Biomedical Sciences, University of Algarve, Faro 8005-139, Portugal

Bárbara Silva, PhD Program in Biomedical Sciences, Faculty of Medicine and Biomedical Sciences, University of Algarve, Faro 8005-139, Portugal

José Bragança, Faculty of Medicine and Biomedical Sciences, Algarve Biomedical Center-Research Institute, University of Algarve, Faro 8005-139, Portugal

José Bragança, Champalimaud Research Program, Champalimaud Centre for the Unknown, Lisbon 1000-001, Portugal

Corresponding author: José Bragança, Associate Professor, PhD, Faculty of Medicine and Biomedical Sciences, Algarve Biomedical Center-Research Institute, University of Algarve, Campus of Gambelas, Building 8, Room 2.22, Faro 8005-139, Portugal. jebraganca@ualg.pt

Abstract

The potential of induced pluripotent stem cells (iPSCs) for modeling and treating metabolic associated fatty liver disease (MAFLD) and metabolic associated steatohepatitis (MASH) is emerging. MAFLD is a growing global health concern, currently with limited treatment options. While primary mesenchymal stem cells hold promise, iPSCs offer a versatile alternative due to their ability to differentiate into various cell types, including iPSC-derived mesenchymal stem cells. However, challenges remain, including optimizing differentiation protocols, ensuring cell safety, and addressing potential tumorigenicity risks. In addition, iPSCs offer the possibility to generate complex cellular models, including three-dimensional organoid models, which are closer representations of the human disease than animal models. Those models would also be valuable for drug discovery and personalized medicine approaches. Overall, iPSCs and their derivatives offer new perspectives for advancing MAFLD/MASH research and developing novel therapeutic strategies. Further research is needed to overcome current limitations

and translate this potential into effective clinical applications.

Key Words: Metabolic associated fatty liver disease; Metabolic associated steatohepatitis; Nonalcoholic fatty liver disease; Nonalcoholic steatohepatitis; Mesenchymal stem cells; Induced pluripotent stem cells; *In vitro* liver models

Core Tip: Induced pluripotent stem cells (iPSCs) show promise for modeling and treating nonalcoholic fatty liver disease and nonalcoholic steatohepatitis. iPSCs can generate various cell types, including cells for therapy or disease modeling. Challenges remain, but iPSCs offer potential for drug discovery and personalized medicine approaches for nonalcoholic fatty liver disease/nonalcoholic steatohepatitis.

Citation: Silva B, Bragança J. Induced pluripotent stem cell-derived mesenchymal stem cells for modeling and treating metabolic associated fatty liver disease and metabolic associated steatohepatitis: Challenges and opportunities. *World J Stem Cells* 2025; 17(2): 99331

URL: https://www.wjgnet.com/1948-0210/full/v17/i2/99331.htm

DOI: https://dx.doi.org/10.4252/wjsc.v17.i2.99331

INTRODUCTION

Metabolic associated fatty liver disease (MAFLD) encompasses a spectrum of liver conditions linked to metabolic dysfunction, with its more severe manifestation being metabolic associated steatohepatitis (MASH), characterized by inflammation and liver damage. Previously, these conditions were known as nonalcoholic fatty liver disease (NAFLD) and nonalcoholic steatohepatitis (NASH), respectively. Although MAFLD and MASH are the newly proposed nomenclature, this review will use the traditional terms NAFLD and NASH to maintain consistency with most of the existing literature and facilitate comparisons with previous studies.

NAFLD is the most common chronic liver disease worldwide, affecting approximately 30% of the global population and 70% of patients with type 2 diabetes mellitus. It is expected to increase to more than 400 million people in the United States, Europe, and Southeast Asia by 2030[1-3]. NAFLD typically stems from overnutrition, resulting in lipid accumulation in the liver. This leads to dysregulation of lipid metabolism, causing oxidative stress, endoplasmic reticulum (ER) stress, lipid peroxidation, inflammation, and tissue fibrosis[4].

NAFLD is diagnosed when more than 5% of the hepatocytes show fat accumulation. This can be detected through liver biopsy or imaging techniques in patients who consume little or no alcohol and do not have factors that contribute to fatty liver disease[5]. Commonly, these patients also have coexisting metabolic disorders, such as obesity, diabetes mellitus, and dyslipidemia. Additional factors, such as genetic and epigenetic factors or changes in gut microbiome, can contribute to NAFLD[3,6].

NAFLD is divided into two main categories. The first is nonalcoholic fatty liver, with hepatocytes exhibiting fat accumulation without liver injury, affecting approximately 75% of patients. The second category is NASH, which is considered the advanced form of NAFLD. In NASH, hepatocytes show steatosis and inflammation, and fibrosis is frequently present in the liver[3,6]. NAFLD can progress to NASH, which can consequently lead to cirrhosis and hepatocellular carcinoma. The precipitating factors for this progression include a high-fat diet, genetic factors, oxidative stress, and inflammation caused by high levels of cytokines or changes in the gut microbiome[7,8].

Several therapies are being studied for the treatment of NAFLD, including the regulation of metabolism through peroxisome proliferator-activated receptor (PPAR) agonists, thyroid hormone receptor beta-agonists, and fibroblast growth factor analogues. Other research areas focus on the gut microbiome, targeting oxidative stress, microRNA, and apoptosis inhibitors[7]. However, there is currently no approved therapy for NAFLD, despite multiple drugs being tested in clinical trials[9], and the most common therapeutic approach involves lifestyle changes, such as adjustments of diet and physical activity.

The use of stem cells, particularly of primary tissue-derived mesenchymal stem cells (MSCs), and their secreted factors has been widely studied as a promising alternative therapeutic for treating NAFLD/NASH patients. Jiang *et al*[10] provided a comprehensive overview of the current situation of the utility of tissue-derived MSCs to address NAFLD/NASH in a recent volume of the *World Journal of Stem Cells*. However, significant progress has been made with induced pluripotent stem cells (iPSCs), particularly in understanding the reprogramming process and differentiation methodologies. These advancements position iPSC as a potential source of MSCs and MSC-derived factors for disease treatment and as a means to model the disease with human cells. In this review, we focused on the potential of iPSC and iPSC-derived MSCs (iMSCs) for modeling and as treatment alternatives of NAFLD/NASH.

MSCS AND NAFLD/NASH

MSCs are multipotent cells readily available in bone marrow (BM-MSC), adipose tissue (AD-MSC), and perinatal tissues, such as umbilical cord tissue, among other tissues/organs. These cells have the ability to adhere to plastic *in vitro* and must be able to differentiate into adipocytes, chondrocytes, and osteoblasts. MSCs are characterized by the expression surface markers such as CD73 and CD90 and the absence of CD11b, CD14, CD19, CD34, CD45, CD79, and HLA-HR expression[11]. However, depending on the donors, MSCs may exhibit some heterogeneity, and some AD-MSCs have been shown to display CD34[12].

MSCs are, nonetheless, a versatile type of stem cells with multiple promising autologous or allogeneic clinical and tissue engineering applications that are explored. Those cells present several advantages including their potential to differentiate into various cell types under appropriate conditions, such as adipocytes, chondrocytes, osteoblasts, and others. In addition, MSCs have a high proliferative ability and low immunogenicity and display immunomodulatory properties that are valuable for the treatment of inflammatory and autoimmune diseases. Therefore, MSCs are a promising therapeutic alternative for the treatment of NAFLD/NASH[13]. Indeed, MSCs may exert several beneficial effects at different stages of NAFLD/NASH by: (1) Secretion of trophic factors and extracellular vesicles (EVs), which induce proproliferative and antiapoptotic effects; (2) Secretion of proteins responsible for triglyceride synthesis and reduction of lipid concentrations, which limit metabolism dysregulation and consequent inflammation; (3) Reduction of fibrosis through paracrine effects and expression of metalloproteinases, which degrade fibrotic matrix; and (4) Regulation of the immune response by inducing a shift in macrophage polarity and reducing T cell activation[13-18].

Despite the properties of MSCs, no registered clinical trials (research performed on November 20, 2024) specifically mentioned "mesenchymal stem cells," "NASH," or "NAFLD" in the Clinicaltrials.gov data base. However, there is a multi-institutional clinical trial registered in the Japanese UMIN Clinical Trial Registry (UMIN000022601) that investigated the potential to treat liver cirrhosis in patients with NASH or fatty liver disease with autologous AD-MSCs. In this pioneering trial, 7 patients injected with AD-MSC *via* intrahepatic arterial infusion showed an improvement in serum albumin concentration and thrombin activity, with no adverse effect detected, demonstrating the efficacy and safety of this approach. These promising results emphasize the need for further studies with extended observational periods to fully elucidate the ability of AD-MSCs to treat NASH or fatty liver disease and determine long-term efficiency and safety of this strategy to treat these conditions[19].

IPSCS AND IMSCS

The generation of human iPSCs has unveiled new possibilities for disease modeling, drug discovery, and regenerative medicine[20]. Indeed, iPSCs are a category of pluripotent stem cells generally derived from somatic cells *via* the exogenous coexpression of the transcription factors octamer-binding transcription factor 4 (OCT4), sex-determining region Y-box 2, Kruppel-like factor 4, and c-MYC (also known as Yamanaka factors), which display properties similar to those of embryonic stem cells with less ethical concerns[21]. Human iPSCs can also be generated from patient-specific cells, enabling the establishment of cellular model systems to study diseases and test drugs or therapies personalized to the patient. Human iPSCs have some drawbacks, such as interclonal and intraclonal heterogeneity in gene expression acquired during the reprogramming process, (epi)genetic variability and genomic instability, and the potential to develop teratomas, among others[20]. Of interest, iPSCs can be used to alter the genome through CRISPR-based methodologies to evaluate the impact of genes or genetic variants in the disease of interest.

iMSCs are a promising alternative to primary MSCs, displaying high proliferation rate and low susceptibility for senescence and showing robust characteristics of standard MSCs[22]. Like primary MSCs, iMSCs express standard MSC superficial markers, have the ability of self-renewal and differentiation, and may even have a propensity for a better proliferation capacity than primary MSCs, as demonstrated by Wei *et al*[22]. These features make iMSCs excellent cellular models for studying new drugs that can even be adapted for personalized treatments if iMSCs are derived from the patient's iPSCs (Figure 1). In addition, iMSCs may be used for cell-based therapies and are suited to generate a large quantity of cells often necessary for therapeutic approaches[23].

However, iPSC-derived cells have some drawbacks. Indeed, iPSCs themselves acquire the potential for teratoma formation during the reprogramming process, which raises significant safety concerns in the use of iPSC-derived cells that may not be properly depleted of undifferentiated iPSC[24]. Teratomas are benign tumors composed of multiple germ layer cell types. Thus, robust safety profiles of produced iMSCs must be carefully established to ensure their safe clinical application. Thus, iMSC usage faces limitations, necessitating the optimization of differentiation protocols and the assessment of cell quality and safety before any clinical applications.

To ensure that iPSCs differentiate properly with no undifferentiated iPSCs remaining among them, cell sorting methodologies (flow cytometry and fluorescence-activated cell sorting, magnetic bead separation based on antibodies targeting pluripotent specific markers) may be used either for removal of undifferentiated iPSCs or to isolate properly differentiated iMSCs harboring specific MSCs markers. Complementary methods, such as immunohistochemistry and quantitative PCR, may also be used to confirm the elimination of cells that do not present proper markers of iMSCs to improve the safety and purity of iPSC-derived therapies[23,25-27].

Although, genomic alterations are not desirable in cells destined for clinical applications, some strategies are developed to introduce "suicide genes" into iPSCs allowing for their selective elimination of undifferentiated cells by administering a specific drug or agent[28]. The establishment of standard, efficient, and reliable differentiation protocols is essential for consistent production of functional iMSCs and is paramount for their clinical application. Indeed, any variability in iMSC

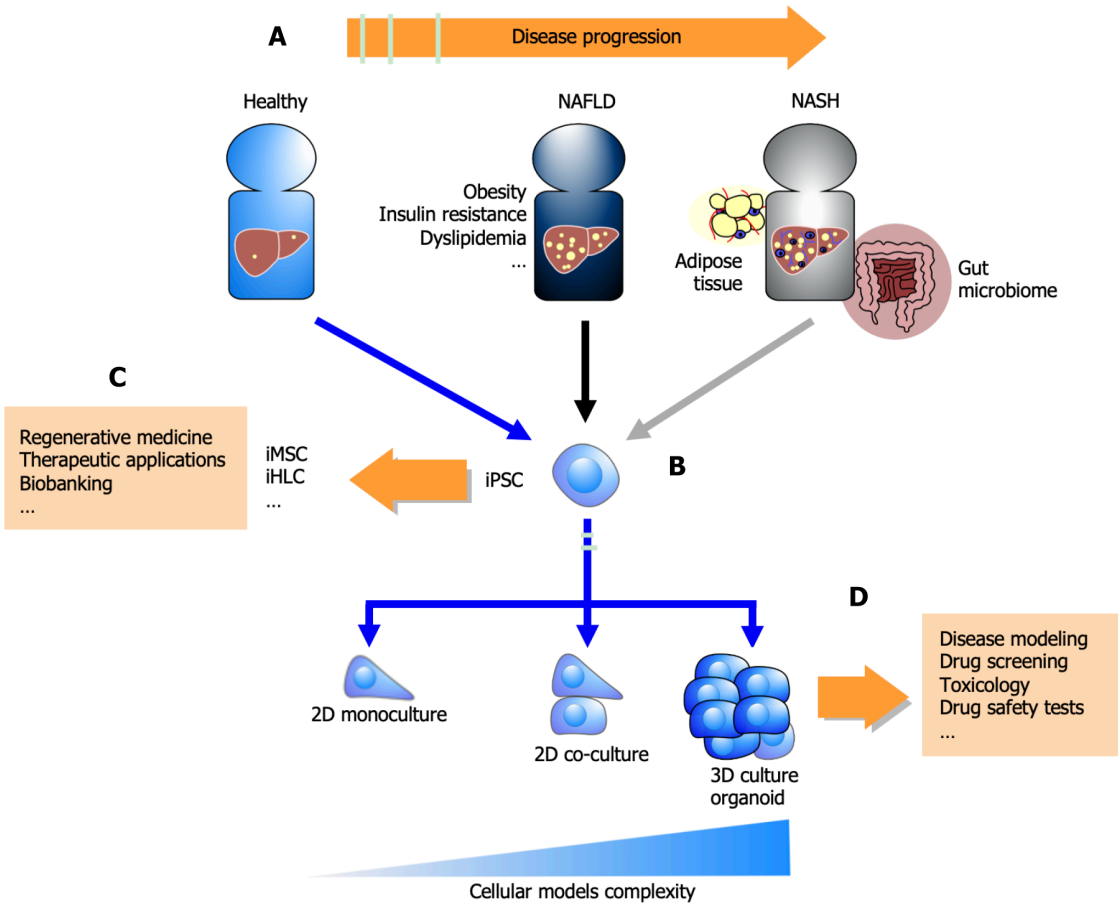

Figure 1 Applications of human induced pluripotent stem cells for nonalcoholic fatty liver/non-alcoholic steatohepatitis disease modeling and therapy. A: Nonalcoholic fatty liver (NAFLD) arises from abnormal lipid accumulation in hepatocytes unrelated to excessive alcohol consumption and is associated with dyslipidemia, insulin resistance, obesity, metabolic syndrome, and type 2 diabetes. The progression of NAFLD to nonalcoholic steatohepatitis (NASH) can be triggered by lipid peroxidation, mitochondrial dysfunction, oxidative stress, hepatocyte apoptosis, the production of proinflammatory cytokines, and alterations in the microbiome. NASH may further deteriorate into cirrhosis due to the development of liver scarring and advanced hepatocellular damage; B: Induced pluripotent stem cells (iPSCs) can be reprogrammed from somatic cells of healthy individuals or patients with NAFLD/NASH; C: Functional hepatocytes, mesenchymal stem cells, and other cell types can be derived from iPSCs for use in regenerative medicine and other therapeutic approaches. Additionally, iPSCs and their derived cells can be characterized and preserved in biobanks worldwide for allogenic cell-based therapies in human leukocyte antigen-matched patients; D: Cells differentiated from iPSCs can be used to create two-dimensional (2D) monocultures, 2D co-cultures, and complex 3D cellular systems, such as liver organoids, to model normal or diseased hepatic tissue. These human *in vitro* liver models are valuable for studying NAFLD/NASH disease progression as well as for testing drugs to assess their efficacy, safety, and toxicity. If the iPSCs are derived from a patient, these models can help identify drugs with better efficacy for treating that specific patient, enabling personalized medicine. iMSC: Induced pluripotent stem cell-derived mesenchymal stem cell; iHLC: Induced pluripotent stem cell-derived hepatocyte-like cell.

properties may result in unpredictable therapeutic outcomes. Moreover, inconsistent differentiation processes may result in heterogeneous iMSC populations impairing their clinical effectiveness. Additionally, the maintenance of protocol reproducibility and quality of iMSCs have to be achieved in large-scale production systems to provide the necessary cell numbers for clinical usage. Of importance, these processes will have to preserve the immunomodulatory function of iMSCs that are crucial for NAFLD/NASH treatment. Therefore, optimizing and standardizing differentiation protocols are vital to ensure that iMSCs are produced consistently with the necessary functional characteristics, thereby supporting their successful clinical application.

Despite iMSCs and primary MSCs exhibiting similar functional characteristics, there are differences in their overall gene expression profiles. For instance, Frobel *et al*[29] reported that genes associated with T cell activation and immune response were expressed at higher levels in primary BM-MSCs compared with iMSCs. Consequently, iMSCs demonstrated a reduced immunomodulatory effect attributed to their decreased ability to suppress T cell proliferation [29]. Diederichs and Tuan[30] found significant differences in gene expression related to differentiation between iMSCs and BM-MSCs from the same donor, with iMSCs showing inferior trilineage differentiation potential compared with BM-MSCs, highlighting that they are not identical entities.

Building on these studies, Xu *et al*[31] compared various iMSC and BM-MSC lines to further investigate their differences. They showed that both cell types were able to efficiently differentiate into osteoblasts, but iMSCs displayed a reduced capacity to differentiate into adipocytes and chondrocytes. iMSCs exhibited a gene expression profile similar to vascular progenitor cells derived from mesodermal origins, possibly explaining their limited capacity to differentiate into the three pilar cell types, namely adipocytes, chondrocytes, and osteoblasts, in comparison with primary MSCs. This underscores the authors' call for broader assessments beyond the International Society for Cellular Therapy,

recommending the inclusion of diverse mesodermal progenitor markers in future evaluations[31].

The immunomodulatory effects of MSCs are mainly attributed to paracrine signals, which include EVs secreted by those cells. Thus, MSC-derived EVs are viewed as therapeutic replacement to MSCs for the treatment of several diseases. Of particular interest for liver-related diseases, MSC-derived EVs are small and accumulate in the liver when delivered by systemic injection. Making the liver a privileged target of EVs could be used to minimize the homeostatic hepatic imbalance during disease[32,33]. For efficient EV-based therapies, a large quantity of EVs would be required, and primary MSCs do not produce large amounts of EVs. Therefore, iMSCs are considered a better source for EV production, as their numbers or iPSCs before differentiation can be expanded in culture for long periods without undergoing senescence.

Moreover, Kim *et al*[34] demonstrated that EVs derived from pan PPAR agonist-stimulated iMSCs were able to treat NASH in both *in vitro* (primary hepatocytes) and *in vivo* (mouse) models by promoting tissue repair, reducing ER stress, stimulating mitochondrial biogenesis, and decreasing reactive oxygen species generation. These results indicate that priming of iMSCs may result in EVs with enhanced capacity to treat NAFLD, and more research has to be performed in this field. Despite some drawbacks, iMSCs appear to be promising cells for drug testing, personalized therapies, and large-scale cell and EV production, which have great potential for treating liver diseases by targeting hepatic repair mechanisms. Nevertheless, optimizing differentiation protocols and ensuring cell safety are crucial before clinical applications can be realized.

MODELLING NAFLD/NASH

To understand the etiology and pathophysiology of NAFLD/NASF and test potential therapies, animal models have been very valuable. Those models are numerous and to some extent reflect the genetic, metabolic, and behavioral abnormalities that contribute to NAFLD/NASH. They provide valuable insights into the specific pathways and mechanisms underlying the pathology. However, these models do not completely reproduce the full spectrum of heterogeneity and complexity observed in human NAFLD/NASH pathology. The mouse model that most closely mimics human NAFLD is called "Diet-induced Animal Model of Nonalcoholic Fatty Liver Disease". Mice are fed a high-fat and fructose diet, leading to progressive stages of NAFLD and eventually liver cancer. However, this model is genetically constrained, and the phenotype takes a few months to develop[35].

Furthermore, ethical and public pressure is increasing to minimize or even abolish the use of animals in scientific, medical, and other procedures to preserve animal welfare and reduce pain and suffering. This is also scientifically justified by the genetic, physiological, and other differences between animals and humans, which can lead to inaccurate modeling of human diseases. Additionally, novel human two-dimensional (2D) and three-dimensional (3D) cell-based *in vitro* models are now available and are alternatives offering more relevant and humane research approaches for disease studies and drug development.

2D CULTURE CELL MODELS

NAFLD is a disease centered on hepatocyte dysfunction. Thus human primary hepatocytes, iPSC-derived hepatocytes, and hepatoma cell lines are interesting cellular systems for studying NAFLD (Figure 1). Primary human hepatocytes (PHHs) are the most abundant cell type in the liver and are responsible for liver-specific functions[35]. Thus, PHHs are commonly used as an *in vitro* model to study liver diseases due to their ease of isolation from liver resection or tissue. However, PHHs have some limitations, such as interdonor variability that makes reproducibility difficult and their ephemeral capacity to proliferate and maintain their liver-specialized functions[36,37]. Despite those limitations, PHHs are physiologically relevant for NAFLD investigation, and their exposure to free fatty acids (FFAs) (oleic or palmitic acid) replicates liver steatosis *in vitro*. Those cells were successfully used to unravel pathways contributing to liver injury, such as transforming growth factor β[38] and to identify protector molecules of hepatocytes, such as GLP-1 analogues that promote autophagy and reduce hepatocyte ER stress-induced apoptosis[39]. GLP-1 is an incretin involved in insulin secretion, satiety, and the suppression of glucagon release when nutrients are digested[40,41]. In the presence of an agonist, a decrease in the fatty acid load within hepatocytes is observed, making it a potential therapeutic target for NAFLD/NASH[39].

Human hepatoma cell lines, such as HepG2 and Huh-7, were derived from cancers and adapted to *in vitro* culture and conserved some of properties of primary hepatocytes. However, they are genomically instable and fail to be fully representative of a primary hepatocyte since they present an altered metabolism and lack the expression of some drug-metabolizing enzymes[36,42]. Nevertheless, these models have been utilized to elucidate some mechanisms underlying the pathology of NAFLD and define some drugs with potential for treatment of the disease. Indeed, exposing HepG2 cells to oleic acid results in lipid accumulation, elevated production of tumor necrosis factor-α, decreased expression of PPARα, increased lipid peroxidation and apoptosis, and reduced cellular proliferation, which are key events contributing to the pathogenesis and progression of NAFLD[43]. The Huh-7 cell line, which shows an expression profile of metabolic enzymes similar to those of PHHs, has been used to test drugs to improve steatosis, such as toyocamycin and an inhibitor of the transcription factor X-box binding protein 1[37,44]. Overall, hepatoma cell lines are not the best cells to model NAFLD/NASH.

The pluripotent nature of human iPSC and embryonic stem cells enables their differentiation virtually into any cell of the adult organism, and protocols have been established to generate hepatocyte-like cells (iHLCs) from those cells. iHLCs express hepatocyte-specific proteins and display biochemical functions specific to liver. Of interest, the exposition of iHLCs to oleic acid led to the accumulation of FFA and metabolic changes recapitulating the characteristics of NAFLD, with an upregulation of genes associated to lipid or glucose metabolism and to a PPAR-related pathway. Interestingly, the treatment of iHLCs with compounds modulating PPAR activity has demonstrated the beneficial effects of PPARα activation seen in patients by reducing the expression of enzymes involved in lipid and cholesterol synthesis[36]. Thus, iHLCs are promising models for NAFLD *in vitro* despite their limitations, such as an immature state compared with primary hepatocytes. Several strategies have been proposed to promote the maturation of iHLCs: (1) Adjusting amino acid levels in the culture media to increase CYP3A4 activity[45]; (2) Using small molecules such as activin A, LY294002 or FH1[46,47]; and (3) Co-culture with other cell types, such as fibroblasts[48].

Another group used undifferentiated iPSCs to study NAFLD by directly placing these cells in contact with oleate to verify their capacity to accumulate lipids. Compared with iHLCs, iPSCs did not present different levels of oleate. They demonstrated the potential of patient-derived iPSCs for initial research on NAFLD and other diseases characterized by lipid accumulation, particularly genetic factors. This allows the identification of high-risk individuals and the understanding of variations in treatment response[49].

To increase the complexity and attractiveness of 2D models, several research groups have developed co-culture systems. Barbero-Becerra *et al*[50] tested a co-culture of Huh-7 hepatocytes and LX-2 human hepatic stellate cells (HSCs) using cell inserts that allow the cells to grow independently while sharing the same culture medium. HSCs are specialized liver cells storing vitamin A, supporting liver regeneration by secreting growth factors, and producing and remodeling the extracellular matrix (ECM) to maintain liver structure. Upon liver injury, HSCs become activated and transform into myofibroblast-like cells, producing excessive ECM, especially type I collagen, leading to liver fibrosis and potentially cirrhosis.

In NAFLD, HSC activation is a key event in the progression from simple steatosis to NASH and fibrosis. HSCs also play a role in immunomodulation by interacting with immune cells and regulating inflammation[51]. The study concluded that the response of HSCs to FFA exposure and its effect on Huh-7 hepatocytes is independent of FFA exposure but requires cell-to-cell or proximity contact with hepatocytes. This is mediated by genes involved in ECM remodeling, such as *α-COL1* and matrix metalloproteinase-2, which exert regulatory effects *via* paracrine mediators[50]. A significant challenge of these 2D models is optimizing cell culture conditions for the various cell types involved[37].

For a better replication of the (patho)physiological characteristics and context through 2D models, several research groups have developed co-culture models. For instance, Barbero-Becerra *et al*[50] tested a co-culture of Huh-7 hepatoma cells and LX-2 human HSCs, where the two cell types grow separated by inserts allowing only the exchange of diffusible molecules and proximity contacts. Supplementation of FFA to this co-culture 2D cell complex led to the indirect activation of HSCs through cell-cell or proximal molecular interactions with Huh-7. This activation was attributed to the expression of genes involved in ECM remodeling, such as α-COL1 and matrix metalloproteinase-2, and paracrine mediators[50].

3D MODELS FOR NAFLD/NASH

Unlike 2D cellular models, 3D co-culture models recreate a more realistic 3D environment of the hepatic organ/tissue with spatial organization of cells and physiology that are a more accurate representation of cell-cell interactions occurring in NAFLD/NASH disease processes. Methods to produce 3D models may include hydrogels, synthetic scaffolds, and spheroid cellular formation. Other groups used microfluidic devices using PHHs or HepG2 hepatoma cells, where cells were exposed to FFA during a defined time point and metabolic and phenotypic changes were observed[52,53]. The standard method involves a 2D sandwich culture, in which hepatocytes are placed between two layers of collagen[54]. 3D spheroid models originated from PHHs of healthy and pathological donors have been used to study steatosis and insulin resistance. Despite variations among donors, such as age and phenotypes, spheroids exposed to FFA for 21 days mimicked pathological effects such as hepatic steatosis and triglyceride accumulation. Notably, the induced steatosis was reversible, suggesting that this model is ideal for studying NAFLD[55]. In 3D spheroids, PHHs were viable for more than 21 days allowing potential high throughput screening experiments. However, the generation of these models remains time-consuming and requires exhaustive validation.

ORGANOIDS TO INVESTIGATE NAFLD/ NASH

In 2009, Sato *et al*[56] successfully generated the first intestinal organoids (“mini-guts”) from intestinal stem cells, demonstrating the feasibility of producing complex. 3D structures that replicate the architecture and functions of specific organs. This groundbreaking achievement spurred significant interest across various research fields, inspiring the generation of organoids from numerous tissues and organs. Consequently, organoid models have become invaluable tools for studying diseases, drug testing, and applications in regenerative medicine.

Organoids are essentially 3D miniaturized and simplified versions of organs produced *in vitro* from stem cells. They arise from stem cells cultured under conditions that support spatial self-organization and differentiation, enabling them to mimic the cell-type composition, structural characteristics, and key functions of the original organ. Compared to traditional 2D cell cultures, organoids are more physiologically relevant, offering a more accurate architectural and

functional complexity representation of organs *in vivo*[57-59]. Moreover, organoids can be maintained long-term in culture, cryopreserved, biobanked without genetic alterations, and derived from stem cells or iPSCs to create personalized models[60].

Hepatic organoids, for instance, replicate the *in vivo* characteristics of liver tissue, including 3D cellular interactions and interactions with the ECM. Moreover, as multicellular structures, the organoids display functional units such as bile duct-like structures and express metabolic and detoxifying enzymes, transporters, and proteins involved in secretion of bile and other metabolites. Importantly, these organoids can be generated from patient-specific liver tissues or iPSCs and preserve genetic traits unique to each individual donor, which are critical for personalized medicine as they may influence drug metabolism and response. Personalized organoids may be instrumental to test and identify the medication with the more effective effects and least toxicity for the donor individual. Thus, organoids not only provide a powerful platform to advance our understanding of NAFLD/NASH mechanisms pathophysiology, but they may facilitate the development of improved therapeutic strategies[61].

Generating hepatic organoids from iPSCs involves protocols designed to guide the transition from 2D cells into self-organized 3D structures through different stages of differentiation. Once formed, these organoids are cultured under specific conditions to support either their expansion or differentiation into various hepatic lineages, including unicellular or multicellular hepatic organoids[61].

In vitro modeling of NAFLD using organoids can follow similar methods to traditional 2D approaches. Typically, a high concentration of FFAs is used to transition from simple steatosis and inflammation to fibrosis. Ramli *et al*[62] analyzed the gene expression profiles of organoids, comparing those exposed to FFAs with those not exposed, using samples from healthy individuals and those from patients with NASH. They found that organoids incubated with FFA exhibited gene expression patterns akin to those in liver tissues from patients with NASH[62].

By using iPSCs from healthy and diseased patients, Ouchi *et al*[63] established multicellular organoids composed of hepatocytes, stellate-like cells, and Kupffer-like cells, recapitulating progressive inflammation, steatosis, and fibrosis, in response to high doses of FFAs. This method proposed a novel approach to personalized treatments for inflammation and fibrosis in humans, enabling the identification of new therapies[63].

Hendriks *et al*[64] utilized expandable human fetal liver organoids to reproduce steatosis either by loading high doses of FFAs, expression of a patatin-like phospholipase domain-containing 3 variant (I148M) associated with a high risk of NAFLD, or by knockout of APOB or MTTP (mutations in these genes are linked to lipid disorders). Exposure of wild-type organoids to low concentrations of FFAs had no effect since the hepatocytes present within the organoids were able to metabolize those lipids, while at higher concentrations, hepatocytes progressively accumulated lipids. Organoids harboring patatin-like phospholipase domain-containing 3 variants or null for either APOB or MTTP showed high intracellular lipid accumulation[64]. Thus, liver organoids derived from stem cells or patient-specific iPSCs, hold potential for understanding NAFLD/NASH progression due to their ability to mimic disease hallmarks like steatosis and fibrosis.

DISCUSSION

NAFLD is an increasing health problem worldwide, which carries the risk of progression to more severe conditions, such as NASH, and even cirrhosis and hepatocellular carcinoma[3,6]. Despite many therapeutic approaches that are under investigation, including the search for metabolic regulators and novel strategies targeting oxidative stress and inflammation, no approved pharmacological therapy is currently available for NAFLD. MSCs have emerged as attractive cells for the treatment of NAFLD since these cells with immunomodulation and tissue regenerative properties are easily harvested from many tissues[13]. An ongoing clinical trial exploring autologous AD-MSCs for liver cirrhosis associated with NASH or fatty liver disease provides encouraging preliminary results, demonstrating improvements in liver function without adverse effects[19]. Despite the positive results of this clinical trial, further research is needed to understand the long-term safety and efficacy of AD-MSCs. Compared to current treatment options for NAFLD/NASH, which primarily focus on lifestyle modifications and managing symptoms, stem cell therapies offer the potential for a more targeted and regenerative approach.

A drawback of employing MSCs in therapies is cell heterogeneity where they can significantly impact the efficacy and consistency of treatments and impair the implementation of standardized MSC preparation[65,66]. A critical point in the production of an MSC-based advanced therapy medicinal product is its quality control, which includes identity, purity, safety, and potency tests because it enhances its safety and efficacy for administration to patients[66]. Therefore, it is essential to identify additional key control points like the assessment of heterogeneity through transcriptome sequencing, along with the monitoring of chromosomal instability and tumorigenicity[66]. *In vitro* culture of MSCs can result in the accumulation of genetic and epigenetic changes, exhibiting genetic instability that could account for their tumorigenic potential.

A significant challenge in developing MSC-based products is the considerable heterogeneity among cell sources, which display varying marker profiles, gene expressions, differentiation potentials, and immunomodulatory and paracrine characteristics. Additionally, factors such as the donor's age and health, along with the manufacturing process (encompassing culture medium composition, substrate properties, and oxygen concentration) are likely to influence the features of MSCs in various mechanisms[66].

To date, numerous single-cell transcriptome studies have been performed to explore MSCs heterogeneity. A study demonstrated that BM-MSCs presented higher transcriptomic heterogeneity than AD-MSCs, suggesting that adipose-tissue derived cells are more suitable for certain cell transplantation treatments[67]. Another study used 361 single MSCs

derived from two umbilical cord-MSC donors and demonstrated that umbilical cord-MSCs expanded *in vitro* present limited heterogeneity and are associated with cell cycle status[68]. Nonetheless, these two studies have limitations, including a small donor pool and the focus on only one or two tissue types. In response, Wang *et al*[69] conducted large-scale multiplexing single-cell RNA sequencing to create an atlas comprising 130000 single MSC transcriptomes from various tissues, including bone marrow, umbilical cord, adipose tissue, and dermis, sourced from 11 donors. This study revealed significant global variability among tissues, highlighting that ECM-related inflammation, aging, and antigen processing and presentation differ greatly within tissue-specific subpopulations, yet these variations are not linked to cell cycle status[69].

To date, the characterization of iMSCs and their heterogeneity have not been the primary focus of MSC transcriptome studies. Indeed, a unique transcriptome analysis has compared pluripotent stem cells, intermediate cells involved in iMSC derivation, mature iMSCs, BM-MSCs, and fibroblast gene expression. This study showed that iPSC-derived MSCs share a similar immunophenotype with BM-MSCs. While pluripotency markers are silenced, the epigenetic signature linked to the iPSC origin remains intact, which does not impede the differentiation potential of iPSCs. Additionally, as somatic cells were reprogrammed into iMSCs, genes associated with mesenchymal identity and lineage commitment were activated. A group of 52 genes with a higher expression profile distinguished MSC types from other cell types[70].

Another important consideration is the tumorigenic potential of MSCs. Stucky *et al*[71] used single-cell RNA sequencing to analyze MSCs during osteogenic differentiation and identified a subpopulation of differentiation-resistant MSCs. These cells exhibited upregulated expression of the *YAP1* gene network, which is involved in stemness, proliferation, and epithelial-mesenchymal transition, a key processes in cancer initiation and progression. They performed a meta-analysis of clinical cancer data, demonstrating a high degree of coexpression among CDH6, YAP1, and OCT4 across various solid tumors. These findings suggested that the *YAP1* gene network plays a key role in the tumorigenicity of MSC subclones that are resistant to differentiation[71]. Conversely, Malvicini *et al*[72] demonstrated that OCT4 is fundamental to MSC to differentiate into adipocytes and osteoblasts. Collectively, these studies underscore the necessity of a balanced expression of these factors in MSCs to maintain their multipotency and prevent tumorigenicity and the necessity to understand MSCs gene expression dynamics to develop safe and reliable an advanced therapy medicinal products.

The ability to generate patient-specific iPSCs has opened avenues for tailoring treatments and setting up complex *in vitro* models to unravel disease mechanisms at a molecular level. It is crucial for advancing precision medicine approaches in NAFLD/NASH. Indeed, functional and well-characterized iMSCs and iHLCs represent a promising opportunity for (personalized) therapies[20]. Functional iHLCs could be reintroduced in the diseased liver to substitute lost functional hepatocytes. On the other hand, iMSCs could be substitutes to tissue MSCs, which are still unstable and difficult to culture for reaching large numbers of cells required for therapies. However, ethical considerations surrounding the use of iPSCs and potential side effects of MSC therapy need to be carefully addressed. Indeed, the use of iPSC-derived cells in therapy generally lacks long-term safety data. Addressing these concerns is crucial, as both iPSCs and iMSCs may present risks of tumorigenicity if not carefully selected. Additionally, it is essential to provide clear and accurate information to patients participating in early-phase clinical trials, as they may have unrealistic expectations or misunderstandings regarding the efficacy of these pioneering therapies.

Both iMSC and iHLCs are useful for disease modeling, drug screening, and personalized therapies[20,23]. Of interest, EVs and proteins secreted by MSCs display the cellular properties to modulate lipid metabolism, reduce inflammation, and promote tissue repair. Therefore, EVs could be substituted for MSCs for NAFLD/NASH treatments in a safer manner than cells since they do not bear genomic DNA material[32,33]. Further research into priming strategies, such as enhancing EV production from iMSCs through targeted molecular interventions, holds promise for enhancing therapeutic efficacy in NAFLD/NASH. Overall, while challenges persist, the potential of stem cells, particularly iMSCs and their secreted EVs, in reshaping the landscape of NAFLD treatment underscores their importance as a focal point for future research and clinical translation efforts. Importantly, optimizing differentiation protocols of desired cells and production/isolation of EVs, ensuring safety, and addressing regulatory concerns are required before stem cell-based therapies can be widely implemented clinically[31]. Beyond priming strategies for EVs, exploring broader future research directions in the field, such as optimizing cell delivery methods or combination therapies with existing treatments, would provide a more comprehensive picture.

Hepatic, intestinal, and many organoids, which are *in vitro* structural and functional representations of the organs, have originated from stem cells including iPSC to represent dysfunctional organs or healthy organs[60]. Hepatic organoids are promising cellular structures for retracing the etiology and progression of NAFLD/NASH[61,63]. However, improvements are needed to optimize their use. Reproducibility in size and cellular organization, especially in multicellular organoids, must be enhanced, as structural variations can affect cell interactions and responses to stimuli. Organoid models created from iPSCs exhibit low hepatic maturity, affecting disease modeling and drug testing. A key limitation is their insufficient vascularization, which limits nutrient and stimulus distribution, restricts organoid size, and obstructs the formation of complex structures for *in vivo* pathology modeling[61]. Those different organoids could be coupled through microfluidic devices to provide a more controlled environment and simulate blood flow for the exchange of metabolites and proteins.

Overall, iPSC and iPSC-derived cells are promising for modeling NAFLD/NASH and the discovery of novel therapeutic strategies. However, while challenges persist, the potential of stem cells, particularly iMSCs and their secreted EVs, in reshaping the landscape of NAFLD treatment underscores their importance as a focal point for future research and clinical translation efforts.

CONCLUSION

Stem cell-based therapies, particularly those utilizing MSCs and HLCs derived from iPSCs, hold significant promise for the treatment of NAFLD/NASH. Unlike current therapies that primarily focus on symptom management, iPSC-derived therapies offer the potential to replace damaged cells and tissues in the liver, promoting the restoration of liver functionality. However, for these therapies to become clinically viable, several critical challenges must be addressed. A key challenge lies in the optimization of cell differentiation protocols to generate high-quality, functional iPSC-derived HLCs and iMSCs that closely replicate the characteristics of their *in vivo* counterparts. Furthermore, scaling up the production of these cell populations, essential for clinical applications, without compromising their functionality may constitute a significant obstacle. Safety concerns also play a central role in the clinical translation of iPSC-derived therapies. A primary concern is the risk of tumorigenicity associated with the use of iPSC-derived cells, such as iMSCs. Rigorous screening and quality control measures are essential at every stage of cell generation and clinical application. Protocols must include mechanisms for detecting and eliminating undifferentiated iPSCs in the final therapeutic cell population to mitigate the risk of teratoma formation. Additionally, the detection of chromosomal abnormalities in these cells should be incorporated into quality control protocols to ensure the safety and stability of the cells used in therapy.

In parallel, the utilization of advanced models such as organoids and single-cell profiling techniques will significantly enhance the understanding of the underlying mechanisms of NAFLD and NASH. These innovative models allow for detailed disease modeling and drug screening, facilitating the development of more effective and personalized therapeutic strategies. The translational potential of iPSC-derived therapies is particularly noteworthy in the context of personalized medicine. By generating patient-specific iPSCs and liver models, such as liver organoids, researchers can better investigate the unique genetic and environmental factors that contribute to NAFLD/NASH. These models offer a robust platform for drug screening, efficacy assessment, and prediction of treatment outcomes on an individualized basis. Moreover, iMSCs demonstrate the capability to modulate fibrosis and inflammation in NASH, providing a targeted therapeutic approach that may surpass the limited efficacy of conventional pharmacological treatments in reversing disease progression.

The integration of iPSC-derived cells into clinical practice holds the potential to transform the treatment landscape for liver diseases by offering regenerative and personalized solutions that traditional therapies cannot achieve. Crucial to the success of these therapies is the development of robust strategies to ensure the engraftment, long-term survival, and proper integration of transplanted cells within the host liver tissue. Addressing these factors is vital for achieving sustained therapeutic outcomes and enhancing patient responses to treatment.

Ethical considerations surrounding iPSC-based therapies must also be addressed. This includes ensuring that informed patient consent provides accurate and comprehensive information, particularly for individuals participating in early-phase clinical trials. Transparent communication regarding the potential adverse effects of these therapies, as well as contingency plans in case of unexpected outcomes, is essential. Furthermore, the accessibility of such cutting-edge therapies must be equitable, ensuring that all patients, irrespective of their socioeconomic status or geographic location, have the opportunity to benefit from these advancements.

While significant challenges remain, the potential of iPSC-derived therapies to address the unmet needs in NAFLD/NASH treatment is substantial. With continued optimization of differentiation protocols, safety measures, and scalability, along with the integration of personalized medicine strategies, these therapies could bring about a transformative shift toward more effective, individualized interventions for liver disease.

FOOTNOTES

Author contributions: Silva B and Bragança J contributed to the conceptualization; Silva B contributed to the writing of the original draft; Bragança J contributed to reviewing and editing, project administration, and funding acquisition; All authors read and agreed to the published version of the manuscript.

Supported by American Heart Association Award, No. 24IVPHA1288417; and FCT Fellowships, No. 2022.13253.BDANA.

Conflict-of-interest statement: All authors report no relevant conflicts of interest for this article.

Country of origin: Portugal

ORCID number: Bárbara Silva 0000-0002-3314-7936; José Bragança 0000-0001-9566-400X.

S-Editor: Wang JJ
L-Editor: Filipodia
P-Editor: Zhang XD

REFERENCES

1 **Estes C**, Razavi H, Loomba R, Younossi Z, Sanyal AJ. Modeling the epidemic of nonalcoholic fatty liver disease demonstrates an exponential increase in burden of disease. *Hepatology* 2018; **67**: 123-133 [PMID: 28802062 DOI: 10.1002/hep.29466]

2 **Mantovani A**, Dalbeni A. Treatments for NAFLD: State of Art. *Int J Mol Sci* 2021; **22**: 2350 [PMID: 33652942 DOI: 10.3390/ijms22052350]

3 **Parola M**, Pinzani M. Liver fibrosis in NAFLD/NASH: from pathophysiology towards diagnostic and therapeutic strategies. *Mol Aspects Med* 2024; **95**: 101231 [PMID: 38056058 DOI: 10.1016/j.mam.2023.101231]

4 **Sanyal AJ**. Past, present and future perspectives in nonalcoholic fatty liver disease. *Nat Rev Gastroenterol Hepatol* 2019; **16**: 377-386 [PMID: 31024089 DOI: 10.1038/s41575-019-0144-8]

5 **Samy AM**, Kandeil MA, Sabry D, Abdel-Ghany AA, Mahmoud MO. From NAFLD to NASH: Understanding the spectrum of non-alcoholic liver diseases and their consequences. *Heliyon* 2024; **10**: e30387 [PMID: 38737288 DOI: 10.1016/j.heliyon.2024.e30387]

6 **Chalasani N**, Younossi Z, Lavine JE, Charlton M, Cusi K, Rinella M, Harrison SA, Brunt EM, Sanyal AJ. The diagnosis and management of nonalcoholic fatty liver disease: Practice guidance from the American Association for the Study of Liver Diseases. *Hepatology* 2018; **67**: 328-357 [PMID: 28714183 DOI: 10.1002/hep.29367]

7 **Yang Z**, Wang L. Current, emerging, and potential therapies for non-alcoholic steatohepatitis. *Front Pharmacol* 2023; **14**: 1152042 [PMID: 37063264 DOI: 10.3389/fphar.2023.1152042]

8 **Yang Z**, Xia Q, Lu D, Yue H, Zhang J, Li Y, Zhang B, Li X, Cao M. Human mesenchymal stem cells treatment improved hepatic lesions and reversed gut microbiome disorder in non-alcoholic steatohepatitis. *Aging (Albany NY)* 2020; **12**: 21660-21673 [PMID: 33168782 DOI: 10.18632/aging.103962]

9 **Domingues I**, Leclercq IA, Beloqui A. Nonalcoholic fatty liver disease: Current therapies and future perspectives in drug delivery. *J Control Release* 2023; **363**: 415-434 [PMID: 37769817 DOI: 10.1016/j.jconrel.2023.09.040]

10 **Jiang Y**, Yusoff NM, Du J, Moses EJ, Lin JT. Current perspectives on mesenchymal stem cells as a potential therapeutic strategy for non-alcoholic fatty liver disease. *World J Stem Cells* 2024; **16**: 760-772 [PMID: 39086561 DOI: 10.4252/wjsc.v16.i7.760]

11 **Dominici M**, Le Blanc K, Mueller I, Slaper-Cortenbach I, Marini F, Krause D, Deans R, Keating A, Prockop Dj, Horwitz E. Minimal criteria for defining multipotent mesenchymal stromal cells. The International Society for Cellular Therapy position statement. *Cytotherapy* 2006; **8**: 315-317 [PMID: 16923606 DOI: 10.1080/14653240600855905]

12 **Viswanathan S**, Shi Y, Galipeau J, Krampera M, Leblanc K, Martin I, Nolta J, Phinney DG, Sensebe L. Mesenchymal stem versus stromal cells: International Society for Cell & Gene Therapy (ISCT®) Mesenchymal Stromal Cell committee position statement on nomenclature. *Cytotherapy* 2019; **21**: 1019-1024 [PMID: 31526643 DOI: 10.1016/j.jcyt.2019.08.002]

13 **Korkida F**, Stamatopoulou A, Roubelakis MG. Recent Advances in Mesenchymal Stem/Stromal Cell-Based Therapy for Alcohol-Associated Liver Disease and Non-alcoholic Fatty Liver Disease. *Stem Cells Transl Med* 2024; **13**: 107-115 [PMID: 38016185 DOI: 10.1093/stcltm/szad082]

14 **Nickel S**, Christ M, Schmidt S, Kosacka J, Kühne H, Roderfeld M, Longerich T, Tietze L, Bosse I, Hsu MJ, Stock P, Roeb E, Christ B. Human Mesenchymal Stromal Cells Resolve Lipid Load in High Fat Diet-Induced Non-Alcoholic Steatohepatitis in Mice by Mitochondria Donation. *Cells* 2022; **11**: 1829 [PMID: 35681524 DOI: 10.3390/cells11111829]

15 **Watanabe Y**, Tsuchiya A, Seino S, Kawata Y, Kojima Y, Ikarashi S, Starkey Lewis PJ, Lu WY, Kikuta J, Kawai H, Yamagiwa S, Forbes SJ, Ishii M, Terai S. Mesenchymal Stem Cells and Induced Bone Marrow-Derived Macrophages Synergistically Improve Liver Fibrosis in Mice. *Stem Cells Transl Med* 2019; **8**: 271-284 [PMID: 30394698 DOI: 10.1002/sctm.18-0105]

16 **Duarte S**, Baber J, Fujii T, Coito AJ. Matrix metalloproteinases in liver injury, repair and fibrosis. *Matrix Biol* 2015; **44-46**: 147-156 [PMID: 25599939 DOI: 10.1016/j.matbio.2015.01.004]

17 **Siapati EK**, Roubelakis MG, Vassilopoulos G. Liver Regeneration by Hematopoietic Stem Cells: Have We Reached the End of the Road? *Cells* 2022; **11**: 2312 [PMID: 35954155 DOI: 10.3390/cells11152312]

18 **Winkler S**, Borkham-Kamphorst E, Stock P, Brückner S, Dollinger M, Weiskirchen R, Christ B. Human mesenchymal stem cells towards non-alcoholic steatohepatitis in an immunodeficient mouse model. *Exp Cell Res* 2014; **326**: 230-239 [PMID: 24786317 DOI: 10.1016/j.yexcr.2014.04.017]

19 **Sakai Y**, Fukunishi S, Takamura M, Kawaguchi K, Inoue O, Usui S, Takashima S, Seki A, Asai A, Tsuchimoto Y, Nasti A, Bich Ho TT, Imai Y, Yoshimura K, Murayama T, Yamashita T, Arai K, Yamashita T, Mizukoshi E, Honda M, Wada T, Harada K, Higuchi K, Kaneko S. Clinical trial of autologous adipose tissue-derived regenerative (stem) cells therapy for exploration of its safety and efficacy. *Regen Ther* 2021; **18**: 97-101 [PMID: 34095367 DOI: 10.1016/j.reth.2021.04.003]

20 **Bragança J**, Lopes JA, Mendes-Silva L, Almeida Santos JM. Induced pluripotent stem cells, a giant leap for mankind therapeutic applications. *World J Stem Cells* 2019; **11**: 421-430 [PMID: 31396369 DOI: 10.4252/wjsc.v11.i7.421]

21 **Takahashi K**, Tanabe K, Ohnuki M, Narita M, Ichisaka T, Tomoda K, Yamanaka S. Induction of pluripotent stem cells from adult human fibroblasts by defined factors. *Cell* 2007; **131**: 861-872 [PMID: 18035408 DOI: 10.1016/j.cell.2007.11.019]

22 **Wei H**, Tan G, Manasi, Qiu S, Kong G, Yong P, Koh C, Ooi TH, Lim SY, Wong P, Gan SU, Shim W. One-step derivation of cardiomyocytes and mesenchymal stem cells from human pluripotent stem cells. *Stem Cell Res* 2012; **9**: 87-100 [PMID: 22683798 DOI: 10.1016/j.scr.2012.04.003]

23 **Zhao C**, Ikeya M. Generation and Applications of Induced Pluripotent Stem Cell-Derived Mesenchymal Stem Cells. *Stem Cells Int* 2018; **2018**: 9601623 [PMID: 30154868 DOI: 10.1155/2018/9601623]

24 **Jung Y**, Bauer G, Nolta JA. Concise review: Induced pluripotent stem cell-derived mesenchymal stem cells: progress toward safe clinical products. *Stem Cells* 2012; **30**: 42-47 [PMID: 21898694 DOI: 10.1002/stem.727]

25 **Fang IM**, Yang CM, Yang CH, Chiou SH, Chen MS. Transplantation of induced pluripotent stem cells without C-Myc attenuates retinal ischemia and reperfusion injury in rats. *Exp Eye Res* 2013; **113**: 49-59 [PMID: 23726881 DOI: 10.1016/j.exer.2013.05.007]

26 **Kim D**, Kim CH, Moon JI, Chung YG, Chang MY, Han BS, Ko S, Yang E, Cha KY, Lanza R, Kim KS. Generation of human induced pluripotent stem cells by direct delivery of reprogramming proteins. *Cell Stem Cell* 2009; **4**: 472-476 [PMID: 19481515 DOI: 10.1016/j.stem.2009.05.005]

27 **Okita K**, Nagata N, Yamanaka S. Immunogenicity of induced pluripotent stem cells. *Circ Res* 2011; **109**: 720-721 [PMID: 21921270 DOI: 10.1161/RES.0b013e318232e187]

28 **Shi ZD**, Tchao J, Wu L, Carman AJ. Precision installation of a highly efficient suicide gene safety switch in human induced pluripotent stem

cells. *Stem Cells Transl Med* 2020; **9**: 1378-1388 [PMID: 32662231 DOI: 10.1002/sctm.20-0007]
29 **Frobel J**, Hemeda H, Lenz M, Abagnale G, Joussen S, Denecke B, Sarić T, Zenke M, Wagner W. Epigenetic rejuvenation of mesenchymal stromal cells derived from induced pluripotent stem cells. *Stem Cell Reports* 2014; **3**: 414-422 [PMID: 25241740 DOI: 10.1016/j.stemcr.2014.07.003]
30 **Diederichs S**, Tuan RS. Functional comparison of human-induced pluripotent stem cell-derived mesenchymal cells and bone marrow-derived mesenchymal stromal cells from the same donor. *Stem Cells Dev* 2014; **23**: 1594-1610 [PMID: 24625206 DOI: 10.1089/scd.2013.0477]
31 **Xu M**, Shaw G, Murphy M, Barry F. Induced Pluripotent Stem Cell-Derived Mesenchymal Stromal Cells Are Functionally and Genetically Different From Bone Marrow-Derived Mesenchymal Stromal Cells. *Stem Cells* 2019; **37**: 754-765 [PMID: 30779868 DOI: 10.1002/stem.2993]
32 **Wu R**, Fan X, Wang Y, Shen M, Zheng Y, Zhao S, Yang L. Mesenchymal Stem Cell-Derived Extracellular Vesicles in Liver Immunity and Therapy. *Front Immunol* 2022; **13**: 833878 [PMID: 35309311 DOI: 10.3389/fimmu.2022.833878]
33 **Zhang B**, Tian X, Hao J, Xu G, Zhang W. Mesenchymal Stem Cell-Derived Extracellular Vesicles in Tissue Regeneration. *Cell Transplant* 2020; **29**: 963689720908500 [PMID: 32207341 DOI: 10.1177/0963689720908500]
34 **Kim GU**, Sung SE, Kang KK, Choi JH, Lee S, Sung M, Yang SY, Kim SK, Kim YI, Lim JH, Seo MS, Lee GW. Therapeutic Potential of Mesenchymal Stem Cells (MSCs) and MSC-Derived Extracellular Vesicles for the Treatment of Spinal Cord Injury. *Int J Mol Sci* 2021; **22** [PMID: 34948463 DOI: 10.3390/ijms222413672]
35 **Underhill GH**, Khetani SR. Emerging trends in modeling human liver disease in vitro. *APL Bioeng* 2019; **3**: 040902 [PMID: 31893256 DOI: 10.1063/1.5119090]
36 **Graffmann N**, Ring S, Kawala MA, Wruck W, Ncube A, Trompeter HI, Adjaye J. Modeling Nonalcoholic Fatty Liver Disease with Human Pluripotent Stem Cell-Derived Immature Hepatocyte-Like Cells Reveals Activation of PLIN2 and Confirms Regulatory Functions of Peroxisome Proliferator-Activated Receptor Alpha. *Stem Cells Dev* 2016; **25**: 1119-1133 [PMID: 27308945 DOI: 10.1089/scd.2015.0383]
37 **Müller FA**, Sturla SJ. Human in vitro models of nonalcoholic fatty liver disease. *Curr Opin Toxicol* 2019; **16**: 9-16 [DOI: 10.1016/j.cotox.2019.03.001]
38 **Wanninger J**, Neumeier M, Hellerbrand C, Schacherer D, Bauer S, Weiss TS, Huber H, Schäffler A, Aslanidis C, Schölmerich J, Buechler C. Lipid accumulation impairs adiponectin-mediated induction of activin A by increasing TGFbeta in primary human hepatocytes. *Biochim Biophys Acta* 2011; **1811**: 626-633 [PMID: 21070865 DOI: 10.1016/j.bbalip.2010.11.001]
39 **Sharma S**, Mells JE, Fu PP, Saxena NK, Anania FA. GLP-1 analogs reduce hepatocyte steatosis and improve survival by enhancing the unfolded protein response and promoting macroautophagy. *PLoS One* 2011; **6**: e25269 [PMID: 21957486 DOI: 10.1371/journal.pone.0025269]
40 **Andersen A**, Lund A, Knop FK, Vilsbøll T. Glucagon-like peptide 1 in health and disease. *Nat Rev Endocrinol* 2018; **14**: 390-403 [PMID: 29728598 DOI: 10.1038/s41574-018-0016-2]
41 **McGlone ER**, Hope DCD, Davies I, Dore M, Goldin R, Jones B, Liu Z, Li JV, Vorkas PA, Khoo B, Carling D, Minnion J, Bloom SR, Tan TM. Chronic treatment with glucagon-like peptide-1 and glucagon receptor co-agonist causes weight loss-independent improvements in hepatic steatosis in mice with diet-induced obesity. *Biomed Pharmacother* 2024; **176**: 116888 [PMID: 38861859 DOI: 10.1016/j.biopha.2024.116888]
42 **Gerets HH**, Tilmant K, Gerin B, Chanteux H, Depelchin BO, Dhalluin S, Atienzar FA. Characterization of primary human hepatocytes, HepG2 cells, and HepaRG cells at the mRNA level and CYP activity in response to inducers and their predictivity for the detection of human hepatotoxins. *Cell Biol Toxicol* 2012; **28**: 69-87 [PMID: 22258563 DOI: 10.1007/s10565-011-9208-4]
43 **Cui W**, Chen SL, Hu KQ. Quantification and mechanisms of oleic acid-induced steatosis in HepG2 cells. *Am J Transl Res* 2010; **2**: 95-104 [PMID: 20182586]
44 **Takahara I**, Akazawa Y, Tabuchi M, Matsuda K, Miyaaki H, Kido Y, Kanda Y, Taura N, Ohnita K, Takeshima F, Sakai Y, Eguchi S, Nakashima M, Nakao K. Toyocamycin attenuates free fatty acid-induced hepatic steatosis and apoptosis in cultured hepatocytes and ameliorates nonalcoholic fatty liver disease in mice. *PLoS One* 2017; **12**: e0170591 [PMID: 28278289 DOI: 10.1371/journal.pone.0170591]
45 **Boon R**, Kumar M, Tricot T, Elia I, Ordovas L, Jacobs F, One J, De Smedt J, Eelen G, Bird M, Roelandt P, Doglioni G, Vriens K, Rossi M, Vazquez MA, Vanwelden T, Chesnais F, El Taghdouini A, Najimi M, Sokal E, Cassiman D, Snoeys J, Monshouwer M, Hu WS, Lange C, Carmeliet P, Fendt SM, Verfaillie CM. Amino acid levels determine metabolism and CYP450 function of hepatocytes and hepatoma cell lines. *Nat Commun* 2020; **11**: 1393 [PMID: 32170132 DOI: 10.1038/s41467-020-15058-6]
46 **Wang L**, Chen YG. Signaling Control of Differentiation of Embryonic Stem Cells toward Mesendoderm. *J Mol Biol* 2016; **428**: 1409-1422 [PMID: 26119455 DOI: 10.1016/j.jmb.2015.06.013]
47 **Yuan Y**, Cotton K, Samarasekera D, Khetani SR. Engineered Platforms for Maturing Pluripotent Stem Cell-Derived Liver Cells for Disease Modeling. *Cell Mol Gastroenterol Hepatol* 2023; **15**: 1147-1160 [PMID: 36738860 DOI: 10.1016/j.jcmgh.2023.01.013]
48 **Berger DR**, Ware BR, Davidson MD, Allsup SR, Khetani SR. Enhancing the functional maturity of induced pluripotent stem cell-derived human hepatocytes by controlled presentation of cell-cell interactions in vitro. *Hepatology* 2015; **61**: 1370-1381 [PMID: 25421237 DOI: 10.1002/hep.27621]
49 **Muñoz A**, Theusch E, Kuang YL, Nalula G, Peaslee C, Dorlhiac G, Landry MP, Streets A, Krauss RM, Iribarren C, Mattis AN, Medina MW. Undifferentiated Induced Pluripotent Stem Cells as a Genetic Model for Nonalcoholic Fatty Liver Disease. *Cell Mol Gastroenterol Hepatol* 2022; **14**: 1174-1176.e6 [PMID: 35863744 DOI: 10.1016/j.jcmgh.2022.07.009]
50 **Barbero-Becerra VJ**, Giraudi PJ, Chávez-Tapia NC, Uribe M, Tiribelli C, Rosso N. The interplay between hepatic stellate cells and hepatocytes in an in vitro model of NASH. *Toxicol In Vitro* 2015; **29**: 1753-1758 [PMID: 26187275 DOI: 10.1016/j.tiv.2015.07.010]
51 **Wang M**, Li L, Xu Y, Du J, Ling C. Roles of hepatic stellate cells in NAFLD: From the perspective of inflammation and fibrosis. *Front Pharmacol* 2022; **13**: 958428 [PMID: 36313291 DOI: 10.3389/fphar.2022.958428]
52 **Gori M**, Simonelli MC, Giannitelli SM, Businaro L, Trombetta M, Rainer A. Investigating Nonalcoholic Fatty Liver Disease in a Liver-on-a-Chip Microfluidic Device. *PLoS One* 2016; **11**: e0159729 [PMID: 27438262 DOI: 10.1371/journal.pone.0159729]
53 **Kostrzewski T**, Cornforth T, Snow SA, Ouro-Gnao L, Rowe C, Large EM, Hughes DJ. Three-dimensional perfused human in vitro model of non-alcoholic fatty liver disease. *World J Gastroenterol* 2017; **23**: 204-215 [PMID: 28127194 DOI: 10.3748/wjg.v23.i2.204]
54 **Dunn JC**, Tompkins RG, Yarmush ML. Long-term in vitro function of adult hepatocytes in a collagen sandwich configuration. *Biotechnol Prog* 1991; **7**: 237-245 [PMID: 1367596 DOI: 10.1021/bp00009a007]
55 **Kozyra M**, Johansson I, Nordling Å, Ullah S, Lauschke VM, Ingelman-Sundberg M. Human hepatic 3D spheroids as a model for steatosis and insulin resistance. *Sci Rep* 2018; **8**: 14297 [PMID: 30250238 DOI: 10.1038/s41598-018-32722-6]
56 **Sato T**, Vries RG, Snippert HJ, van de Wetering M, Barker N, Stange DE, van Es JH, Abo A, Kujala P, Peters PJ, Clevers H. Single Lgr5 stem cells build crypt-villus structures in vitro without a mesenchymal niche. *Nature* 2009; **459**: 262-265 [PMID: 19329995 DOI: 10.1038/nature07935]

57 **Lancaster MA**, Knoblich JA. Organogenesis in a dish: modeling development and disease using organoid technologies. *Science* 2014; **345**: 1247125 [PMID: 25035496 DOI: 10.1126/science.1247125]

58 **Huch M**, Koo BK. Modeling mouse and human development using organoid cultures. *Development* 2015; **142**: 3113-3125 [PMID: 26395140 DOI: 10.1242/dev.118570]

59 **Schutgens F**, Clevers H. Human Organoids: Tools for Understanding Biology and Treating Diseases. *Annu Rev Pathol* 2020; **15**: 211-234 [PMID: 31550983 DOI: 10.1146/annurev-pathmechdis-012419-032611]

60 **Nuciforo S**, Heim MH. Organoids to model liver disease. *JHEP Rep* 2021; **3**: 100198 [PMID: 33241206 DOI: 10.1016/j.jhepr.2020.100198]

61 **Chi KY**, Kim J. Recent advances in liver organoids and their use in in vitro modeling of non-alcoholic fatty liver disease. *Organoid* 2022; **2**: e6 [DOI: 10.51335/organoid.2022.2.e6]

62 **Ramli MNB**, Lim YS, Koe CT, Demircioglu D, Tng W, Gonzales KAU, Tan CP, Szczerbinska I, Liang H, Soe EL, Lu Z, Ariyachet C, Yu KM, Koh SH, Yaw LP, Jumat NHB, Lim JSY, Wright G, Shabbir A, Dan YY, Ng HH, Chan YS. Human Pluripotent Stem Cell-Derived Organoids as Models of Liver Disease. *Gastroenterology* 2020; **159**: 1471-1486.e12 [PMID: 32553762 DOI: 10.1053/j.gastro.2020.06.010]

63 **Ouchi R**, Togo S, Kimura M, Shinozawa T, Koido M, Koike H, Thompson W, Karns RA, Mayhew CN, McGrath PS, McCauley HA, Zhang RR, Lewis K, Hakozaki S, Ferguson A, Saiki N, Yoneyama Y, Takeuchi I, Mabuchi Y, Akazawa C, Yoshikawa HY, Wells JM, Takebe T. Modeling Steatohepatitis in Humans with Pluripotent Stem Cell-Derived Organoids. *Cell Metab* 2019; **30**: 374-384.e6 [PMID: 31155493 DOI: 10.1016/j.cmet.2019.05.007]

64 **Hendriks D**, Brouwers JF, Hamer K, Geurts MH, Luciana L, Massalini S, López-Iglesias C, Peters PJ, Rodríguez-Colman MJ, Chuva de Sousa Lopes S, Artegiani B, Clevers H. Engineered human hepatocyte organoids enable CRISPR-based target discovery and drug screening for steatosis. *Nat Biotechnol* 2023; **41**: 1567-1581 [PMID: 36823355 DOI: 10.1038/s41587-023-01680-4]

65 **Li Z**, Zhang C, Weiner LP, Zhang Y, Zhong JF. Molecular characterization of heterogeneous mesenchymal stem cells with single-cell transcriptomes. *Biotechnol Adv* 2013; **31**: 312-317 [PMID: 23266308 DOI: 10.1016/j.biotechadv.2012.12.003]

66 **Rebelatto CLK**, Boldrini-Leite LM, Daga DR, Marsaro DB, Vaz IM, Jamur VR, de Aguiar AM, Vieira TB, Furman BP, Aguiar CO, Brofman PRS. Quality Control Optimization for Minimizing Security Risks Associated with Mesenchymal Stromal Cell-Based Product Development. *Int J Mol Sci* 2023; **24**: 12955 [PMID: 37629136 DOI: 10.3390/ijms241612955]

67 **Zhou W**, Lin J, Zhao K, Jin K, He Q, Hu Y, Feng G, Cai Y, Xia C, Liu H, Shen W, Hu X, Ouyang H. Single-Cell Profiles and Clinically Useful Properties of Human Mesenchymal Stem Cells of Adipose and Bone Marrow Origin. *Am J Sports Med* 2019; **47**: 1722-1733 [PMID: 31100005 DOI: 10.1177/0363546519848678]

68 **Huang Y**, Li Q, Zhang K, Hu M, Wang Y, Du L, Lin L, Li S, Sorokin L, Melino G, Shi Y, Wang Y. Single cell transcriptomic analysis of human mesenchymal stem cells reveals limited heterogeneity. *Cell Death Dis* 2019; **10**: 368 [PMID: 31068579 DOI: 10.1038/s41419-019-1583-4]

69 **Wang Z**, Chai C, Wang R, Feng Y, Huang L, Zhang Y, Xiao X, Yang S, Zhang Y, Zhang X. Single-cell transcriptome atlas of human mesenchymal stem cells exploring cellular heterogeneity. *Clin Transl Med* 2021; **11**: e650 [PMID: 34965030 DOI: 10.1002/ctm2.650]

70 **Luo L**, Zhou Y, Zhang C, Huang J, Du J, Liao J, Bergholt NL, Bünger C, Xu F, Lin L, Tong G, Zhou G, Luo Y. Feeder-free generation and transcriptome characterization of functional mesenchymal stromal cells from human pluripotent stem cells. *Stem Cell Res* 2020; **48**: 101990 [PMID: 32950887 DOI: 10.1016/j.scr.2020.101990]

71 **Stucky A**, Gao L, Li SC, Tu L, Luo J, Huang X, Chen X, Li X, Park TH, Cai J, Kabeer MH, Plant AS, Sun L, Zhang X, Zhong JF. Molecular Characterization of Differentiated-Resistance MSC Subclones by Single-Cell Transcriptomes. *Front Cell Dev Biol* 2022; **10**: 699144 [PMID: 35356283 DOI: 10.3389/fcell.2022.699144]

72 **Malvicini R**, Santa-Cruz D, Pacienza N, Yannarelli G. OCT4 Silencing Triggers Its Epigenetic Repression and Impairs the Osteogenic and Adipogenic Differentiation of Mesenchymal Stromal Cells. *Int J Mol Sci* 2019; **20** [PMID: 31277213 DOI: 10.3390/ijms20133268]

World Journal of Stem Cells

Submit a Manuscript: https://www.f6publishing.com

World J Stem Cells 2025 February 26; 17(2): 103599

DOI: 10.4252/wjsc.v17.i2.103599

ISSN 1948-0210 (online)

MINIREVIEWS

Asthma and stem cell therapy

Qiong-Hua Chen, Jing-Yang Zheng, Da-Chun Wang

Specialty type: Cell and tissue engineering

Provenance and peer review: Unsolicited article; Externally peer reviewed.

Peer-review model: Single blind

Peer-review report's classification

Scientific Quality: Grade B, Grade B, Grade B, Grade B, Grade D

Novelty: Grade B, Grade B, Grade B, Grade C

Creativity or Innovation: Grade B, Grade B, Grade B, Grade C

Scientific Significance: Grade B, Grade B, Grade B, Grade B

P-Reviewer: Liu L; Ventura C; Zhao K

Received: November 29, 2024

Revised: December 23, 2024

Accepted: February 5, 2025

Published online: February 26, 2025

Processing time: 87 Days and 18.9 Hours

Qiong-Hua Chen, Jing-Yang Zheng, Department of Respiratory Medicine, Quanzhou Women's and Children's Hospital, Clinical Medical College of Fujian Medical University, Quanzhou 362000, Fujian Province, China

Da-Chun Wang, The Brown Foundation Institute of Molecular Medicine for the Prevention of Human Diseases, University of Texas Medical School at Houston, Houston, TX 77030, United States

Da-Chun Wang, Stem Cell Laboratory, Second Affiliated Hospital of Fujian Medical University, Quanzhou 362000, Fujian Province, China

Corresponding author: Qiong-Hua Chen, MD, Department of Respiratory Medicine, Quanzhou Women's and Children's Hospital, Clinical Medical College of Fujian Medical University, No. 700 Fengze Street, Fengze District, Quanzhou 362000, Fujian Province, China.
cqionghua283@163.com

Abstract

The global incidence of asthma, a leading respiratory disorder affecting more than 235 million people, has dramatically increased in recent years. Characterized by chronic airway inflammation and an imbalanced response to airborne irritants, this chronic condition is associated with elevated levels of inflammatory factors and symptoms such as dyspnea, cough, wheezing, and chest tightness. Conventional asthma therapies, such as corticosteroids, long-acting β-agonists, and anti-inflammatory agents, often evoke diverse adverse reactions and fail to reduce symptoms and hospitalization rates over the long term effectively. These limitations have prompted researchers to explore innovative therapeutic strategies, including stem cell-related interventions, offering hope to those afflicted with this incurable disease. In this review, we describe the characteristics of stem cells and critically assess the potential and challenges of stem cell-based therapies to improve disease management and treatment outcomes for asthma and other diseases.

Key Words: Asthma; Stem cell; Therapy; Embryonic stem cells; Induced pluripotent stem cells; Mesenchymal stem cells; Adult stem cells

Core Tip: In this review, we provide an overview of the characteristics of stem cells, including embryonic stem cells, induced pluripotent stem cells, mesenchymal stem cells and adult stem cells, along with a summary of stem cell therapies for asthma and associated challenges. This review aims to guide future research endeavors on developing innovative stem cell therapies for asthma and other disorders.

Citation: Chen QH, Zheng JY, Wang DC. Asthma and stem cell therapy. *World J Stem Cells* 2025; 17(2): 103599
URL: https://www.wjgnet.com/1948-0210/full/v17/i2/103599.htm
DOI: https://dx.doi.org/10.4252/wjsc.v17.i2.103599

INTRODUCTION

Asthma, a chronic inflammatory airway disease affecting both children and adults, has seen a notable increase in incidence in recent years. The World Health Organization 2020 report indicates that approximately 235 million individuals suffer from asthma. Despite accounting for less than 1% of the total mortality rate from all causes, asthma significantly impacts human health and imposes a considerable economic burden. The cost of treating severe asthma cases can be 10 times higher than that of conventional therapy, consuming over 50% of global medical resources allotted for asthma[1].

Patients with asthma present with variable clinical and pathological manifestations including restricted airflow, lung tissue remodeling, and typical symptoms such as coughing, wheezing, and chest tightness. Infants frequently present with wheezing, and a significant proportion progress to chronic asthma by 6 years of age. However, three-quarters of school-aged children with asthma outgrow the disease by adulthood[2], while adults with asthma often experience incomplete remission[3,4]. Asthma is driven by an exaggerated T helper type 2 (Th2) immune response characterized by excess numbers of CD4+ T cells that produce interleukin 4 (IL-4) and IL-5. This response leads to the production of allergen-specific immunoglobulin E (IgE) and eosinophil accumulation that trigger chronic airway inflammation, culminating in airway remodeling marked by basement membrane thickening, goblet cell hyperplasia, smooth muscle cell proliferation, inflammatory cell infiltration, and mucus plug formation[5,6].

Traditional asthma therapies, such as corticosteroids, long-acting β-agonists, and anti-inflammatory agents, are often associated with a broad spectrum of adverse effects such as immunosuppression induced by long-term glucocorticoids use that can increase susceptibility to infection, as well as adrenocortical insufficiency, bone damage, electrolyte disorders, high blood pressure, and hyperglycemia[7-9]. Another drawback of conventional treatments lies in their inability to effectively reverse the asthma pathogenic process, thereby contributing to the high prevalence of severe and refractory cases that underscores the urgent need for innovative prevention and treatment strategies.

Stem cells (SCs), which have self-renewal and differentiation capabilities, were first identified in the hematopoietic system in the mid-20th century. A landmark 1963 study conducted by Becker *et al*[10] showed that simple infusion of bone marrow-derived cells into the blood of lethally irradiated animals can reconstitute all blood cell populations, rescuing the animals from death, while recent studies have highlighted their potential as therapies for lung diseases such as asthma [11]. Notably, SCs exhibit a spectrum of potencies, ranging from totipotent to pluripotent, multipotent, and unipotent, each with a progressively narrower range of differentiation potential. Totipotent SCs are capable of differentiating into all cell types found within the embryonic and extraembryonic tissues (*e.g.*, placenta) of a developing organism; pluripotent cells can only differentiate into cell types found within the embryo proper, including germ cells and cells within any germ layer that can differentiate into any cell type found within a mature organism; multipotent cells are capable of differentiating into any cell type found within a specific germ layer; and unipotent cells can only differentiate into a limited number of cell types. Importantly, SCs can be derived using diverse methods from human embryos, adult somatic cells, or by enhancing the SC potential of differentiated somatic cells (Figure 1).

An overview of the characteristics of SCs is presented in this review, including embryonic SCs (ESCs), induced pluripotent SCs (iPSCs), mesenchymal SCs (MSCs), and adult SCs, along with a summary of SC therapies for asthma and associated challenges. This review aims to guide future research endeavors towards developing innovative SC therapies for asthma and other disorders.

ESCs

ESCs, typically harvested from preimplantation blastocysts around 7 to 10 days post-fertilization, offer unparalleled regenerative capabilities. Their capacity for indefinite propagation and differentiation into essentially any specialized cell type within the body sets them apart as a powerful tool for disease treatment and tissue repair[12].

Lin *et al*[13] described a murine asthma model employed to uncover the association between the therapeutic benefits of human ESC (hESC)-derived MSCs (hESC-MSCs) and the expression of crucial mRNAs in lung tissue. These mRNAs are transcribed from genes encoding chemokine C-C motif ligand 11 (CCL11), CCL24, IL-13, IL-33, and the eosinophil-associated, ribonuclease A family, member 11, as assessed using a polymerase chain reaction array[13]. Ultimately, MSCs were successfully obtained from hESCs through a simple two-step protocol that eliminated the need for fluorescence-activated cell sorting, a process that could potentially damage the cells. Following intravenous injection into the tail veins of allergic mice, the transplanted hESC-MSCs suppressed allergic inflammation in the lung tissues of animals by reducing the expression of CCL11, CCL24, IL13, IL33 (expressed in Th2 cells) and the eosinophil-associated, ribonuclease A family,

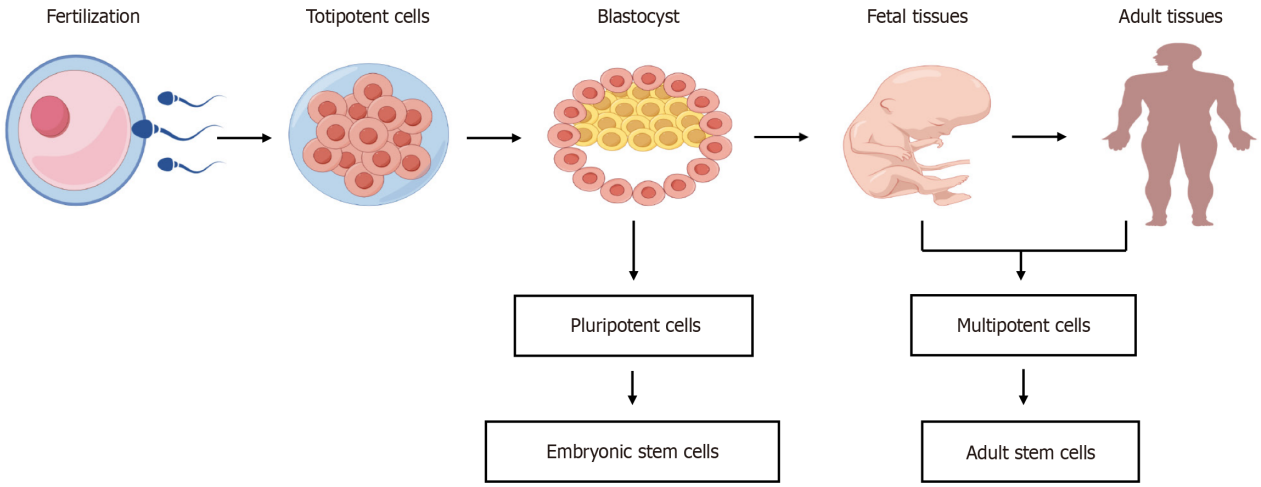

Figure 1 Development and progression and stem cell potency. The figure was drawn by Figdraw. During the earliest embryonic developmental stages, totipotent stem cells, capable of giving rise to any cell type, are present in the zygote during the initial cell divisions following fertilization. With the formation of the blastocyst, stem cells evolve into a pluripotent state, enabling them to differentiate into nearly any cell type, marking a critical step in embryonic development. As development progresses and the primitive streak forms, cells predominantly exhibit multipotent capabilities, restricting their differentiation potential to a narrow array of cell lineages excluding embryonic germ cells. In subsequent developmental phases, stem cells are classified as either 'embryonic' or 'adult,' reflecting their specific differentiation potentials and roles within an organism's cellular hierarchy.

member 11 gene (expressed in eosinophils). Additionally, the transplanted cells restored previously diminished regulatory T cells (Tregs) levels in lung tissues to normal levels. These results suggest that allergic reactions induce elevated expression of these mRNAs, which MSC-mediated immunomodulation inhibits. It is noteworthy that hESC-MSCs share biological characteristics with bone marrow-derived MSCs (BMSCs), including expression of surface markers related to multilineage differentiation and immunomodulatory states, robust proliferation and regenerative capacity and low levels of heterogeneity.

Nevertheless, challenges persist, particularly in ensuring hESC-derived cells' purity, safety, and efficacy before they are widely applied as asthma treatments in clinical settings. For example, MSC therapy has sometimes resulted in poor clinical outcomes due to inherent differences in characteristics among MSCs obtained from different donors[14]. It is, therefore, crucial to evaluate the efficiency of hESC-MSC differentiation by testing hESC-MSC cultures generated using the abovementioned protocol for potential contamination with other cell types, which could trigger unexpected side effects when transplanted. However, it is worth noting that in another study the vast majority of hESC-MSCs strongly expressed classical MSC markers cluster of differentiation 73 (CD73) (> 96.3%), CD90 (> 75.4%), and CD105 (> 99.7%) and were positive for other known MSC markers CD166 (> 45.0%), CD44 (> 98.2%), and CD146 (> 89.0%), while testing negative for the hematopoietic SC marker CD45 (< 8.0%)[13].

Although significant strides have been made in the field of ESC-related regenerative medicine, even highly pure populations of transplantable hESC-derived tissue-specific cells may be unsuitable for tissue regeneration due to low-level expression of human leukocyte antigen I that can trigger immunorejection despite their otherwise low immunogenicity. Accordingly, our laboratory developed a reliable culture and genetic selection procedure yielding the first pure population of transplantable hESCs derived from lung alveolar type II epithelial cells (hESC-ATIICs). After these cells were transplanted into the lungs of severe-combined immunodeficiency mice with bleomycin-induced acute lung injury [15], *in vivo* differentiation of hESC-ATIICs into ATICs was observed associated with repair of damaged lung tissue and long-term restoration of pulmonary function without teratoma formation. At study completion (10 days post-injury), the engrafted cells expressed ATIC phenotypic markers, strongly indicating ongoing or complete differentiation of transplanted ATIICs into ATICs, a noteworthy step towards overcoming the challenge of immunorejection within the context of ESC-derived cell transplantation-induced tissue repair. These results highlight an approach for overcoming immune rejection, paving the way for expanded clinical applications of hESCs and positioning them as a potential "universal donor" SC line with enhanced therapeutic potential.

IPSCs

In 2006, Takahashi and Yamanaka[16] introduced four transcription factors (TFs), organic cation transporter 3/4, sex determining region (SRY) box 2, c-Myc, and Kruppel-like factor 4, into mature cells lacking their expression. Intriguingly, a subset of these modified mature cells reverted to a significantly less-developed ESC-like state, highlighting the successful artificial expansion of cell pluripotency as a transformative achievement ushering in a new era in SC biology. Subsequently, iPSCs collected from an individual could differentiate into any other cell type found within that individual's body, underscoring their potential value as a tool for evaluating the efficacy and safety of 'personalized' drug therapies. However, after extended culture, these cells exhibit noticeable changes in mRNA copy number during reprogramming and epigenetic memory following differentiation and increased *in vivo* tumorigenicity.

Interestingly, treatment of asthmatic mice with iPSC-MSCs or BMSCs prior to the antigenic challenge has been shown to reduce levels of Th2-induced immunoglobulins (*e.g.*, IgE) and cytokines (*e.g.*, IL-4, IL-5, IL-13) in bronchoalveolar and/

or nasal lavage fluid[17,18]. Royce *et al*[19] demonstrated the superior protective effect of intranasally administered iPSCs and mesenchymoangioblast-derived MSCs against ovalbumin (OVA)-induced chronic allergic airway disease and asthma compared to corticosteroids.

In a study by Gao *et al*[20], two distinct sets of human iPSCs were employed to generate MSCs with robust proliferative capacity; heightened expression of recognized adult BMSC markers; and enhanced abilities to engage in adipogenesis, osteogenesis, and chondrogenesis. Specifically, urine cell-derived iPSCs were generated from cells isolated from human urine through reprogramming induced by electroporation of the plasmid pEP4EO2SET2K into the cells. Meanwhile, amniocyte-derived iPSCs were produced through retrovirus-mediated transduction of genes encoding organic cation transporter 4, SRY box 2, Kruppel-like factor 4, and c-Myc TFs into cells isolated from amniotic fluid. Notably, both types of iPSC-MSCs exhibited superior proliferative ability, longer life spans (over 50 passages), and lower rates of cell senescence than MSCs, highlighting their promise as a source of easily generated and well-tolerated MSCs for use in clinical applications. Additionally, these iPSC-MSCs inhibited dendritic cell differentiation, an effect attributed to both cell-cell interactions and iPSC-MSC secretion of IL-10. Unfortunately, safety assessments, including testing of iPSC-MSCs in immunodeficient mice, were lacking in these studies[20]. However, regarding the safety issue, previous studies demonstrated that two other iPSC-MSC clones suppressing allergic airway inflammation[17] were devoid of carcinogenic drifts during four months following their subcutaneous transplantation into severe-combined immunodeficiency mice [21]. In practice, incomplete and random reprogramming of iPSCs by TFs has been observed, associated with abnormal gene expression profiles and necessitating the rigorous screening of iPSCs using various techniques, such as whole genome sequencing, comparative genomic hybridization, single nucleotide polymorphism analysis, before deeming these iPSCs suitable for clinical applications. Within this context, our laboratory has successfully established a novel site-specific insertion-driven targeting strategy for efficiently generating mutation-free, reprogramming factor-free human iPSCs[22]. A refinement of the iPSC methodology is currently in progress, and it is poised to substantially increase the future utilization of iPSCs in therapeutic applications.

MSCs

Over the past half-century, understanding the basic and clinical aspects of asthma MSC-mediated mechanisms has advanced significantly, resulting in the emergence of MSCs as the most extensively studied cell type in experimental cell therapy (Figure 2). Beyond their potential cell replacement applications, certain MSC cell types may be capable of altering the course of a disease without undergoing engraftment. This realization prompted researchers to explore the potential of MSCs to modulate cellular responses to injury or aberrant immune cell activity. In turn, these efforts led to the early identification of a population of BMSCs capable of generating various MSC-derived populations *ex vivo*, giving rise to the concept of MSCs as a customizable tool for regenerating specific types of tissues[23,24]. Currently, MSC-derived colonies arising in culture are recognized for their ability to generate cells that could be induced to differentiate into osteoblasts, adipocytes, or chondrocytes *in vitro*. MSCs may be administered *in vivo via* intravenous, intranasal, or intratracheal routes. However, an ongoing debate persists regarding the criteria for identifying these cells and their specific functions after *in vivo* administration.

MSCs effectively modulate immune responses by suppressing activated T and B cells, inhibiting M1 macrophage differentiation and reducing antigen-presenting cell costimulation[25]. They regulate the Th1/Th2 balance, suppress pathological T cell proliferation, and offer anti-inflammatory[26], antifibrotic[27], anti-apoptotic[28], antimicrobial[29], antioxidative[30], and pro-angiogenic benefits[31]. Additionally, MSCs enhance alveolar fluid clearance[32] and repair pulmonary endothelial and epithelial cell damage[33].

MSCs, specialized cells with critical roles in regulating immune system functions and managing immune responses triggering inflammatory diseases, do not home efficiently to target tissues when infused intravenously[34], resulting in limited MSC colonization and differentiation within target tissues[35]. Despite this limitation, MSCs exert immunoregulatory effects through cell-cell contact involving two key intercellular interaction molecules: Programmed death ligand 1, a costimulatory molecule, and tumor necrosis factor (TNF) ligand superfamily member 6 (TNFSF6)[36]. In one study, during T cell recruitment, BMSCs were found to regulate monocyte chemoattractant protein-1 secretion *via* a Fas-dependent mechanism, leading to T cell apoptosis through a TNFSF6-based mechanism. Subsequently, macrophages were observed to ingest apoptotic T cell debris and release elevated quantities of transforming growth factor beta (TGF-β), triggering enhanced Treg activity and immunotolerance.

MSCs have been evaluated as potential treatments for asthma. In a study conducted by Shin *et al*[37], the therapeutic effects of human umbilical cord-MSCs were evaluated in two murine models of severe asthma, alternaria (alternata-induced) and house dust mite/diesel exhaust particle-induced asthma. Their results revealed significant post-treatment reductions in airway hyperresponsiveness, lung eosinophil levels, and direct inhibition of Th2 cell and type 2 innate lymphoid cell activities. However, Volarevic *et al*[38] revealed that MSC populations exhibited notable diversity in secreted immunoregulatory factor profiles, encompassing TGF-β, hepatocyte growth factor, nitric oxide, indoleamine 2,3-dioxygenase, IL-10, IL-6, leukemia inhibitory factor, IL-1 receptor antagonist, galectins, TNF-stimulated gene 6 protein, human leukocyte antigen-G5, heme oxygenase-1, and prostaglandin E2[38].

Previously, researchers had speculated that the multidirectional differentiation potential of MSCs might lead to their differentiation into fibroblasts and myofibroblasts during asthma progression, triggering the pathological process of airway remodeling[39]. However, recent animal studies demonstrated that MSCs can improve airway remodeling in asthmatic mice[40,41], although the specific mechanism underlying this effect remains unclear. Meanwhile, the paracrine action of MSCs has been linked to the exosome release of biologically active substances that mirrors the observed MSC-induced immunomodulatory effect. MSC exosomes (MSC-Exo) maintained in a conditioned serum-free medium and isolated *via* serial centrifugations were non-immunogenic, well-tolerated by the human body, and equipped with membrane penetration and intrinsic homing capabilities.

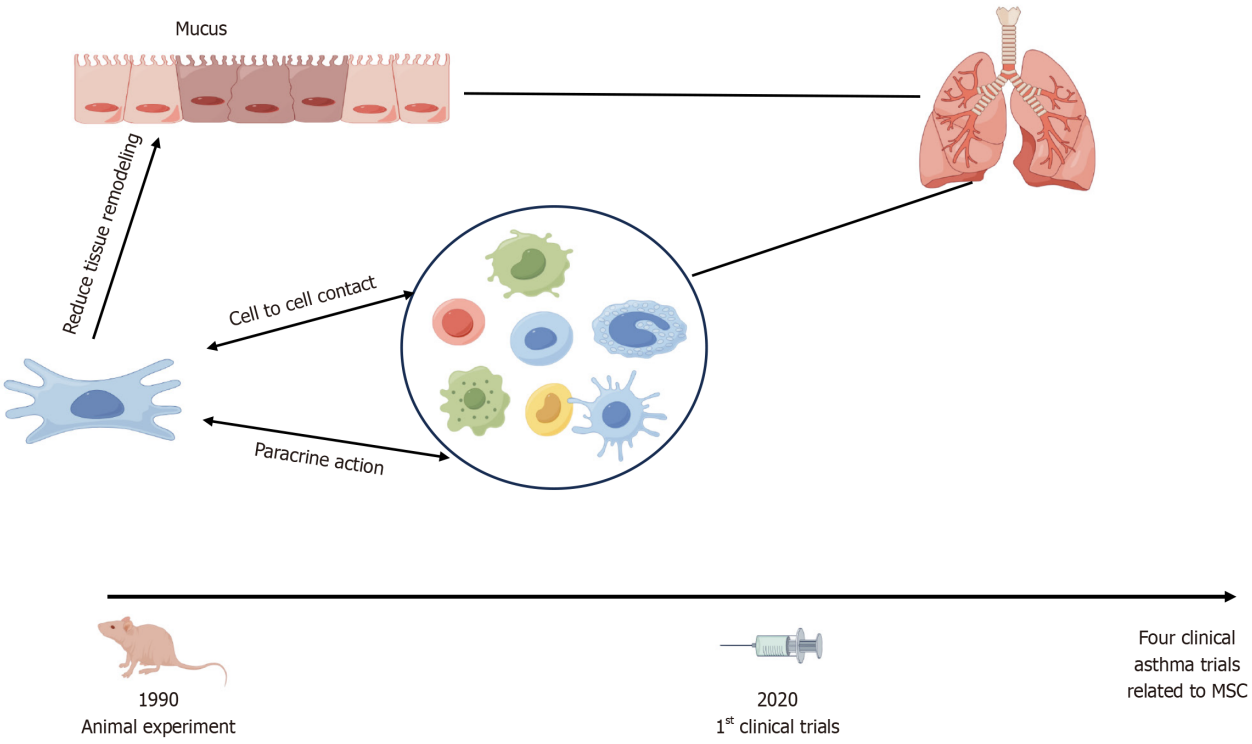

Figure 2 Experimental and clinical investigations into mesenchymal stem cell-mediated mechanisms of asthma causation. The figure was drawn by Figdraw. Mesenchymal stem cells (MSCs) reduce the production of various inflammatory factors, promote the production and release of anti-inflammatory factors, suppress the inflammatory response, restore the T helper type 1/2 balance, and repair damaged epithelial cells, while modulating the immune response through direct cell-to-cell contact. The paracrine action of MSCs is attributed to the release of exosomes containing biologically active substances that effectively mimic MSC immunomodulatory effects. After the MSC-mediated asthma mechanism was elucidated, the first clinical report describing the beneficial effects of bone marrow-derived mononuclear cell therapy in a patient with severe asthma was published in 2020. Currently, four clinical trials grounded in animal experiments are in progress, and they are evaluating the therapeutic effects of systemically administered MSCs registered on the clinicaltrials.gov platform.

MSC-Exo modulate Treg activity by upregulating levels of immunosuppressive cytokines IL-10 and TGF-β1 produced by peripheral blood mononuclear cells of asthmatic patients, a process potentially influenced by antigen-presenting cells [42]. Furthermore, MSC-Exo reversed airway hyperresponsiveness, histopathological changes, and inflammation when administered intratracheally to a severe, steroid-resistant asthma mouse model by reshaping the macrophage polarization profile[43]. MSC-Exo may be an effective therapeutic strategy for Th17-dominant neutrophilic airway inflammation by inhibiting Th17 polarization through the Janus kinase 2/signal transducer and activator of transcription 3 pathway[44]. Kun *et al*[45] found that inhibiting the Notch1/Jagged1 pathway could facilitate the migration of allogeneic BMSCs to injured lung tissues, which promotes immune regulation, corrects the Th1/Th2 imbalance, and enhances the treatment of asthmatic airway inflammation. These effects suggest that MSCs can sense their environment and restore the T cell balance in individuals with disorders primarily associated with aberrant Th1 or Th2 responses[46]. Here, we highlight strategies of MSC-derived extracellular vesicle treatment in asthma models (Figure 3) and summarize findings from the past 3 years[44,47-57], showing that MSC-Exo hold promise as a cell-free therapeutic approach (Table 1). Exosomes are administered *via* intravenous, inhalation, intratracheal, and intranasal. Combined with chemotherapy, small inhibitors, nucleic acids, or immunotherapy could enhance the outcomes in treatment.

Moreover, the differential expression of numerous microRNAs (miRNAs), including miR-146a-5p[57], miR-223-3p[51], miR-138-5p[58], miRNA-let-7, miRNA-155, and miRNA-126, is associated with allergic airway inflammation[59], making these miRNAs potential therapeutic targets in human MSC-based therapy (part of these references are discussed in Table 1). At the same time, the miR-21/activin A receptor type 2A axis has emerged as a crucial mechanism implicated in asthmatic inflammation in both a mouse model of asthma and in human subjects with asthma[60]. Furthermore, human MSCs genetically modified to afford inhibition of miR-138-5p, showed enhanced ability to reduce inflammation and allergic reactions by activating sirtuin 1 and inhibiting the high-mobility group box 1/Toll-like receptor 4 pathway in an asthma mouse model[58]. Shan *et al*[48] found that human bone marrow-MSC-derived exosomes reduced BMSC proliferation and lung injury in asthmatic mice *via* the miR-188/Jumonji, AT-rich interactive domain 2/Wnt/β-catenin pathway. In addition, externally originating MSCs have been observed to migrate towards lung tissue, accumulating at damage sites and then differentiating into type I and type II alveolar epithelial cells that participate in tissue restoration and repair *in vivo*[61,62]. Although their roles in this process remain unclear, the perceived weak differentiation ability of MSCs has prompted researchers to focus increasingly on studying their immunomodulatory effects on the repair of damaged and diseased tissues instead of their transplantation and differentiation behaviors.

Placenta-derived MSCs exerted an anti-IL-5 effect *in vitro* and reduced IL-5 level in culture with peripheral blood mononuclear cells that had been isolated from different subgroups of children with asthma[63]. Concurrently, another study conducted around the same time demonstrated that therapeutic administration of human MSCs to a mouse model

Table 1 Details regarding mesenchymal stem cell-derived extracellular vesicles treatment of asthma models in the past 3 years (2022-2024)

Ref.	MSC-dosage and frequency	MSC-EV source	Asthma animal model	Asthma replication model	Animal numbers	Delivery	Cargo	EV markers
Firouzabadi *et al*[47], 2024	15 μg, 1 time	HBMSC	Male BALB/c mice	Sensitized and challenged with OVA	Total = 43, C = 11, A = 11, T = 21	IV + IT	N/A	CD105, CD63
Shan *et al*[48], 2022	20 μg, 9 times	HBMSC	BALB/c mice	Sensitized and challenged with OVA	Total = 30, C = 10, A = 10, T = 10	IV	MiR-188, miR-124, miR-410, miR-223, miR-130a	CD81, TSG101
Liu *et al*[49], 2022	100 μg, 3 times	MBMSC	BALB/c mice	Sensitized and challenged with OVA	Total = 24, C = 8, A = 8, T = 8	IT	N/A	CD9, CD63, CD81, TSG101
Feng *et al*[50], 2022	NP	NP	Male BALB/c mice	Sensitized and challenged with OVA	Total = 15, C = 5, A = 5, T = 5	NP	Some transfected with miR-301a-3	CD63, CD9
Li *et al*[51], 2023	NP	MBMSC	Male SD rats	Sensitized and challenged with OVA	Total = 32, C = 8, A = 8, T = 16	IV	MiR-223-3p	CD9, CD63, CD81
Xu *et al*[52], 2023	40 μg, 4 times	Hypoxic, HUCMSC	Female BALB/c mice	Sensitized and challenged with OVA	Total = 21, C = 4, A = 5, IV T = 6, INH T = 6	INH and IV	Some vesicles were transfected with miR-146a-5p	TSG101, HSP70
Bandeira *et al*[53], 2023	2×10^9 particles, 1 time	HBMSC	C57BL/6 male mice	Sensitized and challenged with OVA	Total = 15, C = 5, A = 5, T = 5	IN	N/A	Flotillin-1, CD81, and β-actin
Dehnavi *et al*[54], 2023	NP	MAMSC	Female BALB/c mice	Sensitized and challenged with OVA	Total = 20, C = 5, A = 5, OVA-EV T = 5, normal EV T = 5	SL	OVA	CD9, CD63
Asadirad *et al*[55], 2023	NP, 6 times	MAMSC	Female BALB/c mice	Sensitized and challenged with OVA	Total = 20, C = 5, A = 5, T = 10	SL	OVA	CD9, CD63
Luo *et al*[56], 2024	40 μg, 4 times	Hypoxic, HUCMSC	Female BALB/c mice	Sensitized and challenged with OVA	Total = 16, C = 4, A = 6 T = 6	INH	N/A	TSG101, HSP70
Liu *et al*[57], 2024	NP, 3 times	HUCMSC	Female C57BL/6 mice	Sensitized and challenged with DFE	Total = 24, C = 6, A = 6, DFE + EVs T = 6, DFE + 146a-EVs T = 6	INH	MiR-146a-5p	CD63, HSP70, TSG101
He *et al*[44], 2024	2×10^{10} particles, 3 times	Human iPSC-MSCs	Female C57BL/6 mice	Sensitized with OVA and LPS, challenged with OVA	Total = 15, C = 5, A = 5, T = 5	IV	N/A	CD9, CD63, Alix, TSG101, calnexin

A: Asthmatic; C: Control; CD: Cluster of differentiation; DFE: Dermatophagoides farinae extract; EVs: Extracellular vesicles; HBMSC: Human bone marrow mesenchymal stem cell; HSP70: 70-kDa heat shock protein; HUMSC: Human umbilical cord mesenchymal stem cell; IN: Intranasal INH: Inhalation; iPSC-MSC: Induced pluripotent stem cell derived mesenchymal stem cell; IV: Intravenous; IT: Intratracheal; M-AMSC: Murine adipose tissue mesenchymal stem cell; MBMSC: Murine bone marrow mesenchymal stem cell; MSC: Mesenchymal stem cell; N/A: Not applicable; NP: Not provided; OVA: Ovalbumin; SL: Sublingual; T: Treated; TSG101: Tumor susceptibility gene 101.

of allergic asthma positively impacted oxidative stress by decreasing nitrotyrosine levels in lung tissues[64]. Similarly, Hu *et al*[65] reported a reduction in inflammation and oxidative stress to improve therapeutic outcomes in lung injury of acute respiratory distress syndrome by a new technique of integrating biomaterials and therapeutic agents through the fusion of mitochondria with liposomes. Interactions with probiotics also exerted antioxidant effects through the action of antioxidant enzymes[66]. Surprisingly, even nonviable MSCs, such as apoptotic MSCs, have been shown to exert immunosuppressive effects *in vivo*[67].

Shortly after the abovementioned studies were completed, a 12-month study was conducted to evaluate the significance of repeated intravenous MSC infusions. The study's findings revealed that 12-month administration of MSCs initiated after the onset of chronic allergic feline asthma did not lead to reduced airway inflammation and hyperresponsiveness, as assessed using computed tomographic measurements of airway remodeling. However, reduced airway remodeling was observed earlier, after 8 months of treatment[68]. More recently, researchers discovered that a single

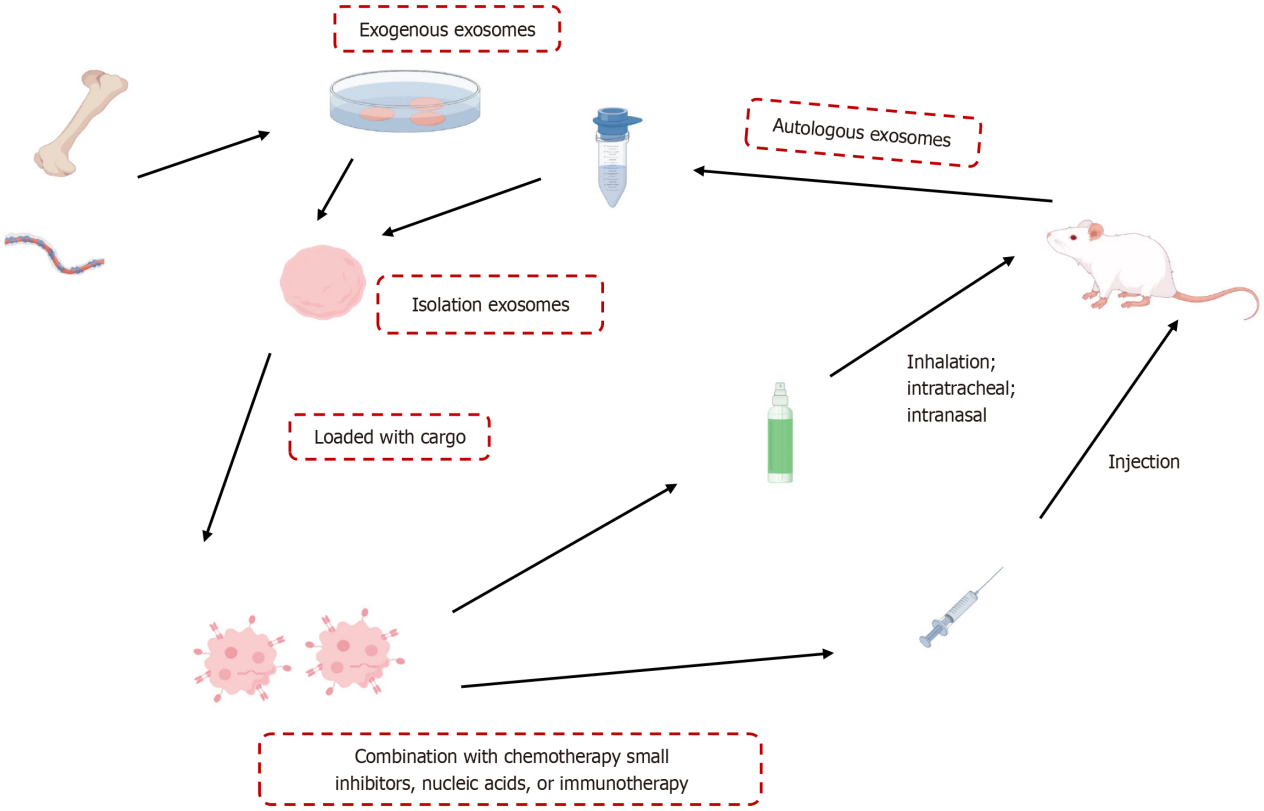

Figure 3 Mesenchymal stem cell-exosomes treatment of asthma models purified exogenous and autologous exosomes derived from mesenchymal stem cells express various functions in treating asthma in animal models. The figure was drawn by Figdraw. Intravenous, inhalation, intratracheal, and intranasal administration for delivering exosomes, as well as the cargo carried by the exosomes, could have important effects on treatment.

injection of human MSCs was significantly more effective than double injections in reducing OVA-induced airway inflammation in a mouse model. Although systemic delivery of cell therapy through infusion is thought to achieve optimal therapeutic efficiency and targeting of lung tissues after optimization of MSC size and treatment frequency[69], both local and systemic administration of a single dose of MSCs were shown to reduce inflammation and lung tissue remodeling in OVA- and aspergillus hyphal extract-induced allergic asthma models[70,71]. Conversely, a single dose of MSCs did not improve lung function or remodeling in house dust mite extract-induced allergic asthma. In contrast, multiple MSC doses reduce lung inflammation, stimulate tissue remodeling, improve lung mechanics, and promote T cell-mediated immunosuppression[70]. Consequently, these outcomes should be carefully considered in future clinical trials when evaluating potential MSC-based asthma therapies.

Most MSC-based trials are currently in their early stages (primarily Phase 1 or 2), with only a limited number progressing to Phase 3[72]. As of May 2020, 68 clinical trials related to MSCs and respiratory diseases were underway, as documented in the clinical registration research database[73]. Among these, coronavirus disease 2019 emerged as the most frequent target condition (31 ongoing trials), followed closely by acute respiratory distress syndrome and chronic obstructive pulmonary disease (10 trials each), idiopathic pulmonary fibrosis (six trials) and asthma (two trials). The remaining nine trials focused on a broad range of diseases, including cystic fibrosis, lung transplantation, pneumoconiosis, radiation-induced injury, and unspecified lung injury. In terms of trial phases, thirty trials were classified as Phase 1, 17 as combined Phase 1/2, 14 as Phase 2, two as combined Phase 2/3, and one as Phase 3.

In 2020, a report revealed treatment outcomes for three individuals who have severe asthma refractory to conventional therapies, including steroids, bronchodilators, and anti-IgE medications are not effective for severe asthma, but SC therapy is effective. These patients received a single intravenous treatment with autologous BMSCs (2×10^7 cells/patient) and then were monitored for 1 year for therapeutic and adverse effects. The study's results demonstrated that administering autologous BMSCs *via* intravenous infusion was safe and effective in improving self-perceived quality of life, as assessed during the early post-procedure phase. Lung function and the 6-minute walk test measurements remained stable throughout[74]. These findings paved the way for future clinical investigations of treatments based on BMSCs or alternative cell types for patients diagnosed with severe asthma.

In 2023, Sharan *et al*[75] reported preliminary findings related to the first participant with asthma enrolled in a Phase 1 clinical trial (Safety of cultured allogeneic adult umbilical cord derived mesenchymal SC intravenous infusion for the treatment of pulmonary diseases, NCT05147688). This trial involved intravenous infusion of cultured MSCs derived from umbilical cord tissue, administered at a dosage of 100 million cells over a 40-minute period. Encouragingly, no adverse events or complications were noted at 2 months and 6 months post-treatment, while improvement in the participant's condition persisted throughout the 6-month follow-up period. These results underscore the potential safety and efficacy of MSC-based therapies for pulmonary diseases, warranting further validation in more extensive clinical trials.

To date, four early-stage clinical studies employing SC therapies for asthma are registered in the clinical trials database, of which three are Phase 1 trials (http://clinicaltrials.gov) (Table 2). Notably, umbilical cord MSCs are the prevailing MSC type utilized in two of these trials, while allogeneic MSCs under evaluation in three of the four trials have exhibited robust immunomodulatory properties. As anticipated, MSCs were predominantly administered *via* the intravenous route (two trials), while intranasal delivery was employed in one trial. It is important to note that these studies are not designed to rule out potential adverse effects of therapy, including uncontrolled MSC proliferation, vascular blockage occurring after intravascular administration, and abnormal differentiation of injected MSCs. Nonetheless, before MSCs can be used for asthma treatment and other clinical applications, MSC dose/dosage, formulation, route of administration, frequency, and indications[76] must be optimized in animal models.

Importantly, MSCs derived from adult or newborn tissues of different donors exhibit limited proliferative capacities, significant variability in quality, rapid loss of differentiation potential, and lower therapeutic efficacy compared to corresponding features of iPSCs and ESCs. Nevertheless, MSCs are still considered an ideal therapeutic option due to their lower immunogenicity and greater ease of preparation. At the same time, iPSCs and ESCs, due to their high proliferation rates, could potentially serve as progenitor cells for generating artificially induced MCSs with therapeutic value. Meanwhile, explorations of the effects of MSC-Exo on the expression of genes related to asthma progression through gene editing could enhance MSC regenerative capacities and effectiveness. Notably, MSC-Exo hold great promise as an alternative to MSCs that may alleviate asthma by regulating the expression of novel miRNAs and other disease-related targets awaiting identification through more comprehensive approaches, such as transcriptomics and proteomics. Such research will enhance understanding of asthma-related pathways and pave the way for developing more targeted and effective therapeutic strategies.

Adult SCs

Adult SCs, also known as tissue-specific SCs, are believed to reside in most tissues and persist throughout an individual's lifetime. These cells are considered crucial for tissue maintenance and repair, particularly in tissues with high cell turnover, such as blood, skin, and intestines, where adult SCs have been clearly identified and studied experimentally[77-79]. Meanwhile, potential adult SC populations have also been reported in tissues with low cell turnover, such as muscle, brain, and kidney[80-83], although one report of adult SCs in lung tissues was retracted[84,85].

In animal models, substantial numbers of bone marrow-derived adult SCs that produce collagen type I and α-smooth muscle actin have been detected in specific tissues, such as lung tissues of mice with OVA-induced chronic asthma[86]. However, adult SC isolation from different tissues can be challenging and an obstacle hindering exploring its potential in regenerative medicine. Within this context, the application of iPSC technology has emerged as a significantly important tool that can stimulate local tissue adult SCs to engage in tissue repair through paracrine signaling and other mechanisms, offering a promising avenue for advancing regenerative medicine.

CHALLENGES ASSOCIATED WITH THE CLINICAL USE OF SCS

Although MSCs demonstrate promising therapeutic potential for asthma, MSC-based treatment strategies remain challenging. For example, restricted *in vitro* growth, stemness decline, and harsh microenvironments hinder transplanted MSCs' therapeutic potential and clinical application prospects[87]. Allogeneic MSC infusion triggers immune memory and boosts innate responses. If their immunosuppressive function is not activated, MSCs can act like antigen-presenting cells and promote inflammation[88]. Adverse effects post-transplantation include fever, chills, headache, back pain, and numbness[89]. Several issues must be addressed before SCs can be harnessed for patient treatment in clinical settings.

The first concern revolves around tissue integration, whereby transplanted cells must seamlessly integrate into surrounding tissues to ensure physiologically beneficial outcomes. Intriguingly, certain types of SCs, such as hESC-derived endothelial cells, exhibit an inherent ability to assemble into tubular structures that can integrate within the vasculature of tissues when inoculated into animals as dispersed cells[90].

A second challenge is the high likelihood that transplanted cells will develop into tumours, with a particularly high risk noted for transplanted pluripotent cells, given their ability to generate teratomas in animal models[91]. Therefore, it is crucial to precisely determine the differentiation states of transplanted cells to avoid the delivery of residual pluripotent cells that might undergo abnormal differentiation *in vivo*. Additionally, culture procedures must be designed to minimize the proliferation of genetically aberrant and potentially hazardous cell types[92]. To address these concerns, assessing pluripotent or other cell types for genetic integrity before transplantation *in vivo* is essential.

A third challenge relates to the ability to control the differentiation of cells into specific cell types, as it can sometimes be challenging to obtain a desired cell type from pluripotent cells. Furthermore, achieving uniformity and consistency of differentiated cells may be difficult, especially when derived from certain progenitor cell types. While these challenges are daunting, they are not insurmountable, although overcoming each obstacle will require substantial effort and focus. Nevertheless, we remain confident that these hurdles will be overcome to pave the way for the continued incorporation of SCs in asthma treatment strategies[12].

CONCLUSION

This review covers fundamental SC traits, including ESCs, iPSCs, MSCs, and adult SCs. It sheds light on SC therapies for

Table 2 Brief description of four clinical asthma trials related to stem cells in the clinical trials database

NCT No	Title	Disease	Source MSCs	Auto/Allo?	Delivery	Phases	Enrollment	Ages eligible for study	Locations
02192736	Safety and feasibility study of intranasal MTF for treatment of asthma	Asthma	UCMSC-CM	Allogeneic	Intra-nasal	1/2	20	18-65 years old	Panama
03137199	Allogeneic human MSCs *via* intravenous delivery in patients with mild asthma	Asthma	BMSCs	Allogeneic	IV	1	6	18-65 years old	United States
04883320	Stem cell strategies for the treatment of chronic asthma	Asthma	MSC	Unspecified	Not provided	Not applicable	15	18-70 years old	United Kingdom
05147688	Safety of cultured allogeneic adult umbilical cord-derived mesenchymal stem cells for pulmonary diseases	Pulmonary diseases, asthma	UCMSC	Allogeneic	IV	1	20	Child, adult, older adult	Antigua and Barbuda

BMSCs: Bone marrow mesenchymal stem cells; MSC: Mesenchymal stem cell; MTF: Mesenchymal trophic factor; UCMSC-CM: Conditioned medium prepared from umbilical cord mesenchymal stem cell; UCMSC: Umbilical cord mesenchymal stem cell.

alleviating asthma. Although the mechanisms by which SCs alleviate asthma are unclear, results of animal experiments suggest that SC-based treatments may relieve asthma symptoms by effectively reducing both airway inflammation and tissue remodeling, improving oxidative stress responses and paracrine functions. Based on these findings, human clinical trials are underway to evaluate SC safety and effectiveness as treatments for asthma and other diseases.

ACKNOWLEDGEMENTS

Professor Da-Chun Wang, the important author of this review, died March 29, 2024. We would like to thank Professor Wang for the support, encouragement, and care. We will always miss him.

FOOTNOTES

Author contributions: Chen QH wrote the manuscript and designed the figures; Chen QH and Wang DC edited the manuscript; Zheng JY designed the figures; Chen QH, Zheng JY, and Wang DC provided administration support; All authors read and approved the final manuscript.

Supported by the Joint Innovation Project Funds of Huaqiao University, No. 2022YX001.

Conflict-of-interest statement: The authors have no conflicts of interest to declare.

Country of origin: China

ORCID number: Qiong-Hua Chen 0000-0002-5684-3379; Jing-Yang Zheng 0000-0002-5202-0121.

S-Editor: Wang JJ
L-Editor: Filipodia
P-Editor: Zheng XM

REFERENCES

1 **Kerkhof M**, Tran TN, Soriano JB, Golam S, Gibson D, Hillyer EV, Price DB. Healthcare resource use and costs of severe, uncontrolled eosinophilic asthma in the UK general population. *Thorax* 2018; **73**: 116-124 [PMID: 28918400 DOI: 10.1136/thoraxjnl-2017-210531]
2 **Guilbert T**, Krawiec M. Natural history of asthma. *Pediatr Clin North Am* 2003; **50**: 523-538 [PMID: 12877234 DOI: 10.1016/s0031-3955(03)00044-0]

3 **Ernst P**, Cai B, Blais L, Suissa S. The early course of newly diagnosed asthma. *Am J Med* 2002; **112**: 44-48 [PMID: 11812406 DOI: 10.1016/s0002-9343(01)01033-6]

4 **Bronnimann S**, Burrows B. A prospective study of the natural history of asthma. Remission and relapse rates. *Chest* 1986; **90**: 480-484 [PMID: 3757559 DOI: 10.1378/chest.90.4.480]

5 **Akkoc T**. Mesenchymal Stem Cells in Asthma. *Adv Exp Med Biol* 2020; **1247**: 101-108 [PMID: 31802444 DOI: 10.1007/5584_2019_460]

6 **Al-Muhsen S**, Johnson JR, Hamid Q. Remodeling in asthma. *J Allergy Clin Immunol* 2011; **128**: 451-62; quiz 463 [PMID: 21636119 DOI: 10.1016/j.jaci.2011.04.047]

7 **Asamoah F**, Kakourou A, Dhami S, Lau S, Agache I, Muraro A, Roberts G, Akdis C, Bonini M, Cavkaytar O, Flood B, Izuhara K, Jutel M, Kalayci Ö, Pfaar O, Sheikh A. Allergen immunotherapy for allergic asthma: a systematic overview of systematic reviews. *Clin Transl Allergy* 2017; **7**: 25 [PMID: 28775845 DOI: 10.1186/s13601-017-0160-0]

8 **Papadopoulos NG**, Agache I, Bavbek S, Bilo BM, Braido F, Cardona V, Custovic A, Demonchy J, Demoly P, Eigenmann P, Gayraud J, Grattan C, Heffler E, Hellings PW, Jutel M, Knol E, Lötvall J, Muraro A, Poulsen LK, Roberts G, Schmid-Grendelmeier P, Skevaki C, Triggiani M, Vanree R, Werfel T, Flood B, Palkonen S, Savli R, Allegri P, Annesi-Maesano I, Annunziato F, Antolin-Amerigo D, Apfelbacher C, Blanca M, Bogacka E, Bonadonna P, Bonini M, Boyman O, Brockow K, Burney P, Buters J, Butiene I, Calderon M, Cardell LO, Caubet JC, Celenk S, Cichocka-Jarosz E, Cingi C, Couto M, Dejong N, Del Giacco S, Douladiris N, Fassio F, Fauquert JL, Fernandez J, Rivas MF, Ferrer M, Flohr C, Gardner J, Genuneit J, Gevaert P, Groblewska A, Hamelmann E, Hoffmann HJ, Hoffmann-Sommergruber K, Hovhannisyan L, Hox V, Jahnsen FL, Kalayci O, Kalpaklioglu AF, Kleine-Tebbe J, Konstantinou G, Kurowski M, Lau S, Lauener R, Lauerma A, Logan K, Magnan A, Makowska J, Makrinioti H, Mangina P, Manole F, Mari A, Mazon A, Mills C, Mingomataj E, Niggemann B, Nilsson G, Ollert M, O'Mahony L, O'Neil S, Pala G, Papi A, Passalacqua G, Perkin M, Pfaar O, Pitsios C, Quirce S, Raap U, Raulf-Heimsoth M, Rhyner C, Robson-Ansley P, Alves RR, Roje Z, Rondon C, Rudzeviciene O, Ruëff F, Rukhadze M, Rumi G, Sackesen C, Santos AF, Santucci A, Scharf C, Schmidt-Weber C, Schnyder B, Schwarze J, Senna G, Sergejeva S, Seys S, Siracusa A, Skypala I, Sokolowska M, Spertini F, Spiewak R, Sprikkelman A, Sturm G, Swoboda I, Terreehorst I, Toskala E, Traidl-Hoffmann C, Venter C, Vlieg-Boerstra B, Whitacker P, Worm M, Xepapadaki P, Akdis CA. Research needs in allergy: an EAACI position paper, in collaboration with EFA. *Clin Transl Allergy* 2012; **2**: 21 [PMID: 23121771 DOI: 10.1186/2045-7022-2-21]

9 **Papi A**, Brightling C, Pedersen SE, Reddel HK. Asthma. *Lancet* 2018; **391**: 783-800 [PMID: 29273246 DOI: 10.1016/S0140-6736(17)33311-1]

10 **Becker AJ**, McCulloch EA, Till JE. Cytological demonstration of the clonal nature of spleen colonies derived from transplanted mouse marrow cells. *Nature* 1963; **197**: 452-454 [PMID: 13970094 DOI: 10.1038/197452a0]

11 **Quan Y**, Wang D. Clinical potentials of human pluripotent stem cells in lung diseases. *Clin Transl Med* 2014; **3**: 15 [PMID: 24995122 DOI: 10.1186/2001-1326-3-15]

12 **Blau HM**, Daley GQ. Stem Cells in the Treatment of Disease. *N Engl J Med* 2019; **380**: 1748-1760 [PMID: 31042827 DOI: 10.1056/NEJMra1716145]

13 **Lin YD**, Fan XL, Zhang H, Fang SB, Li CL, Deng MX, Qin ZL, Peng YQ, Zhang HY, Fu QL. The genes involved in asthma with the treatment of human embryonic stem cell-derived mesenchymal stem cells. *Mol Immunol* 2018; **95**: 47-55 [PMID: 29407576 DOI: 10.1016/j.molimm.2018.01.013]

14 **Kim N**, Cho SG. Overcoming immunoregulatory plasticity of mesenchymal stem cells for accelerated clinical applications. *Int J Hematol* 2016; **103**: 129-137 [PMID: 26662288 DOI: 10.1007/s12185-015-1918-6]

15 **Wang D**, Morales JE, Calame DG, Alcorn JL, Wetsel RA. Transplantation of human embryonic stem cell-derived alveolar epithelial type II cells abrogates acute lung injury in mice. *Mol Ther* 2010; **18**: 625-634 [PMID: 20087316 DOI: 10.1038/mt.2009.317]

16 **Takahashi K**, Yamanaka S. Induction of pluripotent stem cells from mouse embryonic and adult fibroblast cultures by defined factors. *Cell* 2006; **126**: 663-676 [PMID: 16904174 DOI: 10.1016/j.cell.2006.07.024]

17 **Sun YQ**, Deng MX, He J, Zeng QX, Wen W, Wong DS, Tse HF, Xu G, Lian Q, Shi J, Fu QL. Human pluripotent stem cell-derived mesenchymal stem cells prevent allergic airway inflammation in mice. *Stem Cells* 2012; **30**: 2692-2699 [PMID: 22987325 DOI: 10.1002/stem.1241]

18 **Zhang R**, Yin Z, Pan J, Zhai C, Athari SS, Dong L. Effect of transfected induced pluripotent stem cells with Decorin gene on control of lung remodeling in allergic asthma. *J Investig Med* 2023; **71**: 235-243 [PMID: 36803044 DOI: 10.1177/10815589221140590]

19 **Royce SG**, Mao W, Lim R, Kelly K, Samuel CS. iPSC- and mesenchymoangioblast-derived mesenchymal stem cells provide greater protection against experimental chronic allergic airways disease compared with a clinically used corticosteroid. *FASEB J* 2019; **33**: 6402-6411 [PMID: 30768365 DOI: 10.1096/fj.201802307R]

20 **Gao WX**, Sun YQ, Shi J, Li CL, Fang SB, Wang D, Deng XQ, Wen W, Fu QL. Effects of mesenchymal stem cells from human induced pluripotent stem cells on differentiation, maturation, and function of dendritic cells. *Stem Cell Res Ther* 2017; **8**: 48 [PMID: 28253916 DOI: 10.1186/s13287-017-0499-0]

21 **Lian Q**, Zhang Y, Zhang J, Zhang HK, Wu X, Zhang Y, Lam FF, Kang S, Xia JC, Lai WH, Au KW, Chow YY, Siu CW, Lee CN, Tse HF. Functional mesenchymal stem cells derived from human induced pluripotent stem cells attenuate limb ischemia in mice. *Circulation* 2010; **121**: 1113-1123 [PMID: 20176987 DOI: 10.1161/CIRCULATIONAHA.109.898312]

22 **Yan Q**, Quan Y, Sun H, Peng X, Zou Z, Alcorn JL, Wetsel RA, Wang D. A site-specific genetic modification for induction of pluripotency and subsequent isolation of derived lung alveolar epithelial type II cells. *Stem Cells* 2014; **32**: 402-413 [PMID: 24123810 DOI: 10.1002/stem.1570]

23 **Friedenstein AJ**, Petrakova KV, Kurolesova AI, Frolova GP. Heterotopic of bone marrow. Analysis of precursor cells for osteogenic and hematopoietic tissues. *Transplantation* 1968; **6**: 230-247 [PMID: 5654088 DOI: 10.1097/00007890-196803000-00009]

24 **Pittenger MF**, Mackay AM, Beck SC, Jaiswal RK, Douglas R, Mosca JD, Moorman MA, Simonetti DW, Craig S, Marshak DR. Multilineage potential of adult human mesenchymal stem cells. *Science* 1999; **284**: 143-147 [PMID: 10102814 DOI: 10.1126/science.284.5411.143]

25 **Wang M**, Yuan Q, Xie L. Mesenchymal Stem Cell-Based Immunomodulation: Properties and Clinical Application. *Stem Cells Int* 2018; **2018**: 3057624 [PMID: 30013600 DOI: 10.1155/2018/3057624]

26 **Iyer SS**, Rojas M. Anti-inflammatory effects of mesenchymal stem cells: novel concept for future therapies. *Expert Opin Biol Ther* 2008; **8**: 569-581 [PMID: 18407762 DOI: 10.1517/14712598.8.5.569]

27 **El Agha E**, Kramann R, Schneider RK, Li X, Seeger W, Humphreys BD, Bellusci S. Mesenchymal Stem Cells in Fibrotic Disease. *Cell Stem Cell* 2017; **21**: 166-177 [PMID: 28777943 DOI: 10.1016/j.stem.2017.07.011]

28 **Li JW**, Wei L, Han Z, Chen Z. Mesenchymal stromal cells-derived exosomes alleviate ischemia/reperfusion injury in mouse lung by transporting anti-apoptotic miR-21-5p. *Eur J Pharmacol* 2019; **852**: 68-76 [PMID: 30682335 DOI: 10.1016/j.ejphar.2019.01.022]

29 **Silva-Carvalho AÉ**, Cardoso MH, Alencar-Silva T, Bogéa GMR, Carvalho JL, Franco OL, Saldanha-Araujo F. Dissecting the relationship between antimicrobial peptides and mesenchymal stem cells. *Pharmacol Ther* 2022; **233**: 108021 [PMID: 34637839 DOI: 10.1016/j.pharmthera.2021.108021]

30 **Wang X**, Zhao S, Lai J, Guan W, Gao Y. Anti-Inflammatory, Antioxidant, and Antifibrotic Effects of Gingival-Derived MSCs on Bleomycin-Induced Pulmonary Fibrosis in Mice. *Int J Mol Sci* 2021; **23**: 99 [PMID: 35008524 DOI: 10.3390/ijms23010099]

31 **Kim SY**, Lee JH, Kim HJ, Park MK, Huh JW, Ro JY, Oh YM, Lee SD, Lee YS. Mesenchymal stem cell-conditioned media recovers lung fibroblasts from cigarette smoke-induced damage. *Am J Physiol Lung Cell Mol Physiol* 2012; **302**: L891-L908 [PMID: 22307909 DOI: 10.1152/ajplung.00288.2011]

32 **Li JW**, Wu X. Mesenchymal stem cells ameliorate LPS-induced acute lung injury through KGF promoting alveolar fluid clearance of alveolar type II cells. *Eur Rev Med Pharmacol Sci* 2015; **19**: 2368-2378 [PMID: 26214771]

33 **Qin H**, Zhao A. Mesenchymal stem cell therapy for acute respiratory distress syndrome: from basic to clinics. *Protein Cell* 2020; **11**: 707-722 [PMID: 32519302 DOI: 10.1007/s13238-020-00738-2]

34 **Devine SM**, Cobbs C, Jennings M, Bartholomew A, Hoffman R. Mesenchymal stem cells distribute to a wide range of tissues following systemic infusion into nonhuman primates. *Blood* 2003; **101**: 2999-3001 [PMID: 12480709 DOI: 10.1182/blood-2002-06-1830]

35 **Gupta N**, Su X, Popov B, Lee JW, Serikov V, Matthay MA. Intrapulmonary delivery of bone marrow-derived mesenchymal stem cells improves survival and attenuates endotoxin-induced acute lung injury in mice. *J Immunol* 2007; **179**: 1855-1863 [PMID: 17641052 DOI: 10.4049/jimmunol.179.3.1855]

36 **Akiyama K**, Chen C, Wang D, Xu X, Qu C, Yamaza T, Cai T, Chen W, Sun L, Shi S. Mesenchymal-stem-cell-induced immunoregulation involves FAS-ligand-/FAS-mediated T cell apoptosis. *Cell Stem Cell* 2012; **10**: 544-555 [PMID: 22542159 DOI: 10.1016/j.stem.2012.03.007]

37 **Shin JW**, Ryu S, Ham J, Jung K, Lee S, Chung DH, Kang HR, Kim HY. Mesenchymal Stem Cells Suppress Severe Asthma by Directly Regulating Th2 Cells and Type 2 Innate Lymphoid Cells. *Mol Cells* 2021; **44**: 580-590 [PMID: 34462397 DOI: 10.14348/molcells.2021.0101]

38 **Volarevic V**, Gazdic M, Simovic Markovic B, Jovicic N, Djonov V, Arsenijevic N. Mesenchymal stem cell-derived factors: Immuno-modulatory effects and therapeutic potential. *Biofactors* 2017; **43**: 633-644 [PMID: 28718997 DOI: 10.1002/biof.1374]

39 **Saunders R**, Siddiqui S, Kaur D, Doe C, Sutcliffe A, Hollins F, Bradding P, Wardlaw A, Brightling CE. Fibrocyte localization to the airway smooth muscle is a feature of asthma. *J Allergy Clin Immunol* 2009; **123**: 376-384 [PMID: 19081612 DOI: 10.1016/j.jaci.2008.10.048]

40 **Royce SG**, Rele S, Broughton BRS, Kelly K, Samuel CS. Intranasal administration of mesenchymoangioblast-derived mesenchymal stem cells abrogates airway fibrosis and airway hyperresponsiveness associated with chronic allergic airways disease. *FASEB J* 2017; **31**: 4168-4178 [PMID: 28626025 DOI: 10.1096/fj.201700178R]

41 **Mariñas-Pardo L**, Mirones I, Amor-Carro O, Fraga-Iriso R, Lema-Costa B, Cubillo I, Rodríguez Milla MÁ, García-Castro J, Ramos-Barbón D. Mesenchymal stem cells regulate airway contractile tissue remodeling in murine experimental asthma. *Allergy* 2014; **69**: 730-740 [PMID: 24750069 DOI: 10.1111/all.12392]

42 **Du YM**, Zhuansun YX, Chen R, Lin L, Lin Y, Li JG. Mesenchymal stem cell exosomes promote immunosuppression of regulatory T cells in asthma. *Exp Cell Res* 2018; **363**: 114-120 [PMID: 29277503 DOI: 10.1016/j.yexcr.2017.12.021]

43 **Dong B**, Wang C, Zhang J, Zhang J, Gu Y, Guo X, Zuo X, Pan H, Hsu AC, Wang G, Wang F. Exosomes from human umbilical cord mesenchymal stem cells attenuate the inflammation of severe steroid-resistant asthma by reshaping macrophage polarization. *Stem Cell Res Ther* 2021; **12**: 204 [PMID: 33761997 DOI: 10.1186/s13287-021-02244-6]

44 **He BX**, Fang SB, Xie YC, Lou DX, Wu ZC, Li CG, Liu XQ, Zhou ZR, Huang LX, Tian T, Chen DH, Fu QL. Small extracellular vesicles derived from human mesenchymal stem cells prevent Th17-dominant neutrophilic airway inflammation *via* immunoregulation on Th17 cells. *Int Immunopharmacol* 2024; **133**: 112126 [PMID: 38669946 DOI: 10.1016/j.intimp.2024.112126]

45 **Kun W**, Xiaomei C, Lei Y, Huizhi Z. Modulating Th1/Th2 drift in asthma-related immune inflammation by enhancing bone mesenchymal stem cell homing through targeted inhibition of the Notch1/Jagged1 signaling pathway. *Int Immunopharmacol* 2024; **130**: 111713 [PMID: 38387192 DOI: 10.1016/j.intimp.2024.111713]

46 **Le Blanc K**, Mougiakakos D. Multipotent mesenchymal stromal cells and the innate immune system. *Nat Rev Immunol* 2012; **12**: 383-396 [PMID: 22531326 DOI: 10.1038/nri3209]

47 **Firouzabadi SR**, Mohammadi I, Ghafourian K, Kiani A, Hashemi SM. Correction: Mesenchymal Stem Cell-Derived Extracellular Vesicle Therapy for Asthma in Murine Models: A Systematic Review and Meta-analysis. *Stem Cell Rev Rep* 2024; **20**: 1374 [PMID: 38630360 DOI: 10.1007/s12015-024-10718-2]

48 **Shan L**, Liu S, Zhang Q, Zhou Q, Shang Y. Human bone marrow-mesenchymal stem cell-derived exosomal microRNA-188 reduces bronchial smooth muscle cell proliferation in asthma through suppressing the JARID2/Wnt/β-catenin axis. *Cell Cycle* 2022; **21**: 352-367 [PMID: 34974799 DOI: 10.1080/15384101.2021.2020432]

49 **Liu W**, Lin H, Nie W, Wan J, Jiang Q, Zhang A. Exosomal miR-221-3p Derived from Bone Marrow Mesenchymal Stem Cells Alleviates Asthma Progression by Targeting FGF2 and Inhibiting the ERK1/2 Signaling Pathway. *Evid Based Complement Alternat Med* 2022; **2022**: 5910874 [PMID: 35990834 DOI: 10.1155/2022/5910874]

50 **Feng CY**, Bai SY, Li ML, Zhao JY, Sun JM, Bao HJ, Ren Y, Su XM. Adipose-Derived Mesenchymal Stem Cell-Derived Exosomal miR-301a-3p Regulates Airway Smooth Muscle Cells During Asthma by Targeting STAT3. *J Asthma Allergy* 2022; **15**: 99-110 [PMID: 35115789 DOI: 10.2147/JAA.S335680]

51 **Li X**, Yang N. Exosome miR-223-3p in the bone marrow-derived mesenchymal stem cells alleviates the inflammation and airway remodeling through NLRP3-induced ASC/Caspase-1/GSDMD signaling pathway. *Int Immunopharmacol* 2023; **123**: 110746 [PMID: 37549514 DOI: 10.1016/j.intimp.2023.110746]

52 **Xu X**, Wang Y, Luo X, Gao X, Gu W, Ma Y, Xu L, Yu M, Liu X, Liu J, Wang X, Zheng T, Mao C, Dong L. A non-invasive strategy for suppressing asthmatic airway inflammation and remodeling: Inhalation of nebulized hypoxic hUCMSC-derived extracellular vesicles. *Front Immunol* 2023; **14**: 1150971 [PMID: 37090722 DOI: 10.3389/fimmu.2023.1150971]

53 **Bandeira E**, Jang SC, Lässer C, Johansson K, Rådinger M, Park KS. Effects of mesenchymal stem cell-derived nanovesicles in experimental allergic airway inflammation. *Respir Res* 2023; **24**: 3 [PMID: 36604658 DOI: 10.1186/s12931-023-02310-y]

54 **Dehnavi S**, Khodadadi A, Asadirad A, Ghadiri AA. Immune response modulation by allergen loaded into mesenchymal stem cell-derived exosomes as an effective carrier through sublingual immunotherapy. *Immunobiology* 2023; **228**: 152361 [PMID: 36870143 DOI: 10.1016/j.imbio.2023.152361]

55 **Asadirad A**, Ghadiri AA, Amari A, Ghasemi Dehcheshmeh M, Sadeghi M, Dehnavi S. Sublingual prophylactic administration of OVA-loaded MSC-derived exosomes to prevent allergic sensitization. *Int Immunopharmacol* 2023; **120**: 110405 [PMID: 37270928 DOI:

10.1016/j.intimp.2023.110405]
56 **Luo X**, Wang Y, Mao Y, Xu X, Gu W, Li W, Mao C, Zheng T, Dong L. Nebulization of Hypoxic hUCMSC-EVs Attenuates Airway Epithelial Barrier Defects in Chronic Asthma Mice by Transferring CAV-1. *Int J Nanomedicine* 2024; **19**: 10941-10959 [PMID: 39493276 DOI: 10.2147/IJN.S476151]
57 **Liu J**, Xu Z, Yu J, Zang X, Jiang S, Xu S, Wang W, Hong S. MiR-146a-5p engineered hucMSC-derived extracellular vesicles attenuate Dermatophagoides farinae-induced allergic airway epithelial cell inflammation. *Front Immunol* 2024; **15**: 1443166 [PMID: 39364406 DOI: 10.3389/fimmu.2024.1443166]
58 **Tang H**, Han X, Li T, Feng Y, Sun J. Protective effect of miR-138-5p inhibition modified human mesenchymal stem cell on ovalbumin-induced allergic rhinitis and asthma syndrome. *J Cell Mol Med* 2021; **25**: 5038-5049 [PMID: 33973707 DOI: 10.1111/jcmm.16473]
59 **Tang GN**, Li CL, Yao Y, Xu ZB, Deng MX, Wang SY, Sun YQ, Shi JB, Fu QL. MicroRNAs Involved in Asthma After Mesenchymal Stem Cells Treatment. *Stem Cells Dev* 2016; **25**: 883-896 [PMID: 27106170 DOI: 10.1089/scd.2015.0339]
60 **Wu XB**, Wang MY, Zhu HY, Tang SQ, You YD, Xie YQ. Overexpression of microRNA-21 and microRNA-126 in the patients of bronchial asthma. *Int J Clin Exp Med* 2014; **7**: 1307-1312 [PMID: 24995087]
61 **Ai WJ**, Li J, Lin SM, Li W, Liu CZ, Lv WM. R-Smad signaling-mediated VEGF expression coordinately regulates endothelial cell differentiation of rat mesenchymal stem cells. *Stem Cells Dev* 2015; **24**: 1320-1331 [PMID: 25603382 DOI: 10.1089/scd.2014.0253]
62 **Sueblinvong V**, Loi R, Eisenhauer PL, Bernstein IM, Suratt BT, Spees JL, Weiss DJ. Derivation of lung epithelium from human cord blood-derived mesenchymal stem cells. *Am J Respir Crit Care Med* 2008; **177**: 701-711 [PMID: 18063840 DOI: 10.1164/rccm.200706-859OC]
63 **Lin SC**, Liou YM, Ling TY, Chuang YH, Chiang BL. Placenta-Derived Mesenchymal Stem Cells Reduce the Interleukin-5 Level Experimentally in Children with Asthma. *Int J Med Sci* 2019; **16**: 1430-1438 [PMID: 31673233 DOI: 10.7150/ijms.33590]
64 **Malaquias MAS**, Oyama LA, Jericó PC, Costa I, Padilha G, Nagashima S, Lopes-Pacheco M, Rebelatto CLK, Michelotto PV, Xisto DG, Brofman PRS, Rocco PRM, de Noronha L. Effects of mesenchymal stromal cells play a role the oxidant/antioxidant balance in a murine model of asthma. *Allergol Immunopathol (Madr)* 2018; **46**: 136-143 [PMID: 29174587 DOI: 10.1016/j.aller.2017.06.003]
65 **Hu H**, Zhang W, Zhou Y, Zhao K, Kuang J, Liu X, Li G, Xi Y. Engineered mitochondrial ROS scavenger nanocomplex to enhance lung biodistribution and reduce inflammation for the treatment of ARDS. *Adv Compos Hybrid Mater* 2024; **7**: 194 [DOI: 10.1007/s42114-024-00989-1]
66 **Wen X**, Qi LM, Zhao K. Influence of gut bacteria on type 2 diabetes: Mechanisms and therapeutic strategy. *World J Diabetes* 2025; **16**: 100376 [PMID: 39817222 DOI: 10.4239/wjd.v16.i1.100376]
67 **Mathias LJ**, Khong SM, Spyroglou L, Payne NL, Siatskas C, Thorburn AN, Boyd RL, Heng TS. Alveolar macrophages are critical for the inhibition of allergic asthma by mesenchymal stromal cells. *J Immunol* 2013; **191**: 5914-5924 [PMID: 24249728 DOI: 10.4049/jimmunol.1300667]
68 **Trzil JE**, Masseau I, Webb TL, Chang CH, Dodam JR, Cohn LA, Liu H, Quimby JM, Dow SW, Reinero CR. Long-term evaluation of mesenchymal stem cell therapy in a feline model of chronic allergic asthma. *Clin Exp Allergy* 2014; **44**: 1546-1557 [PMID: 25220646 DOI: 10.1111/cea.12411]
69 **Hur J**, Kang JY, Kim YK, Lee SY, Jeon S, Kim Y, Jung CK, Rhee CK. Evaluation of Human MSCs Treatment Frequency on Airway Inflammation in a Mouse Model of Acute Asthma. *J Korean Med Sci* 2020; **35**: e188 [PMID: 32537953 DOI: 10.3346/jkms.2020.35.e188]
70 **Castro LL**, Kitoko JZ, Xisto DG, Olsen PC, Guedes HLM, Morales MM, Lopes-Pacheco M, Cruz FF, Rocco PRM. Multiple doses of adipose tissue-derived mesenchymal stromal cells induce immunosuppression in experimental asthma. *Stem Cells Transl Med* 2020; **9**: 250-260 [PMID: 31746562 DOI: 10.1002/sctm.19-0120]
71 **Lathrop MJ**, Brooks EM, Bonenfant NR, Sokocevic D, Borg ZD, Goodwin M, Loi R, Cruz F, Dunaway CW, Steele C, Weiss DJ. Mesenchymal stromal cells mediate Aspergillus hyphal extract-induced allergic airway inflammation by inhibition of the Th17 signaling pathway. *Stem Cells Transl Med* 2014; **3**: 194-205 [PMID: 24436442 DOI: 10.5966/sctm.2013-0061]
72 **Trounson A**, McDonald C. Stem Cell Therapies in Clinical Trials: Progress and Challenges. *Cell Stem Cell* 2015; **17**: 11-22 [PMID: 26140604 DOI: 10.1016/j.stem.2015.06.007]
73 **Yen BL**, Yen ML, Wang LT, Liu KJ, Sytwu HK. Current status of mesenchymal stem cell therapy for immune/inflammatory lung disorders: Gleaning insights for possible use in COVID-19. *Stem Cells Transl Med* 2020; **9**: 1163-1173 [PMID: 32526079 DOI: 10.1002/sctm.20-0186]
74 **Aguiar FS**, Melo AS, Araújo AMS, Cardoso AP, de Souza SAL, Lopes-Pacheco M, Cruz FF, Xisto DG, Asensi KD, Faccioli L, Salgado ABS, Landesmann MCPP, Goldenberg RCS, Gutfilen B, Morales MM, Rocco PRM, Lapa E Silva JR. Autologous bone marrow-derived mononuclear cell therapy in three patients with severe asthma. *Stem Cell Res Ther* 2020; **11**: 167 [PMID: 32357905 DOI: 10.1186/s13287-020-01675-x]
75 **Sharan J**, Barmada A, Band N, Liebman E, Prodromos C. First Report in a Human of Successful Treatment of Asthma with Mesenchymal Stem Cells: A Case Report with Review of Literature. *Curr Stem Cell Res Ther* 2023; **18**: 1026-1029 [PMID: 36380439 DOI: 10.2174/1574888X18666221115141022]
76 **Shi Y**, Wang Y, Li Q, Liu K, Hou J, Shao C, Wang Y. Immunoregulatory mechanisms of mesenchymal stem and stromal cells in inflammatory diseases. *Nat Rev Nephrol* 2018; **14**: 493-507 [PMID: 29895977 DOI: 10.1038/s41581-018-0023-5]
77 **Gong JK**. Endosteal marrow: a rich source of hematopoietic stem cells. *Science* 1978; **199**: 1443-1445 [PMID: 75570 DOI: 10.1126/science.75570]
78 **Tumbar T**, Guasch G, Greco V, Blanpain C, Lowry WE, Rendl M, Fuchs E. Defining the epithelial stem cell niche in skin. *Science* 2004; **303**: 359-363 [PMID: 14671312 DOI: 10.1126/science.1092436]
79 **Barker N**, van Es JH, Kuipers J, Kujala P, van den Born M, Cozijnsen M, Haegebarth A, Korving J, Begthel H, Peters PJ, Clevers H. Identification of stem cells in small intestine and colon by marker gene Lgr5. *Nature* 2007; **449**: 1003-1007 [PMID: 17934449 DOI: 10.1038/nature06196]
80 **Montarras D**, Morgan J, Collins C, Relaix F, Zaffran S, Cumano A, Partridge T, Buckingham M. Direct isolation of satellite cells for skeletal muscle regeneration. *Science* 2005; **309**: 2064-2067 [PMID: 16141372 DOI: 10.1126/science.1114758]
81 **Reynolds BA**, Weiss S. Generation of neurons and astrocytes from isolated cells of the adult mammalian central nervous system. *Science* 1992; **255**: 1707-1710 [PMID: 1553558 DOI: 10.1126/science.1553558]
82 **Alexander MS**, Rozkalne A, Colletta A, Spinazzola JM, Johnson S, Rahimov F, Meng H, Lawlor MW, Estrella E, Kunkel LM, Gussoni E. CD82 Is a Marker for Prospective Isolation of Human Muscle Satellite Cells and Is Linked to Muscular Dystrophies. *Cell Stem Cell* 2016; **19**: 800-807 [PMID: 27641304 DOI: 10.1016/j.stem.2016.08.006]
83 **Garcia SM**, Tamaki S, Lee S, Wong A, Jose A, Dreux J, Kouklis G, Sbitany H, Seth R, Knott PD, Heaton C, Ryan WR, Kim EA, Hansen SL,

Hoffman WY, Pomerantz JH. High-Yield Purification, Preservation, and Serial Transplantation of Human Satellite Cells. *Stem Cell Reports* 2018; **10**: 1160-1174 [PMID: 29478895 DOI: 10.1016/j.stemcr.2018.01.022]

84 **Kajstura J**, Rota M, Hall SR, Hosoda T, D'Amario D, Sanada F, Zheng H, Ogórek B, Rondon-Clavo C, Ferreira-Martins J, Matsuda A, Arranto C, Goichberg P, Giordano G, Haley KJ, Bardelli S, Rayatzadeh H, Liu X, Quaini F, Liao R, Leri A, Perrella MA, Loscalzo J, Anversa P. Evidence for human lung stem cells. *N Engl J Med* 2011; **364**: 1795-1806 [PMID: 21561345 DOI: 10.1056/NEJMoa1101324]

85 **Drazen JM**. Retraction: Kajstura J *et al*. Evidence for Human Lung Stem Cells. N Engl J Med 2011;364:1795-806. *N Engl J Med* 2018; **379**: 1870 [PMID: 30332555 DOI: 10.1056/NEJMe1813802]

86 **Ou-Yang HF**, Han XP, Zhao F, Ti XY, Wu CG. The role of bone marrow-derived adult stem cells in a transgenic mouse model of allergic asthma. *Respiration* 2012; **83**: 74-80 [PMID: 21968331 DOI: 10.1159/000330013]

87 **Huang S**, Li Y, Zeng J, Chang N, Cheng Y, Zhen X, Zhong D, Chen R, Ma G, Wang Y. Mesenchymal Stem/Stromal Cells in Asthma Therapy: Mechanisms and Strategies for Enhancement. *Cell Transplant* 2023; **32**: 9636897231180128 [PMID: 37318186 DOI: 10.1177/09636897231180128]

88 **François M**, Romieu-Mourez R, Stock-Martineau S, Boivin MN, Bramson JL, Galipeau J. Mesenchymal stromal cells cross-present soluble exogenous antigens as part of their antigen-presenting cell properties. *Blood* 2009; **114**: 2632-2638 [PMID: 19654411 DOI: 10.1182/blood-2009-02-207795]

89 **Averyanov A**, Koroleva I, Konoplyannikov M, Revkova V, Lesnyak V, Kalsin V, Danilevskaya O, Nikitin A, Sotnikova A, Kotova S, Baklaushev V. First-in-human high-cumulative-dose stem cell therapy in idiopathic pulmonary fibrosis with rapid lung function decline. *Stem Cells Transl Med* 2020; **9**: 6-16 [PMID: 31613055 DOI: 10.1002/sctm.19-0037]

90 **Wang ZZ**, Au P, Chen T, Shao Y, Daheron LM, Bai H, Arzigian M, Fukumura D, Jain RK, Scadden DT. Endothelial cells derived from human embryonic stem cells form durable blood vessels in vivo. *Nat Biotechnol* 2007; **25**: 317-318 [PMID: 17322871 DOI: 10.1038/nbt1287]

91 **Thomson JA**, Itskovitz-Eldor J, Shapiro SS, Waknitz MA, Swiergiel JJ, Marshall VS, Jones JM. Embryonic stem cell lines derived from human blastocysts. *Science* 1998; **282**: 1145-1147 [PMID: 9804556 DOI: 10.1126/science.282.5391.1145]

92 **Merkle FT**, Ghosh S, Kamitaki N, Mitchell J, Avior Y, Mello C, Kashin S, Mekhoubad S, Ilic D, Charlton M, Saphier G, Handsaker RE, Genovese G, Bar S, Benvenisty N, McCarroll SA, Eggan K. Human pluripotent stem cells recurrently acquire and expand dominant negative P53 mutations. *Nature* 2017; **545**: 229-233 [PMID: 28445466 DOI: 10.1038/nature22312]

World Journal of Stem Cells

Submit a Manuscript: https://www.f6publishing.com

World J Stem Cells 2025 February 26; 17(2): 100621

DOI: 10.4252/wjsc.v17.i2.100621

ISSN 1948-0210 (online)

ORIGINAL ARTICLE

Retrospective Study

Effect of tandem autologous stem cell transplantation on survival in pediatric patients with high-risk solid tumors in South China

Zi-Yan Luo, Li-Qun Fan, Wen-Ling Guo, Jian-Ping Yang, Zhuo-Yan Li, Yong-Xian Huang, Hua Jiang, Xiao-Hong Zhang

Specialty type: Cell and tissue engineering

Provenance and peer review: Unsolicited article; Externally peer reviewed.

Peer-review model: Single blind

Peer-review report's classification

Scientific Quality: Grade B, Grade B, Grade C, Grade C

Novelty: Grade B, Grade B, Grade C

Creativity or Innovation: Grade B, Grade B, Grade B

Scientific Significance: Grade B, Grade B, Grade C

P-Reviewer: Goebel WS; Guo WC; Li SC

Received: August 21, 2024

Revised: December 6, 2024

Accepted: February 12, 2025

Published online: February 26, 2025

Processing time: 186 Days and 20.1 Hours

Zi-Yan Luo, Li-Qun Fan, Wen-Ling Guo, Jian-Ping Yang, Zhuo-Yan Li, Yong-Xian Huang, Hua Jiang, Division of Hematology and Oncology, Department of Pediatrics, Guangzhou Women and Children's Medical Center, Guangzhou Medical University, Guangzhou 510000, Guangdong Province, China

Xiao-Hong Zhang, Department of Pediatric Hematology Oncology, Guangdong Women and Children Hospital, Guangzhou 510000, Guangdong Province, China

Co-first authors: Zi-Yan Luo and Li-Qun Fan.

Co-corresponding authors: Hua Jiang and Xiao-Hong Zhang.

Corresponding author: Xiao-Hong Zhang, MD, Department of Pediatric Hematology Oncology, Guangdong Women and Children Hospital, No. 318 Renmin Road, Guangzhou 510000, Guangdong Province, China. 2018760286@gzhmu.edu.cn

Abstract

BACKGROUND

Despite advances in treatment, the prognosis for patients with high-risk pediatric solid tumors remains dismal. Tandem autologous stem cell transplantation (ASCT) offers promise for improving outcomes in these patients. This study aimed to examine the efficacy and prognostic factors of tandem ASCT in pediatric patients with high-risk solid tumors.

AIM

To determine the survival outcomes and prognostic factors in pediatric patients with high-risk solid tumors undergoing tandem ASCT.

METHODS

A total of 40 pediatric patients with high-risk solid tumors treated from March 2015 to August 2022 were included in this retrospective study. The diagnoses of the patients included neuroblastoma, germ cell tumors, atypical teratoid/rhabdoid tumor, medulloblastoma, and pineoblastoma. After induction chemotherapy, all patients received tandem ASCT and were allocated into two groups (group A and group B) based on high-dose chemotherapy regimens. Prognostic relevance was evaluated by examining patient characteristics, such as sex, age, lactate dehydrogenase levels, primary site, the number of metastatic sites, and

bone marrow involvement.

RESULTS

The median follow-up duration since the first ASCT was 24 months (range: 1-91 months), with 5-year overall survival (OS) and event-free survival (EFS) rates of 73% and 70%, respectively, for the entire cohort. The 3-year OS rates were 67% for group A and 87% for group B (P = 0.29), with corresponding 3-year EFS rates of 67% and 79% (P = 0.57). Among neuroblastoma patients, the 5-year OS and EFS were 69% and 63% (P = 0.23). Univariable analysis revealed a notable association of age ≥ 36 months and elevated lactate dehydrogenase level at diagnosis with poorer OS. Despite acute adverse effects, all patients demonstrated good tolerance to the treatment, with no occurrences of transplant-related mortality.

CONCLUSION

Tandem ASCT demonstrates promising survival outcomes for patients with high-risk solid tumors, particularly neuroblastoma, with manageable toxicity and no transplant-related mortality.

Key Words: Autologous stem cell transplantation; Pediatric solid tumors; Neuroblastoma; Survival outcomes; Prognostic factors

Core Tip: This study evaluates the efficacy of tandem autologous stem cell transplantation (ASCT) in improving survival outcomes for pediatric patients with high-risk solid tumors, including neuroblastoma. The results demonstrate that tandem ASCT provides encouraging 5-year overall survival and event-free survival rates, with manageable toxicity and no transplant-related mortality. Key prognostic factors, such as age and lactate dehydrogenase levels at diagnosis, were identified. This study highlights the potential of tandem ASCT as a feasible therapeutic option for high-risk pediatric solid tumors, paving the way for further optimizing treatment strategies.

Citation: Luo ZY, Fan LQ, Guo WL, Yang JP, Li ZY, Huang YX, Jiang H, Zhang XH. Effect of tandem autologous stem cell transplantation on survival in pediatric patients with high-risk solid tumors in South China. *World J Stem Cells* 2025; 17(2): 100621
URL: https://www.wjgnet.com/1948-0210/full/v17/i2/100621.htm
DOI: https://dx.doi.org/10.4252/wjsc.v17.i2.100621

INTRODUCTION

The survival rates of pediatric tumors have been reported to be significantly improved, largely due to the adoption of targeted radiation therapy, aggressive surgical procedures, and intensive multiagent chemotherapy[1]. However, significant clinical and biological heterogeneity of solid tumors persists in survival outcomes, particularly neuroblastoma. Over the past few decades, the long-term prognosis for patients with high-risk solid tumors has generally remained poor [2]. Therefore, further exploration of novel therapeutic strategies is crucial for improving clinical outcomes. Autologous stem cell transplantation (ASCT) has been reported to enhance survival rates for high-risk tumors, including neuroblastoma, retinoblastoma, rhabdomyosarcoma, Wilms tumor, non-Hodgkin's lymphoma, Hodgkin's lymphoma, osteosarcoma, Ewing sarcoma, and brain tumors, compared to standard chemotherapy[3-8]. Therefore, to improve the prognosis for patients with high-risk solid tumors, investigation was conducted on the strategies involving high-dose chemotherapy (HDCT) followed by ASCT. In ASCT, the doses of chemotherapeutic agents can be escalated, even exceeding the limits of myeloablation, without increasing toxicity to patients; therefore, higher doses are administered in most ASCT regimens to maximize antitumor cytotoxicity[9]. Several pilot trials have demonstrated the feasibility and safety of ASCT, providing evidence for its role in improving survival outcomes in high-risk pediatric tumors[10-12].

Tandem ASCT, involving two sequential transplants, may offer superior survival outcomes compared to single ASCT. Tandem ASCT allows for two cycles of HDCT, potentially enhancing cytotoxic efficacy and reducing the likelihood of relapse. However, evidence supporting tandem ASCT remains limited, and its long-term efficacy and safety in pediatric solid tumors have yet to be fully established[12]. To address this gap, a retrospective analysis was performed on 40 pediatric patients with high-risk solid tumors receiving tandem ASCT. This study sought to examine the efficacy and safety of tandem ASCT while identifying prognostic factors associated with survival outcomes.

MATERIALS AND METHODS

Patients

This study included 40 pediatric patients with high-risk solid tumors undergoing tandem ASCT at the Guangzhou

Women and Children's Medical Center between March 2015 and August 2022. Patient characteristics are summarized in Table 1. Initial diagnosis and staging were conducted for each patient based on bilateral bone marrow (BM) aspiration, computed tomography scans, and magnetic resonance imaging scans to assess distant metastasis and tumor extent. All patients were classified as stage 3 or stage 4 according to histological examination. Surgery was performed to lessen tumor burden whenever feasible, followed by conventional chemotherapy. Upon receiving 6-15 cycles of induction chemotherapy, patients achieved very good partial remission (VGPR) or complete remission (CR) before proceeding to ASCT. Only patients undergoing tandem ASCT were included in this study.

Tandem ASCT and HDCT regimens

Following induction therapy, patients underwent tandem ASCT as a consolidation therapy. The HDCT regimens adopted in this study are listed in Supplementary Table 1. All patients received etoposide/carboplatin/cyclophosphamide as the first HDCT regimen, with doses tailored to individual cases. For the second HDCT, the allocation of patients into two groups was determined by the timing and conditioning regimen. Patients in group A (n = 21) receiving transplantation before December 2019 were treated with an irinotecan/temozolomide/etoposide/carboplatin/cyclophosphamide regimen developed based on our center's experience. From January 2020, patients in group B (n = 19) who underwent transplantation were administered a busulfan/melphalan regimen following European Society for Blood and Marrow Transplantation guidelines. This regimen has demonstrated improved outcomes in solid tumors, including neuroblastoma, as reported in previous studies[13,14].

Additionally, the interval between the first and second ASCT was at least 12 weeks to reduce cumulative toxicity and facilitate patient recovery. Between the two ASCT procedures, radiotherapy was administered to optimize tumor control while minimizing cumulative toxicity, following expert recommendations from the 2021 International Neuroblastoma Risk Group and the 2024 National Comprehensive Cancer Network guidelines[15]. Radiotherapy targeting the primary tumor site or metastatic sites was delivered to all patients according to their respective manifestations. Radiation doses ranging from 20 to 25 Gy were prescribed in accordance with standard clinical practice and international guidelines. A schematic illustration summarizing the study design was shown in Figure 1.

Peripheral blood stem cell collection

Peripheral blood stem cell (PBSC) collection was carried out based on hematopoietic recovery regardless of complete marrow clearance, in alignment with established guidelines[16]. Blood counts were monitored 3-5 times weekly to track hematopoietic recovery following chemotherapy. After recovery, granulocyte colony-stimulating factor was given to patients daily at a dose of 5-10 μg/kg and maintained until the completion of leukapheresis. PBSC collection was initiated on the fifth day of granulocyte colony-stimulating factor treatment, targeting a minimum yield of 2×10^6 $CD34^+$ cells/kg and 6×10^8 mononuclear leucocyte cells/kg per ASCT. These cells were intended for BM rescue during tandem ASCT. The collected PBSCs were cryopreserved in a liquid nitrogen tank for subsequent use.

Hematological recovery

Neutrophil recovery was defined as the first of three consecutive days with an absolute neutrophil count exceeding 0.5×10^9/L. The definition of platelet recovery was the first transfusion-free day within the past seven days when the platelet count exceeded 20×10^9/L.

Statistical analysis

All statistical analyses were conducted using SPSS software (version 26.0). The Student t-test was used to evaluate the differences between the groups. Survival outcomes, including overall survival (OS) and event-free survival (EFS), were estimated using the Kaplan-Meier method, and survival rates were compared *via* the log-rank test. Univariable analysis was conducted using the χ^2 test to identify prognostic factors for disease progression. $P < 0.05$ was considered statistically significant.

RESULTS

Patient characteristics

A total of 40 patients (29 boys and 11 girls) who underwent tandem ASCT following HDCT were enrolled in this study. Patient characteristics are outlined in Table 1. The median age at diagnosis was 45 months (range: 17-108 months), with 21 patients (52.5%) aged ≥ 36 months and 19 patients (47.5%) aged < 36 months. The most common diagnosis was neuroblastoma (87.5%), followed by the germ cell tumor (5.0%), atypical teratoid/rhabdoid tumor (2.5%), medulloblastoma (2.5%), and pineoblastoma (2.5%). The abdomen was the most frequent primary site (75%), whereas the mediastinum was the second most common (15.0%). Multi-organ (≥ 3) metastasis was present in 70% of patients, and 57.5% had BM involvement at diagnosis. The median lactate dehydrogenase (LDH) level was 675 (range: 227-4003) U/L. All patients received 6-15 cycles of induction chemotherapy (median: 9 cycles) prior to the first ASCT, achieving CR/VGPR.

Hematological recovery

All patients achieved completed hematopoietic engraftment. During the first ASCT, the median time to neutrophil recovery (absolute neutrophil count > 0.5×10^9/L) was 8 days in group A and 10 days in group B, while the time to

Table 1 Patient characteristics, *n* (%)

Characteristics	Group A (*n* = 21)	Group B (*n* = 19)	Total (*n* = 40)	*P* value
Age				0.03[a]
< 36 months	5 (23.8)	14 (73.7)	19 (47.5)	
≥ 36 months	16 (76.2)	5 (26.3)	21 (52.5)	
Sex				0.19
Male	15 (71.4)	14 (73.7)	29 (75)	
Female	6 (28.6)	5 (26.3)	11 (25)	
Diagnosis				0.84
Neuroblastoma	18 (85.7)	17 (89.4)	35 (87.5)	
Germ cell tumor	2 (9.5)	0 (0)	2 (5.0)	
ATRT	1 (4.8)	0 (0)	1 (2.5)	
Medulloblastoma	0 (0)	1 (5.3)	1 (2.5)	
Pineoblastoma	0 (0)	1 (5.3)	1 (2.5)	
Primary site				0.10
Abdomen	15 (71.4)	15 (79.0)	30 (75.0)	
Mediastinum	4 (19.0)	2 (10.5)	6 (15.00)	
Testis	1 (4.8)	0 (0)	1 (2.5)	
Central nervous system	1 (4.8)	2 (10.5)	3 (7.5)	
LDH at diagnosis				0.02[a]
< 1000 U/L	18 (85.7)	13 (68.4)	31 (77.5)	
≥ 1000 U/L	3 (14.3)	6 (31.6)	9 (22.5)	
No. of chemotherapy cycles before HDCT				0.72
≤ 8 cycles	4 (19.0)	1 (5.3)	5 (12.5)	
≥ 9 cycles	17 (81.0)	18 (94.7)	35 (87.5)	
Bone marrow metastasis				0.08
Negative	9 (42.9)	8 (42.1)	17 (42.5)	
Positive	12 (57.1)	11 (57.9)	23 (57.5)	
No. of metastasized organs				0.67
1-2	6 (28.6)	6 (31.6)	12 (30.0)	
≥ 3	15 (71.4)	13 (68.4)	28 (70.0)	

[a]$P < 0.05$.

ATRT: Atypical teratoid/rhabdoid tumor; LDH: Lactate dehydrogenase; HDCT: High-dose chemotherapy.

platelet recovery was 4 days in group A and 9 days in group B. In the second ASCT, neutrophil group B recovery demonstrated faster neutrophil recovery (7 days *vs* 9 days) but required more time for platelet recovery (10 days *vs* 4 days) (Supplementary Figure 1). Differences in engraftment times were attributed to variations in conditioning regimens. Importantly, no obvious increase in toxicity was found in patients receiving extended chemotherapy cycles (10+), possibly due to effective supportive care and individualized dose strategies.

Patient survival

Among the 40 patients, 30 remained alive after a median follow-up of 24 months (range: 1-91 months). As displayed in Figure 1, the 5-year OS and EFS rates were 73% and 70%, respectively (Figure 2A and B). The 3-year OS rates were 67% for group A and 87% for group B (Figure 2C, $P = 0.29$). Similarly, the 3-year EFS rates for patients in groups A and B were 67% and 79% (Figure 2D, $P = 0.57$), respectively. In this cohort, group B demonstrated improved survival trends; however, the differences were not statistically significant.

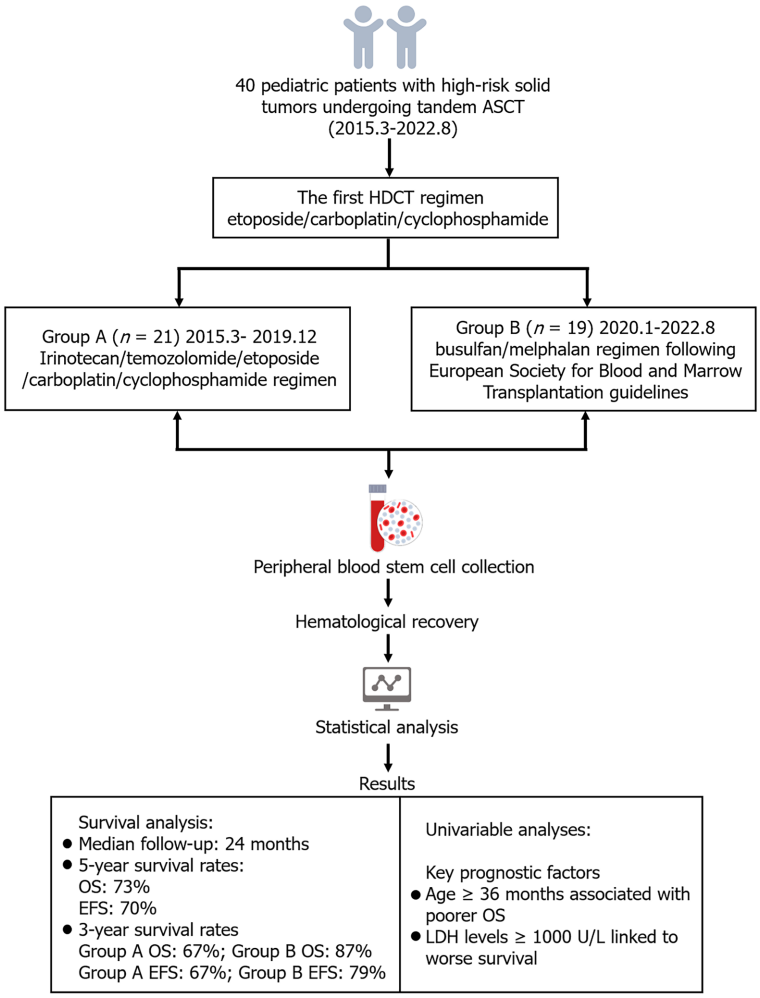

Figure 1 Schematic illustration of the study design. ASCT: Autologous stem cell transplantation; HDCT: High-dose chemotherapy; OS: Overall survival; EFS: Event-free survival; LDH: Lactate dehydrogenase.

Outcomes based on histologic type

The 40 patients were classified into five tumor groups according to histologic diagnosis: The neuroblastoma (n = 35), germ cell tumor (n = 2), atypical teratoid/rhabdoid tumor (n = 1), medulloblastoma (n = 1), and pineoblastoma (n = 1) groups. Survival rates for patients with neuroblastoma and those with other tumors are presented in Figure 2. At the time of follow-up, the 5-year OS rate for patients with neuroblastoma stood at 69%, with all patients with other tumor types still alive (Figure 3A). However, the difference in OS between neuroblastoma and other tumors did not reach statistical significance (P = 0.23).

The 5-year EFS rate was 63% among the subgroup of 35 patients with high-risk neuroblastoma who underwent tandem ASCT (Figure 3B). When comparing conditioning regimens, trends favoring group B were observed among 18 patients in group A and 17 in group B; additionally, the 3-year OS rate was 61% for group A and 87% for group B, with corresponding 3-year EFS rates of 61% and 79% (Figure 3C and D). These differences failed to reach statistical significance (P = 0.44).

Univariable analyses

Univariable analyses were conducted to identify prognostic factors linked to 3-year OS and EFS in patients with high-risk neuroblastoma (Table 2). The OS was significantly worse for patients aged ≥ 36 months at diagnosis than for those aged < 36 months (55.4% *vs* 100%, P = 0.03). Similarly, their 3-year EFS was notably lower (51.3% *vs* 100%, P = 0.03). These findings identified age ≥ 36 months as a critical adverse prognostic factor. Elevated LDH level (≥ 1000 U/L) at diagnosis was markedly associated with poorer OS compared to lower LDH levels (30% *vs* 82%, P = 0.04). Besides, elevated LDH demonstrated a trend toward poorer 3-year EFS (30.0% *vs* 77.4%); however, this difference did not reach statistical significance (P = 0.08).

Additionally, no significant survival differences were identified with respect to sex (P = 0.54) or MYCN amplification. The MYCN-amplified patients exhibited 100% OS (P = 0.10) and EFS (P = 0.12), but their sample size was limited. Survival outcomes were not significantly affected by neuron-specific enolase (NSE) levels (P > 0.05). Overall, these findings highlighted age and LDH levels as key prognostic factors, while sex, MYCN status, and NSE levels were not remarkably associated with survival.

Table 2 Univariable analysis of 35 pediatric patients with high-risk neuroblastoma, *n* (%)

Characteristics	Total (*n* = 35)	3-year OS			3-year EFS		
		mean ± SD	χ^2	*P* value	mean ± SD	χ^2	*P* value
Age							
< 36 months	10 (28.6)	100			100		
≥ 36 months	25 (71.4)	55.4 ± 12.2	4.85	0.03[a]	51.3 ± 12.0	4.85	0.03[a]
Sex							
Male	26 (74.3)	71.8 ± 10.5			67.9 ± 10.7		
Female	9 (25.7)	57.1 ± 18.7	0.37	0.54	57.1 ± 18.7	1.7	0.36
LDH							
< 1000 U/L	25 (71.4)	82.0 ± 8.1			77.4 ± 8.9		
≥ 1000 U/L	10 (28.6)	30.0 ± 22.6	4.32	0.04[a]	30.0 ± 22.6	3.15	0.08
MYCN							
Non-amplified	23 (65.7)	62.4 ± 14.0			57.9 ± 13.7		
Amplified	5 (14.3)	100			100		
Unknown	7 (20.0)	57.1 ± 18.7	2.72	0.10	57.1 ± 18.7	2.43	0.12
NSE							
< 200 ng/mL	10 (28.6)	70.0 ± 14.5			70.0 ± 14.5		
≥ 200 ng/mL	21 (60.0)	68.8 ± 14.8			63.7 ± 14.5		
Unknown	4 (11.4)	50.0 ± 25.0	0.12	0.73	50.0 ± 25.0	0.19	0.66

[a]$P < 0.05$.

OS: Overall survival; EFS: Event-free survival; LDH: Lactate dehydrogenase; NSE: Neuron-specific enolase.

Toxicity of tandem ASCT and adverse events

The toxicities associated with tandem ASCT were summarized in Table 3. Fever, vomiting, and diarrhea were the most common adverse events observed in all patients, followed by hypomagnesemia, hypokalemia, mucositis, elevated liver enzymes, myocarditis, and renal insufficiency. Infections were highly prevalent during the neutropenic period, affecting 92.5% of patients. Among them, respiratory tract infections accounted for the majority, followed by gastrointestinal infections. Detected pathogens included *Escherichia coli*, *Klebsiella pneumoniae*, and *Candida albicans*. Only three patients developed sepsis (systemic inflammatory response syndrome with bacteremia), all of whom responded successfully to antibiotic therapy. In group B, veno-occlusive disease (VOD) occurred in 15.8% of patients; however, this difference between the groups did not achieve statistical significance ($P = 0.24$). Notably, no transplant-related mortality was observed during tandem ASCT, even in patients who received up to 15 cycles of induction chemotherapy. This underscored the effectiveness of supportive care measures.

DISCUSSION

Despite recent progress in therapy, managing high-risk pediatric solid tumors remains challenging, with poor long-term survival rates[17,18]. Tandem ASCT has emerged as a promising strategy for improving outcomes in this population[19]. Numerous studies, including ours, have demonstrated the potential of tandem ASCT to enhance survival in high-risk pediatric patients, particularly those with neuroblastoma. For instance, Adra *et al*[20] highlighted the superior outcomes of tandem ASCT compared to salvage chemotherapy in adults with high-risk testicular granular cell tumor, supporting its role as a standard treatment option for this high-risk group. Therefore, this study retrospectively analyzed the efficacy of tandem ASCT in pediatric patients with high-risk solid tumors.

At least one ASCT is currently regarded as the standard of care for high-risk neuroblastoma, as confirmed by multiple studies and international guidelines[3,21]. The superiority of tandem ASCT over single ASCT remains a topic of debate. According to a large international randomized controlled trial, tandem ASCT improves EFS and OS in high-risk solid tumors as opposed to single ASCT[3]. Survival rates for tandem ASCT have been illustrated to range from 52% to 57%, whereas those for single ASCT are 48.4%[3,20,22]. This study reported 5-year OS and EFS rates of 73% and 70% for patients with high-risk solid tumors treated with tandem ASCT, demonstrating outcomes comparable to or slightly exceeding those reported in the literature. These results highlight the potential benefits of tandem ASCT in this

Table 3 Toxicity in patients with solid tumors who underwent tandem autologous stem cell transplantation, *n* (%)

Parameter	First ASCT		Second ASCT	
	Group A (*n* = 21)	Group B (*n* = 19)	Group A (*n* = 21)	Group B (*n* = 19)
Hematologic toxicity				
Fever (BT ≥ 38.0 °C)	17 (81.1)	18 (94.7)	17 (80.1)	16 (84.2)
Septicemia	2 (9.5)	1 (5.3)	0 (0)	0 (0)
Non-hematologic toxicity				
Mucositis	1 (4.8)	3 (15.8)	2 (9.5)	5 (26.3)
Vomiting	14 (66.7)	16 (84.2)	12 (57.1)	11 (57.9)
Diarrhea	10 (47.6)	13 (68.4)	10 (47.6)	11 (57.9)
Elevated liver enzymes	4 (19.0)	4 (21.1)	1 (4.7)	4 (21.1)
Renal insufficiency	0 (0)	1 (5.3)	0 (0)	1 (5.3)
Hypokalemia	5 (23.8)	10 (52.6)	2 (9.5)	4 (21.1)
Hypomagnesemia	8 (38.0)	6 (31.6)	7 (33.3)	2 (10.5)
Hepatic VOD	0 (0)	0 (0)	0 (0)	3 (15.8)
Myocarditis	2 (9.5)	1 (5.3)	0 (0)	0 (0)
Treatment-related mortality	0		0	

ASCT: Autologous stem cell transplantation; BT: Body temperature; VOD: Veno-occlusive disease.

population.

PBSC collection has emerged as another point of variability in ASCT protocols. Seif *et al*[12] reported that PBSCs collected led to a 3-year EFS of 44.8%, regardless of interim BM assessment. Our cohort, in contrast, demonstrated a markedly higher 5-year EFS of 70%, possibly due to our protocol of collecting PBSCs only when no residual tumor was detected in the BM. Additionally, all patients achieved CR/VGPR after induction chemotherapy, with response rates exceeding the 40%-70% typically reported in the literature[3,23]. These factors likely contributed to the superior outcomes observed in this study.

Univariable analysis revealed that age and LDH levels were identified as significant prognostic factors for survival, consistent with previous studies[24,25]. Patients aged ≥ 36 months at diagnosis exhibited remarkably worse OS and EFS relative to younger patients, highlighting the critical role of age in neuroblastoma risk stratification[26]. Similarly, elevated LDH levels at diagnosis (≥ 1000 U/L) were significantly associated with poorer OS, aligning with its role as a biomarker for aggressive disease. Interestingly, while OS was affected by LDH levels, these levels were not closely related to EFS. Such a result suggested a complex interplay between metabolic activity and treatment resistance. Other commonly reported prognostic factors, including sex, MYCN amplification, and NSE levels, showed no obvious correlation in our cohort, potentially attributed to the small sample size or variations in tumor biology[27-30]. Consequently, larger studies are warranted to verify these findings. Therefore, we hypothesized that more aggressive tumor biology and greater metastatic burden at diagnosis might be reflected by the poorer outcomes observed in children with elevated LDH levels, in line with prior studies[25]. Elevated LDH levels are indicative of rapid cell turnover, tissue damage, and hypoxic environments, which may contribute to resistance to intensive therapy and higher relapse rates. This finding underscores the importance of incorporating LDH levels into risk stratification and treatment planning.

Additionally, this study emphasized the need to consider the similarities between high-risk solid tumors and hematologic malignancies in the context of ASCT. Studies on hematologic cancers have consistently demonstrated the critical role of pre-transplant disease control in improving outcomes[31-33]. For instance, aggressive disease at transplant, characterized by high LDH or residual disease, has been linked to poor post-transplant survival in both settings. These similarities among malignancies could offer valuable insights into risk stratification and conditioning regimens, thereby enhancing the efficacy and safety of ASCT protocols across diverse tumor types.

Furthermore, the safety of ASCT in pediatric patients with high-risk solid tumors has been extensively demonstrated in previous studies[3,23]. As reported in a study, transplant-related mortality rates range from 2% to 15.9% in children undergoing ASCT for solid tumors[34]. However, this study revealed no transplant-related mortality, highlighting the feasibility and safety of tandem ASCT in this population. More importantly, acute toxicities during transplantation were common but manageable, including mucositis, gastrointestinal toxicity, infections, and electrolyte disturbances. Severe adverse effects, such as elevated liver enzymes, renal insufficiency, VOD, and myocarditis, were also observed. Ladenstein *et al*[23] reported a 9% incidence of VOD in neuroblastoma patients undergoing melphalan, aligning with the 7.5% observed in this study. Interestingly, while the incidence of VOD was higher in the busulfan/melphalan regimen, it was not associated with increased transplant-related mortality, further demonstrating the safety of this regimen.

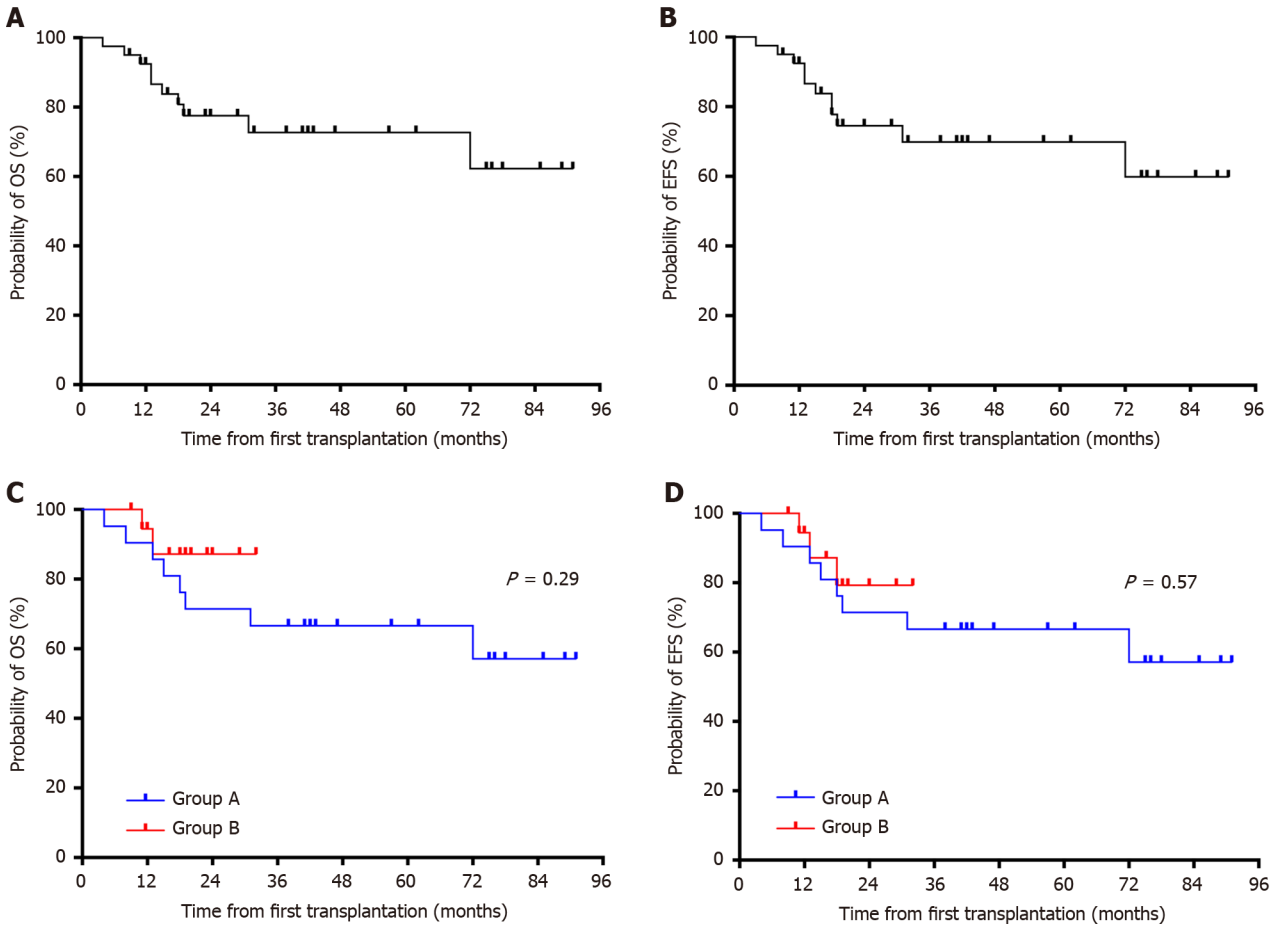

Figure 2 Results of Kaplan-Meier analysis of patient overall survival and event-free survival. A and B: Probabilities of overall survival (A) and event-free survival (B) for patients following the first autologous stem cell transplantation; C and D: Overall survival (C) and event-free survival (D) of patients in different groups after the first autologous stem cell transplantation. OS: Overall survival; EFS: Event-free survival.

Despite the controversy surrounding HDCT regimen selection, emerging evidence suggests potential advantages of certain regimens. Ladenstein *et al*[23] proposed busulfan and melphalan as a standard HDCT regimen for neuroblastoma due to their efficacy in improving EFS and reducing severe adverse events. In this study, the busulfan/melphalan regimen was preferred over the irinotecan/temozolomide regimen, particularly for hematologic recovery and lower toxicity profiles. However, carboplatin, etoposide, and melphalan have been suggested by prior research as effective regimens for transplantation[35]. Variability in reported outcomes underscores the necessity for future randomized studies to identify the optimal conditioning regimen for high-risk solid tumors. Collectively, the toxicity profile observed in this study highlighted the manageable nature of tandem ASCT, even in patients undergoing intensive induction therapy. Although the potential advantages of busulfan/melphalan regimens are observed in this study, the lack of consensus regarding the optimal HDCT regimen warrants further investigation. Future multicenter, prospective studies are critical for establishing evidence-based guidelines for conditioning regimens and toxicity management in pediatric ASCT.

Although the findings are promising, there are several limitations in this study. First, the generalizability of the results is restricted by the retrospective design and small sample size. Given the single-center nature of this study, the potential selection and reporting biases cannot be excluded. Additionally, no formal power calculation was performed, and the study may be underpowered to detect subtle differences in efficacy, safety, and prognostic factors. Future studies should incorporate predefined power analyses to ensure robust statistical comparisons. Moreover, definitive conclusions regarding the superiority of tandem ASCT over alternative approaches are precluded by the absence of a randomized control group. Furthermore, the results may have been confounded by treatment heterogeneity, including differences in conditioning regimens and maintenance therapies. Although the survival outcomes in this cohort were remarkable, the short follow-up period limits the understanding of long-term toxicities and late effects associated with tandem ASCT. Future multicenter, prospective trials with predefined statistical power, standardized treatment protocols, and extended follow-up are needed to validate these findings and develop evidence-based guidelines. These trials should include standardized conditioning regimens, toxicity management protocols, and risk stratification methods to optimize the efficacy and safety of ASCT for high-risk pediatric solid tumors.

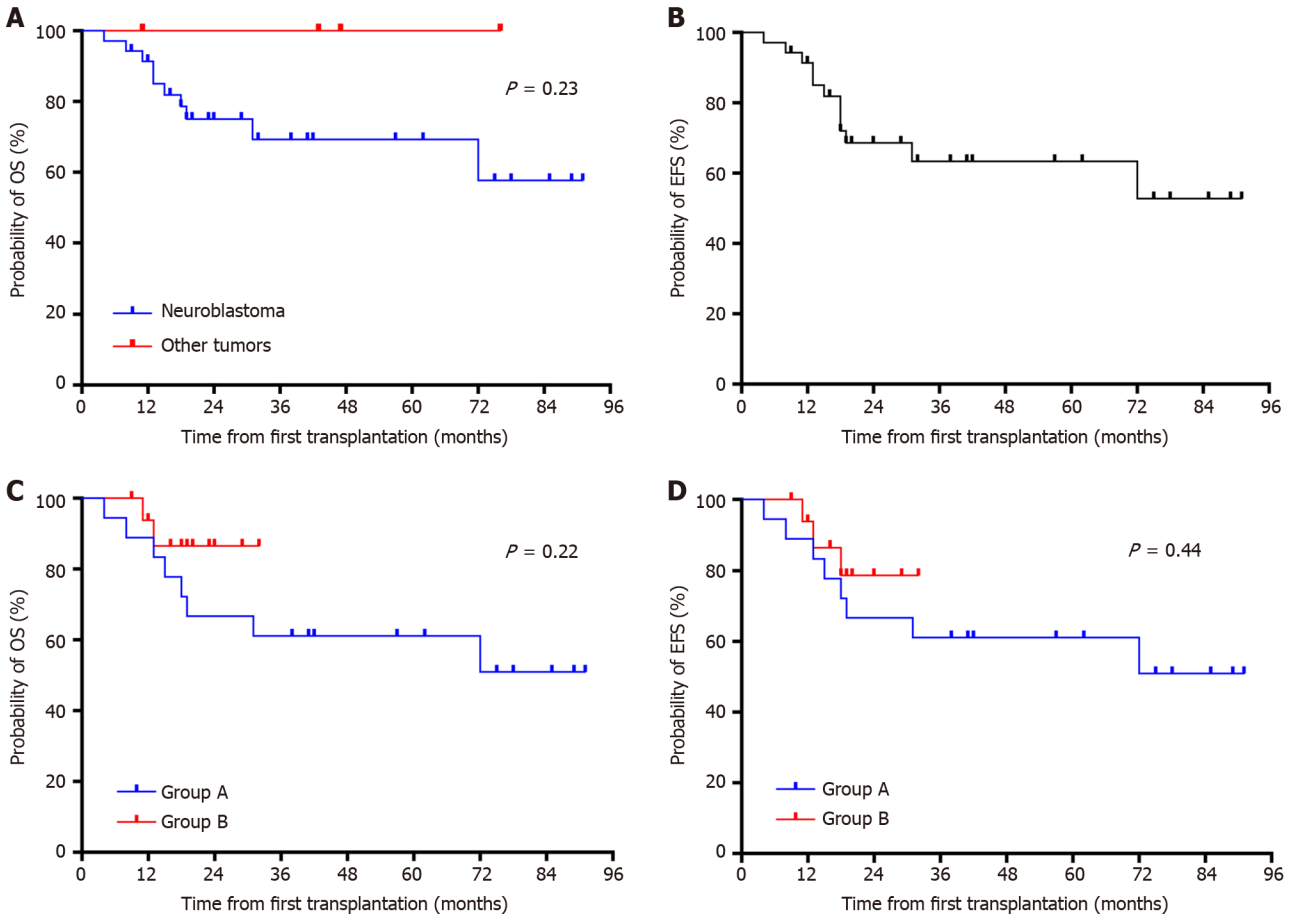

Figure 3 Results of overall survival and event-free survival analysis for patients with neuroblastoma and other tumors. A and B: Probabilities of overall survival (A) and event-free survival (B) in patients with neuroblastoma and other tumors; C and D: Overall survival (C) and event-free survival (D) of patients with neuroblastoma in different groups. OS: Overall survival; EFS: Event-free survival.

CONCLUSION

In summary, this study highlights the effectiveness of tandem ASCT in treating high-risk solid tumors, providing favorable survival outcomes with manageable toxicity. However, limitations, such as the small sample size, single-center design, and short follow-up, warrant caution in interpreting the results. Future multicenter studies with larger cohorts and extended follow-up are needed to confirm these findings and optimize treatment protocols.

FOOTNOTES

Author contributions: Luo ZY and Fan LQ are co-first authors who contributed equally to this work. Luo ZY and Fan LQ both contributed to drafting the initial manuscript; Luo ZY, Fan LQ, Jiang H, and Zhang XH designed and performed the research study; Guo WL, Yang JP, Li ZY, and Huang YX provided help and advice on experiments and analyzed the data. All authors contributed to editorial changes in the manuscript and have read and approved the final manuscript. All authors have contributed significantly to the work and agreed to be accountable for all aspects of the work. Jiang H and Zhang XH as co-corresponding authors, contributed equally to the conceptualization, supervision, and final manuscript revisions, justifying their shared authorship. Jiang H was designed as the primary contact for all journal correspondence.

Supported by Guangzhou Municipal Science and Technology Bureau, Municipal School and College Joint Funding Project, No. 2024A03J1240.

Institutional review board statement: The study was reviewed and approved by the Institutional Review Board of Guangzhou Women and Children's Medical Center, Guangzhou Medical University (Approval No. 2022-12008).

Informed consent statement: Informed consent was obtained from the legal guardians in this study.

Conflict-of-interest statement: All the authors report no relevant conflicts of interest for this article.

Data sharing statement: Data supporting the findings of this study are available from the corresponding author upon request.

Country of origin: China

ORCID number: Hua Jiang 0000-0002-4552-0785; Xiao-Hong Zhang 0009-0008-0419-5200.

S-Editor: Wang JJ
L-Editor: A
P-Editor: Li X

REFERENCES

1 **Lupo PJ**, Spector LG. Cancer Progress and Priorities: Childhood Cancer. *Cancer Epidemiol Biomarkers Prev* 2020; **29**: 1081-1094 [PMID: 32482635 DOI: 10.1158/1055-9965.EPI-19-0941]
2 **Najafi M**, Majidpoor J, Toolee H, Mortezaee K. The current knowledge concerning solid cancer and therapy. *J Biochem Mol Toxicol* 2021; **35**: e22900 [PMID: 34462987 DOI: 10.1002/jbt.22900]
3 **Park JR**, Kreissman SG, London WB, Naranjo A, Cohn SL, Hogarty MD, Tenney SC, Haas-Kogan D, Shaw PJ, Kraveka JM, Roberts SS, Geiger JD, Doski JJ, Voss SD, Maris JM, Grupp SA, Diller L. Effect of Tandem Autologous Stem Cell Transplant vs Single Transplant on Event-Free Survival in Patients With High-Risk Neuroblastoma: A Randomized Clinical Trial. *JAMA* 2019; **322**: 746-755 [PMID: 31454045 DOI: 10.1001/jama.2019.11642]
4 **Ramamurthy A**, Connolly EA, Mar J, Lewin J, Bhadri VA, Phillips MB, Winstanley M, Orme LM, Grimison P, Connor J, Lazarakis S, Hong AM, Omer N, Cayrol J. High-dose chemotherapy for Ewing sarcoma and Rhabdomyosarcoma: A systematic review by the Australia and New Zealand sarcoma association clinical practice guidelines working party. *Cancer Treat Rev* 2024; **124**: 102694 [PMID: 38325070 DOI: 10.1016/j.ctrv.2024.102694]
5 **Kobayashi R**, Inoue M, Takahashi Y, Kikuta A, Ogawa A, Koga Y, Koh K, Hashii Y, Hara J, Kato K, Tabuchi K, Matsumoto K. Autologous Stem Cell Transplantation for Children With Renal Tumors, and Adults With Wilms Tumor: Retrospective Analysis of the Japanese Transplant Registry Unified Management Program. *J Pediatr Hematol Oncol* 2020; **42**: 251-255 [PMID: 32134841 DOI: 10.1097/MPH.0000000000001779]
6 **Kang SH**, Kim W, Lee JS, Suh JK, Kim H, Kim DK, Choi SH, Cho HW, Ju HY, Yoo KH, Sung KW, Koo HH, Seo SW, Im HJ, Lee JW, Koh KN. High-dose chemotherapy followed by autologous stem cell transplantation in pediatric patients with relapsed osteosarcoma. *Pediatr Blood Cancer* 2023; **70**: e30233 [PMID: 36751119 DOI: 10.1002/pbc.30233]
7 **Hara J**, Matsumoto K, Maeda N, Takahara-Matsubara M, Sugimoto S, Goto H. High-dose thiotepa, in conjunction with melphalan, followed by autologous hematopoietic stem cell transplantation in patients with pediatric solid tumors, including brain tumors. *Bone Marrow Transplant* 2023; **58**: 123-128 [PMID: 36329150 DOI: 10.1038/s41409-022-01820-5]
8 **Alnasser SM**, Alharbi KS, Almutairy AF, Almutairi SM, Alolayan AM. Autologous Stem Cell Transplant in Hodgkin's and Non-Hodgkin's Lymphoma, Multiple Myeloma, and AL Amyloidosis. *Cells* 2023; **12**: 2855 [PMID: 38132175 DOI: 10.3390/cells12242855]
9 **Ali MO**, Al Hadidi S. High dose (conditioning) regimens used prior to autologous stem cell transplantation in multiple myeloma. *Transplant Cell Ther* 2022; **28**: 572-580 [PMID: 35750284 DOI: 10.1016/j.jtct.2022.06.013]
10 **George RE**, Li S, Medeiros-Nancarrow C, Neuberg D, Marcus K, Shamberger RC, Pulsipher M, Grupp SA, Diller L. High-risk neuroblastoma treated with tandem autologous peripheral-blood stem cell-supported transplantation: long-term survival update. *J Clin Oncol* 2006; **24**: 2891-2896 [PMID: 16782928 DOI: 10.1200/JCO.2006.05.6986]
11 **Koo J**, Silverman S, Nuechterlein B, Keating AK, Verneris MR, Foreman NK, Mulcahy Levy JM. Safety and feasibility of outpatient autologous stem cell transplantation in pediatric patients with primary central nervous system tumors. *Bone Marrow Transplant* 2019; **54**: 1605-1613 [PMID: 30783209 DOI: 10.1038/s41409-019-0479-3]
12 **Seif AE**, Naranjo A, Baker DL, Bunin NJ, Kletzel M, Kretschmar CS, Maris JM, McGrady PW, von Allmen D, Cohn SL, London WB, Park JR, Diller LR, Grupp SA. A pilot study of tandem high-dose chemotherapy with stem cell rescue as consolidation for high-risk neuroblastoma: Children's Oncology Group study ANBL00P1. *Bone Marrow Transplant* 2013; **48**: 947-952 [PMID: 23334272 DOI: 10.1038/bmt.2012.276]
13 **Proust-Houdemont S**, Pasqualini C, Blanchard P, Dufour C, Benhamou E, Goma G, Semeraro M, Raquin MA, Hartmann O, Valteau-Couanet D. Busulfan-melphalan in high-risk neuroblastoma: the 30-year experience of a single institution. *Bone Marrow Transplant* 2016; **51**: 1076-1081 [PMID: 27042850 DOI: 10.1038/bmt.2016.75]
14 **Granger MM**, Naranjo A, Bagatell R, DuBois SG, McCune JS, Tenney SC, Weiss BD, Mosse YP, Asgharzadeh S, Grupp SA, Hogarty MD, Gastier-Foster JM, Mills D, Shulkin BL, Parisi MT, London WB, Han-Chang J, Panoff J, von Allmen D, Jarzembowski JA, Park JR, Yanik GA. Myeloablative Busulfan/Melphalan Consolidation following Induction Chemotherapy for Patients with Newly Diagnosed High-Risk Neuroblastoma: Children's Oncology Group Trial ANBL12P1. *Transplant Cell Ther* 2021; **27**: 490.e1-490.e8 [PMID: 33823167 DOI: 10.1016/j.jtct.2021.03.006]
15 **Bagatell R**, Park JR, Acharya S, Aldrink J, Allison J, Alva E, Arndt C, Benedetti D, Brown E, Cho S, Church A, Davidoff A, Desai AV, DuBois S, Fair D, Farinhas J, Harrison D, Huang F, Iskander P, Kreissman S, Macy M, Na B, Pashankar F, Pendyala P, Pinto N, Polites S, Rabah R, Shimada H, Slatnick L, Sokol E, Twist C, Vo K, Watt T, Wolden S, Zage P, Schonfeld R, Hang L. Neuroblastoma, Version 2.2024, NCCN Clinical Practice Guidelines in Oncology. *J Natl Compr Canc Netw* 2024; **22**: 413-433 [PMID: 39151455 DOI: 10.6004/jnccn.2024.0040]
16 **Kreissman SG**, Seeger RC, Matthay KK, London WB, Sposto R, Grupp SA, Haas-Kogan DA, Laquaglia MP, Yu AL, Diller L, Buxton A, Park JR, Cohn SL, Maris JM, Reynolds CP, Villablanca JG. Purged versus non-purged peripheral blood stem-cell transplantation for high-risk neuroblastoma (COG A3973): a randomised phase 3 trial. *Lancet Oncol* 2013; **14**: 999-1008 [PMID: 23890779 DOI:

10.1016/S1470-2045(13)70309-7]

17 **Zhang Y**, Zhang WL, Huang DS, Wang YZ, Hu HM, Zhi T, Mei YY. Prognostic factors for intermediate- or high-risk neuroblastomas in children in China. *BMC Pediatr* 2023; **23**: 617 [PMID: 38053080 DOI: 10.1186/s12887-023-04258-w]

18 **Karalexi MA**, Servitzoglou M, Papadakis V, Kachanov D, Česen Mazič M, Baka M, Moschovi M, Kourti M, Polychronopoulou S, Stiakaki E, Hatzipantelis E, Dana H, Stefanaki K, Malama A, Themistocleous MS, Strantzia K, Shamanskaya T, Bouka P, Panagopoulou P, Kantzanou M, Ntzani E, Dessypris N, Petridou ET. Survival patterns of childhood neuroblastoma: an analysis of clinical data from Southern-Eastern European countries. *Eur J Cancer Prev* 2023; **32**: 254-263 [PMID: 32925511 DOI: 10.1097/CEJ.0000000000000614]

19 **Kitko CL**, Bollard CM, Cairo MS, Chewning J, Fry TJ, Pulsipher MA, Shenoy S, Wall DA, Levine JE. Children's Oncology Group's 2023 blueprint for research: Cellular therapy and stem cell transplantation. *Pediatr Blood Cancer* 2023; **70** Suppl 6: e30577 [PMID: 37480158 DOI: 10.1002/pbc.30577]

20 **Adra N**, Abonour R, Althouse SK, Albany C, Hanna NH, Einhorn LH. High-Dose Chemotherapy and Autologous Peripheral-Blood Stem-Cell Transplantation for Relapsed Metastatic Germ Cell Tumors: The Indiana University Experience. *J Clin Oncol* 2017; **35**: 1096-1102 [PMID: 27870561 DOI: 10.1200/JCO.2016.69.5395]

21 **Yan J**, Jie L, Jiaxing Y, Yanna C, Zhanglin L, Zhongyuan L, Daowei W, Guangzong Z, Benfu Z, Jie Y, Qiang Z. Analysis of the efficacy of autologous peripheral blood stem cell transplantation in high-risk neuroblastoma. *Int J Med Sci* 2022; **19**: 1715-1723 [PMID: 36237985 DOI: 10.7150/ijms.76305]

22 **Barrett D**, Fish JD, Grupp SA. Autologous and allogeneic cellular therapies for high-risk pediatric solid tumors. *Pediatr Clin North Am* 2010; **57**: 47-66 [PMID: 20307711 DOI: 10.1016/j.pcl.2010.01.001]

23 **Ladenstein R**, Pötschger U, Pearson ADJ, Brock P, Luksch R, Castel V, Yaniv I, Papadakis V, Laureys G, Malis J, Balwierz W, Ruud E, Kogner P, Schroeder H, de Lacerda AF, Beck-Popovic M, Bician P, Garami M, Trahair T, Canete A, Ambros PF, Holmes K, Gaze M, Schreier G, Garaventa A, Vassal G, Michon J, Valteau-Couanet D; SIOP Europe Neuroblastoma Group (SIOPEN). Busulfan and melphalan versus carboplatin, etoposide, and melphalan as high-dose chemotherapy for high-risk neuroblastoma (HR-NBL1/SIOPEN): an international, randomised, multi-arm, open-label, phase 3 trial. *Lancet Oncol* 2017; **18**: 500-514 [PMID: 28259608 DOI: 10.1016/S1470-2045(17)30070-0]

24 **Ussowicz M**, Mielcarek-Siedziuk M, Musiał J, Stachowiak M, Węcławek-Tompol J, Sęga-Pondel D, Frączkiewicz J, Trelińska J, Raciborska A. Melphalan, Etoposide, and Carboplatin Megatherapy with Autologous Stem Cell Transplantation in Children with Relapsing or Therapy-Resistant Extracranial Germ-Cell Tumors-A Retrospective Analysis. *Cancers (Basel)* 2020; **12**: 3841 [PMID: 33352733 DOI: 10.3390/cancers12123841]

25 **Tian C**, Li Y, Liu S, Chen Z, Zhang Y, Yu Y, Yang H, Zhao H, Zhao Z, Yuan T, Wang Y. Modified conditioning regimen with idarubicin followed by autologous hematopoietic stem cell transplantation for invasive B-cell non-Hodgkin's lymphoma patients. *Sci Rep* 2021; **11**: 4273 [PMID: 33608570 DOI: 10.1038/s41598-021-81944-8]

26 **Kim C**, Choi YB, Lee JW, Yoo KH, Sung KW, Koo HH. Excellent treatment outcomes in children younger than 18 months with stage 4 MYCN nonamplified neuroblastoma. *Korean J Pediatr* 2018; **61**: 53-58 [PMID: 29563945 DOI: 10.3345/kjp.2018.61.2.53]

27 **Moreno L**, Guo D, Irwin MS, Berthold F, Hogarty M, Kamijo T, Morgenstern D, Pasqualini C, Ash S, Potschger U, Ladenstein R, Valteau-Couanet D, Cohn SL, Pearson ADJ, London WB. A nomogram of clinical and biologic factors to predict survival in children newly diagnosed with high-risk neuroblastoma: An International Neuroblastoma Risk Group project. *Pediatr Blood Cancer* 2021; **68**: e28794 [PMID: 33205902 DOI: 10.1002/pbc.28794]

28 **Riley RD**, Heney D, Jones DR, Sutton AJ, Lambert PC, Abrams KR, Young B, Wailoo AJ, Burchill SA. A systematic review of molecular and biological tumor markers in neuroblastoma. *Clin Cancer Res* 2004; **10**: 4-12 [PMID: 14734444 DOI: 10.1158/1078-0432.ccr-1051-2]

29 **Cangemi G**, Reggiardo G, Barco S, Barbagallo L, Conte M, D'Angelo P, Bianchi M, Favre C, Galleni B, Melioli G, Haupt R, Garaventa A, Corrias MV. Prognostic value of ferritin, neuron-specific enolase, lactate dehydrogenase, and urinary and plasmatic catecholamine metabolites in children with neuroblastoma. *Onco Targets Ther* 2012; **5**: 417-423 [PMID: 23226699 DOI: 10.2147/OTT.S36366]

30 **Moroz V**, Machin D, Hero B, Ladenstein R, Berthold F, Kao P, Obeng Y, Pearson ADJ, Cohn SL, London WB. The prognostic strength of serum LDH and serum ferritin in children with neuroblastoma: A report from the International Neuroblastoma Risk Group (INRG) project. *Pediatr Blood Cancer* 2020; **67**: e28359 [PMID: 32472746 DOI: 10.1002/pbc.28359]

31 **Guo W**, Strouse C, Mery D, Siegel ER, Munshi MN, Ashby TC, Cheng Y, Sun F, Wanchai V, Zhang Z, Bailey C, Alapat DV, Peng H, Al Hadidi S, Thanendrarajan S, Schinke C, Zangari M, van Rhee F, Tricot G, Shaughnessy JD Jr, Zhan F. A Risk Stratification System in Myeloma Patients with Autologous Stem Cell Transplantation. *Cancers (Basel)* 2024; **16**: 1116 [PMID: 38539451 DOI: 10.3390/cancers16061116]

32 **Guo W**, Zhan Y, Mery D, Siegel ER, Sun F, Cheng Y, Ashby TC, Zhang Z, Bailey C, Alapat DV, Peng H, Hadidi SA, Thanendrarajan S, Schinke C, Zangari M, van Rhee F, Tricot G, Shaughnessy JD, Zhan F. Prognostic value of ferritin in ASCT MM patients: integration with GEP models and ISS series systems. *Blood Cancer J* 2024; **14**: 30 [PMID: 38355688 DOI: 10.1038/s41408-024-00998-9]

33 **Guo W**, Zhan A, Mery DE, Munshi MN, Makhoul O, Baily C, Zangari M, Tricot G, Peng H, Shaughnessy JD Jr. Application of R2-ISS risk stratification to patients with multiple myeloma treated with autologous stem cell transplants at UAMS. *Blood Adv* 2023; **7**: 6676-6684 [PMID: 37756524 DOI: 10.1182/bloodadvances.2023011096]

34 **Olson TL**, Pollack MM, Dávila Saldaña BJ, Patel AK. Hospital survival following pediatric HSCT: changes in complications, ICU therapies and outcomes over 10 years. *Front Pediatr* 2023; **11**: 1247792 [PMID: 37900687 DOI: 10.3389/fped.2023.1247792]

35 **Perentesis J**, Katsanis E, DeFor T, Neglia J, Ramsay N. Autologous stem cell transplantation for high-risk pediatric solid tumors. *Bone Marrow Transplant* 1999; **24**: 609-615 [PMID: 10490725 DOI: 10.1038/sj.bmt.1701950]

World Journal of Stem Cells

Submit a Manuscript: https://www.f6publishing.com

World J Stem Cells 2025 February 26; 17(2): 96893

DOI: 10.4252/wjsc.v17.i2.96893

ISSN 1948-0210 (online)

ORIGINAL ARTICLE

Basic Study

Nicotinamide adenine dinucleotide rejuvenates septic bone marrow mesenchymal stem cells

Xin Xia, Kun Zhou, Lin-Ying An, Min Zhao, Bin-Le Tian, Jin-Yan Zhao, Zhi-Gang Zhou, Yin Tong

Specialty type: Cell and tissue engineering

Provenance and peer review: Unsolicited article; Externally peer reviewed.

Peer-review model: Single blind

Peer-review report's classification

Scientific Quality: Grade A, Grade B, Grade B

Novelty: Grade B, Grade B

Creativity or Innovation: Grade B, Grade B

Scientific Significance: Grade A, Grade A

P-Reviewer: Gong L; Ventura C; Zhang GK

Received: May 17, 2024

Revised: November 19, 2024

Accepted: January 16, 2025

Published online: February 26, 2025

Processing time: 282 Days and 20 Hours

Xin Xia, Kun Zhou, Lin-Ying An, Min Zhao, Yin Tong, Department of Hematology, Shanghai General Hospital, Shanghai Jiao Tong University School of Medicine, Shanghai 200080, China

Bin-Le Tian, Cancer Center, Shanghai General Hospital, Shanghai Jiao Tong University School of Medicine, Shanghai 200080, China

Jin-Yan Zhao, Department of Laboratory Medicine, Shanghai General Hospital, Shanghai Jiao Tong University School of Medicine, Shanghai 200080, China

Zhi-Gang Zhou, Department of Critical Care Medicine, School of Medicine, Shanghai Jiao Tong University, Shanghai 201620, China

Co-first authors: Xin Xia and Kun Zhou.

Co-corresponding authors: Zhi-Gang Zhou and Yin Tong.

Corresponding author: Yin Tong, PhD, Professor, Department of Hematology, Shanghai General Hospital, Shanghai Jiao Tong University School of Medicine, No. 100 Haining Road, Shanghai 200080, China. 18616909158@163.com

Abstract

BACKGROUND

Sepsis is a severe illness characterized by systemic and multiorgan reactive responses and damage. However, the impact of sepsis on the bone marrow, particularly on bone marrow mesenchymal stem cells (BMSCs), is less reported. BMSCs are critical stromal cells in the bone marrow microenvironment that maintain bone stability and hematopoietic homeostasis; however, the impairment caused by sepsis remains unknown.

AIM

To investigate the effects of sepsis on BMSCs and the underlying mechanisms.

METHODS

BMSCs were obtained from healthy donors and patients with sepsis. We compared the self-renewal capacity, differentiation potential, and hematopoietic supportive ability *in vitro*. Senescence of septic BMSCs was assessed using β-galactosidase staining, senescence-associated secretory phenotype, intracellular reactive oxygen species levels, and the expression of P16 and P21. Finally, the changes in septic BMSCs after nicotinamide adenine dinucleotide (NAD)

treatment were evaluated.

RESULTS

Septic BMSCs showed decreased proliferation and self-renewal, bias towards adipogenic differentiation, and weakened osteogenic differentiation. Additionally, hematopoietic supportive capacity declines in sepsis. The levels of aging markers were significantly higher in the septic BMSCs. After NAD treatment, the proliferation capacity of septic BMSCs showed a recovery trend, with increased osteogenic and hematopoietic supportive capacities. Sepsis resulted in decreased expression of sirtuin 3 (SIRT3) in BMSCs, whereas NAD treatment restored SIRT3 expression, enhanced superoxide dismutase enzyme activity, reduced intracellular reactive oxygen species levels, maintained mitochondrial stability and function, and ultimately rejuvenated septic BMSCs.

CONCLUSION

Sepsis accelerates the aging of BMSCs, as evidenced by a decline in self-renewal and osteogenic capabilities, as well as weakened hematopoietic support functions. These deficiencies can be effectively reversed *via* the NAD/SIRT3/superoxide dismutase pathway.

Key Words: Sepsis; Bone mesenchymal stem cells; Hematopoietic stem cells; Senescence; Nicotinamide adenine dinucleotide

Core Tip: Sepsis often leads to multiorgan dysfunction, including damage to bone marrow mesenchymal stem cells (BMSCs). This damage accelerates the aging of BMSCs, resulting in impaired self-renewal and differentiation abilities and weakened hematopoietic support functions. These changes disrupt hematopoiesis and may even cause long-term immunosuppression and bone loss. Nicotinamide adenine dinucleotide, which protects mitochondrial function, can rejuvenate septic BMSCs and provide a new target for adjunctive therapy to control post-sepsis complications.

Citation: Xia X, Zhou K, An LY, Zhao M, Tian BL, Zhao JY, Zhou ZG, Tong Y. Nicotinamide adenine dinucleotide rejuvenates septic bone marrow mesenchymal stem cells. *World J Stem Cells* 2025; 17(2): 96893
URL: https://www.wjgnet.com/1948-0210/full/v17/i2/96893.htm
DOI: https://dx.doi.org/10.4252/wjsc.v17.i2.96893

INTRODUCTION

Sepsis is a common systemic reactive disease that can damage multiple organs and tissues[1,2]. Current research has predominantly focused on acute organ damage, such as acute lung injury and acute kidney injury, to save lives. However, the impact of sepsis on the bone marrow is often chronic and does not immediately threaten life. Few studies have focused on the damage caused by sepsis in the bone marrow. In our long-term clinical observation, patients still experienced long-term physiological abnormalities, such as persistent lymphocytopenia after discharge, causing unplanned readmissions[3], indicating the presence of prolonged damage to the hematopoietic system. Lymphocytopenia is often accompanied by granulocytosis, which is similar to the hematopoietic composition observed in elderly individuals. Hematopoietic stem cells (HSCs), which are located in the bone marrow at the headquarters of the hematopoietic system, may experience conditions similar to those of elderly individuals. The bone marrow microenvironment is a complex niche of HSCs, including immune and red blood cells at different stages as well as various stromal cells, including endothelial cells, adipocytes, osteoblasts, and neural cells[4]. A crucial cell population in the bone marrow microenvironment is bone marrow mesenchymal stem cells (BMSCs), which have the potential to differentiate into osteoblasts, adipocytes, and chondrocytes to maintain bone marrow stability[5]. BMSCs also secrete various stem cell-supportive factors to maintain their growth niche[6]. Osteoblasts derived from BMSCs form the primary niche for lymphoid progenitor cells. When BMSCs are damaged or aged, their function declines, leading to defects in the growth and multilineage differentiation of HSCs[7]. Therefore, studying sepsis-induced damage to BMSCs and treatment strategies is crucial to restore the chronically impaired HSC niche in patients with sepsis and promote healthy hematopoiesis.

Sepsis continuously consumes immune cells and damages the bone marrow, thereby inhibiting immune system recovery[8]. Although previous studies have shown that sepsis causes osteoblast ablation[9], it is unknown whether this is due to advanced defects in BMSCs. In recent years, increasing attention has been paid to the aging of BMSCs and the resulting bone health issues. Four types of senescence have been proposed: Replicative senescence, oncogene-induced senescence, stress-induced premature senescence, and developmental senescence. Patients with sepsis may be more prone to stress-induced premature senescence due to an inflammatory cytokine storm caused by infection. We compared BMSC differences between healthy individuals and septic patients and found that sepsis-affected BMSCs exhibited a more senescent state, manifested in decreased proliferation and self-renewal capabilities, biased differentiation towards adipogenesis over osteogenesis, and an inability to provide hematopoietic supportive capabilities matching those of

healthy individuals. Additionally, we identified senescence markers in septic BMSCs, including increased levels of reactive oxygen species (ROS), expression of the senescence-associated secretory phenotype (SASP), and markers related to aging P16 and P21.

Nicotinamide adenine dinucleotide (NAD) is essential for activating acetylases, rapidly consuming oxidative free radicals in cells, and aiding in cellular resistance to aging[10-12]. We found that in septic BMSCs, NAD can restore NAD-dependent sirtuin 3 (SIRT3) expression in the mitochondria, which can enhance the activity of superoxide dismutase (SOD) and reduce harmful oxidative free radicals inside the cells[13,14]. Therefore, NAD treatment rejuvenates septic BMSCs and restores their function. It should be noted that our research provides an important reference for other similar adverse conditions, such as radiation and chemical injuries.

MATERIALS AND METHODS

BMSCs culture

All samples were collected from septic patients and healthy donors (HD) aged 26 to 67 years after obtaining informed consent and approval from Shanghai General Hospital. Detailed information on the samples is provided in Supplementary Table 1. To isolate bone marrow mononuclear cells (BMNCs), we used LymphoprepTM (StemCell Technologies, 07801, Canada) following the indicated procedure. Isolated cells were cryopreserved in liquid nitrogen until they were seeded into 12-well plates. BMSCs were cultured in DMEM/F12 supplemented with 10% fetal bovine serum (FBS) (Gibco, A3161001C, MA, United States), 1% penicillin/streptomycin (Gibco, 15070063, MA, United States), 1% insulin transferrin selenium sodium pyruvate additive (Gibco, 51300044, MA, United States), 10 ng/mL epidermal growth factor (PeproTech, AF-100-15, NJ, United States), and 10 ng/mL platelet-derived growth factor BB (PeproTech, AF-100-14B, NJ, United States)[15] at 37 °C in a humidified atmosphere with 5% CO_2. Non-adherent cells were removed after one week, and the remaining cells were continuously expanded. Septic BMSCs were maintained in the above basic medium with an additional 1 mmol/L NAD for 7 days before the experiments began under certain circumstances. Cells from passages 1 to 4 were used in all experiments.

Fibroblast colony-forming unit assay

BMNCs were seeded at a density of one million cells per well in 6-well plates and incubated for 14 days with a weekly medium exchange. The colony formation units were stained with crystal violet (Beyotime, C0121, Shanghai, China) for 10 minutes and counted manually.

CCK-8 assay

A total of 5000 BMSCs derived from both HD and septic samples were seeded per well in 96-well plates. After allowing the cells to adhere for 4 hours, 10 μL of CCK-8 reagent (Yeasen, 40203ES60, Shanghai, China) was added to each well. After incubation for 2 hours, the OD at 450 nm was measured and recorded daily. Growth curves were plotted using GraphPad Prism software.

EdU assay

HD and septic BMSCs (2×10^4) were seeded in 96-well plates, and after 24 hours of adhesion, the medium was supplemented with 50 μM F-ara-EdU (Sigma, T511293, Japan). The cells were fixed 12 hours later. For F-ara-EdU staining, cells were incubated with an EdU staining working solution containing 10 μM Cy3 AZIDE (Thermo, A10266, MA, United States), 1 mmol/L $CuSO_4$ (Sigma, 908940, Japan), and 100 mmol/L (+)-sodium-L-ascorbic (Sigma, A7631, Japan) for 30 minutes at room temperature, followed by washing three times with phosphate-buffered saline (PBS). DAPI was used for nuclear staining. Images were acquired using Operetta.

Quantitative real-time polymerase chain reaction

Total RNA was extracted from cultured BMSCs using TRI Reagent (Sigma, T9424, Japan), following the manufacturer's instructions. cDNA was synthesized using a HiScript III 1st Strand cDNA Synthesis Kit (Vazyme, R312-01, Nanjing, China). Quantitative real-time polymerase chain reaction (qPCR) was performed as previously described using SYBR qPCR SuperMix plus (Novoprotein, E096, Suzhou, China). Primer sequences used in these reactions are listed in Supplementary Table 2. The relative fold-change in expression was calculated using the comparative threshold cycle ($2^{-\Delta\Delta Ct}$) method, as described in previous studies.

Flow cytometry analysis

Single digestive cells were collected and washed twice with cold PBS. Subsequently, they were blocked for 10 minutes on ice (BD Pharmingen, 564220, CA, United States) to prevent nonspecific antibody binding. Mixed antibodies were then added, and the cells were incubated at 4 °C for 30 minutes in the dark. The corresponding isotype controls were prepared using the same procedure. Finally, the stained cells were washed and resuspended in an appropriate volume of PBS containing 0.4% bovine serum albumin before evaluation using a flow cytometer (CYTOFLEX, Beckman). Data analysis was performed using FlowJo_V10 software. The antibodies used in these experiments are listed in Supplementary Table 3.

In vitro osteogenic and adipogenic differentiation

BMSCs at passage three were cultured in an appropriate induction medium for osteogenic and adipogenic differentiation [16,17]. Osteogenic medium was prepared using the MesenCultTM Osteogenic Differentiation Kit (StemCell Technologies, 05465, Canada) supplemented with 2 mmol/L L-glutamine (Gibco, 21051024, MA, United States) and 1% penicillin/streptomycin. The adipogenic medium consisted of DMEM/F12, 10% FBS, 1% penicillin/streptomycin, 1% insulin transferrin selenium sodium pyruvate additive, 60 μM indomethacin (Sigma, I7378, Japan), 10^{-6} M dexamethasone (Sigma, D4902, Japan) and 0.5 mmol/L 3-isobutyl-1-methylxanthine (Sigma, I5879, Japan). Osteogenic differentiation was evaluated after 21 days using Alizarin Red S staining and qPCR, whereas adipogenic differentiation was evaluated using Oil Red O staining and qPCR.

Alizarin Red S staining

Cell layers were fixed using methanol-acetone fixation for 30 minutes and rinsed twice with PBS, followed by 30 minutes of incubation with a 2% Alizarin Red S staining solution (Beyotime, C0138, Shanghai, China). The samples were then washed four times with distilled water, and images were captured under a light microscope. For quantification, a 10% cetylpyridinium chloride solution was used to re-dissolve the dye.

Oil Red O staining

Cells were fixed in 4% formaldehyde for 30 minutes. A stock solution of 0.5% Oil Red O saturated in isopropanol (Sigma, O0625, Japan) was prepared beforehand, and a working solution was created by diluting the stock solution with water in a ratio of 3:2. After fixation, the cells were washed once with isopropanol and incubated in the working solution for 30 minutes. Subsequently, they were washed four times with distilled water, and images were captured under a light microscope. For quantification, 100% isopropanol was used to re-dissolve the dye.

Coculture of hematopoietic stem/progenitor cells and BMSCs

BMSCs were seeded in 24-well plates and expanded for 48 hours. The purified hematopoietic stem/progenitor cells (HSPCs) from HD were seeded at a density of 1×10^4 in transwell chambers (Corning, CLS3413, NY, United States) and cultured in StemSpan SFEM Medium (StemCell Technologies, 09600, Canada) supplemented with 1% penicillin/streptomycin, 100 ng/mL stem cell factor (PeproTech, 300-07, NJ, United States), 100 ng/mL Flt3 L (PeproTech, 300-19, NJ, United States), 20 ng/mL thyroid peroxidase (PeproTech, 300-18, NJ, United States) and 20 ng/mL interleukin 6 (PeproTech, 200-06, NJ, United States)[18]. After 3 days of co-culture, HSPCs were collected and counted using trypan blue. Cellular immunofluorescence was performed to assess proliferative or apoptotic CD34+ HSPC stained with Ki67 or caspase 3 antibodies. The antibodies used in the experiment are listed in Supplementary Table 3. CD34- and Ki67- or caspase-positive cells were counted as observational cells. At least 50 cells per sample were quantified for each random view.

Cellular immunofluorescence

Immunostaining was performed as previously described. Briefly, cells were fixed for 5 minutes at room temperature with 4% formaldehyde. Permeabilization of cell membranes was achieved by treatment with PBS containing 0.2% Triton X-100. Subsequently, the cells underwent a 30-minute blocking step with 0.5% FBS in PBS before incubation with the prepared antibodies at room temperature for 3 hours on a shaker. After incubation with the primary antibody, the cells were washed three times with PBS containing 0.1% Tween-20. They were then incubated with secondary fluorescent antibodies for 1 hour at room temperature. DAPI was utilized for nuclear staining, and images were captured using Operetta.

Isolation of CD34+ HSPCs

CD34+ HSPCs were isolated using the EasySep Human CD34 Positive Selection Kit II protocol (StemCell Technologies, 17856, Canada)[19]. In summary, EasySep Human CD34 Positive Selection Cocktail (StemCell Technologies, 17856C, Canada) was added to BMNCs from a pool of HD at a concentration of approximately 10^8 cells/mL in EasySep buffer, as recommended. The samples were mixed and incubated at room temperature for 10 minutes. RapidSpheres were added and mixed with the samples, followed by incubation at room temperature for 5 minutes. The tube was then placed on an EasySep magnet (StemCell Technologies, 18000, Canada) and incubated at room temperature for 3 minutes. Cells were washed four times, and enriched CD34+ cells were collected in PBS with 2% FBS. For further purification of CD34+ cells, fluorescence-activated cell sorting was performed to obtain pure CD34+ cells. Briefly, antibodies were added to the primary enriched cells and incubated for 30 minutes in the dark at 4 °C. The detailed cell sorting strategy is plotted in Supplementary Figure 1. SONY MA900 was used for sorting.

β-galactosidase staining

The cell layers were fixed at room temperature for 15 minutes. After removing the fixative solution, the cells were washed twice with PBS. Subsequently, the cells were incubated at 37 °C for 12 hours with a working solution prepared according to the manufacturer's instructions (Beyotime, C0602, Shanghai, China). Images were captured under a light microscope.

SOD activity detection

After cell digestion under different treatments, cells were collected and resuspended in cold PBS, and then the cell homogenate was prepared using non-contact automatic ultrasonic liquid processors (Q-sonic, United States). The supernatants were collected after centrifugation, and protein quantification was performed using the BCA Protein

Quantification Kit (Vazyme, E112, Nanjing, China). Subsequently, SOD activity for every 20 μg of protein was measured using Cu/Zn-SOD and Mn-SOD Assay Kit with WST-8 (Beyotime, S0103, Shanghai, China) according to the manufacturer's instructions.

Measurement of mitochondrial membrane potential

BMSCs were seeded in 24-well plates at a density of 5 × 10^4 cells per well and cultured for 24 hours. Subsequently, these cells were utilized for mitochondrial membrane potential (MMP) measurement using the Mitochondrial Membrane Potential Assay Kit with TMRE (Beyotime, C2001S, Shanghai, China), according to the manufacturer's instructions. After rinsing with PBS, the BMSCs were incubated with TMRE working solution at 37 °C for 30 minutes. Nuclear staining was performed using Hoechst 33342. Images were acquired using an inverted fluorescence microscope (Olympus IX73, Japan), and the mean intensity of each sample was calculated using Image J software.

Statistical analysis

All data are presented as mean ± SEM. Statistical analyses were performed using GraphPad Prism software. An unpaired two-tailed Student's *t*-test was used to compare two groups. One-way analysis of variance (ANOVA) was used to compare the three groups. Statistical significance was set at $P < 0.05$.

RESULTS

Sepsis inhibits the proliferation and self-renewal of BMSCs

Purified BMSCs were isolated from bone marrow aspirates of septic patients and HD according to standard protocols [20]. After culturing for 14 days, HD BMSCs exhibited robust growth with a characteristic fibroblastic appearance, whereas septic BMSCs showed significantly altered growth despite maintaining a similar morphology. Upon passage to the second generation, septic BMSCs appeared as disorganized and vesicular structures (Figure 1A) as replicative aging BMSCs. To assess the self-renewal capacity of BMSC in sepsis, we compared the colony formation capacity of BMNC from septic patients and HD (Figure 1B). A markedly reduced number of colony-forming units-fibroblast was observed in septic samples. Regarding replication capacity, a lower EdU-positive rate suggested a decreased capacity for cell reproduction (Figure 1C), and the results of the CCK-8 assay indicated a slower proliferative rate in septic BMSCs (Figure 1D). Furthermore, reduced expression of proliferating cell nuclear antigen was detected in septic BMSCs (Figure 1E). Moreover, we confirmed the immunophenotypes of BMSCs by flow cytometry to determine whether the characteristics of septic BMSCs had undergone any changes. Immunophenotypic analysis showed that both expressed markers were associated with stromal cells (CD73, CD90, and CD105) and were negative for hematopoietic markers (CD45 and CD34) (Figure 1F)[21]. Collectively, these findings demonstrated that sepsis inhibits the proliferation and self-renewal of BMSCs.

Septic BMSCs have stronger adipogenic and poorer osteogenic abilities

To confirm their differentiation potential, we induced adipogenic and osteogenic differentiation of BMSCs *in vitro*. The BMSCs obtained from the septic samples showed reduced osteogenesis capacity (Figure 2A) and stronger adipogenesis capacity (Figure 2B). Quantification of Alizarin Red S and Oil Red O staining revealed a more than 50% decrease in calcium deposition (Figure 2C) and an approximately 12% increase in lipid droplet accumulation (Figure 2D) in septic BMSCs. Furthermore, the lower expression of runt-related transcription factor 2, alkaline phosphatase, and Sp7 transcription factor 7 (osteogenic genes)[22-24] (Figure 2E) and the higher expression of adipogenic genes such as peroxisome proliferator-activated receptor gamma, fatty acid binding protein 4, and perilipin-1[25,26] (Figure 2F) during lineage determination further corroborated our findings.

Diminished HSPC supportive capacity of septic BMSCs

As one of the most crucial functions of BMSCs is to support homeostasis, we aimed to determine whether the defects mentioned above impaired their ability to support HSPCs. We cultured BMSC layers from HD and septic patients, and the same number of purified CD34+ HSPCs (Supplementary Figure 1) was seeded in transwell chambers[27]. Favorable BMSCs can produce supportive cytokines to maintain HSPC expansion and fitness. After three days of coculture, the frequency of Ki67-positive CD34+ cells (Figure 3A) and the total number of CD34+ cells were significantly lower in the septic BMSC group compared to HD group (Figure 3B). In particular, a higher number of apoptotic CD34+ cells was observed in septic BMSCs (Figure 3C and D). Subsequently, we evaluated the production of critical HSC factors such as stem cell factor, C-X-C chemokine ligand 12, and interleukin 7[28,29] in two groups of BMSCs, and the results indicated that the production of supportive cytokines was impaired in septic BMSCs (Figure 3E). These findings suggest that sepsis affects the hematopoietic support capacity of BMSCs.

Septic BMSCs show senescence

Slow proliferation, change in differentiation potency from osteoblasts to adipocytes, and impaired hematopoietic supportive capacity are all characteristic features of aging BMSCs[25]. Therefore, we conducted beta-galactosidase detection, which is a commonly used indicator of senescence. Septic BMSCs exhibited significantly higher staining compared to HD BMSCs (Figure 4A). Furthermore, we measured ROS levels and SASP expression, including transforming growth factor-β, interleukin-6, and interleukin-1β. As depicted in Figure 4B, the mean fluorescence intensity

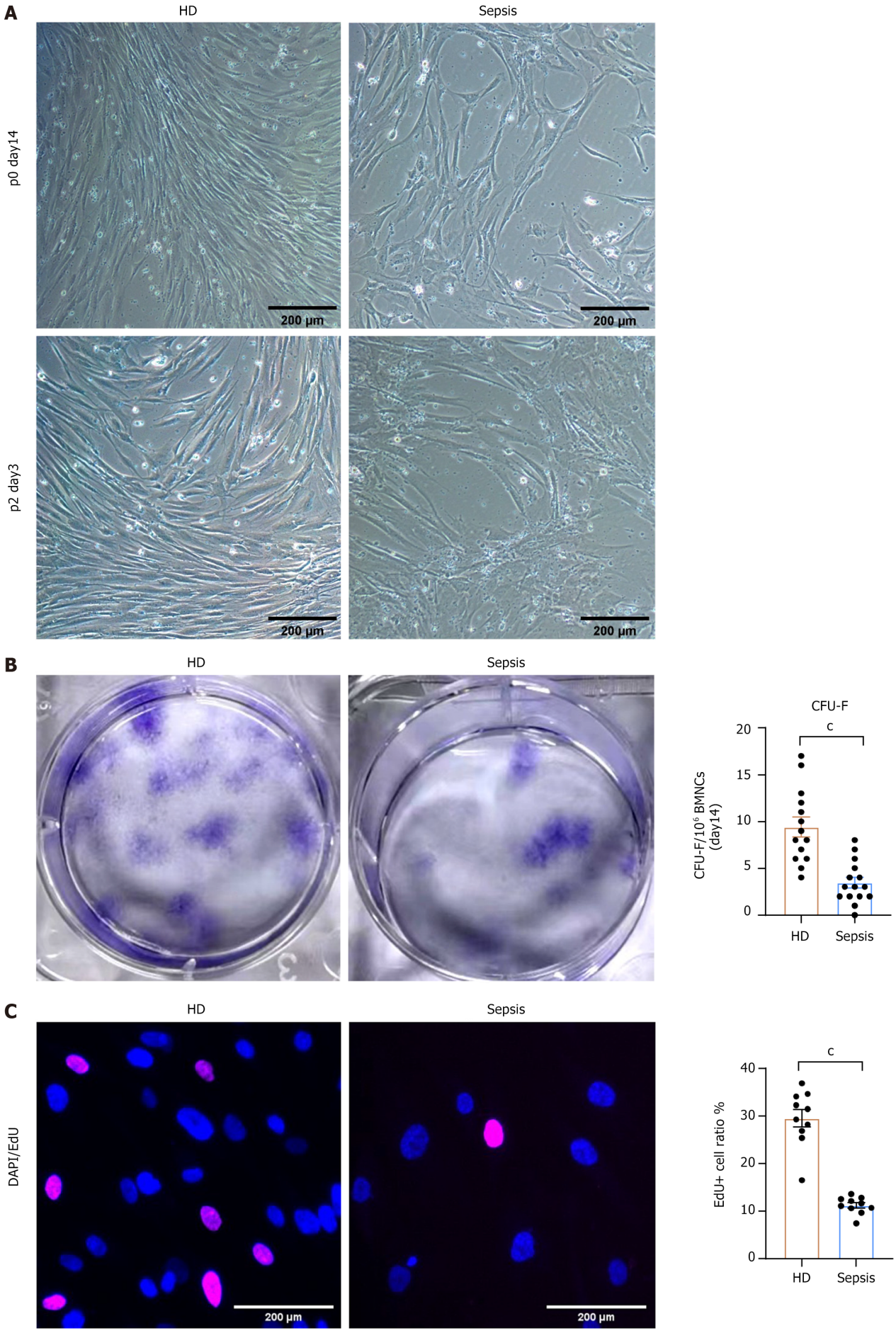
A
HD
Sepsis
p0 day14
p2 day3
200 μm
B
HD
Sepsis
CFU-F
c
CFU-F/10⁶ BMNCs (day14)
20
15
10
5
0
HD
Sepsis
C
HD
Sepsis
DAPI/EdU
200 μm
c
EdU+ cell ratio %
40
30
20
10
0
HD
Sepsis

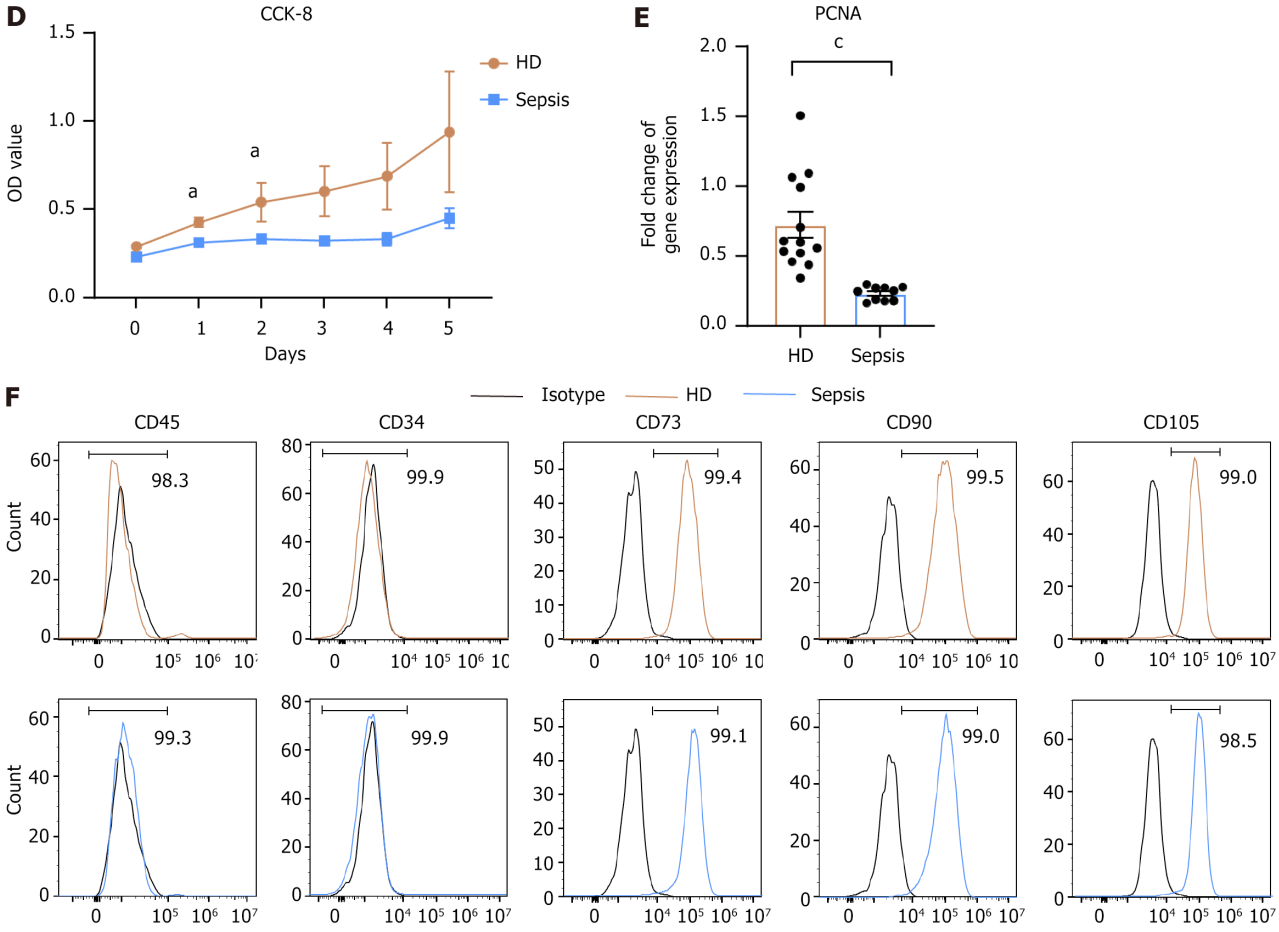

Figure 1 Morphology, clonogenic capacity, proliferation and characterization of bone marrow mesenchymal stem cells. A: Representative images depicting the morphology of *in vitro*-expanded bone marrow mesenchymal stem cells (BMSCs) from healthy donors (HD) and patients with sepsis of various generations; B: Representative images of colony-forming units-fibroblast assays, with results expressed as the number of colony-forming units-fibroblast per one million bone marrow mononuclear cells for HD samples (n = 14) and septic samples (n = 15); C-E: Proliferation of HD and septic BMSCs, C: Merged channel image showing EdU (magenta) and DAPI (blue) staining and the percentage of EdU-positive cells relative to the total number of cells in HD BMSCs (n = 10) and septic BMSCs (n = 10) (C). Growth curves were assessed using the CCK-8 assay for HD BMSCs (n = 10) and septic BMSCs (n = 10) (D). Expression levels of proliferating cell nuclear antigen detected by quantitative real-time polymerase chain reaction (HD: n = 13; sepsis: n = 10) (E); F: Representative flow cytometry images illustrating typical BMSC markers. Positive markers: CD73, CD90, CD105; negative markers: CD34 and CD45. Each error bar represents the mean ± SEM. P values were determined using a t-test ($^aP < 0.05$, $^cP < 0.001$). HD: Healthy donors; CFU-F: Colony-forming units-fibroblast; PCNA: Proliferating cell nuclear antigen.

of intracellular ROS in septic BMSCs was higher than that in HD BMSCs. Elevated expressions of SASP were observed in septic BMSCs (Figure 4C). In addition, classical markers of aging, P16 and P21, were upregulated in septic BMSCs (Figure 4D). Therefore, senescence may be the basis for the functional defects observed in septic BMSCs.

NAD rejuvenates septic BMSCs

As it is well known that NAD interacts with several biological hallmarks of aging[30,31], we aimed to investigate whether septic BMSCs could benefit from NAD treatment. Firstly, we observed a restoration of the proliferation capacity of septic BMSCs after NAD treatment, as evidenced by an increased EdU-positive rate (Figure 5A). Furthermore, we found that NAD treatment contributed to reduced senescence, as demonstrated by a decrease in beta-galactosidase staining (Figure 5B). Thus, we were curious to know whether the differentiation potency had been restored. Thus, we induced osteogenic and adipogenic differentiation in NAD-treated septic BMSCs. Importantly, NAD treatment partially preserved the osteogenesis of septic BMSCs, as indicated by Alizarin Red S staining (Figure 5C and D) and upregulation of osteogenic genes (Figure 5E). On the contrary, the capacity for adipogenesis was inhibited after exposure to NAD, as verified by the decreased accumulation of lipid droplets (Figure 5F and G) and decreased expression of adipogenesis genes (Figure 5H). Additionally, NAD treatment rescued the hematopoietic support capacity of septic BMSCs. We observed better expansion of HSPCs (Supplementary Figure 2A and B) and fewer apoptotic HSPCs co-cultured with NAD-treated septic BMSCs than those with raw septic BMSCs (Supplementary Figure 2C and D). In summary, NAD represents an option to restore the intrinsic characteristics and stromal functions of septic BMSCs *in vitro*.

NAD improves the antioxidant capacity of mitochondria

NAD plays a crucial role in mitochondrial function within cells. As mentioned above, the decline in mitochondrial free radical clearance capacity and increase in ROS levels indicate cellular aging. Therefore, we were curious whether NAD

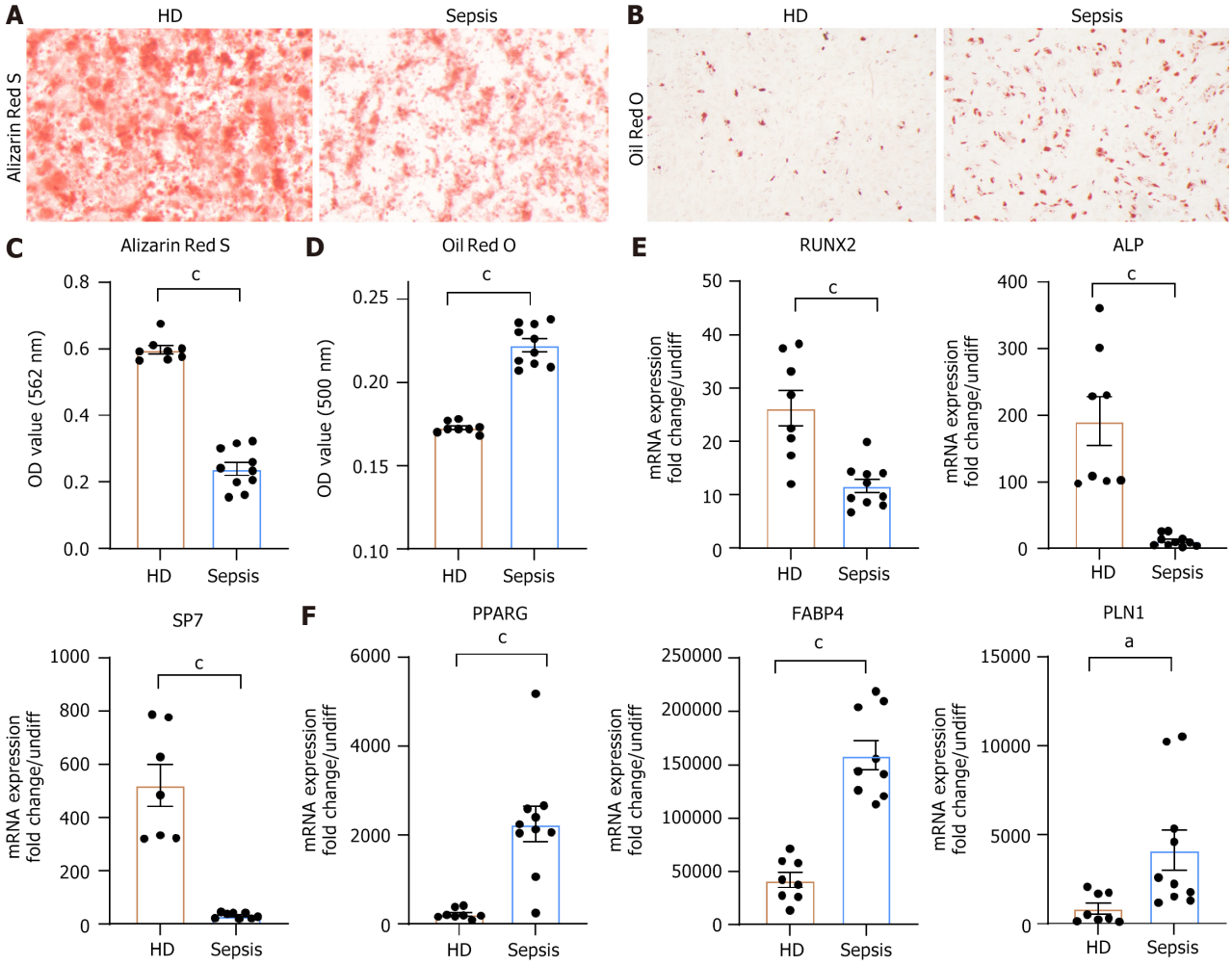

Figure 2 Osteogenic and adipogenic differentiation of bone marrow mesenchymal stem cells. A: Alizarin Red S staining (original magnification, × 4); B: Oil Red O staining (original magnification, × 4); C: Quantification was carried out using cetylpyridinium chloride, and absorbance was measured using a microplate reader at 562 nm; D: Quantification was conducted using isopropanol, and the absorbance was measured using a microplate reader at 500 nm; E: Expression of related genes (runt-related transcription factor 2, alkaline phosphatase, and Sp7 transcription factor 7); F: Expression of related genes (peroxisome proliferator-activated receptor gamma, fatty acid binding protein 4, and perilipin-1). HD: n = 8; sepsis: n = 10. The expression of all genes was assessed using quantitative real-time polymerase chain reaction. Results were expressed as fold change relative to undifferentiated bone marrow mesenchymal stem cells. Each error bar shows the mean ± SEM. P values were determined using a t-test ($^{a}P < 0.05$, $^{c}P < 0.001$). HD: Healthy donors; RUNX2: Runt-related transcription factor 2; ALP: Alkaline phosphatase; SP7: Sp7 transcription factor 7; PPARG: Peroxisome proliferator-activated receptor gamma; FABP4: Fatty acid binding protein 4; PLN1: Perilipin-1.

counteracted the aging BMSC by restoring mitochondrial function. First, we examined the expression levels of the important NAD-dependent deacetylase SIRT3 in different groups of BMSCs. We found a significant decrease in SIRT3 expression in septic BMSCs, which was restored after NAD treatment (Figure 6A). Furthermore, intracellular ROS levels decreased after NAD treatment (Figure 6B). SIRT3 deacetylates SOD enzymes in mitochondria to activate them and improve mitochondrial antioxidant capacity. As depicted in Figure 6C, SOD enzyme activity decreased in septic BMSC but was restored after NAD treatment. On the other hand, abnormal mitochondrial function partially affected mitochondrial integrity, so we detected MMP to evaluate whether mitochondrial function had been damaged. We observed a significant reduction in MMP in septic BMSCs, which was rescued after NAD treatment (Figure 6D). Based on these results, we demonstrated that NAD effectively reversed impaired mitochondrial function in septic BMSCs through the NAD/SIRT3/SOD pathway (Figure 6E).

DISCUSSION

Under natural circumstances, the functionality of BMSCs decreases with age, leading to organ failure and age-related diseases, such as osteoporosis, bone marrow fibrosis, and even HSC aging. Our research indicates that sepsis induces senescence in BMSCs, characterized by inhibited proliferation and self-renewal capabilities and biased differentiation toward adipogenesis rather than osteogenesis, leading to an increased incidence of diseases such as osteoporosis. Furthermore, sepsis-affected senescent BMSCs exhibit reduced hematopoietic support capacity, particularly lymphoid

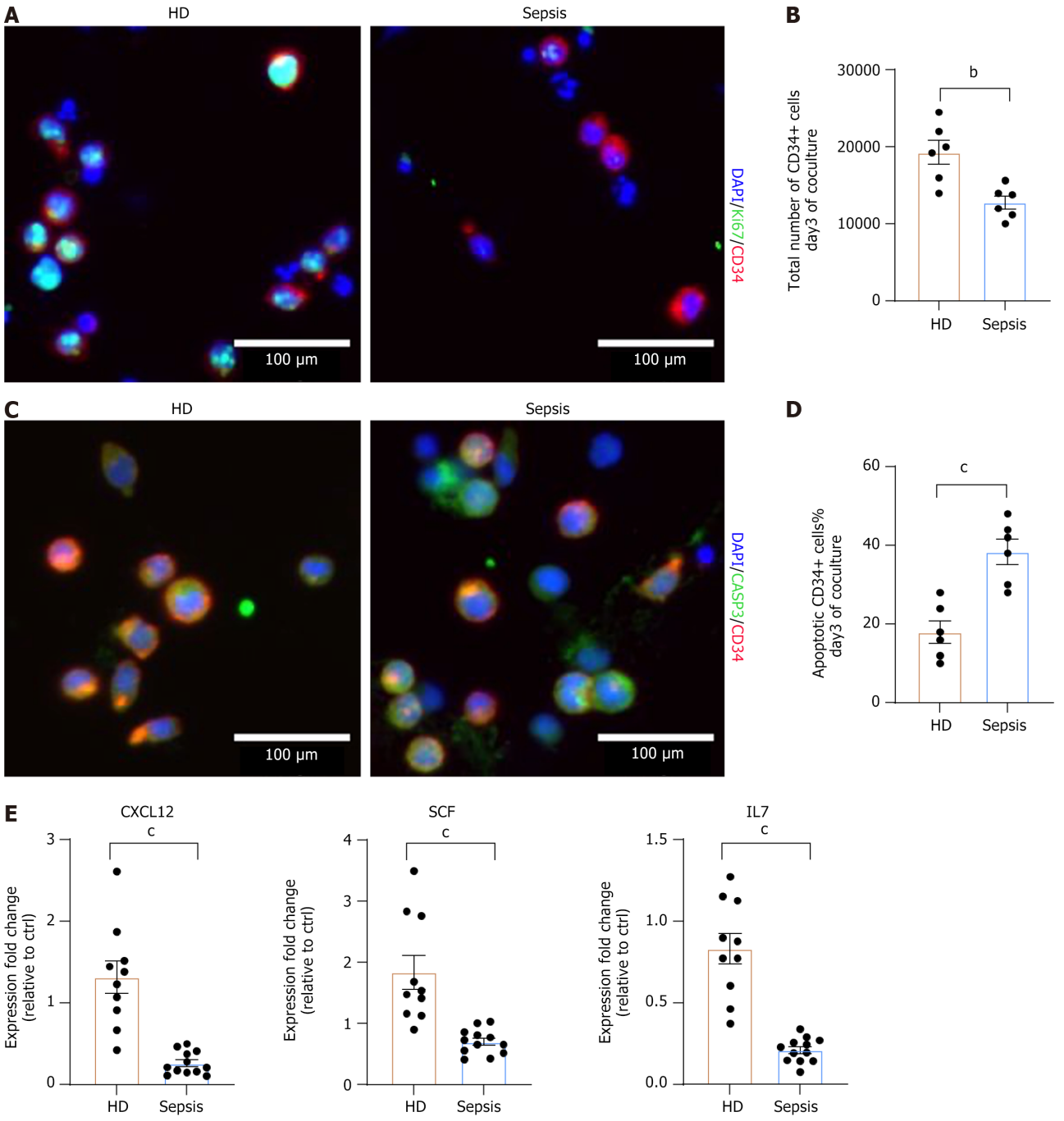

Figure 3 Supportive capacity of bone marrow mesenchymal stem cells. A: Representative fluorescence image showing proliferating hematopoietic stem/progenitor cells (HSPCs) co-cultured with healthy donors (HD) and septic bone marrow mesenchymal stem cells (BMSCs) after 3 days *in vitro*. Ki67 (green), CD34 (red), DAPI (blue); B: Total number of CD34-positive HSPCs after co-culture with HD BMSCs (n = 6) or septic BMSCs (n = 6), starting with an initial number of 10000 cells; C: Representative fluorescence image of apoptotic HSPCs after co-culture; D: Percentages of apoptotic HSPCs (CD34+ and caspase-positive) relative to the total number of cells (HD: n = 6; sepsis: n = 6); E: Expression levels of supportive cytokines (C-X-C chemokine ligand 12, stem cell factor, and interleukin 7) were evaluated by fold change relative to one of the HD samples (HD: n = 10; sepsis: n = 12). Data were mean ± SEM. P values were determined using a t-test ($^bP < 0.01$, $^cP < 0.001$). HD: Healthy donors; CXCL12: C-X-C chemokine ligand 12; SCF: Stem cell factor; IL7: Interleukin 7.

progenitor cells near the endosteum, which impedes the recovery of the immune system in patients with sepsis. Long-term lymphocytopenia weakens immune function and increases the risk of secondary infection and hospitalization.

Our experiments also confirmed a significant increase in SASP in septic BMSCs. These elevated levels of inflammatory factors induce HSC aging. Transforming growth factor-β has been shown to slow the progression of the HSC cell cycle and inhibit self-renewal potential[32]. IL-1β is a crucial cytokine driving HSC in elderly mice[33]. Therefore, aging BMSCs not only do not provide good maintenance capability of HSC but also promote HSC aging. In our study, treatment with NAD effectively improved the hematopoietic supportive capacities of septic BMSCs, achieving the goal of sepsis treatment with a longer-lasting effect and avoiding side effects. In particular, our research suggests that similar phenotypes may exist in other related diseases, such as tendinopathies, tumors, drug-induced injuries, and other conditions in which BMSC damage is possible. Focusing on the aging of BMSCs provides new insights and suggestions

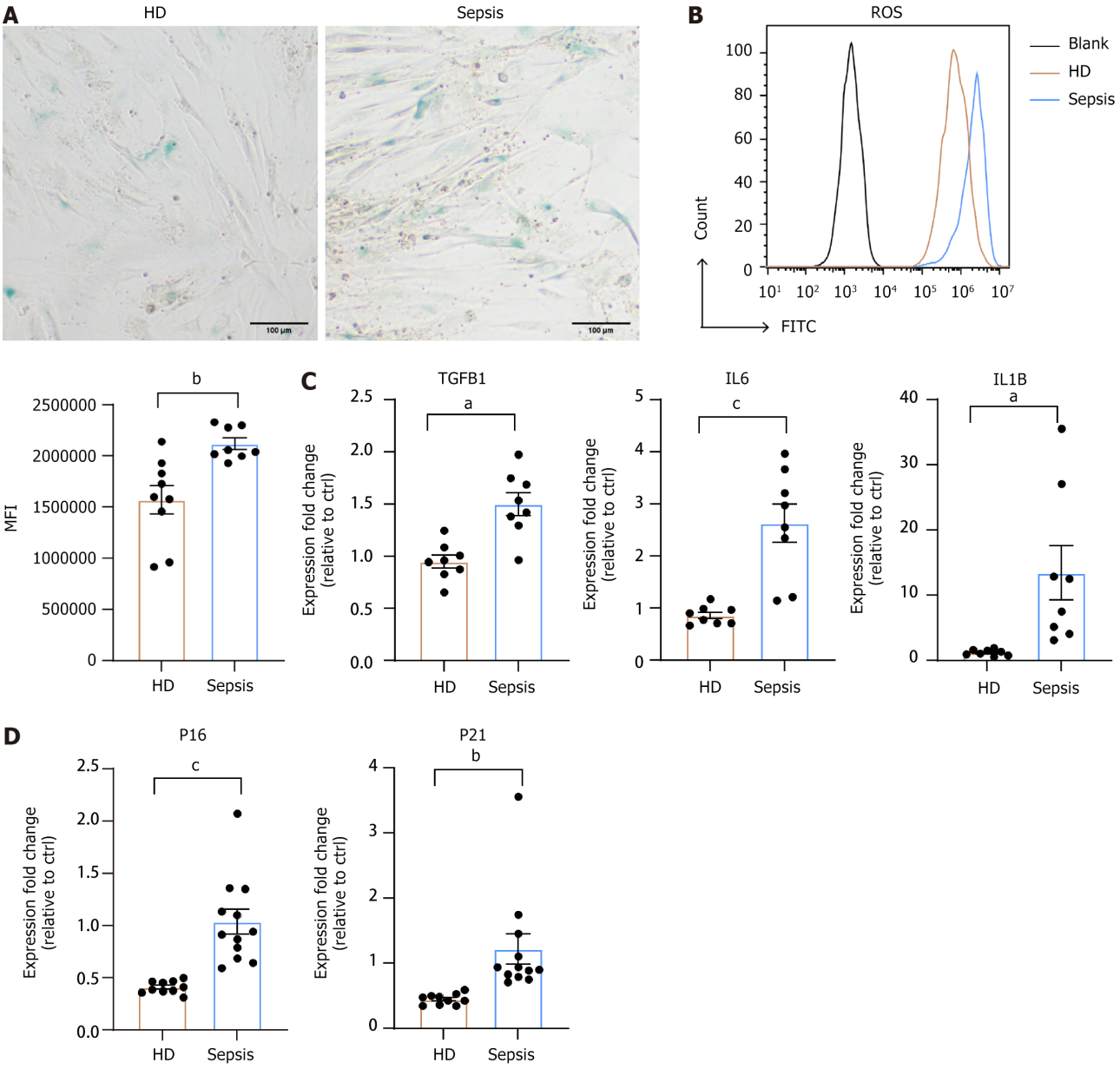

Figure 4 Senescence behavior in healthy donors and septic bone marrow mesenchymal stem cells. A: Representative β-gal staining images of healthy donors (HD) and septic bone marrow mesenchymal stem cells (BMSCs); B: *In vitro* reactive oxygen species levels assessed by flow cytometry, expressed as mean fluorescence intensity of forward scatter for HD BMSCs (n = 9) and septic BMSCs (n = 8); C: Relative senescence-associated secretory phenotype content (transforming growth factor β1, interleukin 6, and interleukin 1β) compared to HD samples in both groups (n = 8); D: Detection of senescence markers (P16, P21) in HD BMSCs (n = 10) and septic BMSCs (n = 12). Data were presented as mean ± SEM. P values were determined by t-test ($^aP < 0.05$, $^bP < 0.01$, $^cP < 0.005$). HD: Healthy donors; ROS: Reactive oxygen species; MFI: Mean fluorescence intensity; TGF: Transforming growth factor; IL: Interleukin.

for the research and treatment of these diseases.

MSCs are widely distributed throughout the body, and their therapeutic purpose has been proven to be efficient with few side effects in many diseases[34,35]. However, the long-standing challenge is to conduct a good expansion of MSCs *in vitro*[36], mainly because of the difficulty in maintaining the stemness of MSCs under culture conditions[37]. Our research suggests that anti-aging measures contribute to maintaining the stemness of MSCs, potentially enhancing the quality and stability of cultured MSCs.

Our limitation lies in needing an in-depth investigation of the exact substances that cause BMSC aging under septic conditions. According to previous reports, aging mechanisms include DNA damage, mitochondrial dysfunction, exosomes, and other intracellular signaling pathways. It remains unclear whether these mechanisms exist in the bone marrow of patients with sepsis and to what extent they contribute to aging. In addition, there are many anti-aging drugs, including natural compounds such as quercetin, resveratrol, spermidine, curcumin, and sulforaphane, and other compounds such as rapamycin, metformin, and NAD enhancers[38], which may have better and more suitable effects on septic BMSC. Determining how to combine and administer these drugs and refining treatment regimens through animal and clinical trials will be the focus of future research.

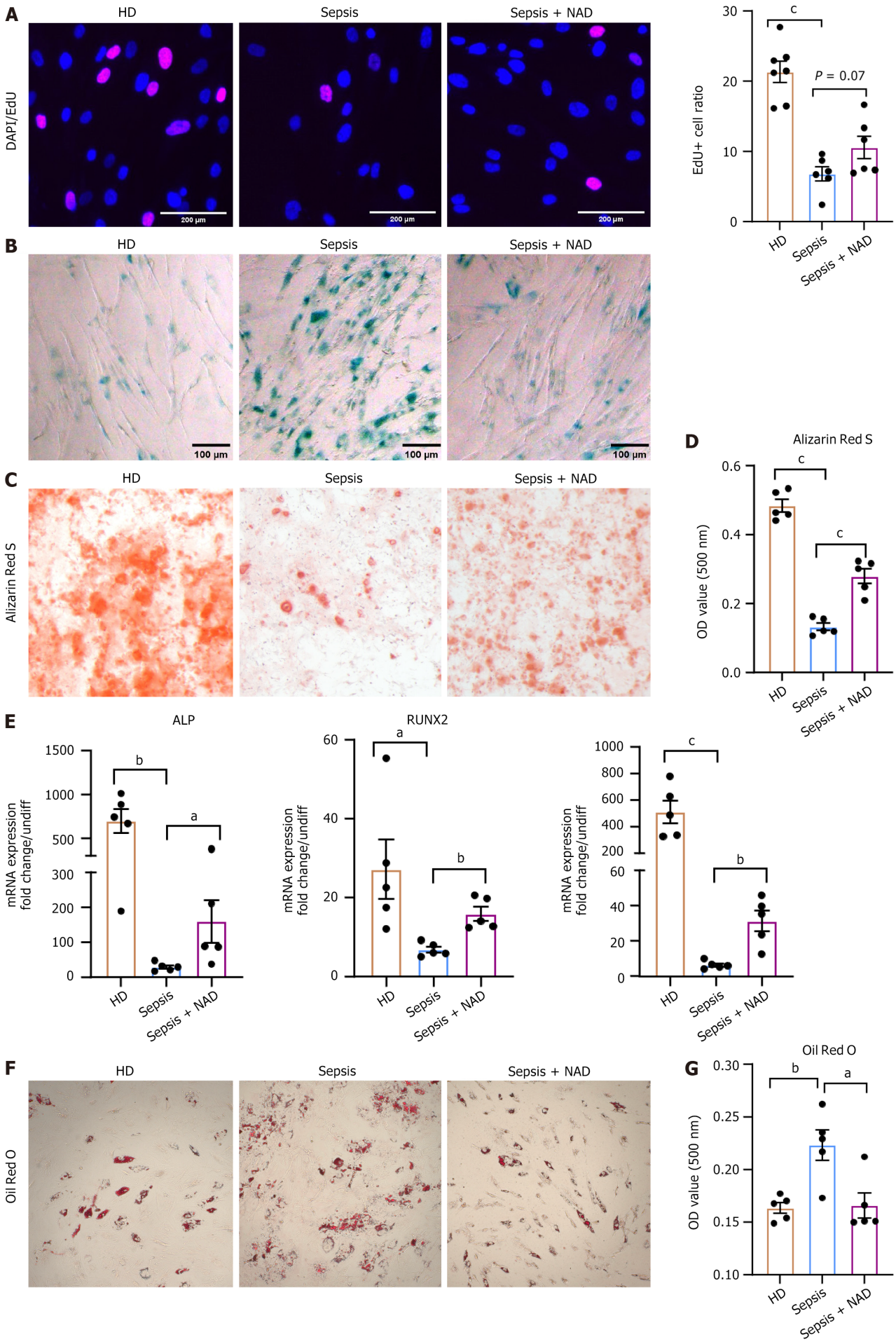
A
HD
Sepsis
Sepsis + NAD
DAPI/EdU
200 μm
EdU+ cell ratio
P = 0.07
B
100 μm
C
Alizarin Red S
D
OD value (500 nm)
E
ALP
RUNX2
mRNA expression fold change/undiff
F
Oil Red O
G

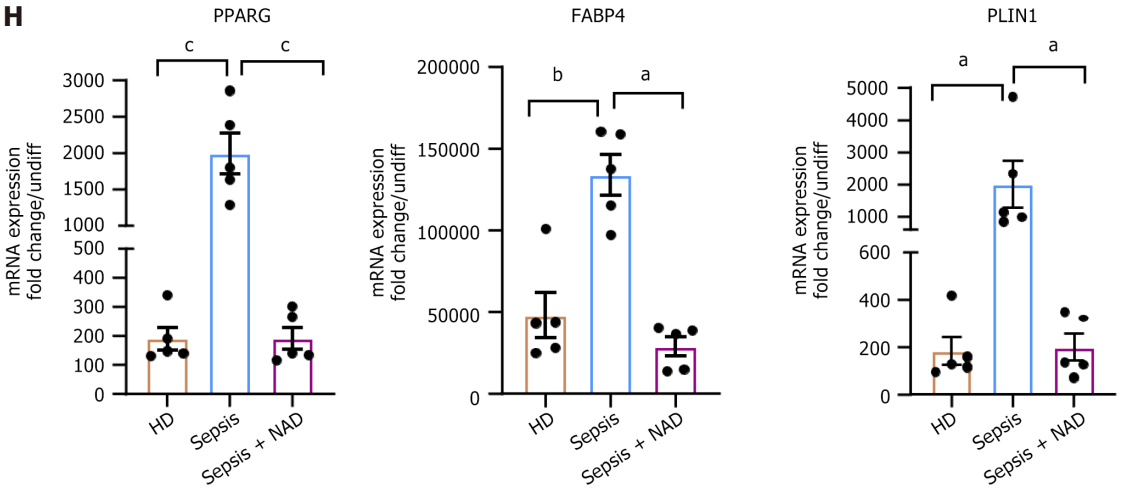

Figure 5 Nicotinamide adenine dinucleotide treatment rescue function of septic bone marrow mesenchymal stem cells. A: Representative images of EdU incorporation, EdU (magenta), and DAPI (blue) staining. The percentage of EdU-positive cells increased after treatment with nicotinamide adenine dinucleotide (NAD) [healthy donors (HD): n = 7; sepsis: n = 6; sepsis with NAD: n = 6]; B: Cellular senescence assessed by β-gal staining in bone marrow mesenchymal stem cells (BMSCs) from three groups; C and D: Alizarin Red S staining (original magnification, × 4) and quantification of calcium precipitation; E: Quantitative real-time polymerase chain reaction analysis of osteogenic genes (runt-related transcription factor 2, alkaline phosphatase, and Sp7 transcription factor 7) in HD BMSCs (n = 5), septic BMSCs (n = 5), and NAD-treated septic BMSCs (n = 5); F and G: Oil Red O staining (original magnification, × 10) and lipid droplet quantification; H: Quantitative real-time polymerase chain reaction analysis of adipogenic genes (peroxisome proliferator-activated receptor gamma, fatty acid binding protein 4, and perilipin-1) in HD BMSCs (n = 5), septic BMSCs (n = 5), and NAD-treated septic BMSCs (n = 5). Results were presented as fold change relative to undifferentiated BMSCs. Error bars represent the mean ± SEM. P values were determined using One-Way ANOVA ($^aP < 0.05$, $^bP < 0.01$, $^cP < 0.001$). HD: Healthy donors; NAD: Nicotinamide adenine dinucleotide; RUNX2: Runt-related transcription factor 2; ALP: Alkaline phosphatase; SP7: Sp7 transcription factor 7; PPARG: Peroxisome proliferator-activated receptor gamma; FABP4: Fatty acid binding protein 4; PLN1: Perilipin-1.

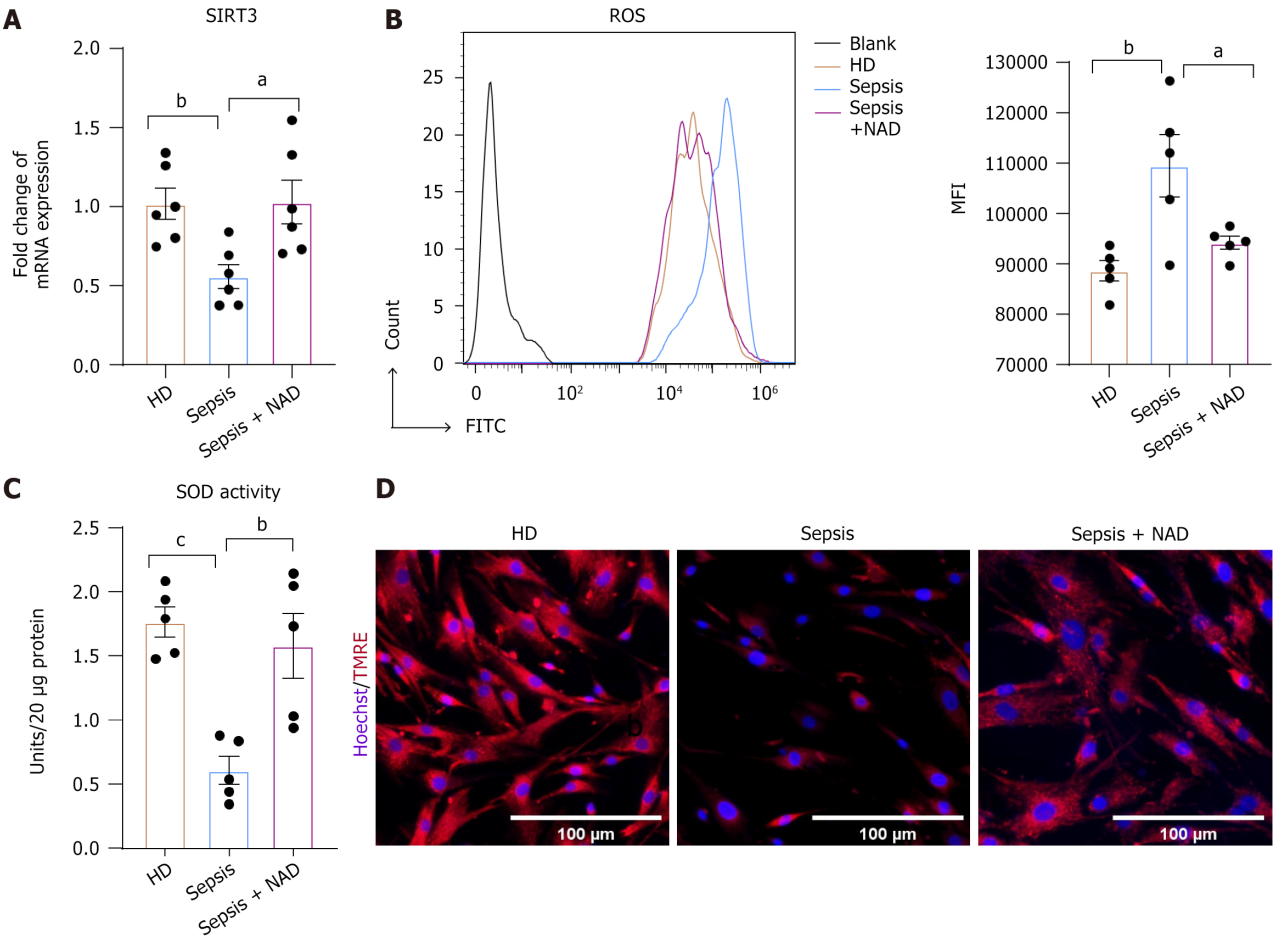

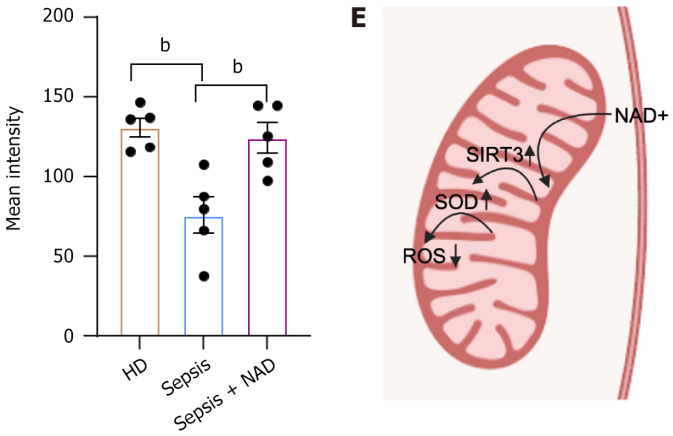

Figure 6 Nicotinamide adenine dinucleotide treatment improves the antioxidant capacity of mitochondria *via* the nicotinamide adenine dinucleotide/sirtuin 3/superoxide dismutase pathway. A: Expression level of sirtuin 3 in healthy donors, septic and nicotinamide adenine dinucleotide (NAD)-treated septic bone marrow mesenchymal stem cells (BMSCs) (n = 6); B: *In vitro* reactive oxygen species levels were expressed as mean fluorescence intensity of forward scatter for healthy donor-, septic-, and NAD-treated septic BMSCs (n = 5); C: Superoxide dismutase activity of every 20 μg of protein from different BMSCs (n = 5); D: Measure mitochondrial membrane potential with TMRE staining to show mitochondrial integrity. TMRE staining (red) and Hoechst 33342 staining (blue). The mean intensity of TMRE staining was calculated with Image J; E: Graph of NAD/sirtuin 3/superoxide dismutase pathway. Error bars represent the mean ± SEM. P values were determined using One-Way ANOVA ($^aP < 0.05$, $^bP < 0.01$, $^cP < 0.001$). HD: Healthy donors; NAD: Nicotinamide adenine dinucleotide; MFI: Mean fluorescence intensity; SIRT3: Sirtuin 3; ROS: Reactive oxygen species; SOD: Superoxide dismutase.

CONCLUSION

We demonstrated that sepsis induces senescence of BMSCs, manifested by decreased proliferative capacity, self-renewal capacity, osteogenic differentiation, and impaired hematopoietic supportive effects. Treatment with the anti-aging drug NAD effectively reversed this damage. These findings improve our understanding of bone marrow complications of sepsis and provide a new treatment option for associated complications.

ACKNOWLEDGEMENTS

The authors thank Mr. An Zeng for technical support during the experiment.

FOOTNOTES

Author contributions: Zhou ZG and Tong Y contributed to the funding acquisition, writing - review & editing and supervision of this manuscript, they contributed equally to this manuscript as co-corresponding authors; Xia X and Zhou K took part in the investigation and visualization, manuscript writing - original draft, they contributed equally to this manuscript as co-first authors; An LY and Zhao M participated in collect samples; Tian BL contributed to the data visualization and interpretation of this manuscript; An LY, Zhao M, and Zhao JY participated in the resources of this study.

Supported by Shanghai Natural Science Foundation, No. 21ZR1452300; and the Clinical Research Innovation Plan of Shanghai General Hospital, No. CCTR-2022B04.

Institutional review board statement: This study was approved by the institutional review board of Shanghai General Hospital, No. [2023]145.

Conflict-of-interest statement: All the authors report no relevant conflicts of interest for this article.

Data sharing statement: No additional data were available.

Country of origin: China

ORCID number: Jin-Yan Zhao 0000-0002-6403-5857; Yin Tong 0000-0001-7551-5509.

S-Editor: Wang JJ
L-Editor: A
P-Editor: Zhang XD

REFERENCES

1 **Fleischmann C**, Scherag A, Adhikari NK, Hartog CS, Tsaganos T, Schlattmann P, Angus DC, Reinhart K; International Forum of Acute Care Trialists. Assessment of Global Incidence and Mortality of Hospital-treated Sepsis. Current Estimates and Limitations. *Am J Respir Crit Care Med* 2016; **193**: 259-272 [PMID: 26414292 DOI: 10.1164/rccm.201504-0781OC]
2 **Singer M**, Deutschman CS, Seymour CW, Shankar-Hari M, Annane D, Bauer M, Bellomo R, Bernard GR, Chiche JD, Coopersmith CM, Hotchkiss RS, Levy MM, Marshall JC, Martin GS, Opal SM, Rubenfeld GD, van der Poll T, Vincent JL, Angus DC. The Third International Consensus Definitions for Sepsis and Septic Shock (Sepsis-3). *JAMA* 2016; **315**: 801-810 [PMID: 26903338 DOI: 10.1001/jama.2016.0287]
3 **Liu D**, Huang SY, Sun JH, Zhang HC, Cai QL, Gao C, Li L, Cao J, Xu F, Zhou Y, Guan CX, Jin SW, Deng J, Fang XM, Jiang JX, Zeng L. Sepsis-induced immunosuppression: mechanisms, diagnosis and current treatment options. *Mil Med Res* 2022; **9**: 56 [PMID: 36209190 DOI: 10.1186/s40779-022-00422-y]
4 **Comazzetto S**, Shen B, Morrison SJ. Niches that regulate stem cells and hematopoiesis in adult bone marrow. *Dev Cell* 2021; **56**: 1848-1860 [PMID: 34146467 DOI: 10.1016/j.devcel.2021.05.018]
5 **Chen Q**, Shou P, Zheng C, Jiang M, Cao G, Yang Q, Cao J, Xie N, Velletri T, Zhang X, Xu C, Zhang L, Yang H, Hou J, Wang Y, Shi Y. Fate decision of mesenchymal stem cells: adipocytes or osteoblasts? *Cell Death Differ* 2016; **23**: 1128-1139 [PMID: 26868907 DOI: 10.1038/cdd.2015.168]
6 **Beerman I**, Luis TC, Singbrant S, Lo Celso C, Méndez-Ferrer S. The evolving view of the hematopoietic stem cell niche. *Exp Hematol* 2017; **50**: 22-26 [PMID: 28189651 DOI: 10.1016/j.exphem.2017.01.008]
7 **Leimkühler NB**, Gleitz HFE, Ronghui L, Snoeren IAM, Fuchs SNR, Nagai JS, Banjanin B, Lam KH, Vogl T, Kuppe C, Stalmann USA, Büsche G, Kreipe H, Gütgemann I, Krebs P, Banz Y, Boor P, Tai EW, Brümmendorf TH, Koschmieder S, Crysandt M, Bindels E, Kramann R, Costa IG, Schneider RK. Heterogeneous bone-marrow stromal progenitors drive myelofibrosis *via* a druggable alarmin axis. *Cell Stem Cell* 2021; **28**: 637-652.e8 [PMID: 33301706 DOI: 10.1016/j.stem.2020.11.004]
8 **Takizawa H**, Fritsch K, Kovtonyuk LV, Saito Y, Yakkala C, Jacobs K, Ahuja AK, Lopes M, Hausmann A, Hardt WD, Gomariz Á, Nombela-Arrieta C, Manz MG. Pathogen-Induced TLR4-TRIF Innate Immune Signaling in Hematopoietic Stem Cells Promotes Proliferation but Reduces Competitive Fitness. *Cell Stem Cell* 2017; **21**: 225-240.e5 [PMID: 28736216 DOI: 10.1016/j.stem.2017.06.013]
9 **Terashima A**, Okamoto K, Nakashima T, Akira S, Ikuta K, Takayanagi H. Sepsis-Induced Osteoblast Ablation Causes Immunodeficiency. *Immunity* 2016; **44**: 1434-1443 [PMID: 27317262 DOI: 10.1016/j.immuni.2016.05.012]
10 **Lautrup S**, Sinclair DA, Mattson MP, Fang EF. NAD(+) in Brain Aging and Neurodegenerative Disorders. *Cell Metab* 2019; **30**: 630-655 [PMID: 31577933 DOI: 10.1016/j.cmet.2019.09.001]
11 **Reiten OK**, Wilvang MA, Mitchell SJ, Hu Z, Fang EF. Preclinical and clinical evidence of NAD(+) precursors in health, disease, and ageing. *Mech Ageing Dev* 2021; **199**: 111567 [PMID: 34517020 DOI: 10.1016/j.mad.2021.111567]
12 **Chini CCS**, Cordeiro HS, Tran NLK, Chini EN. NAD metabolism: Role in senescence regulation and aging. *Aging Cell* 2024; **23**: e13920 [PMID: 37424179 DOI: 10.1111/acel.13920]
13 **Wang T**, Cao Y, Zheng Q, Tu J, Zhou W, He J, Zhong J, Chen Y, Wang J, Cai R, Zuo Y, Wei B, Fan Q, Yang J, Wu Y, Yi J, Li D, Liu M, Wang C, Zhou A, Li Y, Wu X, Yang W, Chin YE, Chen G, Cheng J. SENP1-Sirt3 Signaling Controls Mitochondrial Protein Acetylation and Metabolism. *Mol Cell* 2019; **75**: 823-834.e5 [PMID: 31302001 DOI: 10.1016/j.molcel.2019.06.008]
14 **Mitchell S**, Zhang P, Cannon M, Beaver L, Lehman A, Harrington B, Sampath D, Byrd JC, Lapalombella R. Anti-tumor NAMPT inhibitor, KPT-9274, mediates gender-dependent murine anemia and nephrotoxicity by regulating SIRT3-mediated SOD deacetylation. *J Hematol Oncol* 2021; **14**: 101 [PMID: 34187548 DOI: 10.1186/s13045-021-01107-0]
15 **Li R**, Zhou Y, Cao Z, Liu L, Wang J, Chen Z, Xing W, Chen S, Bai J, Yuan W, Cheng T, Xu M, Yang FC, Zhao Z. TET2 Loss Dysregulates the Behavior of Bone Marrow Mesenchymal Stromal Cells and Accelerates Tet2(-/-)-Driven Myeloid Malignancy Progression. *Stem Cell Reports* 2018; **10**: 166-179 [PMID: 29290626 DOI: 10.1016/j.stemcr.2017.11.019]
16 **Ciuffreda MC**, Malpasso G, Musarò P, Turco V, Gnecchi M. Protocols for in vitro Differentiation of Human Mesenchymal Stem Cells into Osteogenic, Chondrogenic and Adipogenic Lineages. *Methods Mol Biol* 2016; **1416**: 149-158 [PMID: 27236670 DOI: 10.1007/978-1-4939-3584-0_8]
17 **Moseley KF**, Doyle ME, Jan De Beur SM. Diabetic serum from older women increases adipogenic differentiation in mesenchymal stem cells. *Endocr Res* 2018; **43**: 155-165 [PMID: 29521566 DOI: 10.1080/07435800.2018.1441868]
18 **Wei W**, Xu C, Ye ZY, Huang XJ, Yuan JE, Ma TB, Lin HB, Chen XQ. [Biological characteristics of mesenchymal stem cell and hematopoietic stem cell in the co-culture system]. *Sheng Li Xue Bao* 2016; **68**: 691-698 [PMID: 27778036]
19 **Van Egeren D**, Escabi J, Nguyen M, Liu S, Reilly CR, Patel S, Kamaz B, Kalyva M, DeAngelo DJ, Galinsky I, Wadleigh M, Winer ES, Luskin MR, Stone RM, Garcia JS, Hobbs GS, Camargo FD, Michor F, Mullally A, Cortes-Ciriano I, Hormoz S. Reconstructing the Lineage Histories and Differentiation Trajectories of Individual Cancer Cells in Myeloproliferative Neoplasms. *Cell Stem Cell* 2021; **28**: 514-523.e9 [PMID: 33621486 DOI: 10.1016/j.stem.2021.02.001]
20 **Ferrin I**, Beloqui I, Zabaleta L, Salcedo JM, Trigueros C, Martin AG. Isolation, Culture, and Expansion of Mesenchymal Stem Cells. *Methods Mol Biol* 2017; **1590**: 177-190 [PMID: 28353270 DOI: 10.1007/978-1-4939-6921-0_13]
21 **Vieira CP**, McCarrel TM, Grant MB. Novel Methods to Mobilize, Isolate, and Expand Mesenchymal Stem Cells. *Int J Mol Sci* 2021; **22**: 5728 [PMID: 34072061 DOI: 10.3390/ijms22115728]
22 **Kanawa M**, Igarashi A, Fujimoto K, Saskianti T, Nakashima A, Higashi Y, Kurihara H, Kato Y, Kawamoto T. The Identification of Marker Genes for Predicting the Osteogenic Differentiation Potential of Mesenchymal Stromal Cells. *Curr Issues Mol Biol* 2021; **43**: 2157-2166 [PMID: 34940124 DOI: 10.3390/cimb43030150]
23 **Almalki SG**, Agrawal DK. Key transcription factors in the differentiation of mesenchymal stem cells. *Differentiation* 2016; **92**: 41-51 [PMID:

27012163 DOI: 10.1016/j.diff.2016.02.005]

24 **Zhou CC**, Xiong QC, Zhu XX, Du W, Deng P, Li XB, Jiang YZ, Zou SJ, Wang CY, Yuan Q. AFF1 and AFF4 differentially regulate the osteogenic differentiation of human MSCs. *Bone Res* 2017; **5**: 17044 [PMID: 28955517 DOI: 10.1038/boneres.2017.44]

25 **Yang YK**, Ogando CR, Wang See C, Chang TY, Barabino GA. Changes in phenotype and differentiation potential of human mesenchymal stem cells aging in vitro. *Stem Cell Res Ther* 2018; **9**: 131 [PMID: 29751774 DOI: 10.1186/s13287-018-0876-3]

26 **Stefańska K**, Nemcova L, Blatkiewicz M, Żok A, Kaczmarek M, Pieńkowski W, Mozdziak P, Piotrowska-Kempisty H, Kempisty B. Expression Profile of New Marker Genes Involved in Differentiation of Human Wharton's Jelly-Derived Mesenchymal Stem Cells into Chondrocytes, Osteoblasts, Adipocytes and Neural-like Cells. *Int J Mol Sci* 2023; **24**: 12939 [PMID: 37629120 DOI: 10.3390/ijms241612939]

27 **Bucar S**, Branco ADM, Mata MF, Milhano JC, Caramalho Í, Cabral JMS, Fernandes-Platzgummer A, da Silva CL. Influence of the mesenchymal stromal cell source on the hematopoietic supportive capacity of umbilical cord blood-derived CD34(+)-enriched cells. *Stem Cell Res Ther* 2021; **12**: 399 [PMID: 34256848 DOI: 10.1186/s13287-021-02474-8]

28 **Mattiucci D**, Maurizi G, Izzi V, Cenci L, Ciarlantini M, Mancini S, Mensà E, Pascarella R, Vivarelli M, Olivieri A, Leoni P, Poloni A. Bone marrow adipocytes support hematopoietic stem cell survival. *J Cell Physiol* 2018; **233**: 1500-1511 [PMID: 28574591 DOI: 10.1002/jcp.26037]

29 **Cordeiro Gomes A**, Hara T, Lim VY, Herndler-Brandstetter D, Nevius E, Sugiyama T, Tani-Ichi S, Schlenner S, Richie E, Rodewald HR, Flavell RA, Nagasawa T, Ikuta K, Pereira JP. Hematopoietic Stem Cell Niches Produce Lineage-Instructive Signals to Control Multipotent Progenitor Differentiation. *Immunity* 2016; **45**: 1219-1231 [PMID: 27913094 DOI: 10.1016/j.immuni.2016.11.004]

30 **Arslan NP**, Taskin M, Keles ON. Nicotinamide Mononucleotide and Nicotinamide Riboside Reverse Ovarian Aging in Rats Via Rebalancing Mitochondrial Fission and Fusion Mechanisms. *Pharm Res* 2024; **41**: 921-935 [PMID: 38684562 DOI: 10.1007/s11095-024-03704-3]

31 **Wu QJ**, Zhang TN, Chen HH, Yu XF, Lv JL, Liu YY, Liu YS, Zheng G, Zhao JQ, Wei YF, Guo JY, Liu FH, Chang Q, Zhang YX, Liu CG, Zhao YH. The sirtuin family in health and disease. *Signal Transduct Target Ther* 2022; **7**: 402 [PMID: 36581622 DOI: 10.1038/s41392-022-01257-8]

32 **Wang X**, Dong F, Zhang S, Yang W, Yu W, Wang Z, Zhang S, Wang J, Ma S, Wu P, Gao Y, Dong J, Tang F, Cheng T, Ema H. TGF-β1 Negatively Regulates the Number and Function of Hematopoietic Stem Cells. *Stem Cell Reports* 2018; **11**: 274-287 [PMID: 29937145 DOI: 10.1016/j.stemcr.2018.05.017]

33 **Kovtonyuk LV**, Caiado F, Garcia-Martin S, Manz EM, Helbling P, Takizawa H, Boettcher S, Al-Shahrour F, Nombela-Arrieta C, Slack E, Manz MG. IL-1 mediates microbiome-induced inflammaging of hematopoietic stem cells in mice. *Blood* 2022; **139**: 44-58 [PMID: 34525198 DOI: 10.1182/blood.2021011570]

34 **Lotfy A**, AboQuella NM, Wang H. Mesenchymal stromal/stem cell (MSC)-derived exosomes in clinical trials. *Stem Cell Res Ther* 2023; **14**: 66 [PMID: 37024925 DOI: 10.1186/s13287-023-03287-7]

35 **Lan T**, Luo M, Wei X. Mesenchymal stem/stromal cells in cancer therapy. *J Hematol Oncol* 2021; **14**: 195 [PMID: 34789315 DOI: 10.1186/s13045-021-01208-w]

36 **Tsai AC**, Jeske R, Chen X, Yuan X, Li Y. Influence of Microenvironment on Mesenchymal Stem Cell Therapeutic Potency: From Planar Culture to Microcarriers. *Front Bioeng Biotechnol* 2020; **8**: 640 [PMID: 32671039 DOI: 10.3389/fbioe.2020.00640]

37 **Yin JQ**, Zhu J, Ankrum JA. Manufacturing of primed mesenchymal stromal cells for therapy. *Nat Biomed Eng* 2019; **3**: 90-104 [PMID: 30944433 DOI: 10.1038/s41551-018-0325-8]

38 **Moskalev A**, Guvatova Z, Lopes IA, Beckett CW, Kennedy BK, De Magalhaes JP, Makarov AA. Targeting aging mechanisms: pharmacological perspectives. *Trends Endocrinol Metab* 2022; **33**: 266-280 [PMID: 35183431 DOI: 10.1016/j.tem.2022.01.007]

World Journal of Stem Cells

Submit a Manuscript: https://www.f6publishing.com

World J Stem Cells 2025 February 26; 17(2): 99132

DOI: 10.4252/wjsc.v17.i2.99132

ISSN 1948-0210 (online)

ORIGINAL ARTICLE

Basic Study

WDR36 inhibits the osteogenic differentiation and migration of periodontal ligament stem cells

Yi Wang, Feng-Qiu Zhang, Zhi-Peng Fan, Xin-Ling Zhu, Wan-Hao Yan, Xiu-Li Zhang

Specialty type: Cell and tissue engineering

Provenance and peer review: Unsolicited article; Externally peer reviewed.

Peer-review model: Single blind

Peer-review report's classification

Scientific Quality: Grade B, Grade B, Grade C, Grade C, Grade C

Novelty: Grade B, Grade B, Grade B, Grade B

Creativity or Innovation: Grade B, Grade B, Grade B, Grade B

Scientific Significance: Grade A, Grade B, Grade B, Grade B

P-Reviewer: Ou QJ; Satarzadeh M; Ventura C

Received: July 23, 2024

Revised: November 23, 2024

Accepted: January 16, 2025

Published online: February 26, 2025

Processing time: 215 Days and 18.3 Hours

Yi Wang, Department of Wangfujing General School of Stomatology, Capital Medical University, Beijing 100070, China

Feng-Qiu Zhang, Department of Periodontics School of Stomatology, Capital Medical University, Beijing 100070, China

Zhi-Peng Fan, Key Laboratory of Tooth Regeneration and Function Reconstruction, Beijing Stomatological Hospital, School of Stomatology, Beijing 100070, China

Zhi-Peng Fan, Beijing Laboratory of Oral Health, Capital Medical University, Beijing 100070, China

Zhi-Peng Fan, Research Unit of Tooth Development and Regeneration, Chinese Academy of Medical Sciences, Beijing 100070, China

Xin-Ling Zhu, Department of Periodontology, Hangzhou Stomatology Hospital, Hangzhou 310006, Zhejiang Province, China

Wan-Hao Yan, Laboratory of Molecular Signaling and Stem Cells Therapy, Beijing Key Laboratory of Tooth Regeneration and Function Reconstruction, Capital Medical University School of Stomatology, Beijing 100070, China

Xiu-Li Zhang, Department of Stomatology, Civil Aviation General Hospital, Beijing 100123, China

Co-corresponding authors: Feng-Qiu Zhang and Zhi-Peng Fan.

Corresponding author: Feng-Qiu Zhang, Department of Periodontics School of Stomatology, Capital Medical University, No. 9 Fanjiacun Road, Fengtai District, Beijing 100070, China. zhfengqiu@126.com

Abstract

BACKGROUND

Periodontitis is an inflammatory disease caused by the host's immune response and various interactions between pathogens, which lead to the loss of connective tissue and bone. In recent years, mesenchymal stem cell (SC) transplantation technology has become a research hotspot, which can form periodontal ligament, cementum, and alveolar bone through proliferation and differentiation.

AIM
To elucidate the regulatory effects of WD repeat-containing protein 36 (WDR36) on the senescence, migration, and osteogenic differentiation of periodontal ligament SCs (PDLSCs).

METHODS
The migration and chemotaxis of PDLSCs were detected by the scratch-wound migration test and transwell chemotaxis test. Alkaline phosphatase (ALP) activity, Alizarin red staining, calcium content, and real-time reverse transcription polymerase chain reaction (RT-qPCR) of key transcription factors were used to detect the osteogenic differentiation function of PDLSCs. Cell senescence was determined by senescence-associated β-galactosidase staining.

RESULTS
The 24-hour and 48-hour scratch-wound migration test and 48-hour transwell chemotaxis test showed that overexpression of WDR36 inhibited the migration/chemotaxis of PDLSCs. Simultaneously, WDR36 depletion promoted the migration/chemotaxis of PDLSCs. The results of ALP activity, Alizarin red staining, calcium content, and RT-qPCR showed that overexpression of WDR36 inhibited the osteogenic differentiation of PDLSCs, and WDR36 depletion promoted the osteogenic differentiation of PDLSCs. Senescence-associated β-galactosidase staining showed that 0.1 μg/mL icariin (ICA) and overexpression of WDR36 inhibited the senescence of PDLSCs, and WDR36 depletion promoted the osteogenic differentiation of PDLSCs.

CONCLUSION
WDR36 inhibits the migration and chemotaxis, osteogenic differentiation, and senescence of PDLSCs; 0.1 μg/mL ICA inhibits the senescence of PDLSCs. Therefore, WDR36 might serve as a target for periodontal tissue regeneration and the treatment of periodontitis.

Key Words: Periodontal ligament stem cells; Periodontal tissue regeneration; Icariin; WD repeat-containing protein 36; Osteogenic differentiation

Core Tip: Periodontal ligament stem cells (PDLSCs) are an important cell source for periodontal tissue regeneration. They can migrate to injured areas to promote tissue repair, induce osteogenic differentiation for bone tissue regeneration, and delay tissue loss by inhibiting senescence. In this study, we investigated the regulatory function of WD repeat-containing protein 36 (WDR36) on PDLSCs and found that WDR36 inhibited the migration, osteogenic differentiation, and senescence of PDLSCs. Thus, WDR36 may serve as a new candidate target for periodontal tissue regeneration.

Citation: Wang Y, Zhang FQ, Fan ZP, Zhu XL, Yan WH, Zhang XL. WDR36 inhibits the osteogenic differentiation and migration of periodontal ligament stem cells. *World J Stem Cells* 2025; 17(2): 99132
URL: https://www.wjgnet.com/1948-0210/full/v17/i2/99132.htm
DOI: https://dx.doi.org/10.4252/wjsc.v17.i2.99132

INTRODUCTION

Periodontitis is an inflammatory disease caused by the host's immune response and various interactions between pathogens, leading to the loss of connective tissue and bone[1,2]. The main pathological change of periodontitis involves the destruction of alveolar bone, which is the leading cause of tooth loss in adults[3]. Periodontitis also negatively impacts speech, nutrition, quality of life, and self-esteem[4-6]. Moreover, there is a risk of severe systemic inflammation[7,8]. Due to its high incidence, periodontitis has become a huge public health burden worldwide, and the treatment of periodontitis has become a significant health challenge. Thus, the ultimate treatment goal of periodontitis is to reconstruct the lost periodontal tissues with the same physiological structure and function[9].

Current therapies for periodontitis are not very effective for controlling inflammation or regulating immune function. It is especially difficult to achieve ideal regeneration of the lost periodontal tissue[10,11]. Tissue engineering/regenerative medicine is an established research field that combines biomaterials, cell therapy, biomedical engineering, and genetics [12]. Its purpose is to stimulate the regeneration of tissues and organs by implanting biomaterials *in vivo* or constructing substitutes *in vitro*[12]. Adult stem cells (SCs) have a high proliferation potential to differentiate into various cell types depending on the tissue of origin. Additionally, they are responsible for generating new tissues in response to injury and disease *in vivo*. Therefore, therapies based on adult SCs have received widespread attention in treating various degenerative diseases[13]. Notably, there are mesenchymal SCs (MSCs) in teeth and surrounding supporting tissues, which can be isolated and cultured *in vitro* and have the potential for self-renewal and multidirectional differentiation, as well as regeneration and repairing functions[10,11]. Moreover, MSCs can proliferate and differentiate to form new

periodontal tissues[14-16]. Therefore, MSC transplantation technology is expected to be an ideal therapy for periodontal tissue regeneration.

Periodontal ligament SCs (PDLSCs) are among the few MSCs that continue to proliferate in adults. Additionally, their differentiation potential offers great promise for SC-based dental regeneration therapy[17,18]. PDLSCs are clonogenic and highly proliferative pluripotent cells that can regenerate cementum/periodontal ligament-like tissue by differentiating into osteoblast/cementoblast-like cells, adipocytes, chondrocytes, and fibroblasts. They also participate in the repair and steady-state turnover of periodontal tissue[19]. Previous studies have found that regenerated periodontal tissue can be obtained when autologous and allogeneic PDLSCs are transplanted into the periodontal defect area of pigs caused by surgery[16]. Therefore, PDLSCs are the leading candidate SCs among all MSCs, especially for treating periodontal tissue defects[20].

Research on traditional Chinese medicine has recently gained widespread attention, and this treatment method has unique advantages[21]. Icariin (ICA) is the main active flavonoid glycoside isolated from the dried stems and leaves of epimedium (chemical formula: C33H40O15); it has extensive pharmacological effects such as anti-oxidative and antitumor functions. ICA can dose dependently promote proliferation and differentiation, inhibit senescence, and reduce the apoptosis of PDLSCs[22-24]. ICA can also effectively promote bone reconstruction and prevent or delay the progression of bone metastasis-related diseases in rats by regulating the balance between adipogenesis and osteogenesis[23]. Our previous works showed that 0.1 μg/mL ICA could effectively promote proliferation and osteogenic differentiation and inhibit the bone resorption of PDLSCs[25,26]. To clarify the drug target of ICA, the whole-cell protein detection of PDLSCs under the action of 0.1 μg/mL ICA was performed. Western blotting verified the test results, and the target proteins and genes were subsequently screened. It was found that the expression of WD repeat-containing protein 36 (WDR36) was significantly increased.

Initially, WDR36 was discovered in 2005 as the candidate gene of primary open-angle glaucoma. The WDR36 gene is located in chromosome region 5q22.1, which spans a genomic region of approximately 34.7 kb and contains 23 exons that encode a 105 kDa protein (950 amino acids)[27]. WDR36 was found to be highly expressed in the human heart, placenta, liver, kidney, pancreas, and skeletal muscle[27]. By binding proteins, peptides, RNA, or DNA, the WDR domain participates in various cellular functions and is considered a possible drug target[28]. However, the role of WDR36 in MSCs and periodontal tissue regeneration remains unknown.

In this study, we used PDLSCs to clarify the function of WDR36 on the senescence, migration/chemotaxis, and osteogenic differentiation of PDLSCs and expound the potential role of WDR36 in periodontal tissue regeneration.

MATERIALS AND METHODS

Cell cultures

PDLSCs were purchased from Shanghai Optimal Ma Lai Biotechnology Co., Ltd. (Shanghai, China). The cells were cultured according to previously published protocols[29].

Cell sample preparation and proteomics analysis

ICA was purchased from the National Institute for the Control of Pharmaceutical and Biological Products (No. 110737-200415; Beijing, China), with a purity of 98.5%. It is a yellow powder and was sealed and stored at 4 °C. Additionally, 1 mg ICA powder was dissolved in 2 mL phosphate-buffered saline (PBS) and prepared to a 0.5 g/L solution. Then the 0.5 g/L solution was diluted with Alpha Minimum Essential Medium [15% fetal bovine serum (FBS) + 2 mmol/L glutamine + 1% double antibody] to a mass concentration of 0.1 μg/mL ICA solution. The cells were cultured in Dulbecco's Modified Eagle's Medium (DMEM) and cultured in ICA solution for 48 hours. Total protein extraction and sodium dodecyl sulfate polyacrylamide gel electrophoresis (SDS-PAGE) were performed according to previous protocols[30], followed by proteomics analysis according to previous protocols[31].

Plasmid construction and viral infection

The process of plasmid construction and viral infection was previously detailed in our study[29]. In short, plasmids were constructed using standard techniques, and all structures were verified through appropriate enzyme digestion and/or sequencing. Human full-length WDR36 cDNA containing the hemagglutinin (HA) tag was constructed using the whole gene synthesis method. Subsequently, the HA-WDR36 sequence was inserted into the pQCXIN recombinant vector through AgeI and BamH1 restriction sites. Virus packaging was prepared according to the manufacturer's protocol (Clontech Laboratories, Inc., Mountain View, CA, United States). Short hairpin RNA (shRNA)-WDR36 (sh-WDR36) and control shRNA lentivirus were purchased from Genepharma Company (Suzhou, China). The control shRNA sequence was 5'-TTCTCCGAACGTGTCACGT-3', and the sh-WDR36 sequence was 5'-GCGATGGATTGCTCTATTAGG-3'.

Real-time reverse transcription polymerase chain reaction

RNA extraction, cDNA synthesis, and real-time reverse transcription polymerase chain reaction (RT-qPCR) procedures followed previous protocols[30]. RT-PCR was performed using the SYBR Green PCR kit (Qiagen, Hilden, Germany). All primer sequences are shown in Table 1. The $2^{-\Delta\Delta Ct}$ method was utilized to calculate the relative mRNA levels[32]. ΔCts were determined from the Ct normalized with GAPDH. Then we calculated the Pearson's correlation coefficient for each gene using the normalized data to determine the consistency between microarray experiments and RT-qPCR ($P < 0.05$ and $r > 0.9$)[32].

Table 1 Real-time polymerase chain reaction primer sequence

Gene	Primer sequences	Primer product size
GAPDH-forward	5′-CATGAGAAGTATGACAACAGCCT-3′	113 bp
GAPDH-reverse	5′-AGTCCTTCCACGATACCAAAGT-3′	
WDR36-forward	5′-AGCCGTGGATGTTGTTGCTAT-3′	134 bp
WDR36-reverse	5′-GACCATCTGTGCGAAATGAAAT-3′	
OSX-forward	5′-CTCCTGCGACTGCCCTAAT-3′	126 bp
OSX-reverse	5′-TGCGAAGCCTTGCCATAC-3′	
RUNX2-forward	5′-CCAACCCACGAATGCACTATC-3′	78 bp
RUNX2-reverse	5′-CGGACATACCGAGGGACATG-3′	
DLX3-forward	5′-CCAGACGGTGAACCCCTAC-3′	83 bp
DLX3-reverse	5′-CCGACTTGGGCGAGTAAGC-3′	
OPN-forward	5′-ATGATGGCCGAGGTGATAGTGT-3′	76 bp
OPN-reverse	5′-TACTGGATGTCAGGTCTGCGA-3′	
OCN-forward	5′-AAGAGACCCAGGCGCTACCT-3′	110 bp
OCN-reverse	5′-AACTCGTCACAGTCCGGATTG-3′	
DMP1-forward	5′-GAAGAATGGAAGGGTCATTTGG-3′	134 bp
DMP1-reverse	5′-AAGCCACCAGCTAGCCTATAAATGT-3′	

bp: Base pairs; DLX3: Distal-less homeobox 3; DMP1: Dentin matrix protein-1; OCN: Osteocalcin; OPN: Osteopontin; OSX: Osterix; RUNX2: Runt-related transcription factor 2.

Western blot analysis

Total protein extraction and SDS-PAGE were performed according to previous protocols[30]. The protein quantification used in the experiment was 20 μg. The primary antibodies used were anti-WDR36 (Cat No. 73548; Abcam, Cambridge, MA, United States) and mouse monoclonal anti-HA (Clone No. C29F4, Cat No. MMS-101P; Covance Laboratories, Inc., Princeton, NJ, United States). Membranes were probed with monoclonal antibodies against β-actin (Cat No. C1313; Applygen Technologies, Inc., Beijing, China) and GAPDH (Cat No. C1312-100/-250; Applygen), which served as loading controls.

Scratch-wound migration assays

PDLSCs were seeded into a 6-well plate (Corning Costar, Tewksbury, MA, United States) at 4-5 × 10^5 cells/well and cultured in DMEM (Gibco, Thermo Fisher Scientific, Waltham, MA, United States) until the cells were 90% confluent. Then, a 1 mL pipette tip (Corning Costar) was used to scratch three straight wounds every 5 cm in the 6-well plate. After washing the cells with PBS (Gibco) to ensure no residual cell debris, the cells were cultured for 24-48 hours with DMEM. In sequence, three sites in each wound were selected to take pictures at 0 hour, 24 hours, and 48 hours. Image-Pro Plus 6.0 was applied to calculate the void area and height, and the relative width was obtained by the formula relative width = void area/height[33].

Transwell chemotaxis assays

To culture PDLSCs, 600 μL DMEM, supplemented with 15% FBS (Invitrogen, Carlsbad, CA, United States), was added to each well of the 24-well plate. Then the PDLSCs were seeded into the upper transwell chamber (8 μm pore size; Corning Costar) at 2-5 × 10^4 cells/well and cultured for 24-48 hours under the conditions of 37 °C and 5% CO_2. Subsequently, the cells were fixed in 4% paraformaldehyde and stained with 0.1% crystal violet staining solution. Finally, an inverted microscope and a camera system (Olympus, Tokyo, Japan) were used to observe the number of cells in nine randomly selected fields of each well.

Alkaline phosphatase activity assay and Alizarin red staining

PDLSCs were cultured in an osteogenic-inducing medium containing 100 μM/mL ascorbic acid (Cat No. abs580047; Absin, Shanghai, China), 2 mmol/L β-glycerophosphate (Cat No. 819-83-0; Kalamar, Shanghai, China), 1.8 mmol/L potassium dihydrogen phosphate [Cat No. GBW(E)130195; JissKang, Qingdao, China], and 10 nM dexamethasone (Cat No. A1217601; Gibco, Thermo Fisher Scientific, Shanghai, China). According to the manufacturer's experimental procedures, alkaline phosphatase (ALP) activity was detected with an ALP Activity Kit (Sigma-Aldrich, St. Louis, MO, United States). After 14 days of osteogenic induction of PDLSCs, mineralization was detected by 70% ethanol fixation and

2% Alizarin red (Sigma-Aldrich) staining. Then the stained cells were destained with 10% cetylpyridinium chloride in 10 mmol/L sodium phosphate at room temperature for 30 minutes to determine the calcium content.

Preparation of ICA solution and senescence-associated β-galactosidase staining

The Senescence β-Galactosidase Staining Kit (Cell Senescence Testing Kit; GenMed Scientifics Inc., Shanghai, China) was used to detect the effects of ICA and WDR36 on the senescence of PDLSCs. The cells cultured in DMEM and cultured in ICA solution were washed three times with PBS and fixed in 4% paraformaldehyde at room temperature for 30 minutes. The cells were stained overnight with senescence-associated β-galactosidase (SA-β-gal) staining solution (GenMed Scientifics) at 37 °C and randomly selected from five different fields of view from each sample with an optical microscope. Following the selections, the percentage of blue cell was calculated from three independent experiments.

Statistical analyses

All statistical analyses were done using SPSS 16.0 statistical software (IBM SPSS Statistics, Armonk, NY, United States). The Student's *t*-test or one-way analysis of variance was performed to evaluate the statistical significance, with $P \leq 0.05$ considered statistically significant.

RESULTS

WDR36 expression increases with 0.1 μg/mL ICA

The results of cell proteomics analysis showed a significant increase in the expression of WDR36 (see the Supplementary material) after culturing PDLSCs with 0.1 μg/mL ICA for 48 hours. The results were further validated by Western blotting (Figure 1).

WDR36 overexpression inhibits the migration/chemotaxis of PDLSCs

The retroviral vector was used to construct the HA-WDR36 sequence and transfected into PDLSCs. After 7 days of screening with 600 μg/mL G418 antibiotic, the overexpression efficiency was verified by RT-qPCR and Western blotting (Figure 2). The 24-hour and 48-hour wound-healing results showed that the migration distance of the HA-WDR36 group was shorter than that of the control group. The difference was also statistically significant ($P \leq 0.01$), indicating that WDR36 overexpression inhibited the migration function of the PDLSCs (Figure 3A and B). The transwell results also showed that the number of cells passing through the membrane in the vector group was significantly higher than that in the HA-WDR36 group ($P \leq 0.01$), indicating that overexpression of WDR36 inhibited the chemotactic function of the PDLSCs (Figure 3C and D).

WDR36 depletion promotes the migration/chemotaxis of PDLSCs

The sh-WDR36 lentivirus was used to knock down the expression of WDR36 in PDLSCs. After 3 days of screening with 1 μg/mL puromycin, the knockdown efficiency was verified by RT-qPCR and Western blotting (Figure 4). The 48-hour wound-healing results showed that the migration distance of the sh-WDR36 group was longer than that of the control group. The difference was also statistically significant ($P \leq 0.01$), indicating that knocking down WDR36 promoted the migration function of the PDLSCs (Figure 5A and B). Transwell results showed that the number of cells passing through the membrane in the sh-WDR36 group was significantly higher than that in the control group ($P \leq 0.01$), indicating that knocking down WDR36 promoted the chemotactic function of the PDLSCs (Figure 5C and D).

WDR36 overexpression inhibits the osteogenic differentiation of PDLSCs

ALP activity was detected on the third and fifth days of osteogenic induction as an early indicator of osteogenic differentiation. The results showed that compared with the control group, the ALP activity of the experimental group was significantly decreased ($P \leq 0.05$), demonstrating that the overexpression of WDR36 reduced the ALP activity of the PDLSCs. The results showed that WDR36 overexpression inhibited the early osteogenic differentiation of the PDLSCs (Figure 6A and B).

On the 14th day, the osteoblast-induced cells were stained with Alizarin red, and the calcium content was determined. We found that compared with the experimental group, the control group showed more obvious staining, and the calcium content of the control group was also higher than that of the experimental group. Notably, the results were statistically significant ($P \leq 0.05$). The results showed that overexpression of WDR36 inhibited the mineralization of the PDLSCs *in vitro* (Figure 6C and D).

RT-qPCR was used to detect the expression of osteogenic factors Runt-related transcription factor 2 (RUNX2), osterix (OSX), and distal-less homeobox 3 (DLX3) in cells without osteogenic induction. The results showed that the expression of these osteogenic players in the WDR36-overexpressing group was significantly lower than that of the control group ($P \leq 0.05$) (Figure 6E-G). After 1 week of osteogenic induction, the expression of osteopontin (OPN), dentin matrix protein-1 (DMP1), and osteocalcin (OCN) in the WDR36 overexpression group was significantly reduced compared with the control group ($P \leq 0.05$) (Figure 6H-J). After 2 weeks of osteogenic induction, the expression of OPN in the experimental group was significantly lower than that in the control group ($P \leq 0.05$) (Figure 6H).

WDR36 depletion promotes the osteogenic differentiation of the PDLSCs

The ALP activity results showed that compared with the control group, the ALP activity of the experimental group was

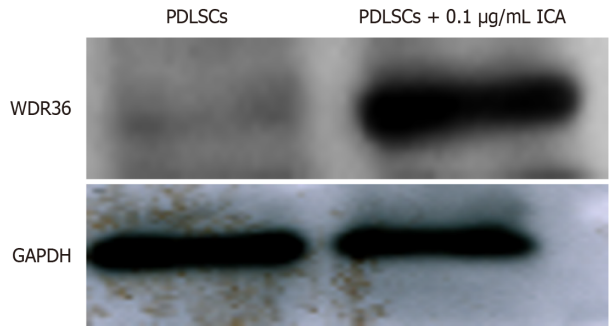

Figure 1 Expression of WD repeat-containing protein 36 in periodontal ligament stem cells with 0.1 μg/mL icariin. Western blot analysis showed that treatment with 0.1 μg/mL icariin (ICA) for 48 hours led to significantly increased expression of WD repeat-containing protein 36 (WDR36) in periodontal ligament stem cells (PDLSCs). Glyceraldehyde-3-phosphate dehydrogenase (GAPDH) served as an internal control.

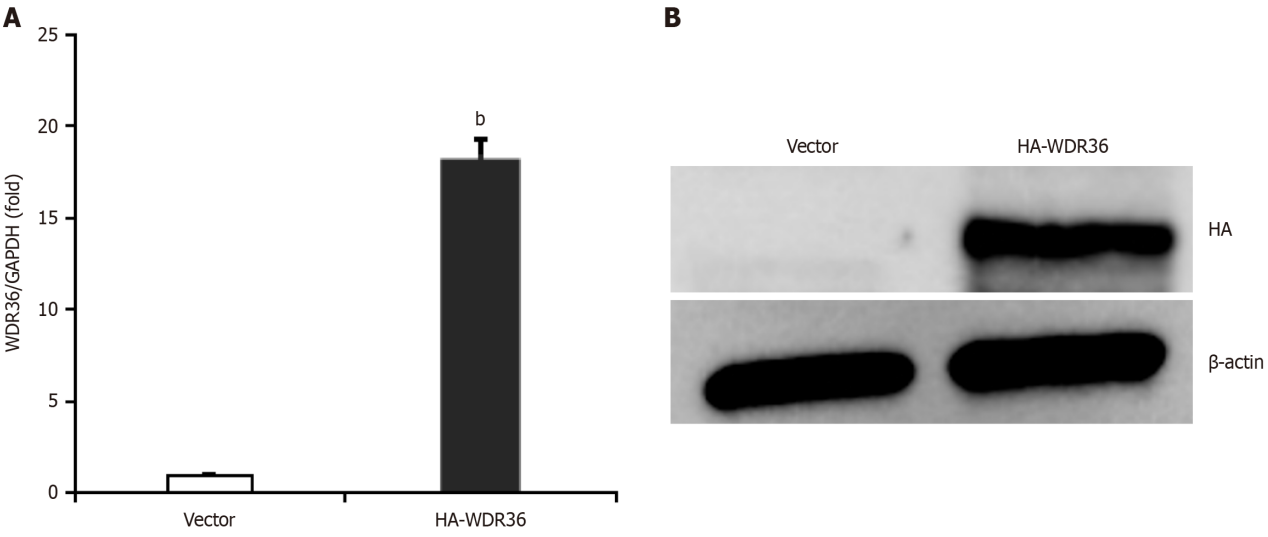

Figure 2 Validation of transfection efficiency of WD repeat-containing protein 36 overexpression. A: Reverse transcriptase-reverse polymerase chain reaction results showed the overexpression efficiency of hemagglutinin-WD repeat-containing protein 36 (HA-WDR36) in periodontal ligament stem cells (PDLSCs). Glyceraldehyde-3-phosphate dehydrogenase (GAPDH) served as an internal control; B: Western blot analysis showed the overexpression efficiency of HA-WDR36 in PDLSCs. β-actin served as an internal control. The statistical significance was measured by the Student's *t*-test. The error bars represent the standard deviation (n = 3). $^{b}P \leq 0.01$.

significantly increased ($P \leq 0.05$). This demonstrates that WDR36 depletion enhanced the ALP activity of the PDLSCs. That is, WDR36 depletion promoted the early osteogenic differentiation of the PDLSCs (Figure 7A and B).

On the 14th day, the osteoblast-induced cells were stained with Alizarin red, and the calcium content was detected. We found that compared with the experimental group, the control group showed less obvious staining, and the calcium content of the control group was also lower than that of the experimental group. Notably, these findings were statistically significant ($P \leq 0.05$). The results show that knockdown of WDR36 promoted the mineralization of PDLSCs *in vitro* (Figure 7C and D).

The expression of osteogenic factors RUNX2, OSX, DLX3, and DMP1 in cells without osteogenic induction was detected by RT-qPCR. The results showed that expression in the sh-WDR36 group was significantly higher than that in the control group ($P \leq 0.05$) (Figure 7E-H). After 1 week of osteogenic induction, the expression of DMP1, OPN, and OCN in the sh-WDR36 group was significantly increased compared with the control group ($P \leq 0.05$) (Figure 7H-J). After 2 weeks of osteogenic induction, the expression of OPN in the experimental group was significantly higher than that in the control group ($P \leq 0.05$) (Figure 7I).

ICA and WDR36 overexpression inhibits the senescence of PDLSCs

The results of SA-β-gal staining and quantitative calculation showed that the number of positive cells in the ICA group was significantly less than that in the group without ICA. In comparison, the number of positive cells in the HA-WDR36 group with or without ICA was significantly lower than that in the control group, indicating that 0.1 μg/mL ICA inhibited the senescence of PDLSCs. The same figure shows that overexpression of WDR36 also significantly inhibited the senescence of PDLSCs ($P \leq 0.01$) (Figure 8).

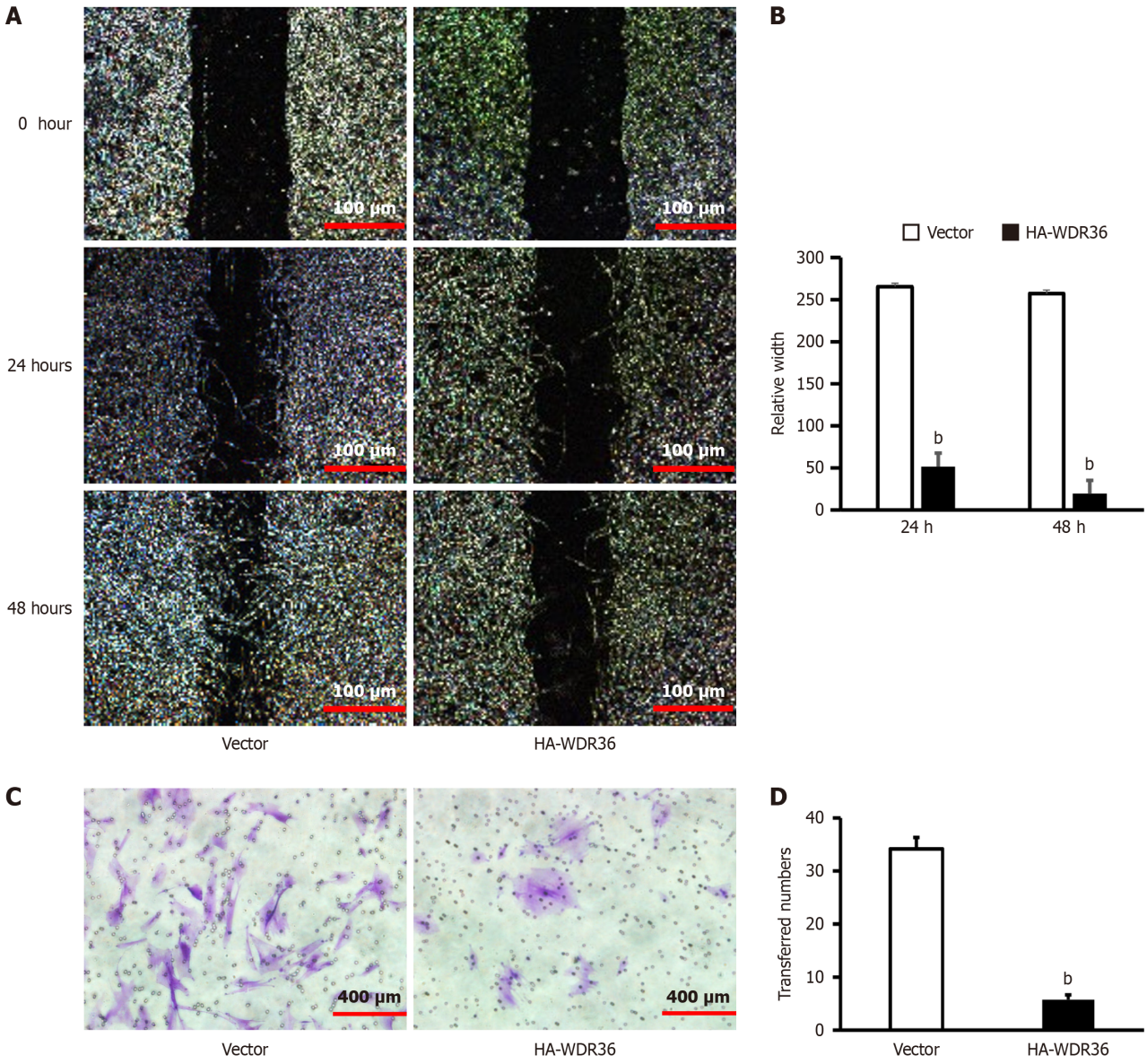

Figure 3 Migration and chemotaxis of WD repeat-containing protein 36 overexpression. A and B: The results for 0 hour, 24 hours, and 48 hours showed that the cell migration distance of the control group was longer than that of the hemagglutinin-WD repeat-containing protein 36 (HA-WDR36) group; C and D: Transwell results showed that the number of cells passing through the membrane in the WDR36 overexpression group was less than that in the control group. The statistical significance was measured by the Student's *t*-test. The error bars represent the standard deviation (n = 3). $^{b}P \leq 0.01$.

WDR36 depletion promotes the senescence of PDLSCs

SA-β-gal staining results showed that the number of positive cells in the ICA group was significantly less than that in the group without ICA. In comparison, the number of positive cells in the sh-WDR36 group with or without ICA was significantly higher than that in the control group, indicating that 0.1 μg/mL ICA inhibited the senescence of PDLSCs. At the same time, WDR36 depletion promoted the senescence of PDLSCs ($P \leq 0.01$) (Figure 9).

DISCUSSION

Our results indicate that WDR36 regulates the migration and chemotaxis, osteogenic differentiation, and senescence of PDLSCs. PDLSCs are the primary source of periodontal tissue regeneration, facilitating tissue repair by migrating to damaged sites. However, due to limited cell number and migration capacity, only a small number of PDLSCs can migrate to the target sites for periodontal tissue regeneration[33-35]. This could lead to less favorable conditions for subsequent periodontal regeneration. We investigated its effect on periodontal tissue regeneration by overexpression and knockdown of WDR36 in PDLSCs. The wound-healing and transwell results showed that overexpression of WDR36 inhibited the migration/chemotaxis of PDLSCs, whereas knocking down WDR36 promoted the migration/chemotaxis of PDLSCs. These findings indicate that WDR36 inhibits the migration/chemotaxis of PDLSCs, and WDR36 depletion is beneficial to the repair of damaged tissues.

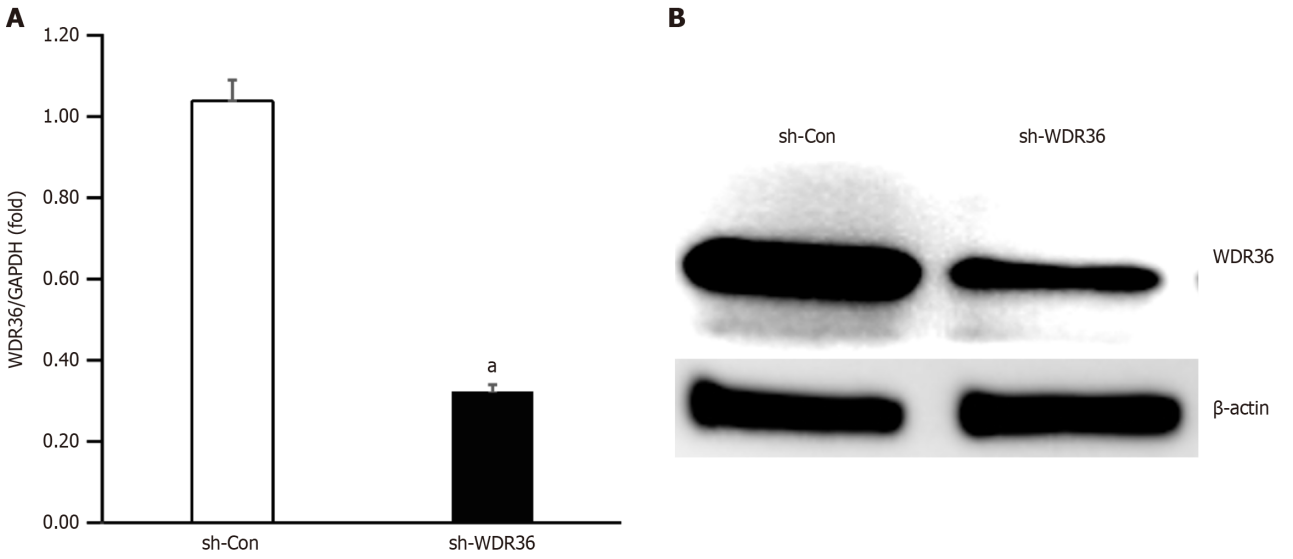

Figure 4 Validation of transfection efficiency of short hairpin RNA-WD repeat-containing protein 36. A: Reverse transcriptase-reverse polymerase chain reaction results showed the knockdown efficiency of short hairpin RNA-WD repeat-containing protein 36 (sh-WDR36) in periodontal ligament stem cells (PDLSCs). Glyceraldehyde-3-phosphate dehydrogenase (GAPDH) was used as an internal control; B: Western blot results showed the knockdown efficiency of sh-WDR36 in PDLSCs. β-actin was used as an internal control. The statistical significance was measured by the Student's *t*-test. The error bars represent the standard deviation (n = 3). $^{a}P \leq 0.05$.

We also studied the osteogenic differentiation function of PDLSCs by observing the osteogenic markers of cells at different times. Tissue non-specific ALP is generally considered a marker in the early process of osteogenesis/dentation and plays a role in bone matrix mineralization[36,37]. We detected the ALP activity and found that overexpression of WDR36 inhibited the ALP activity of PDLSCs while knockdown promoted its activity. The results also demonstrated that WDR36 inhibited the early osteogenesis of PDLSCs. Furthermore, by conducting Alizarin red staining and determining the calcium content, it was found that the overexpression of WDR36 inhibited the mineralization of PDLSCs *in vitro*. By contrast, WDR36 depletion enhanced the mineralization of PDLSCs *in vitro*.

We detected the mRNA expression of some osteogenic markers. The results showed that overexpression of WDR36 downregulated the expression of OCN, OPN, and DMP-1, suggesting that overexpression of WDR36 inhibited the osteogenic function of PDLSCs. OCN, OPN, and DMP-1 expression was upregulated in the WDR36 depletion group, indicating that knocking down WDR36 enhanced the osteogenic function of PDLSCs. RUNX2 is a transcription factor that regulates the transcription of many genes and early osteogenic differentiation. An increase in RUNX2 can promote osteoblast differentiation[38]. Moreover, OSX acts downstream of RUNX2, which maintains the balance of bone metabolism and is an important transcription factor for bone formation[39]. DLX3 plays a crucial role in embryogenesis and morphogenesis. Thus, the increased expression of DLX3 promotes the osteogenic function of MSCs[40]. Notably, our results showed that WDR36 overexpression decreased the expression of RUNX2, OSX, and DLX3 in PDLSCs. Meanwhile, WDR36 depletion increased their expression, suggesting that WDR36 inhibited the osteogenic differentiation of PDLSCs by regulating the transcription of RUNX2, OSX, and DLX3.

It has been shown that deleting the *WDR36* gene in cultured human trabecular meshwork cells can eventually activate the *p53* gene stress-response pathway, leading to cell apoptosis[41]. p53 can respond to various forms of cellular stress and is essential for cell senescence[42,43]. WDR36 is upregulated during human T-cell proliferation, participating in T-cell activation, and is considered a T-cell activation WD repeat protein[44]. However, research on WDR36 in osteogenic differentiation is still in its early stages, and the related mechanisms have not been investigated in the literature. Nonetheless, some works have found that the WD repeat protein, which activates gene transcription *via* chromatin remodeling, can accelerate osteoblast differentiation when overexpressed[45]. Furthermore, the gene *WDR63*, closely related to WDR36, is considered a key promoting factor in osteogenic differentiation[46]. The overexpression of WDR5 could enhance canonical Wnt signaling and osteoblast differentiation[45]. These investigations offer valuable insights and support for future works on the osteogenic differentiation mechanisms of WDR36.

ICA promotes the migration of bone marrow MSCs through hypoxia-inducible factor-1 alpha and further regulates the expression of chemokine receptor type 4[47]. ICA at a concentration of 0.01 mg/L effectively promotes the proliferation of PDLSCs and enhances the expression of osteoprotegerin (OPG) at both the mRNA and protein levels, thereby inhibiting alveolar bone resorption[25]. ICA can also promote the osteogenic differentiation of PDLSCs and stimulate the expression of osteogenic genes including ALP, OC, and type I collagen[25]. ICA promoted osteoblast proliferation by stimulating the expression of bone morphogenetic protein-2 (BMP-2) and OPG proteins and upregulating the mRNA expression of *BMP-2*, *OPG*, and *ALP*[23]. Some studies have found that ICA can promote the proliferation and differentiation of osteoblasts and induce the expression of RUNX2, OPG, and OSX through estrogen receptor-mediated pathways, BMP-2/Smad4 signaling pathways, and Wnt/β-catenin signaling pathways to increase the calcium content and promote bone formation [23,48,49]. Furthermore, ICA can downregulate the expression of RANKL through the nuclear factor kappa B and mitogen-activated protein kinases pathways to inhibit the proliferation, differentiation, and migration of osteoclasts, thus

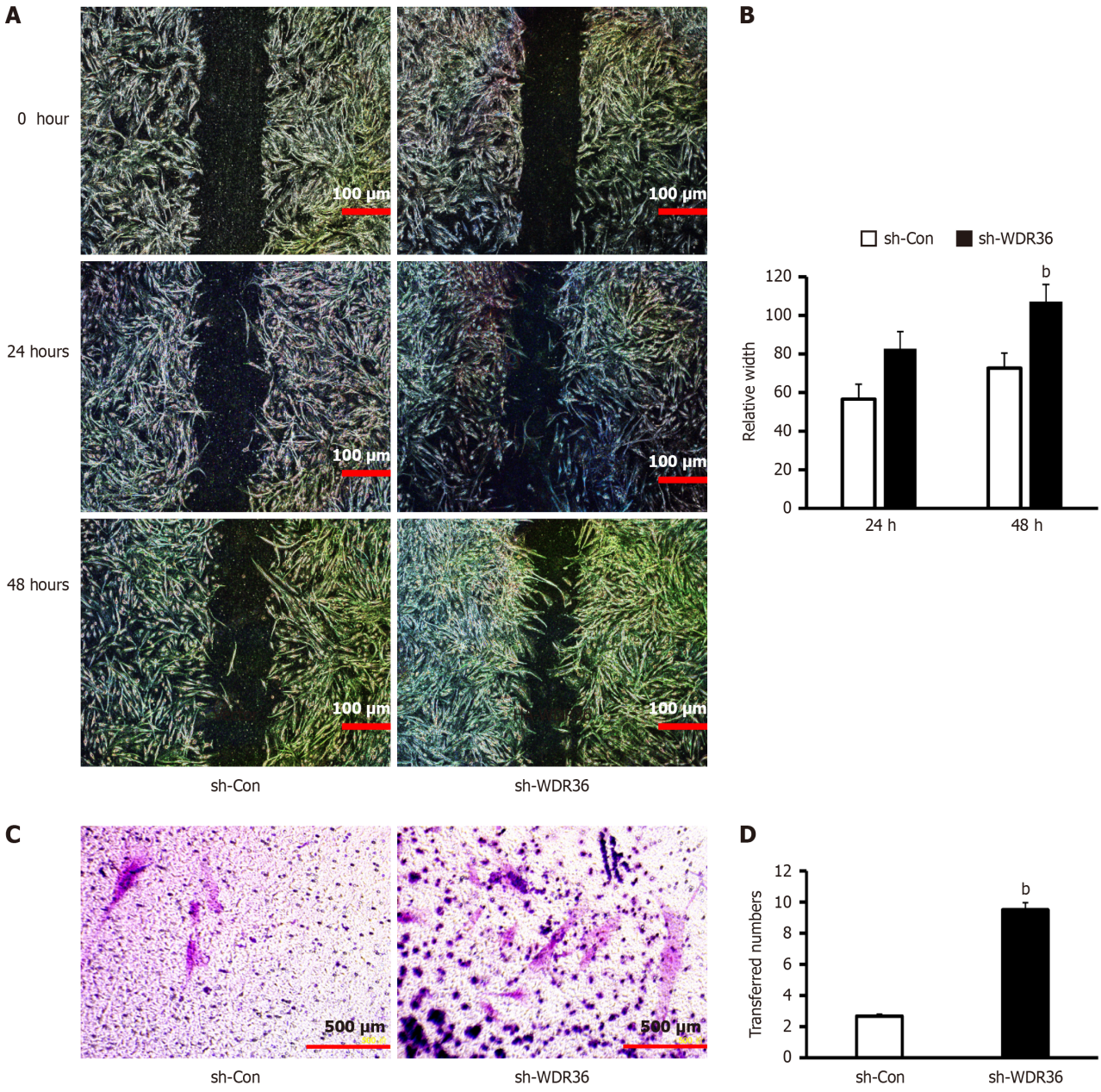

Figure 5 Migration and chemotaxis of short hairpin RNA-WD repeat-containing protein 36. A and B: The results for 0 hour and 24 hours showed that there were no significant differences between the short hairpin RNA-WD repeat-containing protein 36 (sh-WDR36) group and the control group. The 48 hours results showed that the cell migration distance of the control group was shorter than that of the sh-WDR36 group; C and D: Transwell results showed more cells passing through the membrane in the WDR36 depletion group than in the control group, and there was a statistically significant difference. The statistical significance was measured by the Student's *t*-test. The error bars represent the standard deviation (n = 3). $^{b}P \leq 0.01$.

reducing bone resorption[50]. Our study revealed that ICA led to the increased expression of WDR36. However, it was found that the overexpression of WDR36 inhibited the migration and osteogenic differentiation of PDLSCs. This indicates that ICA and WDR36 exhibit antagonistic effects on osteogenic function. The contradictory results could be attributed to the negative feedback regulatory role of WDR36. The negative feedback loop is a crucial regulatory motif within cells that helps reduce the stochasticity of protein levels. Protein-mediated transcriptional regulation is a common form that has negative feedback mechanism, where the protein involved inhibits its own transcription[51]. Within the WD-repeat gene family, while both WDR63 and WDR5 exhibit promotion of osteogenic function[45,46], WDR7 and WDR8 both demonstrate inhibition of the osteogenic process[52,53]. The detected downregulation of WDR8 expression in the endochondral ossification process shows that the WDR8 might serve as an antagonist in endochondral ossification through a negative feedback regulatory mechanism[53].

Senescence is an inevitable physiological process of various organisms and the leading cause of many chronic diseases. The gradual weakening of the function of human organs characterizes it. With senescence, periodontal tissue's anti-inflammation, anti-infection, and healing capacities gradually decrease. Additionally, the accumulated secretion of senescent cells may destroy tissue structure and function, affect SC function, cause environmental imbalance, and induce diseases[54]. MSCs also have anti-inflammatory, anti-fibrotic, and neuroprotective effects and can improve endothelial

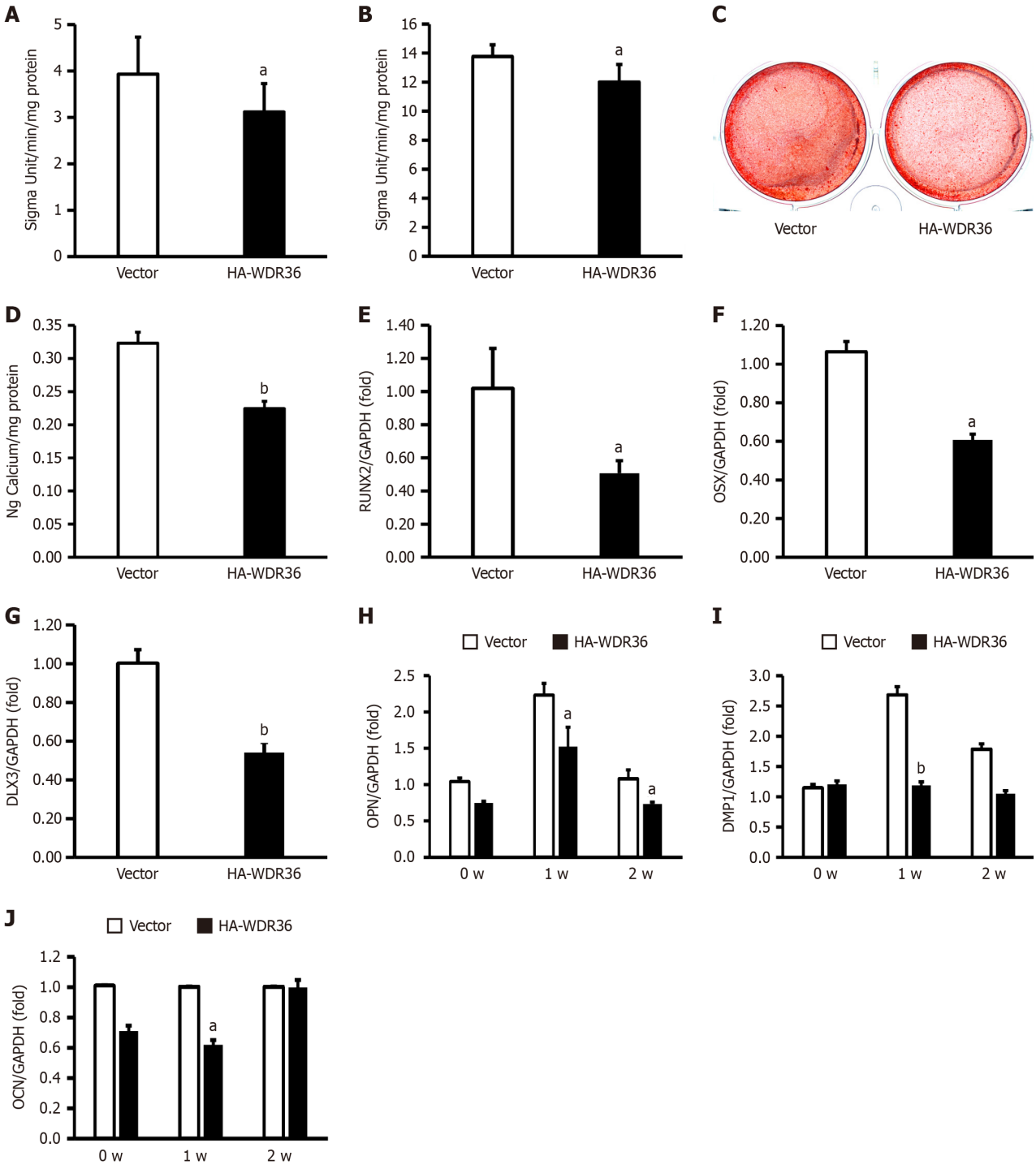

Figure 6 Osteogenic differentiation of WD repeat-containing protein 36 overexpression. A: Alkaline phosphatase (ALP) activity results on the third day; B: ALP activity results on the fifth day; C: Alizarin red staining; D: Calcium quantitative analysis; E: Expression of Runt-related transcription factor 2 (RUNX2) in the WD repeat-containing protein 36 (WDR36) overexpression group was significantly lower than that in the control group; F: Osterix (OSX) expression in the WDR36 overexpression group was significantly lower than that in the control group; G: Distal-less homeobox 3 (DLX3) in the WDR36 overexpression group was significantly lower than that in the control group; H: After 1 week and 2 weeks of osteogenic induction, osteopontin (OPN) expression in the WDR36 overexpression group was significantly lower than that in the control group; I: After 1 week of osteogenic induction, the expression of dentin matrix protein-1 (DMP1) in the WDR36 overexpression group was significantly lower than that in the control group. However, there were no statistically significant differences between the two groups at 0 week and 2 weeks; J: After 1 week of osteogenic induction, osteocalcin (OCN) expression in the WDR36 overexpression group was significantly lower than that in the control group. At 0 week and 2 weeks, no statistically significant differences between the two groups were observed. The statistical significance was measured by the Student's *t*-test. The error bars represent the standard deviation ($n = 3$). $^{a}P \leq 0.05$; $^{b}P \leq 0.01$.

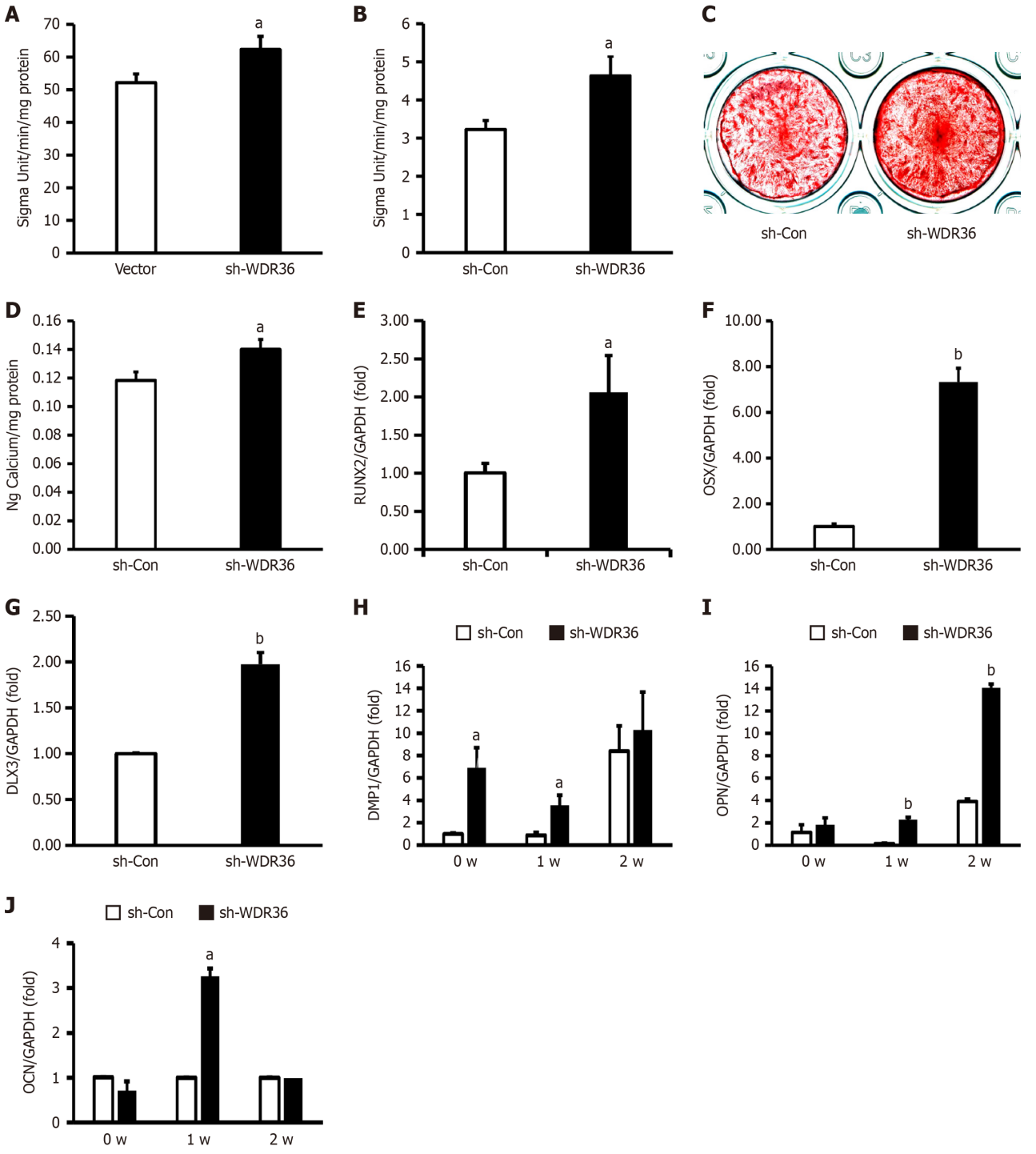

Figure 7 Osteogenic differentiation of short hairpin RNA-WD repeat-containing protein 36. A: Alkaline phosphatase (ALP) activity results on the third day; B: ALP activity results on the fifth day; C: Alizarin red staining; D: Calcium quantitative analysis; E: Expression of Runt-related transcription factor 2 (RUNX2) in the WD repeat-containing protein 36 (WDR36) depletion group was significantly higher than that in the control group; F: Osterix (OSX) expression in the WDR36 depletion group was significantly higher than that in the control group; G: Distal-less homeobox 3 (DLX3) in the WDR36 depletion group was significantly higher than that in the control group; H: At 0 week and 1 week of osteogenic induction, the expression of dentin matrix protein-1 (DMP1) in the WDR36 depletion group was significantly higher than that in the control group. At 2 weeks, there were no statistically significant differences between the two groups; I: The difference in osteopontin (OPN) expression between the WDR36 depletion group and the control group was not statistically significant. However, after 1 week and 2 weeks of osteogenic induction, OPN expression in the depletion group was significantly higher than that in the control group; J: At 1 week of osteogenic induction, OCN expression in the WDR36 depletion group was significantly higher than that in the control group. However, there were no statistically significant differences between the two groups at 0 week and 2 weeks. The statistical significance was measured by the Student's *t*-test. The error bars represent the standard deviation ($n = 3$). $^{a}P \leq 0.05$; $^{a}P \leq 0.01$.

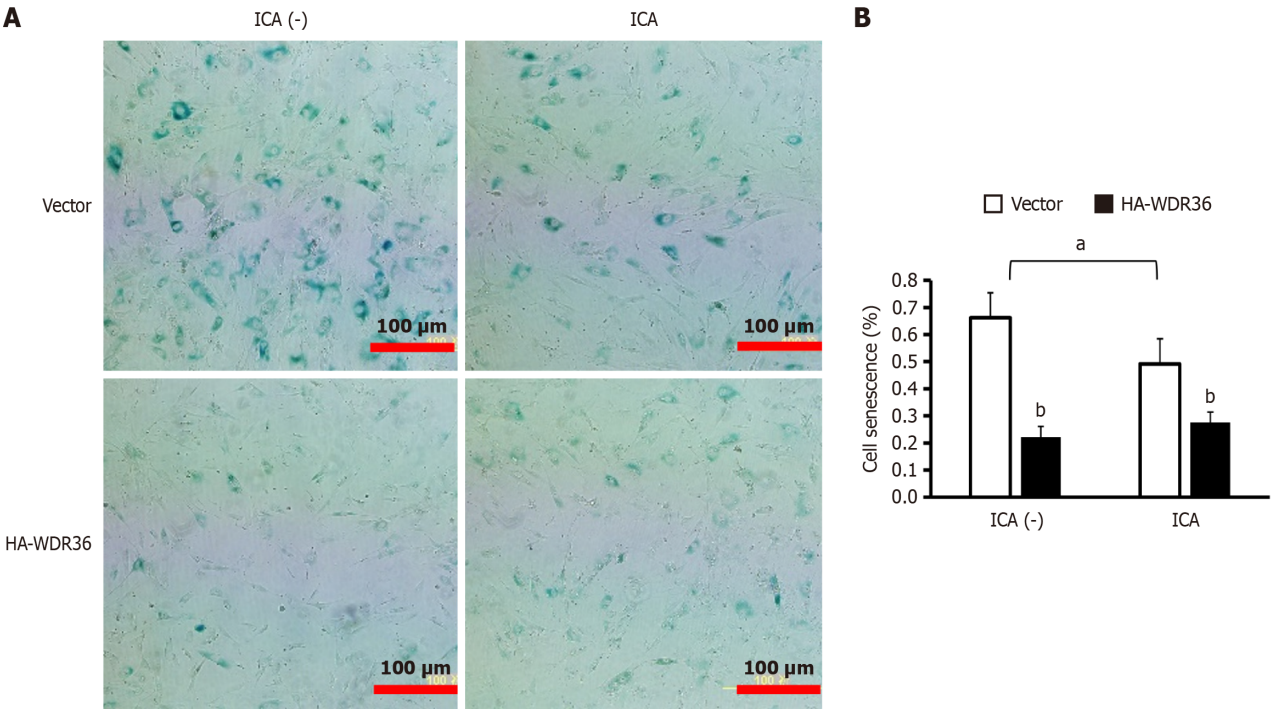

Figure 8 Senescence of 0.1 μg/mL icariin and WD repeat-containing protein 36 overexpression. A: Senescence-associated β-galactosidase staining results; B: Senescence-associated β-galactosidase staining results showed that the number of positive cells in the icariin (ICA) group was significantly less than that in the group without ICA. By contrast, the number of positive cells in the hemagglutinin-WD repeat-containing protein 36 (HA-WDR36) group with or without ICA was significantly lower than that in the control group, which indicates that 0.1 μg/mL ICA inhibited the senescence of periodontal ligament stem cells (PDLSCs), and overexpression of WDR36 inhibited the senescence of PDLSCs. The statistical significance was measured by the Student's *t*-test. The error bars represent the standard deviation (n = 3). $^{a}P \leq 0.05$; $^{b}P \leq 0.01$.

and mitochondrial functions, which makes MSCs attractive candidate cells for alleviating age-related diseases. Previous studies have also shown that ICA has antioxidant effects and can inhibit cell aging[13]. Treatment with 5 μM ICA during *in vitro* aging significantly reduced reactive oxygen species activity. Moreover, it increased the mRNA expression of glutathione and antioxidant genes. Additionally, 5 μM ICA prevented spindle defects and chromosome misalignment while increasing the mRNA expression of cytoplasmic maturation factor genes. It also inhibited apoptosis, increased the mRNA expression of anti-apoptotic genes, and decreased the mRNA expression of pro-apoptotic genes[22]. Therefore, we studied the effects of ICA and WDR36 on the senescence of PDLSCs. In 1995, Dimri *et al*[43] first proposed a marker enzyme to identify SA-β-gal, the product of the lysosomal β-gal gene beta-galactosidase (*GLB1*). In senescent cells, GLB1 significantly increases mRNA and protein levels, and the activity of β-gal is also correspondingly increased[30]. At a pH of 6.0, SA-β-gal can specifically recognize senescent cells *in vitro* and *in vivo*, and the positive staining rate increases with aging. Our results showed that the overexpression of WDR36 inhibited the senescence of PDLSCs, while the deletion of WDR36 promoted the senescence of PDLSCs. Simultaneously, we found that 0.1 μg/mL ICA inhibited the senescence of PDLSCs. Based on these findings, it was found that while WDR36 and ICA exhibit opposing functions in osteogenic process, they demonstrated a synergistic effect in terms of senescence-related functions. Although the negative feedback of WDR36 counteracted some anti-senescence effects, overexpression of WDR36 with ICA still exhibited some anti-senescence functions in PDLSCs. Previous investigations have also confirmed that the upregulation of WDR7 in rat PDLSCs could exert protective effects against hydrogen peroxide-induced oxidative stress, which is a significant factor contributing to cellular aging[55,56]. However, more works on the feedback mechanism of WDR36 are needed, such as the feedback regulatory pathways of WDR36 and the identification of key regulators within these pathways. These could reduce the negative impact of the feedback regulation on osteogenesis and anti-aging functions, and provide the possibility for our research to be applied clinically in the treatment of periodontal diseases in the future.

Although some studies have demonstrated the regulatory role of WD-repeat protein in osteogenic differentiation[45], research on WDR36 in osteogenesis is still lacking. As such, our study has addressed this research gap. Presently, the treatment of periodontitis primarily involves medication, basic therapy, surgical interventions, and supportive care. However, the effectiveness of these treatment modalities is not sufficiently ideal, especially in achieving optimal regeneration of lost periodontal tissues. PDLSCs can potentially promote the regeneration of periodontal tissues, while ICA can dose dependently stimulate the proliferation, differentiation, and deceleration of senescence of PDLSCs. Through our work, we demonstrated that targeting WDR36 effectively regulates the osteogenic differentiation of PDLSCs. This finding could introduce a novel approach to the regenerative treatment of periodontitis.

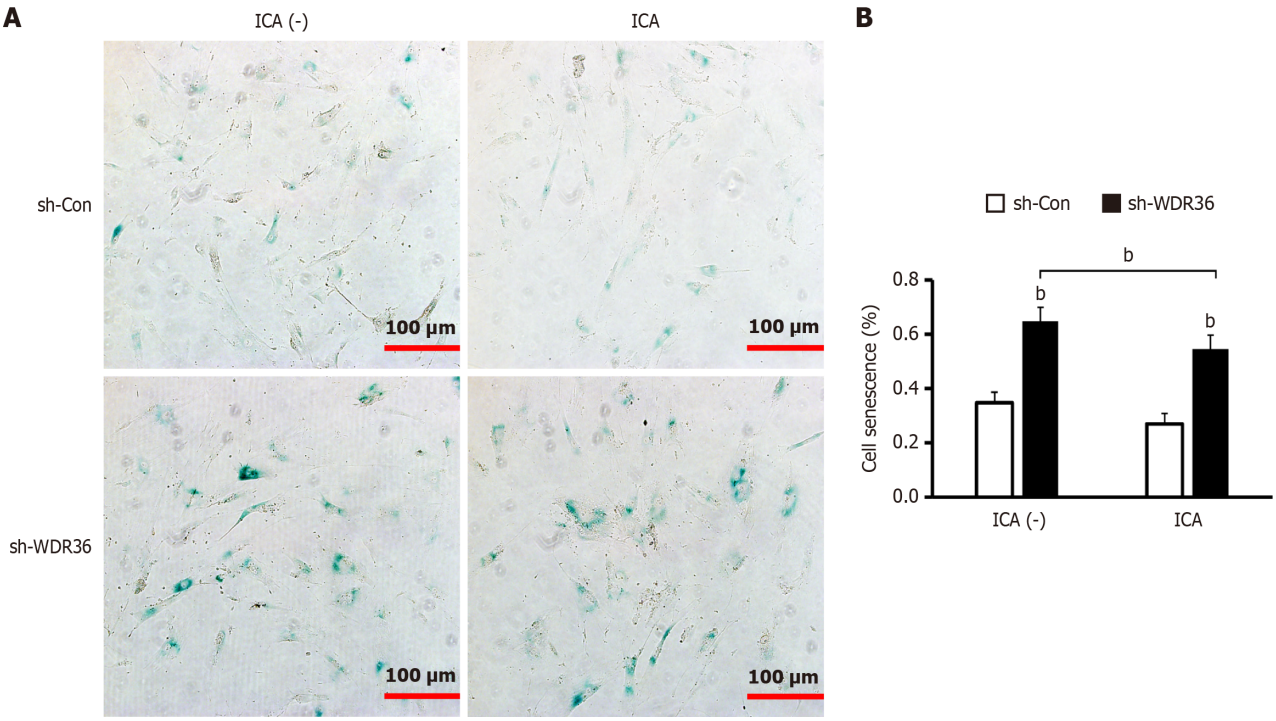

Figure 9 Senescence of 0.1 μg/mL icariin and short hairpin RNA- WD repeat-containing protein 36. A: Senescence-associated β-galactosidase staining results; B: Senescence-associated β-galactosidase staining results showed that the number of positive cells in the icariin (ICA) group was significantly less than that in the group without ICA. By contrast, the number of positive cells in the short hairpin RNA-WD repeat-containing protein 36 (sh-WDR36) group with or without ICA was significantly higher than that in the control group, which indicates that 0.1 μg/mL ICA inhibited the senescence of periodontal ligament stem cells (PDLSCs), and WDR36 depletion promoted the senescence of PDLSCs. The statistical significance was measured by the Student's *t*-test. The error bars represent the standard deviation (n = 3). $^{b}P \leq 0.01$.

CONCLUSION

In conclusion, WDR36 has regulatory effects on PDLSCs. As such, it inhibits the migration and chemotaxis, osteogenic differentiation, and senescence of PDLSCs. 0.1 μg/mL ICA inhibits the senescence of PDLSCs. Thus, our results provide new ideas and candidate targets for periodontal tissue regeneration and the treatment of periodontitis.

ACKNOWLEDGEMENTS

The authors gratefully thank the reviewers for their improvements to the manuscript.

FOOTNOTES

Author contributions: Wang Y wrote the manuscript; Zhang FQ and Fan ZP conceptualized the study, revised and formatted the content of the manuscript, and verified spelling, punctuation, and grammatical errors; Wang Y, Zhu XL, Yan WH, and Zhang XL carried out the experiments and analyzed the data. The collaboration between Zhang FQ and Fan ZP was essential for the publication of this manuscript. Both authors contributed equally to the research, including study design, revised and formatted the content of the manuscript, and verified spelling, punctuation, and grammatical errors. This statement confirms that both Zhang FQ and Fan ZP share equal responsibility and contribution as co-corresponding authors of this work. All authors contributed to the preparation of the manuscript.

Supported by Beijing Natural Science Foundation, No. 7192076.

Institutional review board statement: Institutional review board approval was not needed for this study because the cells used in this study were commercially obtained from LMAI Bio Company (Shanghai, China), which complies with all relevant ethical guidelines for cell procurement and distribution. These cells were further modified by surface marking in our laboratory for the purposes of this research. As no human or animal subjects were involved in the collection of the cells used, no additional ethical approval was required.

Conflict-of-interest statement: The authors have no conflicts of interest to declare.

Data sharing statement: The datasets generated during the current work are available from the corresponding authors on reasonable

request.

Country of origin: China

ORCID number: Yi Wang 0009-0005-0904-7635; Feng-Qiu Zhang 0000-0001-5782-0761; Zhi-Peng Fan 0000-0003-0629-3476.

S-Editor: Wang JJ
L-Editor: Filipodia
P-Editor: Zheng XM

REFERENCES

1 **Checchi V**, Maravic T, Bellini P, Generali L, Consolo U, Breschi L, Mazzoni A. The Role of Matrix Metalloproteinases in Periodontal Disease. *Int J Environ Res Public Health* 2020; **17**: 4923 [PMID: 32650590 DOI: 10.3390/ijerph17144923]
2 **Kurgan S**, Kantarci A. Molecular basis for immunohistochemical and inflammatory changes during progression of gingivitis to periodontitis. *Periodontol 2000* 2018; **76**: 51-67 [PMID: 29194785 DOI: 10.1111/prd.12146]
3 **He S**, Zhou Q, Luo B, Chen B, Li L, Yan F. Chloroquine and 3-Methyladenine Attenuates Periodontal Inflammation and Bone Loss in Experimental Periodontitis. *Inflammation* 2020; **43**: 220-230 [PMID: 31720989 DOI: 10.1007/s10753-019-01111-0]
4 **Helal O**, Göstemeyer G, Krois J, Fawzy El Sayed K, Graetz C, Schwendicke F. Predictors for tooth loss in periodontitis patients: Systematic review and meta-analysis. *J Clin Periodontol* 2019; **46**: 699-712 [PMID: 31025366 DOI: 10.1111/jcpe.13118]
5 **Schwendicke F**, Schmietendorf E, Plaumann A, Sälzer S, Dörfer CE, Graetz C. Validation of multivariable models for predicting tooth loss in periodontitis patients. *J Clin Periodontol* 2018; **45**: 701-710 [PMID: 29611218 DOI: 10.1111/jcpe.12900]
6 **Costa CR**, Amorim BR, de Magalhães P, De Luca Canto G, Acevedo AC, Guerra EN. Effects of Plants on Osteogenic Differentiation and Mineralization of Periodontal Ligament Cells: A Systematic Review. *Phytother Res* 2016; **30**: 519-531 [PMID: 26822584 DOI: 10.1002/ptr.5568]
7 **Chapple IL**, Van der Weijden F, Doerfer C, Herrera D, Shapira L, Polak D, Madianos P, Louropoulou A, Machtei E, Donos N, Greenwell H, Van Winkelhoff AJ, Eren Kuru B, Arweiler N, Teughels W, Aimetti M, Molina A, Montero E, Graziani F. Primary prevention of periodontitis: managing gingivitis. *J Clin Periodontol* 2015; **42** Suppl 16: S71-S76 [PMID: 25639826 DOI: 10.1111/jcpe.12366]
8 **Nagarajan S**, Chandra RV. Perception of oral health related quality of life (OHQoL-UK) among periodontal risk patients before and after periodontal therapy. *Community Dent Health* 2012; **29**: 90-94 [PMID: 22482257]
9 **Sculean A**, Chapple IL, Giannobile WV. Wound models for periodontal and bone regeneration: the role of biologic research. *Periodontol 2000* 2015; **68**: 7-20 [PMID: 25867976 DOI: 10.1111/prd.12091]
10 **Trubiani O**, Pizzicannella J, Caputi S, Marchisio M, Mazzon E, Paganelli R, Paganelli A, Diomede F. Periodontal Ligament Stem Cells: Current Knowledge and Future Perspectives. *Stem Cells Dev* 2019; **28**: 995-1003 [PMID: 31017047 DOI: 10.1089/scd.2019.0025]
11 **Nagata M**, Iwasaki K, Akazawa K, Komaki M, Yokoyama N, Izumi Y, Morita I. Conditioned Medium from Periodontal Ligament Stem Cells Enhances Periodontal Regeneration. *Tissue Eng Part A* 2017; **23**: 367-377 [PMID: 28027709 DOI: 10.1089/ten.TEA.2016.0274]
12 **Brouwer KM**, Lundvig DM, Middelkoop E, Wagener FA, Von den Hoff JW. Mechanical cues in orofacial tissue engineering and regenerative medicine. *Wound Repair Regen* 2015; **23**: 302-311 [PMID: 25787133 DOI: 10.1111/wrr.12283]
13 **Cable J**, Fuchs E, Weissman I, Jasper H, Glass D, Rando TA, Blau H, Debnath S, Oliva A, Park S, Passegué E, Kim C, Krasnow MA. Adult stem cells and regenerative medicine-a symposium report. *Ann N Y Acad Sci* 2020; **1462**: 27-36 [PMID: 31655007 DOI: 10.1111/nyas.14243]
14 **Liu J**, Ruan J, Weir MD, Ren K, Schneider A, Wang P, Oates TW, Chang X, Xu HHK. Periodontal Bone-Ligament-Cementum Regeneration *via* Scaffolds and Stem Cells. *Cells* 2019; **8**: 537 [PMID: 31167434 DOI: 10.3390/cells8060537]
15 **Cho YD**, Kim KH, Ryoo HM, Lee YM, Ku Y, Seol YJ. Recent Advances of Useful Cell Sources in the Periodontal Regeneration. *Curr Stem Cell Res Ther* 2019; **14**: 3-8 [PMID: 30112999 DOI: 10.2174/1574888X13666180816113456]
16 **Hu L**, Liu Y, Wang S. Stem cell-based tooth and periodontal regeneration. *Oral Dis* 2018; **24**: 696-705 [PMID: 28636235 DOI: 10.1111/odi.12703]
17 **Soudi A**, Yazdanian M, Ranjbar R, Tebyanian H, Yazdanian A, Tahmasebi E, Keshvad A, Seifalian A. Role and application of stem cells in dental regeneration: A comprehensive overview. *EXCLI J* 2021; **20**: 454-489 [PMID: 33746673 DOI: 10.17179/excli2021-3335]
18 **Queiroz A**, Albuquerque-Souza E, Gasparoni LM, de França BN, Pelissari C, Trierveiler M, Holzhausen M. Therapeutic potential of periodontal ligament stem cells. *World J Stem Cells* 2021; **13**: 605-618 [PMID: 34249230 DOI: 10.4252/wjsc.v13.i6.605]
19 **Seo BM**, Miura M, Gronthos S, Bartold PM, Batouli S, Brahim J, Young M, Robey PG, Wang CY, Shi S. Investigation of multipotent postnatal stem cells from human periodontal ligament. *Lancet* 2004; **364**: 149-155 [PMID: 15246727 DOI: 10.1016/S0140-6736(04)16627-0]
20 **Huang GT**, Gronthos S, Shi S. Mesenchymal stem cells derived from dental tissues vs. those from other sources: their biology and role in regenerative medicine. *J Dent Res* 2009; **88**: 792-806 [PMID: 19767575 DOI: 10.1177/0022034509340867]
21 **Sharifi S**, Moghaddam FA, Abedi A, Maleki Dizaj S, Ahmadian S, Abdolahinia ED, Khatibi SMH, Samiei M. Phytochemicals impact on osteogenic differentiation of mesenchymal stem cells. *Biofactors* 2020; **46**: 874-893 [PMID: 33037744 DOI: 10.1002/biof.1682]
22 **Yoon JW**, Lee SE, Park YG, Kim WJ, Park HJ, Park CO, Kim SH, Oh SH, Lee DG, Pyeon DB, Kim EY, Park SP. The antioxidant icariin protects porcine oocytes from age-related damage in vitro. *Anim Biosci* 2021; **34**: 546-557 [PMID: 32777912 DOI: 10.5713/ajas.20.0046]
23 **Xie L**, Liu N, Xiao Y, Liu Y, Yan C, Wang G, Jing X. In Vitro and In Vivo Osteogenesis Induced by Icariin and Bone Morphogenetic Protein-2: A Dynamic Observation. *Front Pharmacol* 2020; **11**: 1058 [PMID: 32760277 DOI: 10.3389/fphar.2020.01058]

24 **Song L**, Zhao J, Zhang X, Li H, Zhou Y. Icariin induces osteoblast proliferation, differentiation and mineralization through estrogen receptor-mediated ERK and JNK signal activation. *Eur J Pharmacol* 2013; **714**: 15-22 [PMID: 23764463 DOI: 10.1016/j.ejphar.2013.05.039]

25 **Ding Q**, Zhang F, Ma Y. [Effect of icariin on osteoblastic differentiation gene expression of human periodontal ligament cells]. *Beijing Daxue Xuebao (Yixueban)* 2013; **45**: 975-978

26 **Ding Q**, Zhang F. [Effect of icariin on the expression of receptor activator nudear factor.κB ligand and osteoprotegerin of human periodontal ligament cells]. *Zhonghua Kouqiang Yixue Zazhi* 2013; **48**: 68-71 [DOI: 10.3760/cma.j.issn.1002-0098.2013.02.002]

27 **Monemi S**, Spaeth G, DaSilva A, Popinchalk S, Ilitchev E, Liebmann J, Ritch R, Héon E, Crick RP, Child A, Sarfarazi M. Identification of a novel adult-onset primary open-angle glaucoma (POAG) gene on 5q22.1. *Hum Mol Genet* 2005; **14**: 725-733 [PMID: 15677485 DOI: 10.1093/hmg/ddi068]

28 **Blankenbach KV**, Bruno G, Wondra E, Spohner AK, Aster NJ, Vienken H, Trautmann S, Ferreirós N, Wieland T, Bruni P, Meyer Zu Heringdorf D. The WD40 repeat protein, WDR36, orchestrates sphingosine kinase-1 recruitment and phospholipase C-β activation by G(q)-coupled receptors. *Biochim Biophys Acta Mol Cell Biol Lipids* 2020; **1865**: 158704 [PMID: 32244061 DOI: 10.1016/j.bbalip.2020.158704]

29 **Liu D**, Wang Y, Jia Z, Wang L, Wang J, Yang D, Song J, Wang S, Fan Z. Demethylation of IGFBP5 by Histone Demethylase KDM6B Promotes Mesenchymal Stem Cell-Mediated Periodontal Tissue Regeneration by Enhancing Osteogenic Differentiation and Anti-Inflammation Potentials. *Stem Cells* 2015; **33**: 2523-2536 [PMID: 25827480 DOI: 10.1002/stem.2018]

30 **Liu H**, Han X, Yang H, Cao Y, Zhang C, Du J, Diao S, Fan Z. GREM1 inhibits osteogenic differentiation, senescence and BMP transcription of adipose-derived stem cells. *Connect Tissue Res* 2021; **62**: 325-336 [PMID: 32151168 DOI: 10.1080/03008207.2020.1736054]

31 **Kim JA**, Vetrivel P, Kim SM, Ha SE, Kim HH, Bhosale PB, Heo JD, Lee WS, Senthil K, Kim GS. Quantitative Proteomics Analysis for the Identification of Differential Protein Expression in Calf Muscles between Young and Old SD Rats Using Mass Spectrometry. *ACS Omega* 2021; **6**: 7422-7433 [PMID: 33778255 DOI: 10.1021/acsomega.0c05821]

32 **Zhang W**, Dong R, Diao S, Du J, Fan Z, Wang F. Differential long noncoding RNA/mRNA expression profiling and functional network analysis during osteogenic differentiation of human bone marrow mesenchymal stem cells. *Stem Cell Res Ther* 2017; **8**: 30 [PMID: 28173844 DOI: 10.1186/s13287-017-0485-6]

33 **Zhang J**, Zhang C, Yang H, Han X, Fan Z, Hou B. Depletion of PRDM9 enhances proliferation, migration and chemotaxis potentials in human periodontal ligament stem cells. *Connect Tissue Res* 2020; **61**: 498-508 [PMID: 31096797 DOI: 10.1080/03008207.2019.1620224]

34 **Liang Q**, Du L, Zhang R, Kang W, Ge S. Stromal cell-derived factor-1/Exendin-4 cotherapy facilitates the proliferation, migration and osteogenic differentiation of human periodontal ligament stem cells in vitro and promotes periodontal bone regeneration in vivo. *Cell Prolif* 2021; **54**: e12997 [PMID: 33511708 DOI: 10.1111/cpr.12997]

35 **Chen Z**, Liu HL. Restoration of miR-1305 relieves the inhibitory effect of nicotine on periodontal ligament-derived stem cell proliferation, migration, and osteogenic differentiation. *J Oral Pathol Med* 2017; **46**: 313-320 [PMID: 27604968 DOI: 10.1111/jop.12492]

36 **Yu Z**, Gauthier P, Tran QT, El-Ayachi I, Bhatti FU, Bahabri R, Al-Habib M, Huang GT. Differential Properties of Human ALP(+) Periodontal Ligament Stem Cells vs Their ALP(-) Counterparts. *J Stem Cell Res Ther* 2015; **5**: 292 [PMID: 26807329 DOI: 10.4172/2157-7633.1000292]

37 **Ye G**, Li C, Xiang X, Chen C, Zhang R, Yang X, Yu X, Wang J, Wang L, Shi Q, Weng Y. Bone morphogenetic protein-9 induces PDLSCs osteogenic differentiation through the ERK and p38 signal pathways. *Int J Med Sci* 2014; **11**: 1065-1072 [PMID: 25136261 DOI: 10.7150/ijms.8473]

38 **Vimalraj S**, Arumugam B, Miranda PJ, Selvamurugan N. Runx2: Structure, function, and phosphorylation in osteoblast differentiation. *Int J Biol Macromol* 2015; **78**: 202-208 [PMID: 25881954 DOI: 10.1016/j.ijbiomac.2015.04.008]

39 **Chen D**, Li Y, Zhou Z, Xing Y, Zhong Y, Zou X, Tian W, Zhang C. Synergistic inhibition of Wnt pathway by HIF-1α and osteoblast-specific transcription factor osterix (Osx) in osteoblasts. *PLoS One* 2012; **7**: e52948 [PMID: 23300831 DOI: 10.1371/journal.pone.0052948]

40 **Sun S**, Yu M, Fan Z, Yeh IT, Feng H, Liu H, Han D. DLX3 regulates osteogenic differentiation of bone marrow mesenchymal stem cells *via* Wnt/β-catenin pathway mediated histone methylation of DKK4. *Biochem Biophys Res Commun* 2019; **516**: 171-176 [PMID: 31202458 DOI: 10.1016/j.bbrc.2019.06.029]

41 **Skarie JM**, Link BA. The primary open-angle glaucoma gene WDR36 functions in ribosomal RNA processing and interacts with the p53 stress-response pathway. *Hum Mol Genet* 2008; **17**: 2474-2485 [PMID: 18469340 DOI: 10.1093/hmg/ddn147]

42 **Blanco-Marchite C**, Sánchez-Sánchez F, López-Garrido MP, Iñigez-de-Onzoño M, López-Martínez F, López-Sánchez E, Alvarez L, Rodrí guez-Calvo PP, Méndez-Hernández C, Fernández-Vega L, García-Sánchez J, Coca-Prados M, García-Feijoo J, Escribano J. WDR36 and P53 gene variants and susceptibility to primary open-angle glaucoma: analysis of gene-gene interactions. *Invest Ophthalmol Vis Sci* 2011; **52**: 8467-8478 [PMID: 21931130 DOI: 10.1167/iovs.11-7489]

43 **Dimri GP**, Lee X, Basile G, Acosta M, Scott G, Roskelley C, Medrano EE, Linskens M, Rubelj I, Pereira-Smith O. A biomarker that identifies senescent human cells in culture and in aging skin in vivo. *Proc Natl Acad Sci U S A* 1995; **92**: 9363-9367 [PMID: 7568133 DOI: 10.1073/pnas.92.20.9363]

44 **Mao M**, Biery MC, Kobayashi SV, Ward T, Schimmack G, Burchard J, Schelter JM, Dai H, He YD, Linsley PS. T lymphocyte activation gene identification by coregulated expression on DNA microarrays. *Genomics* 2004; **83**: 989-999 [PMID: 15177553 DOI: 10.1016/j.ygeno.2003.12.019]

45 **Zhu ED**, Demay MB, Gori F. Wdr5 is essential for osteoblast differentiation. *J Biol Chem* 2008; **283**: 7361-7367 [PMID: 18201971 DOI: 10.1074/jbc.M703304200]

46 **Diao S**, Yang DM, Dong R, Wang LP, Wang JS, Du J, Wang SL, Fan Z. Enriched trimethylation of lysine 4 of histone H3 of WDR63 enhanced osteogenic differentiation potentials of stem cells from apical papilla. *J Endod* 2015; **41**: 205-211 [PMID: 25498833 DOI: 10.1016/j.joen.2014.09.027]

47 **Zhu H**, Wang X, Han Y, Zhang W, Xin W, Zheng X, Zhang J. Icariin promotes the migration of bone marrow stromal cells *via* the SDF-1α/HIF-1α/CXCR4 pathway. *Drug Des Devel Ther* 2018; **12**: 4023-4031 [PMID: 30538428 DOI: 10.2147/DDDT.S179989]

48 **Xue L**, Jiang Y, Han T, Zhang N, Qin L, Xin H, Zhang Q. Comparative proteomic and metabolomic analysis reveal the antiosteoporotic molecular mechanism of icariin from Epimedium brevicornu maxim. *J Ethnopharmacol* 2016; **192**: 370-381 [PMID: 27422162 DOI: 10.1016/j.jep.2016.07.037]

49 **Yang A**, Yu C, Lu Q, Li H, Li Z, He C. Mechanism of Action of Icariin in Bone Marrow Mesenchymal Stem Cells. *Stem Cells Int* 2019; **2019**: 5747298 [PMID: 31089330 DOI: 10.1155/2019/5747298]

50 **Xu Q**, Chen G, Liu X, Dai M, Zhang B. Icariin inhibits RANKL-induced osteoclastogenesis *via* modulation of the NF-κB and MAPK signaling pathways. *Biochem Biophys Res Commun* 2019; **508**: 902-906 [PMID: 30538045 DOI: 10.1016/j.bbrc.2018.11.201]

51 **Singh A**. Negative feedback through mRNA provides the best control of gene-expression noise. *IEEE Trans Nanobioscience* 2011; **10**: 194-

200 [PMID: 22020106 DOI: 10.1109/tnb.2011.2168826]

52 **Yumimoto K**, Matsumoto M, Onoyama I, Imaizumi K, Nakayama KI. F-box and WD repeat domain-containing-7 (Fbxw7) protein targets endoplasmic reticulum-anchored osteogenic and chondrogenic transcriptional factors for degradation. *J Biol Chem* 2013; **288**: 28488-28502 [PMID: 23955342 DOI: 10.1074/jbc.M113.465179]

53 **Koshizuka Y**, Ikegawa S, Sano M, Nakamura K, Nakamura Y. Isolation, characterization, and mapping of the mouse and human WDR8 genes, members of a novel WD-repeat gene family. *Genomics* 2001; **72**: 252-259 [PMID: 11401440 DOI: 10.1006/geno.2000.6475]

54 **Du T**, Liu N, Gu B, Li L, Yuan Y, Zhang W, Zhang T. Effects of Aging on the Proliferation and Differentiation Capacity of Human Periodontal Ligament Stem Cells. *Chin Med Sci J* 2017; **32**: 83-81 [PMID: 28693688 DOI: 10.24920/J1001-9294.2017.012]

55 **Pole A**, Dimri M, Dimri GP. Oxidative stress, cellular senescence and ageing. *AIMS Mol Sci* 2016; **3**: 300-324 [DOI: 10.3934/molsci.2016.3.300]

56 **Feng Y**, Fu X, Lou X. Notch pathway deactivation mediated by F-box/WD repeat domain-containing 7 ameliorates hydrogen peroxide-induced apoptosis in rat periodontal ligament stem cells. *Arch Oral Biol* 2019; **100**: 93-99 [PMID: 30822705 DOI: 10.1016/j.archoralbio.2019.02.010]

World Journal of Stem Cells

Submit a Manuscript: https://www.f6publishing.com

World J Stem Cells 2025 February 26; 17(2): 99326

DOI: 10.4252/wjsc.v17.i2.99326

ISSN 1948-0210 (online)

ORIGINAL ARTICLE

Basic Study

Effects of macrophages on the osteogenic differentiation of adipose tissue-derived stem cells in two-dimensional and three-dimensional cocultures

He-Ao Zhang, Bo-Yu Zhang, Hong-Bo Tang

Specialty type: Cell and tissue engineering

Provenance and peer review: Unsolicited article; Externally peer reviewed.

Peer-review model: Single blind

Peer-review report's classification

Scientific Quality: Grade B, Grade B, Grade D

Novelty: Grade B, Grade B, Grade C

Creativity or Innovation: Grade B, Grade B, Grade C

Scientific Significance: Grade B, Grade B, Grade C

P-Reviewer: Gangadaran P; Kuhlmann C

Received: July 19, 2024

Revised: November 24, 2024

Accepted: January 23, 2025

Published online: February 26, 2025

Processing time: 219 Days and 14.4 Hours

He-Ao Zhang, Bo-Yu Zhang, Hong-Bo Tang, Department of Plastic and Cosmetic Surgery, Tongji Hospital, Tongji Medical College, Huazhong University of Science and Technology, Wuhan 430030, Hubei Province, China

Co-first authors: He-Ao Zhang and Bo-Yu Zhang.

Corresponding author: Hong-Bo Tang, Professor, Department of Plastic and Cosmetic Surgery, Tongji Hospital, Tongji Medical College, Huazhong University of Science and Technology, No. 1095 Jiefang Avenue, Wuhan 430030, Hubei Province, China. tthhbb@sohu.com

Abstract

BACKGROUND

Fracture is one of the most pervasive injuries in the musculoskeletal system, and there is a complex interaction between macrophages and adipose tissue-derived stem cells (ADSCs) in fracture healing. However, two-dimensional (2D) coculture of macrophages and ADSCs can not accurately mimic the *in vivo* cell microenvironment.

AIM

To establish both 2D and 3D osteogenic coculture models to investigate the interaction between macrophages and ADSCs.

METHODS

After obtaining ADSCs from surgery and inducing differentiation of the THP1 cell line, we established 2D and 3D osteogenic coculture models. To assess the level of osteogenic differentiation, we used alizarin red staining and measured the relative expression levels of osteogenic differentiation markers osteocalcin, Runt-related transcription factor 2, and alkaline phosphatase through polymerase chain reaction. Verification was conducted by analyzing the expression changes of N-cadherin and the activation of the Wnt/β-catenin signaling pathway using western blotting.

RESULTS

In this study, it was discovered that macrophages in 3D culture inhibited osteogenic differentiation of ADSCs, contrary to the effect in 2D culture. This observation confirmed the significance of intricate intercellular connections in the 3D

culture environment. Additionally, the 3D culture group exhibited significantly higher N-cadherin expression and showed reduced β-catenin and Wnt1 protein levels compared to the 2D culture group.

CONCLUSION

Macrophages promoted ADSC osteogenic differentiation in 2D culture conditions but inhibited it in 3D culture. The 3D culture environment might inhibit the Wnt/β-catenin signaling pathway by upregulating N-cadherin expression, ultimately hindering the osteogenic differentiation of ADSCs. By investigating the process of osteogenesis in ADSCs, this study provides novel ideas for exploring 3D osteogenesis in ADSCs, fracture repair, and other bone trauma repair.

Key Words: Fracture; Adipose tissue-derived stem cells; Osteogenic differentiation; Three-dimensional cell culture; N-cadherin

Core Tip: The macrophages in three-dimensional (3D) culture inhibited osteogenic differentiation of adipose tissue-derived stem cells (ADSCs), contrary to the effect in 2D culture. The 3D culture environment might inhibit the Wnt/β-catenin signaling pathway by increasing N-cadherin expression, and consequently, inhibiting osteogenic differentiation of ADSCs. This study offers a refined protocol for the exploration of ADSCs osteogenesis and provides novel ideas for exploring 3D osteogenesis in ADSCs, fracture repair, and other bone trauma repair.

Citation: Zhang HA, Zhang BY, Tang HB. Effects of macrophages on the osteogenic differentiation of adipose tissue-derived stem cells in two-dimensional and three-dimensional cocultures. *World J Stem Cells* 2025; 17(2): 99326
URL: https://www.wjgnet.com/1948-0210/full/v17/i2/99326.htm
DOI: https://dx.doi.org/10.4252/wjsc.v17.i2.99326

INTRODUCTION

Fracture is one of the most pervasive injuries in the musculoskeletal system. The complex physiological process of fracture healing has been extensively studied[1]. Following bone injury, a variety of inflammatory cells participate in the response, and the inflammatory response at the injury site affects the process of osteogenic differentiation[2]. Bone tissue engineering is a critical and innovative field in the treatment of bone injuries. Multiple relevant studies have been conducted, offering a valuable clinical foundation for the treatment of bone defects[3,4]. Owing to their unique ability to differentiate into osteogenic lineages, several stem cell types, including adipose tissue-derived stem cells (ADSCs), bone marrow mesenchymal stem cells (MSCs), and embryonic stem cells, have garnered significant attention in bone tissue engineering in recent years[5]. Among these, ADSCs, which are tissue stem cells that possess multidirectional differentiation potential and are present in the stromal vascular fraction (SVF) of adipose tissue, offer several benefits, such as easy availability of materials, plentiful sources, and the ability to interact with other inflammatory cells[6]. Therefore, ADSCs are widely used as stem cell sources for bone tissue engineering research. Following bone injury, macrophages are essential for regulating inflammatory responses[7]. Under the chemotaxis of mediators released by macrophages, MSCs and pericytes derived from bone marrow and other tissues migrate toward the trauma site and differentiate into osteoblasts to contribute to tissue repair[8].

Complex interactions exist between macrophages and ADSCs, consequently affecting the activity, function, and potential clinical applications of ADSCs[9]. Our previous studies established a two-dimensional (2D) coculture model of macrophages with ADSCs[10], and we discovered that macrophages promoted the osteogenic differentiation of ADSCs. Although 2D culture is the standard technique for *in vitro* cell culture, its ability to accurately mimic the complex microenvironment of cells *in vivo*, including the intricate cellular matrix, vascular and nutrient transport, and growth patterns, is limited[11]. In 3D culture, each cell can be surrounded by surrounding cells or an extracellular matrix, which corresponds to the normal *in vivo* ecological niche[12]. It is a good simulation of cell-cell junctions and cell-substrate interactions. In addition, the 3D coculture models can have more cell connections and morphogenetic movements than can the 2D coculture models in terms of cell adhesion, cell migration, and inflammatory activation processes, which can better mimic the *in vivo* environment[13-15]. Using 3D culture technology, we further established a 3D coculture model of macrophages and ADSCs by inoculating the cells with biocompatible scaffolds[16] or allowing them to aggregate into small spheres[17] to further elucidate the relationship between macrophages and ADSCs[18,19].

Interestingly, the results of the 3D culture model showed that macrophages inhibited the osteogenic differentiation of ADSCs, which was completely opposite to the results of the 2D culture model. These results confirmed that both the 2D and 3D culture models exerted different influences on the macrophage-ADSC interaction. N-cadherin-mediated intercellular junctions also play an important role in interfering with the osteogenesis of ADSCs[20]. This suggests that under 3D culture conditions, intercellular junctions form complex interactions that may have a significant impact on cellular functions[21,22].

N-cadherin is a single-stranded transmembrane glycoprotein that promotes adhesion between homologous and heterotypic cells in a calcium-dependent manner. As a member of the calcineurin family, N-cadherin plays crucial roles in regulating the development and function of the brain, nervous system, hematopoietic system, vasculature, skeletal muscle, heart, and microenvironment[23]. N-cadherin promotes osteogenic differentiation in the early stages but is challenging to identify in fully differentiated osteoblasts, indicating varying roles in different stages of osteogenic differentiation[24]. Our previous study revealed that N-cadherin plays a different role in osteogenic differentiation at different time points and that N-cadherin is expressed in macrophages, whereas it is not expressed in ADSCs, which is consistent with previously reported findings. In addition, Wnt/β-catenin signaling plays a vital role in regulating the stem cell resting phase and drug resistance[25]. E-cadherin is also crucial for macrophage function through the Wnt/β-catenin signaling pathway. However, the effect of N-cadherin on macrophages has not been reported[26,27]. In our previous study, by investigating the effect of macrophages on the osteogenic differentiation of ADSCs, we found that intercellular connectivity exerted an important influence on cellular function in a 3D environment and that the differential expression of N-cadherin was an important factor affecting stem cell osteogenesis.

In previous studies, osteogenic 2D and 3D coculture models of ADSCs and macrophages were established to investigate the role of macrophages in the osteogenic differentiation of ADSCs. The degree of osteogenic differentiation was assessed through Alizarin red staining and quantitative analysis of osteogenic markers using polymerase chain reaction (PCR), while western blotting was employed to analyze proteins involved in relevant signaling pathways. By exploring the pathophysiological processes underlying ADSC osteogenesis, this study provides a refined protocol for studying osteogenic differentiation in ADSCs and offers novel insights into 3D osteogenesis, fracture repair, and regeneration of bone tissue after trauma.

MATERIALS AND METHODS

Acquisition and characterization of ADSCs

Young, healthy patients aged between 20 and 30 underwent liposuction to extract adipose tissue from their waist, abdomen, or thighs. All operations were performed through the ethical committee of Tongji Hospital. The tissue was digested with collagenase, filtered through a screen, and centrifuged in a density gradient to obtain the SVF. The SVFs were then inoculated into culture flasks at a density of $1 \times 10^5/cm^2$, and the wall cells obtained after 3-5 passes were considered ADSCs[28]. The cells were either preserved through freezing or cultured for further progeny. To evaluate the differentiation potential of ADSCs, the cells were cultured in osteogenic, adipogenic, and chondrogenic induction media. Differentiation outcomes were assessed using Alcian blue staining for chondrogenesis, Oil Red O staining for adipogenesis, and Alizarin red staining for osteogenesis. Additionally, the expression of surface markers, including CD29, CD44, CD31, and CD34, was analyzed *via* flow cytometry to characterize the ADSCs.

Induced differentiation of the THP-1 cell line

The THP-1 monocyte cell line was purchased, cultured, and passaged in RPMI-1640 medium supplemented with 10% foetal bovine serum, which could be used for macrophage-induced differentiation after 3 generations. The induction protocol was as follows: THP-1 cells were induced to become macrophages after 48 hours by the addition of 50 ng/mL phorbol-12-myristate-13-acetate[29].

2D coculture of ADSCs-macrophages

To investigate the differences in ADSC and macrophage coculture under different conditions, 2D cocultures were divided into two groups. In the 2D-ADSC group, 5×10^4 ADSCs were cultured alone, and in the 2D-ADSC-THP-1 group, 5×10^4 ADSCs and 5×10^4 macrophages were cultured together. In 2D culture, the direct coculture method was used to obtain ADSCs and THP-1-differentiated macrophages, which were mixed according to the cell types and numbers of the above groups in 24-well plates and then cultured for 28 days by the addition of osteogenic medium (containing 10 nM dexamethasone, 100 μM ascorbic acid, and 10 mmol/L sodium β-glycerophosphate).

3D coculture of ADSCs-macrophages

To investigate the differences in ADSC and macrophage coculture under different conditions, 3D cocultures were divided into two groups. In the 3D-ADSC group, 5×10^4 ADSCs were cultured alone, and in the 3D-ADSC-THP-1 group, 5×10^4 ADSCs and 5×10^4 macrophages were cultured together. 3D culture was performed by the suspension drop method; 10 cm diameter Petri dishes were prepared with 15 mL of phosphate buffered saline (PBS), and the lid of each Petri dish was turned over and placed on an ultraclean table. For coculture, the concentration of macrophages was adjusted to 2.86×10^6/mL, and then the macrophages were mixed with an equal volume and concentration of ADSCs. For individual cultures, the concentration of ADSCs was adjusted to 2.86×10^6/mL, and then the ADSCs were mixed with an equal volume of medium. The cell suspension was mixed well, and the cell suspension was pushed onto the inside of the Petri dish lid with a micropipette at 35 μL per spot so that the cell suspension had a hemispherical protrusion. The lid was carefully flipped over the dish, and the mixture was incubated in the incubator for 3 days until the cells aggregated to form spheres. Finally, the pellets were transferred to 48-well nonadherent culture plates and incubated with osteogenic medium for 28 days.

For live-cell staining of cultured spheroplasts, the viability of the spheroplasts was assessed after spheroplast formation using the Calcein-AM/PI Toxicity Assay Kit (Yesen, China). The spheroids were washed twice with PBS and incubated in

PBS containing 2 μM calcein-AM and 1.5 μM PI for 15 minutes at room temperature. The samples were observed *via* a SOPTOP CX40 microscope (Shanghai, China).

Alizarin red staining and Semiquantification

The cells were fixed in 4% paraformaldehyde for 10 minutes after 14 and 28 days of osteogenic differentiation and then washed with distilled water. After the cells were stained for 2 minutes with Alizarin red staining, they were cleaned once more with distilled water and photographed using a microscope. Alizarin red was analyzed by quantitative detection using the colorimetric method. After the distilled water was removed, the plates remained at room temperature until they were completely dry. After 280 μL of 10% acetic acid was added, the plate was agitated for 30 minutes. The mixture was then transferred to an EP tube and heated for 10 minutes to 85 °C before being chilled on ice for 5 minutes. Following 20 minutes of centrifugation at 16000 × *g*, 100 μL of the supernatant was transferred into a tube along with 40 μL of 10% ammonium hydroxide. After the finished solution was transferred to a 96-well plate, a microplate reader was used to measure the absorbance at 405 nm.

Quantitative real-time PCR

To extract total RNA from the cell precipitates, we used RNAiso Plus (Takara Biomedical Technology, China). To obtain stable cDNA, Hieff first-strand cDNA Synthesis Super Mix (Yeasen, China) was then used following the manufacturer's instructions. To assess mRNA expression precisely, SYBR green real-time PCR Master Mix (Yeasen, China) was utilized. The primer sequences are shown in Supplementary Table 1.

Western blotting

Western blotting was used to identify protein expression. The cell samples were homogenized using cell lysis buffer (Cell Signaling Technology, United States), and the supernatant was obtained *via* centrifugation. The extracted proteins were separated on 10% or 8% SDS-polyacrylamide gels and subsequently transferred onto polyvinylidene fluoride membranes (Bio-Rad, United States) through electrotransfer. After the membranes were blocked for 1 hour, they were incubated overnight at 4 °C with primary antibodies. Following thorough washing, the membranes were incubated with HRP-conjugated secondary antibodies (Proteintech, Chicago, IL, United States) at a 1:5000 dilution for 2 hours at room temperature. Using the ECL western blotting kit (Proteintech, Chicago, IL, United States), the protein bands were detected and quantified using ImageLab software. The antibodies used are shown in Supplementary Table 2.

Statistical analysis

The data in the article are presented as the means ± SDs. Quantitative outcomes were evaluated using one-way ANOVA, with statistical significance defined as $P < 0.05$. All the statistical analyses were conducted using SPSS Statistics 25 software (IBM, New York, NY, United States).

RESULTS

Successful isolation and characterization of ADSCs

To obtain ADSCs, adipose tissue obtained from microtia surgery was digested with collagenase, screened, and subjected to density gradient centrifugation to obtain the SVF. After the SVFs were inoculated and passaged for 3-5 passages, we isolated and extracted human ADSCs. In passages 1-2, only a small number of cells adhered to the wall and were in a low-density state, forming a large, flattened monolayer. In passages 3-5, the stem cell growth morphology favored a long spindle shape and displayed a fibroblast-like morphology with abundant cytoplasm and nucleoli in parallel or swirling growth arrangements in a favorable culture state (Figure 1A). In the context of macrophage culture, normal THP-1 cells exhibited a complete morphology, good refractive qualities, and existed as single cells in suspension. After 48 hours of phorbol-12-myristate-13-acetate induction, the cells were wall-adherent round or oval shaped and larger in size (Figure 1B). ADSCs were incubated with fluorescence-conjugated antibodies and analyzed using flow cytometry. The results demonstrated that ADSCs were positive for the MSC surface markers CD29 and CD44 but negative for the endothelial marker CD31 and the hematopoietic marker CD34 (Figure 1C). Additionally, Alizarin red, Oil Red O, and Alcian blue staining confirmed the osteogenic, adipogenic, and chondrogenic differentiation capabilities of the ADSCs (Figure 1D-F). Therefore, ADSCs were successfully isolated and characterized.

Osteogenic differentiation effects of macrophages on ADSCs in 2D or 3D culture

Figure 2A presents a physical image of the 3D cell culture model that was prepared using the hanging drop method. Live cell staining revealed that the cells inside the spheres had good viability with negligible cell death during sphere formation, and most of the cells demonstrated strong proliferative activity capacity (Figure 2B). Images captured by the microscope revealed variations in the spheres between the two groups of cells. The ADSC spheres had a smoother and more uniform structure, whereas the ADSC-THP-1 spheres were irregular and had a larger diameter. These cell spheres were cultured in nonadherent plates and adhered to the bottom of the plates, maintaining a roughly spherical shape in the first 14 days. After 21 days of culture, the cells were detached from the spheres and subsequently proliferated by adhering to the bottom of the culture plate (Figure 2C).

After 14 and 28 days of osteogenic culture, the 2D-ADSC-THP-1 group displayed greater calcium deposition than did the 2D-ADSC group, as shown by alizarin red staining (Figure 3A). As determined by colorimetry, macrophages

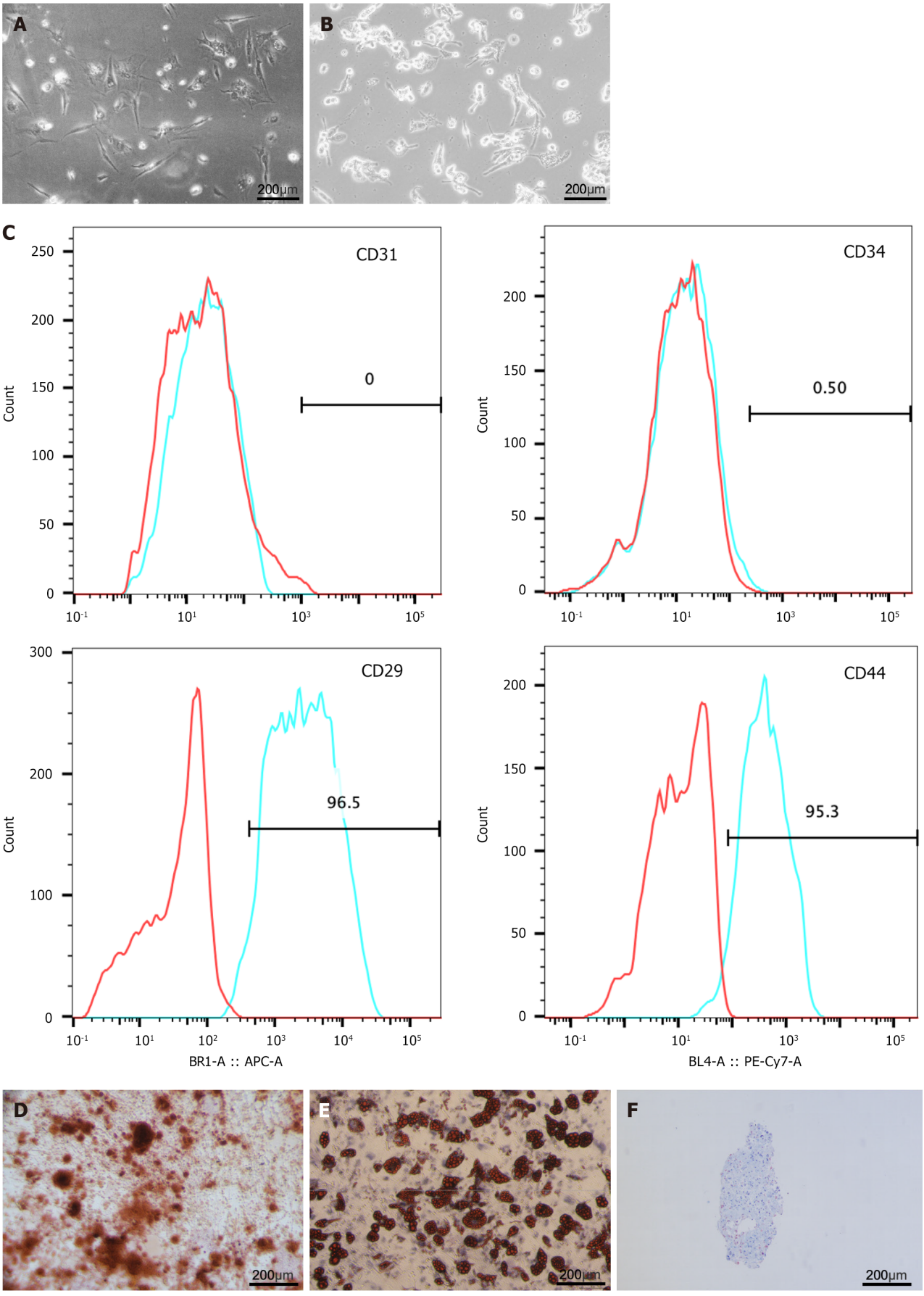

Figure 1 The isolation, extraction and characterisation of adipose tissue-derived stem cell and THP1. A: Cell culture micrographs of adipose tissue-derived stem cells; B: Cell culture micrographs of THP1; C: Flow cytometry showed adipose tissue-derived stem cells positive for CD29 and CD44, negative for CD31 and CD34; D-F: Osteogenic, adipogenic, and chondrogenic differentiations measured by Alizarin Red staining, Oil Red O staining, and Alcian Blue staining.

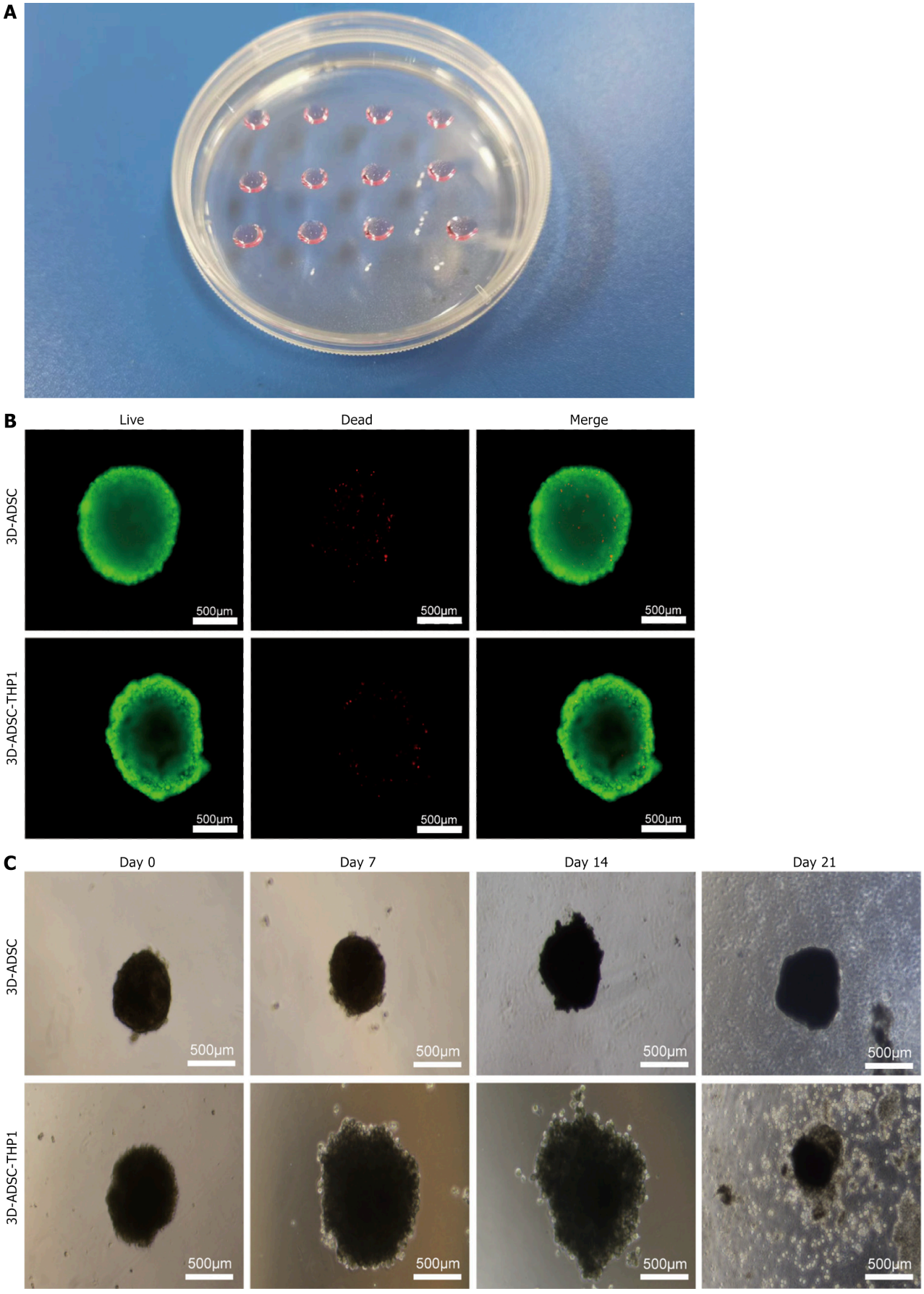

Figure 2 Three-dimensional culture of adipose tissue-derived stem cells. A: Macro photographs of three-dimensional culture cell; B: Immunofluorescence staining of alive and dead stem cells; C: Three-dimensional cultured cell spheroids recorded on day 0, 7, 14, and 21, and the cells are gradually detached from the and migrated to the culture plate with the prolongation of culture time. 3D: Three-dimensional; ADSC: Adipose tissue-derived stem cell.

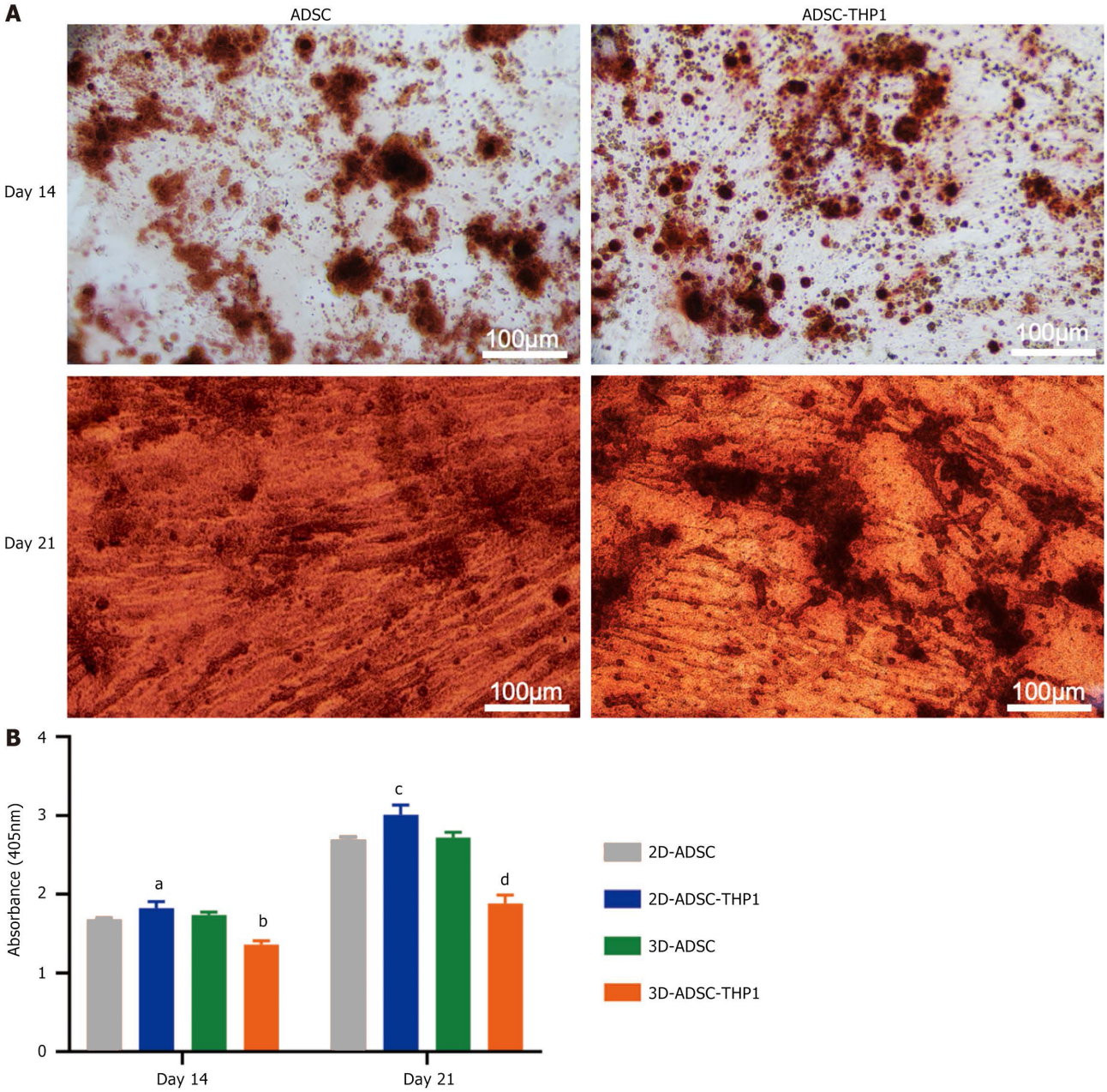

Figure 3 Osteogenic differentiation of adipose tissue-derived stem cells. A: Alizarin red staining of adipose tissue-derived stem cell (ADSC) and ADSC-THP1 in two-dimensional culture at 14 and 28 days; B: Semiquantitative measurement of calcium deposits formed during osteogenic differentiation of ADSCs in each group by alizarin red staining colorimetry. [a]*P* < 0.05 *vs* day14 two-dimensional-adipose tissue-derived stem cell, [b]*P* < 0.001 *vs* day14 three-dimensional-adipose tissue-derived stem cell, [c]*P* < 0.05 *vs* day28 two-dimensional-adipose tissue-derived stem cell, [d]*P* < 0.001 *vs* day28 three-dimensional-adipose tissue-derived stem cell. 3D: Three-dimensional; 2D: Two-dimensional; ADSC: Adipose tissue-derived stem cell.

effectively induced osteogenic differentiation of ADSCs in the 2D culture groups at 14 and 28 days. In contrast, macrophages hindered the osteogenic differentiation of ADSCs in the 3D culture groups. All the differences were statistically significant (Figure 3B).

Osteogenic marker gene expression was analyzed *via* quantitative real-time PCR. The results of alkaline phosphatase (*ALP*) gene expression on day 7 revealed no significant difference between the 2D-ADSC and 2D-ADSC-THP-1 groups, but the ALP expression in the 3D-ADSC-THP-1 group was lower than that in the 3D-ADSC group. On day 14, *ALP* gene expression was notably elevated in the 2D-ADSC-THP-1 group compared with the 2D-ADSC group. In contrast, the 3D-ADSC-THP-1 group presented significantly lower *ALP* gene expression than the 3D-ADSC group did (Figure 4A). On both day 7 and day 14, the expression levels of osteocalcin (OCN) and Runt-related transcription Factor 2 (RUNX2) were elevated in the 2D-ADSC-THP-1 group compared with those in the 2D-ADSC group, whereas they were reduced in the 3D-ADSC-THP-1 group compared with those in the 3D-ADSC group (Figure 4B and C).

The osteogenic differentiation function of ADSCs involves the Wnt signaling pathway

The levels of N-cadherin and proteins involved in the Wnt/β-catenin signaling pathway were quantified *via* western blotting analysis within each group (Figure 5A and B). The results revealed that the 3D-ADSC-THP-1 group presented a

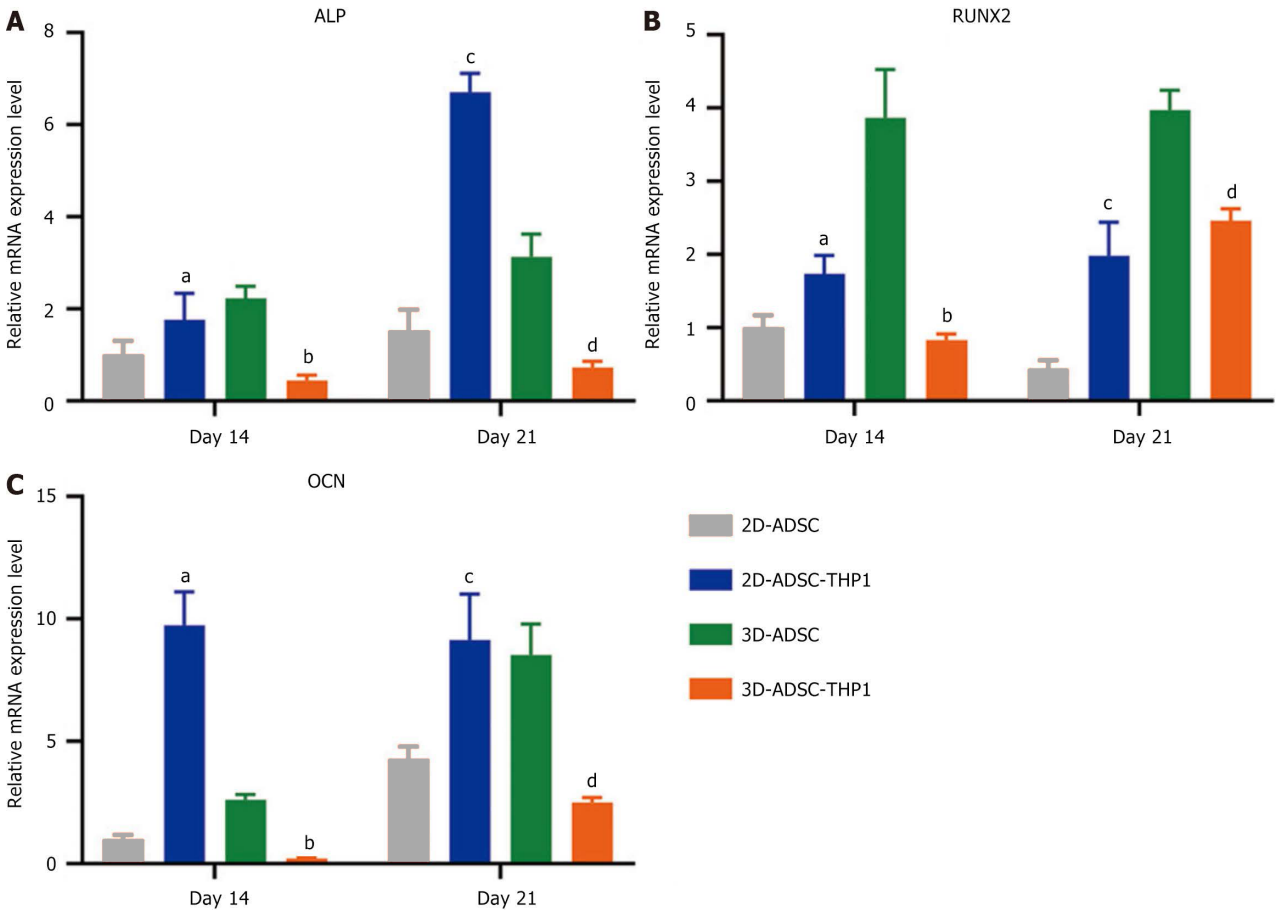

Figure 4 Expression of osteogenic gene markers in adipose tissue-derived stem cells. A: Relative expression of alkaline phosphatase in each group on day 7 and 14 ($^{a}P < 0.05$ *vs* day 7 two-dimensional-adipose tissue-derived stem cell (2D-ADSC), $^{b}P < 0.001$ *vs* day 7 three-dimensional (3D)-ADSC, $^{c}P < 0.001$ *vs* day 14 2D-ADSC, $^{d}P < 0.01$ *vs* day 14 3D-ADSC); B: Relative expression of Runt-related transcription factor 2 mRNA in each group on day 7 and 14 ($^{a}P < 0.05$ *vs* day 7 2D-ADSC, $^{b}P < 0.01$ *vs* day 7 3D-ADSC, $^{c}P < 0.01$ *vs* day 14 2D-ADSC, $^{d}P < 0.01$ *vs* day 14 3D-ADSC); C: Relative expression of osteocalcin in each group on day 7 and 14 ($^{a}P < 0.001$ *vs* day 7 2D-ADSC, $^{b}P < 0.001$ *vs* day 7 3D-ADSC, $^{c}P < 0.05$ *vs* day 14 2D-ADSC, $^{d}P < 0.01$ *vs* day 14 3D-ADSC). ALP: Alkaline phosphatase; RUNX2: Runt-related transcription factor 2; OCN: Osteocalcin; 3D: Three-dimensional; 2D: Two-dimensional; ADSC: Adipose tissue-derived stem cell.

significantly greater level of N-cadherin expression than did the 2D-ADSC-THP-1 group (Figure 5B). In addition, the protein expression of β-catenin and Wnt1 was reduced in the 3D-ADSC-THP-1 group (Figure 5B). These findings indicate that 3D culture might inhibit the Wnt/β-catenin signaling pathway by increasing the expression of N-cadherin, thus inhibiting the osteogenic differentiation of ADSCs.

DISCUSSION

Fractures are prevalent injuries to the musculoskeletal system, with complex interactions occurring between macrophages and ADSCs during the healing process[30]. There have been no relevant studies exploring the changes in N-cadherin expression in macrophages and MSCs during osteogenesis in ADSCs, particularly in the context of 2D and 3D cultures. Therefore, this study established osteogenic 2D and 3D coculture models and investigated the relationship between macrophages and ADSCs through the induction of cell aggregation into small spheres.

The use of coculture systems has rapidly become a suitable tool for studying cell-cell interactions in tissue engineering and regenerative medicine[18,19]. Previous studies explored 2D coculture systems to determine the cell-cell interactions between macrophages and ADSCs[6]. However, traditional 2D culture inadequately mimics the real microenvironment of *in vivo* cell interactions, ignoring the effects of the complex cellular matrix, vascular transport, nutrient transport, and growth patterns compared with 3D culture when studying the interaction between macrophages and ADSCs[12,31,32]. For example, primary articular chondrocytes and hepatocytes rapidly lose their normal phenotype when removed from *in vitro* culture and placed in 2D cell cultures, but this loss can be mitigated or even reversed by 3D culture methods[33,34]. The aggregation of ADSCs into 3D multicellular spheroids enhances their resistance to hypoxia-induced cell injury and apoptosis, differentiation potential, and growth factor production and release[35,36]. Our study established a 3D coculture model of macrophages and ADSCs, which can better mimic the real microenvironment of cells *in vivo* and explore the relationship between macrophages and ADSCs more comprehensively.

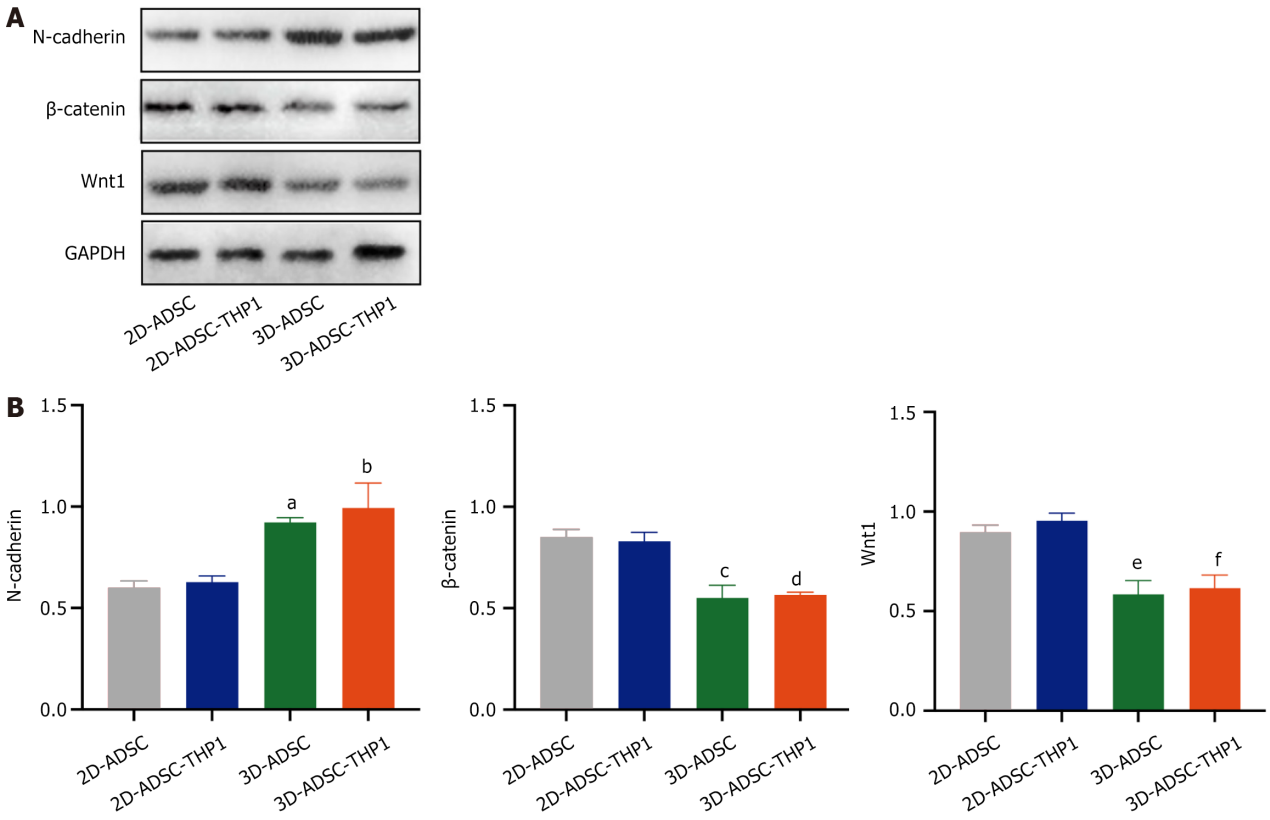

Figure 5 Quantification of pathway proteins. A: Measurement of N-cadherin and Wnt1, β-catenin signaling pathway protein expression in each group using western blotting; B: Quantitative analysis of western blotting in each group. [a]*P* < 0.01 *vs* two-dimensional-adipose tissue-derived stem cell (N-cadherin), [b]*P* < 0.001 *vs* two-dimensional-adipose tissue-derived stem cell-THP1 (N-cadherin), [c]*P* < 0.001 *vs* two-dimensional-adipose tissue-derived stem cell (β-catenin), [d]*P* < 0.001 *vs* two-dimensional-adipose tissue-derived stem cell-THP1 (β-catenin), [e]*P* < 0.01 *vs* two-dimensional-adipose tissue-derived stem cell (Wnt1), [f]*P* < 0.001 *vs* two-dimensional-adipose tissue-derived stem cell-THP1 (Wnt1). 3D: Three-dimensional; 2D: Two-dimensional; ADSC: Adipose tissue-derived stem cell.

Previous studies have explored the effects of macrophages on the osteogenic differentiation of MSCs but reported different effects. Fernandes *et al*[37] reported that macrophage-conditioned medium (CM) and oncostatin M in CM significantly promoted osteogenic differentiation[37]. However, Chen *et al*[38] reported that CM inhibited bone morphogenetic protein 2-induced osteogenic differentiation of human MSCs. The culture environment may be one of the factors influencing the results. In this study, we obtained different results in different culture models by establishing 2D and 3D osteogenic coculture models. Under 2D culture conditions, macrophages promoted ADSC osteogenic differentiation, whereas under 3D culture conditions, macrophages inhibited ADSC osteogenic differentiation. Compared with those in 2D culture, the intercellular adhesive junctions in 3D culture more precisely imitated the proliferation and osteogenic alterations of ADSCs *in vivo*. Moreover, the intricate intercellular bonds in the 3D culture setting could significantly impact the osteogenic differentiation of ADSCs.

N-cadherin is a classical cadherin that mediates intercellular adhesion between neural cells and many other types of nonneural cells[39]. Previous studies have demonstrated that N-calmodulin, which is expressed predominantly by osteoblasts, can control bone formation and bone mass[40]. N-calmodulin directly interacts with the Wnt coreceptors lipoprotein receptor-related protein 5 and lipoprotein receptor-related protein 6, thereby inhibiting Wnt/β-catenin signaling, osteoblast differentiation, and bone formation[41]. In this study, we further revealed that 3D culture conditions might inhibit the Wnt/β-catenin signaling pathway by increasing the expression of N-cadherin, thereby inhibiting the osteogenic differentiation of ADSCs.

This study provides a better understanding of the pathophysiological process of ADSC osteogenesis and a more extensive investigation of ADSC osteogenesis. On the contrary, exploration of the potential molecular mechanisms of ADSC osteogenesis provides a more theoretical basis for the clinical promotion of new targets for bone trauma repair. These results could provide a basis for the clinical application of ADSCs, enabling the rational modulation of macrophage activity or the use of macrophage-targeting drugs to increase the osteogenic differentiation capacity and efficiency of ADSCs. By modifying the culture environment, the osteogenic differentiation process can be precisely and directionally regulated. Moreover, employing a 3D coculture of macrophages and ADSCs allows simulation of the immune cell infiltration environment in bone defects, facilitating a deeper understanding of the functionality and potential osteogenic mechanisms of ADSCs as materials for bone tissue engineering.

However, there are still some issues to be considered in this study. First, the ADSCs used in this study were derived from a limited number of donors, which may not fully represent the characteristics of ADSCs across different ages, sexes, or pathological conditions. Although the 2D coculture model is more closely aligned with the *in vivo* environment than the 3D coculture model is, there are still some simplified treatments that may not fully replicate the mechanical microen-

vironment and biomechanical environment of bone tissue. Furthermore, the samples of ADSCs used in this study were derived from a limited number of donors, which may have resulted in an inability to fully represent the characteristics of ADSCs across different age groups, sexes, or pathological states, and different types of macrophages may have different degrees of influence on the osteogenic differentiation of ADSCs. Osteogenic differentiation is a highly dynamic, long-term process, and the signaling requirements and pathway activity may differ significantly at different stages of differentiation. A single observation of the results and the focus on only the N-cadherin-regulated Wnt signaling pathway may not fully capture the temporal dynamics of the signaling pathways. Future studies can further explore alternative molecular mechanisms to achieve a more comprehensive understanding of the osteogenic differentiation mechanism of ADSCs. In addition, this study was performed only at the cellular level, and future studies can further investigate the osteogenic differentiation effects of macrophages in animal experiments.

CONCLUSION

Macrophages promoted ADSC osteogenic differentiation in 2D culture conditions but inhibited it in 3D culture. Compared with 2D cultures, ADSCs in 3D cultures maintained high levels of activity. Additionally, the 3D culture environment might inhibit the Wnt/β-catenin signaling pathway by upregulating N-cadherin expression, ultimately hindering the osteogenic differentiation of ADSCs. Furthermore, the intercellular adhesive connections in the 3D-ADSC-THP-1 coculture were able to simulate the proliferation and osteogenic changes of ADSCs better than those in the other cocultures, thus influencing the osteogenic differentiation of ADSCs. By investigating the process of osteogenesis in ADSCs, this study provides novel ideas for exploring 3D osteogenesis in ADSCs, fracture repair, and other types of bone trauma repair.

FOOTNOTES

Author contributions: Zhang HA and Zhang BY designed the research, conducted the study, and wrote the manuscript, they contributed equally to this manuscript are co-first authors; Tang HB revised and supervised the manuscript.

Institutional review board statement: The experiments were approved by the ethical committee of the Tongji Hospital, Tongji Medical College at the Huazhong University of Science and Technology in China (IRB ID: TJ-IRB20220740).

Conflict-of-interest statement: All the authors report no relevant conflicts of interest for this article.

Data sharing statement: All data displayed in this study can be obtained in the article. Further questions can be directed to the corresponding author.

Country of origin: China

ORCID number: Hong-Bo Tang 0009-0001-4462-6895.

S-Editor: Wang JJ
L-Editor: A
P-Editor: Zhang XD

REFERENCES

1 **Ensrud KE**. Epidemiology of fracture risk with advancing age. *J Gerontol A Biol Sci Med Sci* 2013; **68**: 1236-1242 [PMID: 23833201 DOI: 10.1093/gerona/glt092]
2 **Caplan AI**. MSCs: The Sentinel and Safe-Guards of Injury. *J Cell Physiol* 2016; **231**: 1413-1416 [PMID: 26565391 DOI: 10.1002/jcp.25255]
3 **Dong R**, Bai Y, Dai J, Deng M, Zhao C, Tian Z, Zeng F, Liang W, Liu L, Dong S. Engineered scaffolds based on mesenchymal stem cells/preosteoclasts extracellular matrix promote bone regeneration. *J Tissue Eng* 2020; **11**: 2041731420926918 [PMID: 32551034 DOI: 10.1177/2041731420926918]
4 **Marolt Presen D**, Traweger A, Gimona M, Redl H. Mesenchymal Stromal Cell-Based Bone Regeneration Therapies: From Cell Transplantation and Tissue Engineering to Therapeutic Secretomes and Extracellular Vesicles. *Front Bioeng Biotechnol* 2019; **7**: 352 [PMID: 31828066 DOI: 10.3389/fbioe.2019.00352]
5 **Iaquinta MR**, Mazzoni E, Bononi I, Rotondo JC, Mazziotta C, Montesi M, Sprio S, Tampieri A, Tognon M, Martini F. Adult Stem Cells for Bone Regeneration and Repair. *Front Cell Dev Biol* 2019; **7**: 268 [PMID: 31799249 DOI: 10.3389/fcell.2019.00268]
6 **Zhang Y**, Böse T, Unger RE, Jansen JA, Kirkpatrick CJ, van den Beucken JJJP. Macrophage type modulates osteogenic differentiation of

adipose tissue MSCs. *Cell Tissue Res* 2017; **369**: 273-286 [PMID: 28361303 DOI: 10.1007/s00441-017-2598-8]

7 **Einhorn TA**, Gerstenfeld LC. Fracture healing: mechanisms and interventions. *Nat Rev Rheumatol* 2015; **11**: 45-54 [PMID: 25266456 DOI: 10.1038/nrrheum.2014.164]

8 **Rickard AJ**, Young MJ. Corticosteroid receptors, macrophages and cardiovascular disease. *J Mol Endocrinol* 2009; **42**: 449-459 [PMID: 19158233 DOI: 10.1677/JME-08-0144]

9 **Pajarinen J**, Lin T, Gibon E, Kohno Y, Maruyama M, Nathan K, Lu L, Yao Z, Goodman SB. Mesenchymal stem cell-macrophage crosstalk and bone healing. *Biomaterials* 2019; **196**: 80-89 [PMID: 29329642 DOI: 10.1016/j.biomaterials.2017.12.025]

10 **Tang H**, Husch JFA, Zhang Y, Jansen JA, Yang F, van den Beucken JJJP. Coculture with monocytes/macrophages modulates osteogenic differentiation of adipose-derived mesenchymal stromal cells on poly(lactic-co-glycolic) acid/polycaprolactone scaffolds. *J Tissue Eng Regen Med* 2019; **13**: 785-798 [PMID: 30771241 DOI: 10.1002/term.2826]

11 **Aijian AP**, Garrell RL. Digital microfluidics for automated hanging drop cell spheroid culture. *J Lab Autom* 2015; **20**: 283-295 [PMID: 25510471 DOI: 10.1177/2211068214562002]

12 **Fennema E**, Rivron N, Rouwkema J, van Blitterswijk C, de Boer J. Spheroid culture as a tool for creating 3D complex tissues. *Trends Biotechnol* 2013; **31**: 108-115 [PMID: 23336996 DOI: 10.1016/j.tibtech.2012.12.003]

13 **Salmenperä P**, Kankuri E, Bizik J, Sirén V, Virtanen I, Takahashi S, Leiss M, Fässler R, Vaheri A. Formation and activation of fibroblast spheroids depend on fibronectin-integrin interaction. *Exp Cell Res* 2008; **314**: 3444-3452 [PMID: 18824166 DOI: 10.1016/j.yexcr.2008.09.004]

14 **Kang HG**, Jenabi JM, Zhang J, Keshelava N, Shimada H, May WA, Ng T, Reynolds CP, Triche TJ, Sorensen PH. E-cadherin cell-cell adhesion in ewing tumor cells mediates suppression of anoikis through activation of the ErbB4 tyrosine kinase. *Cancer Res* 2007; **67**: 3094-3105 [PMID: 17409416 DOI: 10.1158/0008-5472.CAN-06-3259]

15 **Kim Y**, Rajagopalan P. 3D hepatic cultures simultaneously maintain primary hepatocyte and liver sinusoidal endothelial cell phenotypes. *PLoS One* 2010; **5**: e15456 [PMID: 21103392 DOI: 10.1371/journal.pone.0015456]

16 **Claes L**, Recknagel S, Ignatius A. Fracture healing under healthy and inflammatory conditions. *Nat Rev Rheumatol* 2012; **8**: 133-143 [PMID: 22293759 DOI: 10.1038/nrrheum.2012.1]

17 **Tang H**, Zhang Y, Jansen JA, van den Beucken JJJP. Effect of monocytes/macrophages on the osteogenic differentiation of adipose-derived mesenchymal stromal cells in 3D co-culture spheroids. *Tissue Cell* 2017; **49**: 461-469 [PMID: 28684045 DOI: 10.1016/j.tice.2017.06.002]

18 **Kirkpatrick CJ**, Fuchs S, Unger RE. Co-culture systems for vascularization--learning from nature. *Adv Drug Deliv Rev* 2011; **63**: 291-299 [PMID: 21281686 DOI: 10.1016/j.addr.2011.01.009]

19 **Kirkpatrick CJ**. Modelling the regenerative niche: a major challenge in biomaterials research. *Regen Biomater* 2015; **2**: 267-272 [PMID: 26816650 DOI: 10.1093/rb/rbv018]

20 **Di Benedetto A**, Brunetti G, Posa F, Ballini A, Grassi FR, Colaianni G, Colucci S, Rossi E, Cavalcanti-Adam EA, Lo Muzio L, Grano M, Mori G. Osteogenic differentiation of mesenchymal stem cells from dental bud: Role of integrins and cadherins. *Stem Cell Res* 2015; **15**: 618-628 [PMID: 26513557 DOI: 10.1016/j.scr.2015.09.011]

21 **Vallés G**, Bensiamar F, Crespo L, Arruebo M, Vilaboa N, Saldaña L. Topographical cues regulate the crosstalk between MSCs and macrophages. *Biomaterials* 2015; **37**: 124-133 [PMID: 25453943 DOI: 10.1016/j.biomaterials.2014.10.028]

22 **Haÿ E**, Laplantine E, Geoffroy V, Frain M, Kohler T, Müller R, Marie PJ. N-cadherin interacts with axin and LRP5 to negatively regulate Wnt/beta-catenin signaling, osteoblast function, and bone formation. *Mol Cell Biol* 2009; **29**: 953-964 [PMID: 19075000 DOI: 10.1128/MCB.00349-08]

23 **Cao ZQ**, Wang Z, Leng P. Aberrant N-cadherin expression in cancer. *Biomed Pharmacother* 2019; **118**: 109320 [PMID: 31545265 DOI: 10.1016/j.biopha.2019.109320]

24 **Fontana F**, Xiang J, Su X, Tycksen E, Nassau R, Fox G, Leanza G, Weilbaecher K, Civitelli R. N-cadherin in osteolineage cells modulates stromal support of tumor growth. *J Bone Oncol* 2021; **28**: 100356 [PMID: 33912383 DOI: 10.1016/j.jbo.2021.100356]

25 **Li L**, Bhatia R. Stem cell quiescence. *Clin Cancer Res* 2011; **17**: 4936-4941 [PMID: 21593194 DOI: 10.1158/1078-0432.CCR-10-1499]

26 **Murray IR**, West CC, Hardy WR, James AW, Park TS, Nguyen A, Tawonsawatruk T, Lazzari L, Soo C, Péault B. Natural history of mesenchymal stem cells, from vessel walls to culture vessels. *Cell Mol Life Sci* 2014; **71**: 1353-1374 [PMID: 24158496 DOI: 10.1007/s00018-013-1462-6]

27 **Fontana F**, Hickman-Brecks CL, Salazar VS, Revollo L, Abou-Ezzi G, Grimston SK, Jeong SY, Watkins M, Fortunato M, Alippe Y, Link DC, Mbalaviele G, Civitelli R. N-cadherin Regulation of Bone Growth and Homeostasis Is Osteolineage Stage-Specific. *J Bone Miner Res* 2017; **32**: 1332-1342 [PMID: 28240364 DOI: 10.1002/jbmr.3112]

28 **Varma MJ**, Breuls RG, Schouten TE, Jurgens WJ, Bontkes HJ, Schuurhuis GJ, van Ham SM, van Milligen FJ. Phenotypical and functional characterization of freshly isolated adipose tissue-derived stem cells. *Stem Cells Dev* 2007; **16**: 91-104 [PMID: 17348807 DOI: 10.1089/scd.2006.0026]

29 **Freytes DO**, Kang JW, Marcos-Campos I, Vunjak-Novakovic G. Macrophages modulate the viability and growth of human mesenchymal stem cells. *J Cell Biochem* 2013; **114**: 220-229 [PMID: 22903635 DOI: 10.1002/jcb.24357]

30 **Mosser DM**, Edwards JP. Exploring the full spectrum of macrophage activation. *Nat Rev Immunol* 2008; **8**: 958-969 [PMID: 19029990 DOI: 10.1038/nri2448]

31 **Laschke MW**, Schank TE, Scheuer C, Kleer S, Shadmanov T, Eglin D, Alini M, Menger MD. In vitro osteogenic differentiation of adipose-derived mesenchymal stem cell spheroids impairs their in vivo vascularization capacity inside implanted porous polyurethane scaffolds. *Acta Biomater* 2014; **10**: 4226-4235 [PMID: 24998773 DOI: 10.1016/j.actbio.2014.06.035]

32 **Yamaguchi Y**, Ohno J, Sato A, Kido H, Fukushima T. Mesenchymal stem cell spheroids exhibit enhanced in-vitro and in-vivo osteoregenerative potential. *BMC Biotechnol* 2014; **14**: 105 [PMID: 25479895 DOI: 10.1186/s12896-014-0105-9]

33 **Yoon HH**, Bhang SH, Shin JY, Shin J, Kim BS. Enhanced cartilage formation *via* three-dimensional cell engineering of human adipose-derived stem cells. *Tissue Eng Part A* 2012; **18**: 1949-1956 [PMID: 22881427 DOI: 10.1089/ten.TEA.2011.0647]

34 **Bhang SH**, Cho SW, La WG, Lee TJ, Yang HS, Sun AY, Baek SH, Rhie JW, Kim BS. Angiogenesis in ischemic tissue produced by spheroid grafting of human adipose-derived stromal cells. *Biomaterials* 2011; **32**: 2734-2747 [PMID: 21262528 DOI: 10.1016/j.biomaterials.2010.12.035]

35 **Bierwolf J**, Lutgehetmann M, Feng K, Erbes J, Deichmann S, Toronyi E, Stieglitz C, Nashan B, Ma PX, Pollok JM. Primary rat hepatocyte culture on 3D nanofibrous polymer scaffolds for toxicology and pharmaceutical research. *Biotechnol Bioeng* 2011; **108**: 141-150 [PMID: 20824672 DOI: 10.1002/bit.22924]

36 **von der Mark K**, Gauss V, von der Mark H, Müller P. Relationship between cell shape and type of collagen synthesised as chondrocytes lose their cartilage phenotype in culture. *Nature* 1977; **267**: 531-532 [PMID: 559947 DOI: 10.1038/267531a0]

37 **Fernandes TJ**, Hodge JM, Singh PP, Eeles DG, Collier FM, Holten I, Ebeling PR, Nicholson GC, Quinn JM. Cord blood-derived macrophage-lineage cells rapidly stimulate osteoblastic maturation in mesenchymal stem cells in a glycoprotein-130 dependent manner. *PLoS One* 2013; **8**: e73266 [PMID: 24069182 DOI: 10.1371/journal.pone.0073266]

38 **Chen C**, Uludağ H, Wang Z, Rezansoff A, Jiang H. Macrophages inhibit migration, metabolic activity and osteogenic differentiation of human mesenchymal stem cells in vitro. *Cells Tissues Organs* 2012; **195**: 473-483 [PMID: 22156615 DOI: 10.1159/000330686]

39 **Miyamoto Y**, Sakane F, Hashimoto K. N-cadherin-based adherens junction regulates the maintenance, proliferation, and differentiation of neural progenitor cells during development. *Cell Adh Migr* 2015; **9**: 183-192 [PMID: 25869655 DOI: 10.1080/19336918.2015.1005466]

40 **Mbalaviele G**, Shin CS, Civitelli R. Cell-cell adhesion and signaling through cadherins: connecting bone cells in their microenvironment. *J Bone Miner Res* 2006; **21**: 1821-1827 [PMID: 17002562 DOI: 10.1359/jbmr.060811]

41 **Haÿ E**, Buczkowski T, Marty C, Da Nascimento S, Sonnet P, Marie PJ. Peptide-based mediated disruption of N-cadherin-LRP5/6 interaction promotes Wnt signaling and bone formation. *J Bone Miner Res* 2012; **27**: 1852-1863 [PMID: 22576936 DOI: 10.1002/jbmr.1656]

World Journal of Stem Cells

Submit a Manuscript: https://www.f6publishing.com

World J Stem Cells 2025 February 26; 17(2): 101030

DOI: 10.4252/wjsc.v17.i2.101030

ISSN 1948-0210 (online)

ORIGINAL ARTICLE

Basic Study

Fetal mice dermal mesenchymal stem cells promote wound healing by inducing M2 type macrophage polarization

Zhen-Yu Xia, Yi Wang, Nian Shi, Mei-Qi Lu, Yun-Xiang Deng, Yong-Jun Qi, Xing-Lei Wang, Jie Zhao, Du-Yin Jiang

Specialty type: Cell and tissue engineering

Provenance and peer review: Unsolicited article; Externally peer reviewed.

Peer-review model: Single blind

Peer-review report's classification

Scientific Quality: Grade A, Grade B, Grade B

Novelty: Grade A, Grade A, Grade B

Creativity or Innovation: Grade A, Grade B, Grade B

Scientific Significance: Grade A, Grade B, Grade B

P-Reviewer: Gu ZW; Yang Y

Received: September 2, 2024

Revised: December 9, 2024

Accepted: February 7, 2025

Published online: February 26, 2025

Processing time: 174 Days and 17.3 Hours

Zhen-Yu Xia, Yi Wang, Nian Shi, Mei-Qi Lu, Yun-Xiang Deng, Cheeloo College of Medicine, Shandong University, Jinan 250012, Shandong Province, China

Yong-Jun Qi, Department of Plastic Surgery & Burns, The Second Hospital of Shandong University, Jinan 250033, Shandong Province, China

Xing-Lei Wang, Jie Zhao, Du-Yin Jiang, Emergency Medicine Center, The Second Hospital of Shandong University, Jinan 250033, Shandong Province, China

Co-corresponding authors: Jie Zhao and Du-Yin Jiang.

Corresponding author: Du-Yin Jiang, MD, Emergency Medicine Center, The Second Hospital of Shandong University, No. 247 Beiyuan Street, Jinan 250033, Shandong Province, China. jduyin0227@163.com

Abstract

BACKGROUND

Mesenchymal stem cells, found in various tissues, possess significant healing and immunomodulatory properties, influencing macrophage polarization, which is essential for wound repair. However, chronic wounds present significant therapeutic challenges, requiring novel strategies to improve healing outcomes.

AIM

To investigate the potential of fetal dermal mesenchymal stem cells (FDMSCs) in enhancing wound healing through modulation of macrophage polarization, specifically by promoting the M2 phenotype to address inflammatory responses in chronic wounds.

METHODS

FDMSCs were isolated from BalB/C mice and co-cultured with RAW264.7 macrophages to assess their effects on macrophage polarization. Flow cytometry, quantitative reverse transcriptase polymerase chain reaction, and histological analyses were employed to evaluate shifts in macrophage phenotype and wound healing in a mouse model. Statistical analysis was performed using GraphPad Prism.

RESULTS

FDMSCs induced macrophage polarization from the M1 to M2 phenotype, as demonstrated by a reduction in pro-inflammatory markers (inducible nitric oxide synthase, interleukin-6) and an increase in anti-inflammatory markers [mannose receptor (CD206), arginase-1] in co-cultured RAW264.7 macrophages. These shifts were confirmed by flow cytometry. In an acute skin wound model, FDMSC-treated mice exhibited faster wound healing, enhanced collagen deposition, and improved vascular regeneration compared to controls. Significantly higher expression of arginase-1 further indicated an enriched M2 macrophage environment.

CONCLUSION

FDMSCs effectively modulate macrophage polarization from M1 to M2, reduce inflammation, and enhance tissue repair, demonstrating their potential as an immunomodulatory strategy in wound healing. These findings highlight the promising therapeutic application of FDMSCs in managing chronic wounds.

Key Words: Fetal dermal mesenchymal stem cells; Macrophage polarization; Wound healing; Immunomodulation; M2 phenotype

Core Tip: This study investigates the role of fetal dermal mesenchymal stem cells in wound healing by modulating macrophage polarization towards a pro-healing M2 phenotype. Using flow cytometry, reverse transcriptase polymerase chain reaction, and histology, we demonstrate that fetal dermal mesenchymal stem cells promote a reparative immune environment, accelerating wound closure, enhancing collagen deposition, and supporting vascular regeneration in a mouse model.

Citation: Xia ZY, Wang Y, Shi N, Lu MQ, Deng YX, Qi YJ, Wang XL, Zhao J, Jiang DY. Fetal mice dermal mesenchymal stem cells promote wound healing by inducing M2 type macrophage polarization. *World J Stem Cells* 2025; 17(2): 101030
URL: https://www.wjgnet.com/1948-0210/full/v17/i2/101030.htm
DOI: https://dx.doi.org/10.4252/wjsc.v17.i2.101030

INTRODUCTION

Mesenchymal stem cells (MSCs) are multipotent precursor cells with self-renewal capacity, found in various tissues such as bone marrow, adipose tissue, umbilical cord blood, dental pulp, dermis, and the endometrial lining of the uterus[1]. MSCs are known for their robust regenerative properties, including the ability to migrate to injury sites, differentiate into various cell types, and release cytokines, growth factors, and chemokines that promote tissue repair[2]. In addition to their direct regenerative effects, MSCs modulate the immune response during healing, particularly by influencing macrophage behavior, which plays a critical role in tissue repair and inflammation resolution[3]. This immunomodulatory function enhances the healing process, positioning MSCs as promising candidates for treating chronic wounds, autoimmune disorders, and inflammation-driven diseases[4,5].

Macrophages are critical immune cells involved in the inflammatory, proliferative, and remodeling phases of wound healing[6]. Initially, granulocytes and monocytes are recruited to the injury site, with monocytes differentiating into pro-inflammatory M1 macrophages characterized by high CD86 and programmed death-ligand 1 expression[7]. These M1 macrophages secrete inflammatory mediators such as inducible nitric oxide synthase (iNOS), tumor necrosis factor-alpha, interleukin-1 beta (IL-1β), and IL-6, and play a key role in phagocytosis and debris clearance[8]. As healing progresses, macrophages transition to an anti-inflammatory M2 phenotype, marked by high mannose receptor (CD206), arginase-1 (Arg-1), and FIZZ1 expression, along with the secretion of transforming growth factor-beta and IL-10[9]. M2 macrophages support tissue repair by promoting angiogenesis and collagen deposition[10]. They also produce cytokines like vascular endothelial growth factor and fibroblast growth factor to stimulate fibroblast and endothelial cell activity[11]. An overabundance of pro-inflammatory macrophages in chronic wounds can impair healing by hindering tissue remodeling [12]. Recent research has revealed that macrophage polarization is more complex than the classical M1/M2 dichotomy, with various intermediate phenotypes influencing the wound healing process. These phenotypes, shaped by factors such as the tissue microenvironment, activation timing, and the presence of other immune cells, demonstrate that macrophage polarization exists on a spectrum. This dynamic understanding is essential for developing more targeted immunomodulatory therapies for chronic wounds and inflammation[13].

Fetal dermal MSCs (FDMSCs) are a distinct category of MSCs extracted from the dermal tissue of BalB/C mice on the fifteenth day of gestation. In comparison to adult MSCs, including those sourced from bone marrow and adipose tissue, FDMSCs exhibit enhanced multidirectional differentiation potential, decreased immunogenicity, and a significant correlation with the scarless healing properties inherent to fetal skin. Previous studies have demonstrated that FDMSCs play a crucial role in promoting wound healing and angiogenesis, with evidence showing that they facilitate tissue repair by inducing macrophage polarization toward the M2 phenotype[14,15]. This study aims to investigate the role of FDMSCs in modulating macrophage polarization, specifically promoting the transition from the pro-inflammatory M1

phenotype to the anti-inflammatory M2 phenotype, and to evaluate their impact on wound healing.

MATERIALS AND METHODS

Animals

BalB/C mice, aged 6 to 8 weeks, were procured from Jinan Pengyue Laboratory Animal Breeding Co., Ltd. and were maintained in groups at the Animal Facility of our hospital. All animal care and experimental techniques were conducted in accordance with the protocols sanctioned by the Institutional Animal Care and Use Committee at our hospital. Furthermore, all procedures were conducted in compliance with applicable rules and legislation to guarantee the ethical treatment of animals. This study adhered to ARRIVE principles, and all techniques are documented to guarantee transparency and reproducibility of the experimental processes. Upon the completion of the experiments, euthanasia was performed to alleviate suffering. Mice were executed *via* CO_2 inhalation, followed by cervical dislocation as a supplementary method to confirm death, in compliance with the American Veterinary Medical Association euthanasia recommendations. All treatments were performed under the oversight of veterinary personnel to guarantee humane care.

Cells isolation and culture

FDMSC was isolated from the dorsal dermis of BalB/C mice on gestational day 15. The epidermis and dermis were dissociated using neutral protease, followed by digestion of the dermis with type I collagenase. The FDMSCs were subjected to filtration using a 70-micrometer filter and subsequently cultivated in DMEM low glucose medium (HyClone, UT, United States) supplemented with 10% fetal bovine serum (Gibco, CA, United States) and 1% Penicillin-Streptomycin at a concentration of 100 U/mL (Gibco, CA, United States).

Flow cytometry

The surface markers of FDMSCs and M1/M2 type RAW264.7 were evaluated by flow cytometry. Macrophages were stimulated to the M1 phenotype using 100 ng/mL lipopolysaccharide (LPS) and 20 ng/mL interferon (IFN)-β, and to the M2 phenotype using 20 ng/mL IL-4 for intracellular cytokine detection. In summary, 5×10^5 cells were harvested and resuspended in phosphate buffered saline buffer, followed by a 15-minute incubation with particular antibodies in the dark. The cells were subsequently rinsed with phosphate buffered saline solution and evaluated by flow cytometry. Results were evaluated using FlowJo Software (Ashland, OR, United States).

Co-culture of FDMSCs and RAW264.7

Co-culture investigations were conducted utilizing 0.4 μm pore transwell chambers (Corning, CA, United States). RAW264.7 cells were cultured in the lower compartment and polarized to the M1 phenotype using 100 ng/mL LPS and 20 ng/mL IFN-β; 20 ng/mL IL-4 was employed to produce the M2 macrophage phenotype. The FDMSCs were cultured in the upper chamber. Co-culture for a duration of 24 hours prior to evaluation.

Acute skin wound healing model and FDMSCs treatment

Mice were randomly assigned to control and FDMSCs-treated groups. A full-thickness skin splinting model in mice with a diameter of 1 cm was established. In the control group, 100 μL of normal saline was administered at the wound's periphery. In the FDMSCs group, 100 μL of normal saline containing approximately 10^6 FDMSCs was administered. The injury was dressed with sterile gauze.

Total RNA extraction and quantitative reverse transcriptase polymerase chain reaction

Total cellular RNA was extracted using a TRIzol reagent (Invitrogen, Carlsbad, CA, United States), according to the manufacturer's instructions. Isolated total RNA was then subjected to reverse transcription using Oligo dT primer and PrimeScript® RTase (Takara, Dalian, China), according to the manufacturer's instructions. Quantitative reverse transcriptase polymerase chain reaction was performed with SYBR® Premix Ex Taq™ II (Takara, Dalian, China) using the C1000™ Thermal Cycler (Bio-Rad, Hercules, CA, United States). The expression levels of the target genes were normalized to that of the housekeeping gene, β-actin.

Histological analysis

The excised tissues from wound sites were preserved in 4% paraformaldehyde for 24 hours and subsequently dehydrated using graded ethanol. Following the embedding of collected tissues in paraffin, the samples were sectioned into 4 μm thick slices. Hematoxylin and eosin (HE) staining was performed to examine the histological alterations in the wound healing process. The Masson's trichrome staining assay was conducted to assess collagen maturity in accordance with the manufacturer's guidelines. Microscopic images were obtained and analyzed using Image J software.

Statistical analysis

Statistical analysis was conducted on GraphPad Prism 8. Three or more separate experiments were conducted for each outcome, and the mean and standard deviation were computed. One-way ANOVA or Student's *t*-test were employed to identify statistically significant differences. A *P* value of less than 0.05 was deemed statistically significant.

RESULTS

Characterization of FDMSC and M1/2 macrophages

In accordance with the MSC identification criterion, we discovered three biomarkers: CD29, CD44, and CD45. Among these, CD29 and CD44 were highly expressed, while CD45 was little expressed. RAW264.7 was stimulated with conditioned media for 24 hours, and the expression levels of CD86 and CD206 were assessed using flow cytometry. In comparison to uninduced RAW264.7 cells, M1-type macrophages exhibited elevated expression of CD86, while M2-type macrophages demonstrated increased expression of CD206. The induction with 100 ng/mL LPS, 20 ng/mL IFN-γ, and 20 ng/mL IL-4 effectively generated M1/2-type macrophages for further tests (Figure 1).

FDMSCs facilitate the phenotype switch of RAW264.7 from M1 to M2 type

We investigated the influence of FDMSCs on macrophage polarization through a coculture method. Prior to co-culture, RAW264.7 was polarized to the M1 phenotype using LPS and IFN-γ, followed by co-culturing with FDMSCs. We identified the gene expression of iNOS and IL-6, which are hallmark pro-inflammatory components of M1 macrophages. In comparison to the control group, the expressions of iNOS and IL-6 in M1 macrophages co-cultured with FDMSC were decreased. Furthermore, we identified the expression of the anti-inflammatory cytokine IL-10. The expression of the *IL-10* gene was elevated in the MSC group relative to the control group. Ultimately, we identified two cell markers, CD86 and CD206, by flow cytometry. The results indicated a decrease in CD86 expression, indicative of M1 polarization, and an increase in CD206 expression, indicative of M2 polarization. Consequently, we have demonstrated that FDMSC can diminish the polarization of M1 macrophages, decrease the expression levels of pro-inflammatory factors IL-6 and iNOS; concurrently, it can facilitate the transformation of M1 macrophages to the M2 phenotype, resulting in an elevated expression level of IL-10 (Figure 2).

FDMSC promotes macrophage polarization towards M2

We employed the identical methodology to investigate the influence of FDMSCs on M2-polarized macrophages, which were induced to the M2 phenotype using IL-4 prior to co-culture. We subsequently analyze the distinctive cellularity that indicates the degree of polarization of M2 macrophages.

Following FDMSC injection, the gene expression of *IL-10* in M2 macrophages was elevated in comparison to the control group. The flow cytometry data indicated a reduction in CD86 expression and an elevation in CD206 expression relative to the control group. Furthermore, we observed that the expression of the *Arg-1* gene in M2 macrophages increased following the administration of FDMSC, in comparison to the control group. It may be inferred that FDMCS can enhance macrophage polarization towards the M2 phenotype and elevate the gene expression of key anti-inflammatory proteins IL-10 and Arg-1 (Figure 3).

FDMSCs promote acute wound healing in mice

We developed a model of acute total trauma in mice and treated the trauma with FDMSCs. The healing process demonstrated that trauma in the FDMSCs intervention group resolved more rapidly than in the non-intervention control group, achieving substantial healing by day 14 (Figure 4A). ImageJ software was employed to quantify the disparity in wound healing rates between the two groups, revealing that the wound healing rate was accelerated in the FDMSCs intervention group (Figure 4B). Ultimately, we excised the entire skin from the day 14 trauma for paraffin embedding, followed by HE and Masson staining to examine the healing process of the damage. In HE stains, the FDMSCs exhibited closely grouped fibroblasts, an increased number of neoplastic capillaries, and discernible neoplastic hair follicles in comparison to the control group. Masson staining revealed a greater abundance of neoplastic collagen fibers (Figure 4C and D). Subsequently, we assessed the area filled by blue-stained collagen fibers in Masson-stained sections utilizing ImageJ software, and the results indicated that the FDMSCs intervention group facilitated collagen deposition in comparison to the control group (Figure 4E). This indicated that FDMSCs facilitated the healing of acute full-thickness wounds in mice, encompassing the enhancement of collagen deposition, vascular regeneration, and re-epithelialization.

To further substantiate the role of FDMSCs in the wound healing process, we collected wound specimens on day 14 and assessed the expression of iNOS and Arg-1 *via* quantitative reverse transcriptase polymerase chain reaction. The results indicated that Arg-1 expression was elevated in the FDMSCs-intervention group relative to the control group (Figure 4F), whereas no statistically significant difference was noted for iNOS. This indicates a potentially elevated proportion of M2-type macrophages in the FDMSCs group during the wound healing process, hence facilitating wound repair.

DISCUSSION

Our study reveals the innovative potential of FDMSCs for wound healing, highlighting their capability to shift macrophage polarization from M1 to M2, thereby fostering an anti-inflammatory milieu conducive to tissue repair. This effect was validated through co-culture experiments showing decreased pro-inflammatory markers and increased anti-inflammatory markers. Further, FDMSC treatment markedly improved wound closure, collagen deposition, and vascular regeneration in a mouse model, supported by increased expression of the M2 marker Arg-1. These findings underscore the therapeutic promise of FDMSCs for chronic wound management and tissue regeneration, leveraging their low immunogenicity and high biocompatibility. This research advances the field of regenerative medicine, offering new

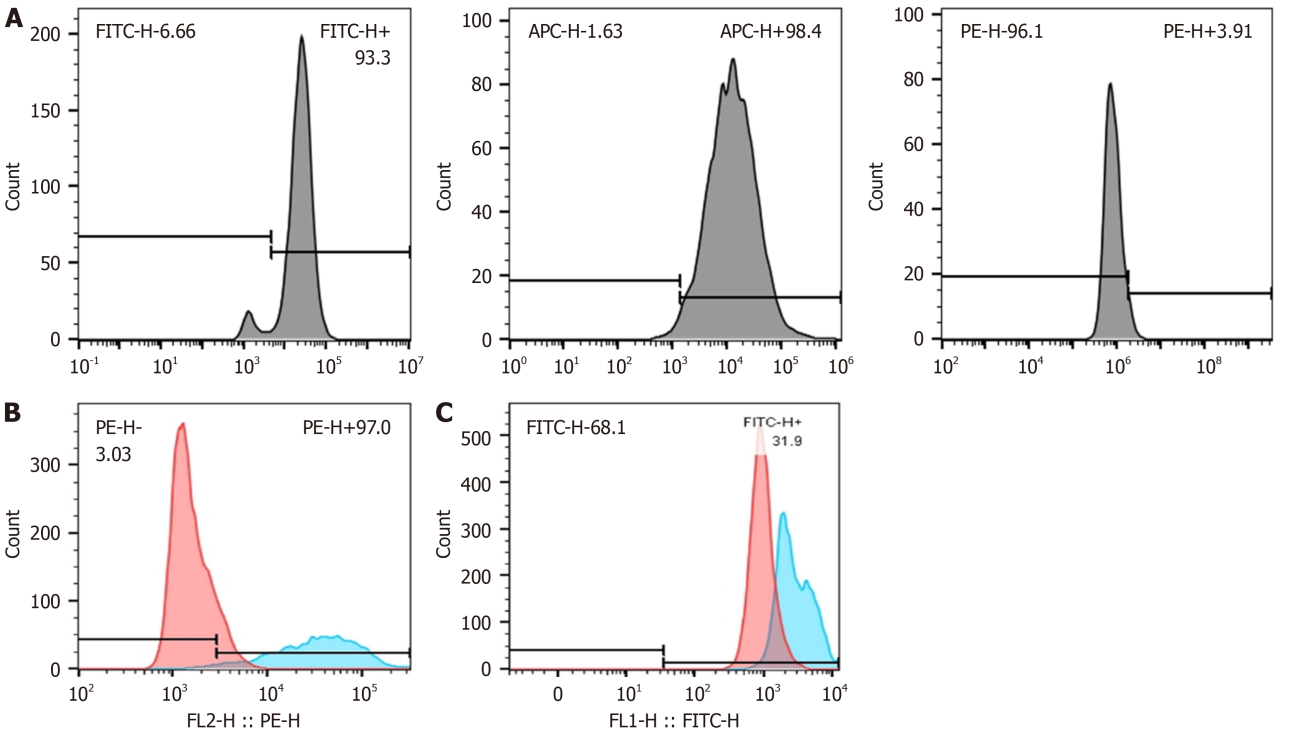

Figure 1 Characterization of fetal dermal mesenchymal stem cell M1/2 macrophages. A: Detection of CD29 (FITC), CD44 (APC), and CD45 (PE) expression, characteristic markers of mesenchymal stem cells by flow cytometry; B: Flow cytometric analysis of CD86 (PE) cell surface marker expression (red - RAW264.7, blue - M1-type macrophages induced); C: Flow cytometric analysis of CD206 (FITC) cell surface marker expression (red - RAW264.7, blue - M2-type macrophages induced).

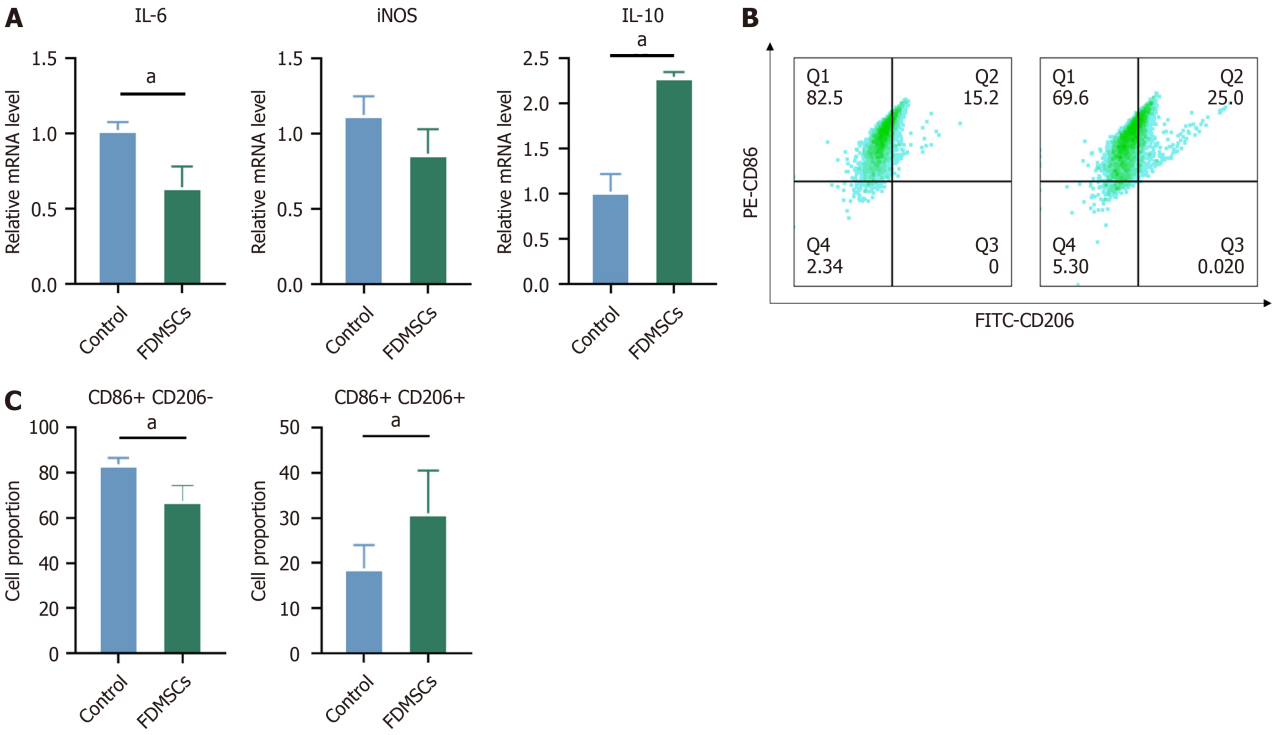

Figure 2 Fetal dermal mesenchymal stem cells facilitate the phenotypic switch of RAW264.7 from M1 to M2 type. A: Quantitative reverse transcriptase polymerase chain reaction analysis of genes characterizing M1, including interleukin-6 and inducible nitric oxide synthase, and the anti-inflammatory factor interleukin-10; B and C: Cells were immunostained with PE-CD86 and FITC-CD206 antibodies and analyzed by flow cytometry. $^{a}P < 0.05$. IL: Interleukin; iNOS: Inducible nitric oxide synthase; FDMSC: Fetal dermal mesenchymal stem cell.

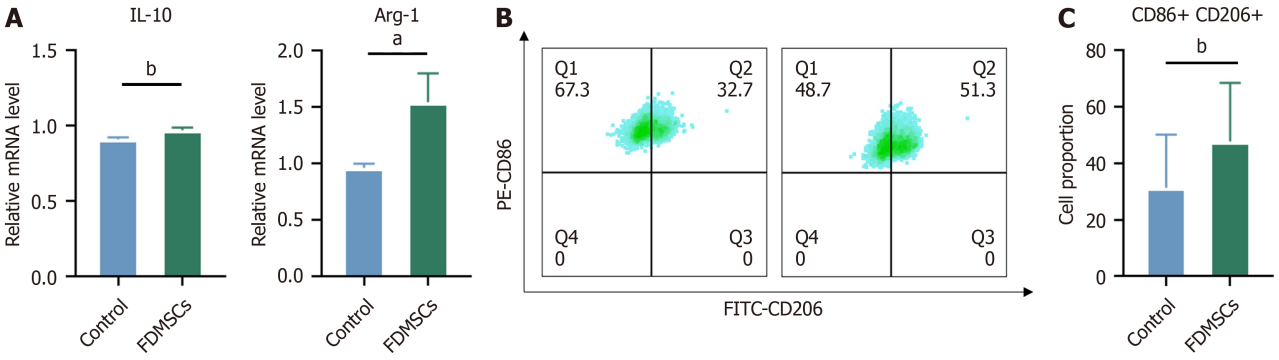

Figure 3 Fetal dermal mesenchymal stem cell promotes macrophage polarization towards M2. A: Quantitative reverse transcriptase polymerase chain reaction analysis of genes characterizing M2, including interleukin-10 and arginase-1; B and C: Cells were immunostained with PE-CD86 and FITC-CD206 antibodies and analyzed by flow cytometry. $^{a}P < 0.05$; $^{b}P < 0.01$. IL: Interleukin; Arg-1: Arginase-1; FDMSC: Fetal dermal mesenchymal stem cell.

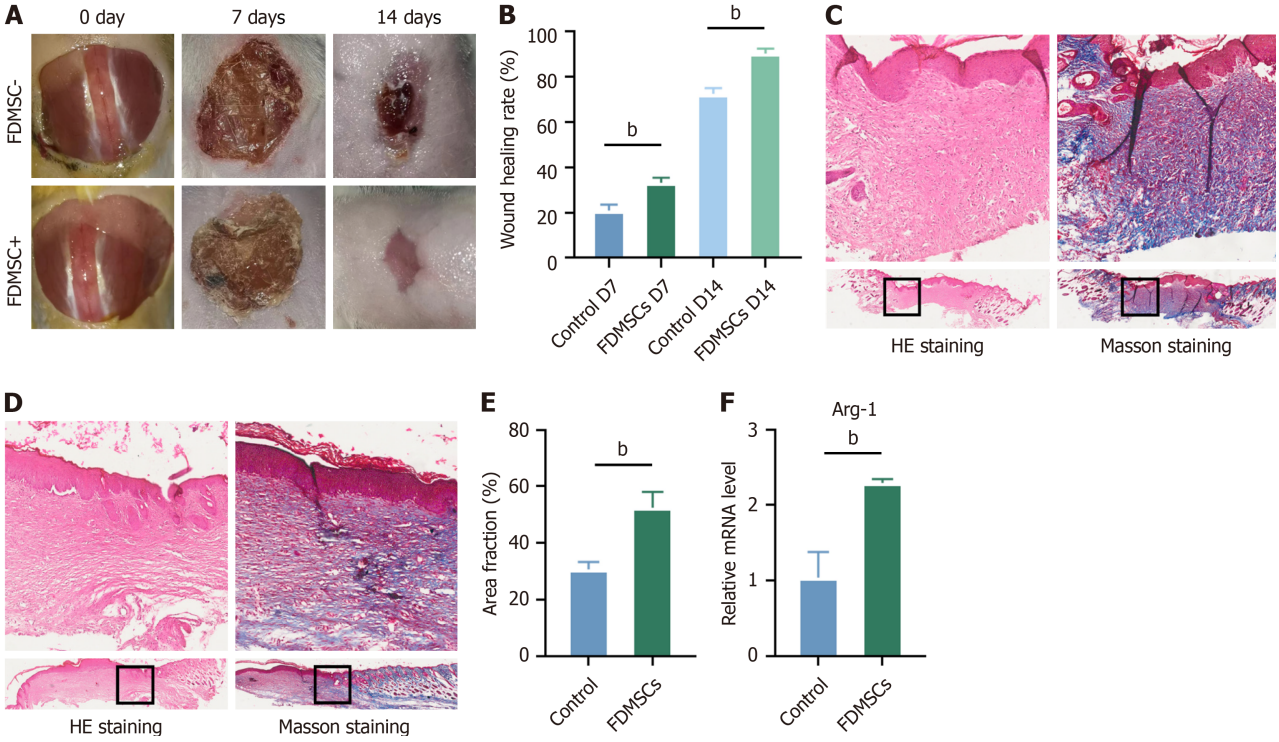

Figure 4 Evaluation of wound healing and tissue analysis in mice following thoracoscopic surgery. A: Mice were euthanized on postoperative days 0, 7, and 14; wound healing was photographed and documented; B: Analysis of wound healing rate; C and D: Hematoxylin and eosin and Masson's trichrome staining of traumatized skin on day 14 (× 40 magnification); E: The area of blue-stained collagen in Masson's trichrome-stained sections was quantified using ImageJ software and statistically analyzed; F: Mouse trauma tissue extracted on day 14 for quantitative reverse transcriptase polymerase chain reaction analysis to detect arginase-1 expression. $^{b}P < 0.01$. HE: Hematoxylin and eosin; Arg-1: Arginase-1; FDMSC: Fetal dermal mesenchymal stem cell.

strategies for treating non-healing wounds and enhancing tissue repair outcomes. Current therapies for wound healing primarily involve the use of growth factors, stem cell therapies, and skin grafts. However, these approaches often face limitations such as prolonged healing times, immune rejection, and risk of scarring. Our study introduces FDMSCs as a promising alternative. FDMSCs promote macrophage polarization toward the M2 phenotype, enhancing tissue regeneration, collagen deposition, and vascularization. Compared to existing methods, FDMSC-based treatment offers potential advantages in reducing inflammation, accelerating healing, and improving scar-free recovery, providing a more sustainable, less invasive option for wound care.

Numerous studies have documented the beneficial effects of MSCs on various diseases, particularly through their influence on macrophage polarization, which impacts the progression of certain inflammatory disorders, myocardial infarction, spinal cord injury, and wound healing[16,17]. MSCs operate by multiple mechanisms, including the secretion of diverse cytokines and exosomes, facilitation of angiogenesis, tissue healing, immunological modulation, and cell recruitment. Our prior research has established that FDMSCs contribute positively to angiogenesis, wound healing, and keloid management. We concentrated on the impact of FDMSC on macrophage polarization. During tissue regeneration, MSCs can facilitate the change of macrophages from the inflammatory M1 phenotype to the anti-inflammatory M2

phenotype[18]. Bone marrow MSCs and human placenta MSCs have been shown to suppress M1 marker expression and facilitate polarization towards the M2 phenotype, characterized by decreased levels of tumor necrosis factor-alpha and iNOS, alongside increased levels of IL-10, CD206, and Arg1.

Macrophages engage in tissue repair *via* phenotypic conversion, facilitate the phagocytosis of pathogenic microbes and cellular debris during the inflammatory phase, release various essential cytokines during this period, and aid in cell recruitment[19]. During the tissue repair phase, it demonstrates an anti-inflammatory activity, releases various cytokines, and activates fibroblasts and endothelial cells. Research has established that MSCs are pivotal in cardiac healing and the reduction of fibrosis following acute kidney damage *via* macrophage polarization[20].

FDMSC, a type of MSC isolated from fetal mouse dermis, has low immunogenicity and excellent biocompatibility. Its dermal origin suggests a superior capacity for *in situ* skin wound repair and it is considered a crucial cell in scarless healing. The interaction between FDMSCs and macrophages, essential immune cells in tissue regeneration, remains unexplored. This study demonstrates that coculturing FDMSC with macrophages facilitates the polarization of macrophages towards the M2 phenotype, hence reducing inflammation and enhancing tissue healing. Flow cytometry revealed that, relative to the control group, CD206 expression in M1 and M2 macrophages rose and CD86 expression reduced following FDMSC intervention, suggesting that FDMSC can promote macrophage polarization towards the M2 phenotype. Subsequent polymerase chain reaction results indicated that FDMSC could not only suppress the expression of pro-inflammatory factors IL-6 and iNOS in M1 macrophages but also enhance the expression of the anti-inflammatory factor IL-10, thereby mitigating the pro-inflammatory effects of M1 macrophages. Following FDMSC intervention in M2 macrophages, the expression of the anti-inflammatory factor IL-10 and the growth factor transforming growth factor-beta increased, enhancing their capacity to control inflammation and facilitate tissue repair. The results indicate that FDMSC can drive macrophage polarization towards the M2 phenotype, hence augmenting the macrophages' capacity to suppress inflammation and facilitate tissue regeneration.

To further validate the characteristics of FDMSCs, we conducted a morphological examination and confirmed their typical fibroblast-like spindle-shaped appearance under a microscope, which is consistent with MSC properties. Additionally, the multipotent differentiation potential of FDMSCs was demonstrated through their ability to differentiate into adipocytes, osteocytes, and chondrocytes under specific culture conditions, as expected for MSCs. This differentiation capacity underscores the functional versatility of FDMSCs. Furthermore, to ensure the purity of the FDMSC population, we assessed the expression of negative markers, including CD45, CD34, and HLA-DR, all of which were absent, further confirming their mesenchymal identity. Prior to the injection of FDMSCs into the wound healing model, we ensured that the number and viability of the cells met stringent quality control standards. Cell counting was performed using a hemocytometer, and cell viability was assessed by the Trypan blue exclusion assay. Only FDMSCs with a viability greater than 95% were used, ensuring that only healthy and functional cells were administered. These rigorous procedures were carried out immediately prior to injection, ensuring the reproducibility and reliability of the experimental outcomes.

While our study demonstrates the promising therapeutic potential of FDMSCs in promoting wound healing and macrophage polarization, several limitations need to be addressed. First, the mouse model used in this study, though informative, may not fully replicate the complexity of human chronic wounds. In particular, human-specific factors such as age, comorbidities, and impaired immune responses are not adequately modeled. To improve clinical relevance, future studies should incorporate advanced models such as diabetic or aged mice, which more closely resemble the delayed and inflammatory healing seen in human patients. Additionally, while FDMSCs showed effective wound healing in the short term, long-term outcomes, including the potential for fibrosis, scarring, and immune responses post-treatment, remain unexplored. These aspects are crucial for assessing the translational potential of FDMSC therapy. Finally, while we assessed macrophage polarization, a more comprehensive evaluation of immune responses, including cytokine profiling and T-cell interactions, is needed to fully understand the immunomodulatory effects of FDMSCs.

To address these limitations, future studies should employ clinically relevant models, such as 3D bioprinted human skin constructs or diabetic wound models, to better simulate human wound healing. We also plan to investigate the potential differential effects of male and female hormones on FDMSC efficacy in wound healing, as hormonal variations may influence immune responses and healing dynamics. Additionally, we will explore the optimization of co-culture durations to determine whether extending or shortening the co-culture period enhances macrophage polarization and macrophage-driven healing outcomes. These directions will provide deeper insights into the mechanisms of FDMSC action and further validate their clinical applicability.

CONCLUSION

Our research demonstrates that FDMSC can induce a phenotypic transition of RAW264.7 from M1 to M2, hence inhibiting inflammation during the initial phase of wound healing and enhancing tissue regeneration in the subsequent phase. This establishes a basis for more research on FDMSCs in relation to wound healing *via* the immunomodulation of macrophages.

FOOTNOTES

Author contributions: Xia ZY and Wang Y contributed to the conceptualization of this study; Xia ZY and Shi N took part in the data curation; Xia ZY and Lu MQ participated in the formal analysis of this manuscript; Xia ZY and Deng YX contributed to the methodology;

Xia ZY and Qi YJ contributed to the resources; Xia ZY and Wang XL contributed to the software; Xia ZY wrote the original draft; Zhao J and Jiang DY contributed to the writing - review & editing. Zhao J and Jiang DY are co-corresponding of this manuscript. Jiang DY provided guidance on the methodological design; Zhao J and Jiang DY jointly guided the conceptualization of our study, and completed the final revisions and confirmation of the manuscript.

Supported by National Natural Science Foundation of China, No. 81873934; and Jinan Science and Technology Planning Project, No. 202225065.

Institutional animal care and use committee statement: Ethical approval for all animal experiments conducted in this study was granted by the Institutional Animal Care and Use Committee at the Second Hospital of Shandong University (Approval No. KYLL-2023LW013). All animal procedures were carried out in strict accordance with institutional guidelines.

Conflict-of-interest statement: All the authors report no relevant conflicts of interest for this article.

Data sharing statement: The datasets used and/or analyzed during the present study are available from the corresponding author on reasonable request.

ARRIVE guidelines statement: The authors have read the ARRIVE guidelines, and the manuscript was prepared and revised according to the ARRIVE guidelines.

Country of origin: China

ORCID number: Du-Yin Jiang 0009-0009-6700-4982.

S-Editor: Wang JJ
L-Editor: A
P-Editor: Xu ZH

REFERENCES

1 **Uccelli A**, Moretta L, Pistoia V. Mesenchymal stem cells in health and disease. *Nat Rev Immunol* 2008; **8**: 726-736 [PMID: 19172693 DOI: 10.1038/nri2395]
2 **Zheng G**, Ge M, Qiu G, Shu Q, Xu J. Mesenchymal Stromal Cells Affect Disease Outcomes *via* Macrophage Polarization. *Stem Cells Int* 2015; **2015**: 989473 [PMID: 26257791 DOI: 10.1155/2015/989473]
3 **Bian D**, Wu Y, Song G, Azizi R, Zamani A. The application of mesenchymal stromal cells (MSCs) and their derivative exosome in skin wound healing: a comprehensive review. *Stem Cell Res Ther* 2022; **13**: 24 [PMID: 35073970 DOI: 10.1186/s13287-021-02697-9]
4 **Yu Y**, Yue Z, Xu M, Zhang M, Shen X, Ma Z, Li J, Xie X. Macrophages play a key role in tissue repair and regeneration. *PeerJ* 2022; **10**: e14053 [PMID: 36196399 DOI: 10.7717/peerj.14053]
5 **Chen C**, Liu T, Tang Y, Luo G, Liang G, He W. Epigenetic regulation of macrophage polarization in wound healing. *Burns Trauma* 2023; **11**: tkac057 [PMID: 36687556 DOI: 10.1093/burnst/tkac057]
6 **Mosser DM**, Edwards JP. Exploring the full spectrum of macrophage activation. *Nat Rev Immunol* 2008; **8**: 958-969 [PMID: 19029990 DOI: 10.1038/nri2448]
7 **DiPietro LA**, Wilgus TA, Koh TJ. Macrophages in Healing Wounds: Paradoxes and Paradigms. *Int J Mol Sci* 2021; **22**: 950 [PMID: 33477945 DOI: 10.3390/ijms22020950]
8 **Rauchenwald T**, Handle F, Connolly CE, Degen A, Seifarth C, Hermann M, Tripp CH, Wilflingseder D, Lobenwein S, Savic D, Pölzl L, Morandi EM, Wolfram D, Skvortsova II, Stoitzner P, Haybaeck J, Konschake M, Pierer G, Ploner C. Preadipocytes in human granulation tissue: role in wound healing and response to macrophage polarization. *Inflamm Regen* 2023; **43**: 53 [PMID: 37904253 DOI: 10.1186/s41232-023-00302-5]
9 **Murray PJ**. Macrophage Polarization. *Annu Rev Physiol* 2017; **79**: 541-566 [PMID: 27813830 DOI: 10.1146/annurev-physiol-022516-034339]
10 **Fantin A**, Vieira JM, Gestri G, Denti L, Schwarz Q, Prykhozhij S, Peri F, Wilson SW, Ruhrberg C. Tissue macrophages act as cellular chaperones for vascular anastomosis downstream of VEGF-mediated endothelial tip cell induction. *Blood* 2010; **116**: 829-840 [PMID: 20404134 DOI: 10.1182/blood-2009-12-257832]
11 **Wynn TA**, Vannella KM. Macrophages in Tissue Repair, Regeneration, and Fibrosis. *Immunity* 2016; **44**: 450-462 [PMID: 26982353 DOI: 10.1016/j.immuni.2016.02.015]
12 **Zhao R**, Liang H, Clarke E, Jackson C, Xue M. Inflammation in Chronic Wounds. *Int J Mol Sci* 2016; **17**: 2085 [PMID: 27973441 DOI: 10.3390/ijms17122085]
13 **Abumaree MH**, Al Jumah MA, Kalionis B, Jawdat D, Al Khaldi A, Abomaray FM, Fatani AS, Chamley LW, Knawy BA. Human placental mesenchymal stem cells (pMSCs) play a role as immune suppressive cells by shifting macrophage differentiation from inflammatory M1 to anti-inflammatory M2 macrophages. *Stem Cell Rev Rep* 2013; **9**: 620-641 [PMID: 23812784 DOI: 10.1007/s12015-013-9455-2]
14 **Martinez FO**, Gordon S. The M1 and M2 paradigm of macrophage activation: time for reassessment. *F1000Prime Rep* 2014; **6**: 13 [PMID: 24669294 DOI: 10.12703/P6-13]

15 **Luque-Campos N**, Bustamante-Barrientos FA, Pradenas C, García C, Araya MJ, Bohaud C, Contreras-López R, Elizondo-Vega R, Djouad F, Luz-Crawford P, Vega-Letter AM. The Macrophage Response Is Driven by Mesenchymal Stem Cell-Mediated Metabolic Reprogramming. *Front Immunol* 2021; **12**: 624746 [PMID: 34149687 DOI: 10.3389/fimmu.2021.624746]

16 **Wang M**, Zhang G, Wang Y, Liu T, Zhang Y, An Y, Li Y. Crosstalk of mesenchymal stem cells and macrophages promotes cardiac muscle repair. *Int J Biochem Cell Biol* 2015; **58**: 53-61 [PMID: 25462160 DOI: 10.1016/j.biocel.2014.11.003]

17 **Wise AF**, Williams TM, Kiewiet MB, Payne NL, Siatskas C, Samuel CS, Ricardo SD. Human mesenchymal stem cells alter macrophage phenotype and promote regeneration *via* homing to the kidney following ischemia-reperfusion injury. *Am J Physiol Renal Physiol* 2014; **306**: F1222-F1235 [PMID: 24623144 DOI: 10.1152/ajprenal.00675.2013]

18 **Maggini J**, Mirkin G, Bognanni I, Holmberg J, Piazzón IM, Nepomnaschy I, Costa H, Cañones C, Raiden S, Vermeulen M, Geffner JR. Mouse bone marrow-derived mesenchymal stromal cells turn activated macrophages into a regulatory-like profile. *PLoS One* 2010; **5**: e9252 [PMID: 20169081 DOI: 10.1371/journal.pone.0009252]

19 **Ni R**, Jiang L, Zhang C, Liu M, Luo Y, Hu Z, Mou X, Zhu Y. Biologic Mechanisms of Macrophage Phenotypes Responding to Infection and the Novel Therapies to Moderate Inflammation. *Int J Mol Sci* 2023; **24**: 8358 [PMID: 37176064 DOI: 10.3390/ijms24098358]

20 **Liu Y**, Xu R, Gu H, Zhang E, Qu J, Cao W, Huang X, Yan H, He J, Cai Z. Metabolic reprogramming in macrophage responses. *Biomark Res* 2021; **9**: 1 [PMID: 33407885 DOI: 10.1186/s40364-020-00251-y]

World Journal of Stem Cells

Submit a Manuscript: https://www.f6publishing.com

World J Stem Cells 2025 February 26; 17(2): 101395

DOI: 10.4252/wjsc.v17.i2.101395

ISSN 1948-0210 (online)

ORIGINAL ARTICLE

Basic Study

Exosomal miR-203 from bone marrow stem cells targets the SOCS3/NF-κB pathway to regulate neuroinflammation in temporal lobe epilepsy

Wei Wang, Jian Yin

Specialty type: Cell and tissue engineering

Provenance and peer review: Unsolicited article; Externally peer reviewed.

Peer-review model: Single blind

Peer-review report's classification

Scientific Quality: Grade B, Grade C

Novelty: Grade B, Grade B

Creativity or Innovation: Grade B, Grade C

Scientific Significance: Grade C, Grade C

P-Reviewer: Hiramoto K; Wang GF

Received: November 28, 2024

Revised: December 27, 2024

Accepted: February 11, 2025

Published online: February 26, 2025

Processing time: 87 Days and 22.6 Hours

Wei Wang, Jian Yin, Department of Neurosurgery, The Second Affiliated Hospital of Dalian Medical University, Dalian 116023, Liaoning Province, China

Corresponding author: Jian Yin, PhD, Chief Physician, Department of Neurosurgery, The Second Affiliated Hospital of Dalian Medical University, No. 467 Zhongshan Road, Shahekou District, Dalian 116023, Liaoning Province, China. yin_dmu@sina.com

Abstract

BACKGROUND

Epilepsy is a prevalent chronic neurological disorder affecting 50 million individuals globally, with temporal lobe epilepsy (TLE) being the most common form. Despite advances in antiepileptic drug development, over 30% of patients suffer from drug-resistant epilepsy, which can lead to severe cognitive impairments and adverse psychosocial outcomes.

AIM

To explore the role of bone marrow mesenchymal stem cell (BMSC)-derived exosomal miR-203 in the regulation of neuroinflammation in a mouse model of epilepsy, providing a theoretical basis for the development of targeted microRNA delivery therapies for drug-resistant epilepsy.

METHODS

Adult male C57BL/6 mice were divided into a control group and a TLE model of 30 mice each, and the TLE model group was established by injecting kainic acid. BMSCs were isolated from the mice, and exosomes were purified using ultracentrifugation. Exosomal miR-203 was identified and characterized using high-throughput sequencing and quantitative reverse-transcription polymerase chain reaction. The uptake of exosomes by hippocampal neurons and the subsequent effects on neuroinflammatory markers were assessed using *in vitro* cell culture models.

RESULTS

Exosomal miR-203 exhibited a significant upregulation in BMSCs derived from epileptic mice. *In vitro* investigations demonstrated the efficient internalization of these exosomes by hippocampal neurons, resulting in downregulation of suppressor of cytokine signaling 3 expression and activation of the nuclear factor

kappaB pathway, ultimately leading to enhanced secretion of pro-inflammatory cytokines.

CONCLUSION
Our study identifies exosomal miR-203 as a key regulator of neuroinflammation in a mouse model of epilepsy. The findings suggest that targeting miR-203 may offer a novel therapeutic strategy for epilepsy by modulating the suppression of cytokine signaling 3/nuclear factor kappaB pathway, thus providing a potential avenue for the development of cell-free therapeutics.

Key Words: Epilepsy; Neuroinflammation; MiR-203; Exosomes; Bone marrow mesenchymal stem cells; Suppressor of cytokine signaling; Nuclear factor kappaB

Core Tip: This study highlights the role of bone marrow mesenchymal stem cell-derived exosomal miR-203 in regulating neuroinflammation in a mouse model of temporal lobe epilepsy. These findings suggest that miR-203 modulates the suppressor of cytokine signaling 3/nuclear factor kappaB pathway, leading to increased neuroinflammation. This pathway activation promotes the secretion of proinflammatory cytokines, contributing to the pathology of epilepsy. Targeting miR-203 may offer a novel therapeutic approach for drug-resistant epilepsy by reducing neuroinflammation and improving patient outcomes, offering potential for future cell-free therapeutic strategies.

Citation: Wang W, Yin J. Exosomal miR-203 from bone marrow stem cells targets the SOCS3/NF-κB pathway to regulate neuroinflammation in temporal lobe epilepsy. *World J Stem Cells* 2025; 17(2): 101395
URL: https://www.wjgnet.com/1948-0210/full/v17/i2/101395.htm
DOI: https://dx.doi.org/10.4252/wjsc.v17.i2.101395

INTRODUCTION

Epilepsy, a prevalent neurological disorder characterized by recurrent seizures, affects approximately 50 million people worldwide[1]. Temporal lobe epilepsy (TLE), the most common form of epilepsy, is associated with hyperexcitability of neurons, hippocampal damage, neuronal apoptosis, activation of astrocytes and microglia, neuroinflammation, oxidative stress, and cognitive impairment[2-4]. Despite advancements in antiepileptic drugs, over 30% of patients suffer from drug-resistant epilepsy (DRE)[5], which can lead to more severe memory and cognitive deficits as well as adverse psychosocial outcomes[6].

Neuroinflammation plays a critical role in the pathophysiology of epilepsy. Sustained inflammation exacerbates TLE through synaptic reorganization, mossy fiber sprouting, and neuronal damage, leading to recurrent seizures. The suppression of cytokine signaling 3 (SOCS3) has been implicated in the modulation of neuroinflammatory responses. SOCS3 is a negative feedback regulator of cytokine signaling that can inhibit the activation of the Janus kinase/signal transducer and activator of the transcription pathway, which is involved in the production of proinflammatory cytokines [7]. In the context of TLE, overactivation of neuroinflammatory pathways, such as the nuclear factor kappaB (NF-κB) pathway, can lead to a chronic inflammatory state that contributes to seizure progression and resistance to antiepileptic drugs[8]. While numerous basic and clinical studies have contributed to the development of antiepileptic drugs, a deeper understanding of the pathomechanisms by which TLE suppresses neuroinflammatory responses and apoptotic processes is needed, thereby improving patient memory and cognitive abilities and enhancing their quality of life.

MicroRNAs (miRNAs) play crucial roles in the differentiation, proliferation, and death of neuronal cells, and are known to regulate neurotransmitter release and neuroinflammatory responses[9-13]. In the context of epilepsy pathogenesis, miRNAs are thought to exert regulatory effects through the precise control of gene expression, influencing the behavior and interactions of neural cells[14-16]. Among various miRNAs implicated in neurological disorders, miR-203 has garnered attention because of its potential role in modulating neuroinflammation. The miR-203 targets SOCS3, a key negative regulator of cytokine signaling pathways[17]. SOCS3 inhibits the activation of the Janus kinase/signal transducer and activator of the transcription pathway, which is crucial for the production of proinflammatory cytokines such as tumor necrosis factor (TNF)-α and interleukin (IL)-6[18,19]. By binding to the 3′ untranslated region of *SOCS3* mRNA, miR-203 can lead to the degradation of *SOCS3* mRNA or block its translation, thereby reducing SOCS3 protein levels[20-22]. Downregulation of SOCS3 enhances the activation of proinflammatory pathways, contributing to the neuroinflammatory state associated with epilepsy. Understanding the interplay between miR-203 and SOCS3 could provide valuable insights into the molecular mechanisms underlying epilepsy and identify potential therapeutic targets for the management of neuroinflammation in epilepsy.

Exosomes are extracellular vesicles of endocytic origin that are important mediators of intercellular communication in the nervous system[23]. These nanoscale vesicles, measuring 30-100 nm in diameter, exhibit favorable characteristics, such as the ability to evade clearance by the reticuloendothelial system[24], cross the blood-brain barrier[25], and target specific cells within the central nervous system[26]. They have been implicated in the modulation of neuroinflammation

and immune responses, and have potential as therapeutic agents against various neurological disorders[27].

This study investigated the role of exosomal miR-203 derived from bone marrow mesenchymal stem cells (BMSCs) in the regulation of neuroinflammation in a mouse model of epilepsy. We hypothesized that miR-203, which is differentially expressed in BMSC-derived exosomes from epileptic mice, modulates neuroinflammation by targeting the SOCS3/NF-κB pathway, a key regulator of the inflammatory response. By elucidating the mechanisms by which exosomal miR-203 influences neuroinflammation, this study provides a foundation for the development of targeted miRNA delivery strategies to improve outcomes in patients with DRE.

MATERIALS AND METHODS

Animal model and ethical approval

To establish a reliable animal model of epilepsy for studying the effects of exosomal miR-203 on neuroinflammation, 60 adult male C57BL/6 mice, aged 8-10 weeks and weighing 20-28 g, were randomly divided into two groups: A TLE model group and a control group, each consisting of 30 mice. The randomization process was conducted using a random number table to ensure that each mouse had an equal chance of being allocated to either group. Specifically, we assigned a unique number to each mouse and referred to a random number table to determine the group assignment. Mice with numbers corresponding to a randomly selected sequence were placed in the TLE model group, whereas the others were assigned to the control group. The TLE model group was injected with kainic acid at dose of 15-20 mg/kg to induce TLE. The Racine scale was used to quantify the severity of the seizures, allowing for a standardized assessment of epilepsy induction. All experimental procedures involving animals were conducted in strict accordance with the guidelines of the Institutional Animal Care and Use Committee of Dalian Medical University (No. JL-WW-2022120601) to ensure the ethical and humane treatment of the animals.

Racine scale

Epileptic seizures were classified according to Racine grading criteria, with grade 0 indicating the absence of convulsive seizures. Grade I indicates ear and face convulsions, whereas grade II indicates myoclonus without an upright position. Grade III denotes myoclonus in the orthostatic position. Grade IV represents generalized tetanic seizures and grade V represents tonic-clonic seizures accompanied by loss of postural control. In the epileptic status model, mice exhibiting class V or higher seizures lasting for 40 minutes were considered successful if they remained in good condition after resolution.

Isolation of BMSCs and exosome extraction

Bone marrow was extracted from the femurs of mice to ensure sterile conditions to maintain cell viability and purity. Extracted marrow was cultured in Dulbecco's modified Eagle's medium supplemented with 10% fetal bovine serum and 1% penicillin/streptomycin under standard cell culture conditions (37 °C, 5% CO_2). Mononuclear cells from the bone marrow were isolated *via* density-gradient centrifugation using Ficoll-Paque PLUS solution. The interphase containing mononuclear cells was collected, washed, and cultured to allow the BMSCs to adhere. Once a sufficient number of BMSCs were obtained, the culture supernatant was collected and centrifuged at 2000 × *g* for 30 minutes at 4 °C to remove cells and debris. The supernatant was then filtered through a 0.45 μm filter to remove larger vesicles. Exosomes were pelleted by ultracentrifugation at 100000 × *g* for 70 minutes at 4 °C. The pellet was resuspended in phosphate-buffered saline (PBS), and this step was repeated to ensure purity. The final exosome pellet was resuspended in a minimal volume of PBS and stored at -80 °C for further analysis.

Characterization of exosomes

Exosome samples were initially adsorbed onto copper grids and stained with uranyl acetate to verify the identity, purity, and characteristics of the extracted exosomes. Subsequently, their morphology and size were evaluated *via* a transmission electron microscopy to confirm the typical "cup-shaped" appearance associated with exosomes. The size distribution and concentration of the exosomes were then determined using nanoparticle tracking analysis, providing a quantitative assessment of the exosome populations within the sample. Furthermore, western blotting or immunofluorescence assays employing specific antibodies were employed to identify surface markers, such as CD9 and CD63, on exosomes by confirming their origin as vesicles derived from exosomal sources. Additionally, fluorescent dyes (*e.g.*, PKH67) have been used to label exosomes and track their uptake by target cells. This facilitated visualization under a confocal microscope and quantification using flow cytometry to ensure efficient internalization into cellular entities.

Differential miRNA analysis of exosomes derived from BMSCs

To extract and quantify the total RNA from BMSC-derived exosomes, the exosome pellet was resuspended in RNase-free water, and an appropriate volume of RNA lysis buffer was added to facilitate membrane disruption and RNA release. Following a 5-minute incubation at room temperature, chloroform was added to the mixture, which was then vortexed and centrifuged to separate the phases. The upper aqueous phase, enriched with RNA, was carefully transferred to a new tube and isopropanol was added to precipitate the RNA. After centrifugation, the supernatant was removed and the RNA pellet was washed with 75% ethanol. The dried RNA pellet was resuspended in RNase-free water and its concentration and purity were determined using a spectrophotometer. RNA integrity was assessed by agarose gel electrophoresis, confirming the suitability of the extracted RNA for downstream applications, such as gene expression analysis and

miRNA profiling. All steps were conducted in an RNase-free environment using RNase-free reagents to prevent contamination and ensure the reliability of the results.

Following the ligation of the extracted RNA with 5′ and 3′ adapters, cDNA reverse transcription was performed to serve as a template for constructing the miRNA library. The resulting library was subjected to PE150 sequencing to generate sequence data. To identify the differentially expressed miRNAs in BMSC-derived exosomes, raw sequencing reads were quality-checked and trimmed using FastQC and Trimmomatic to remove low-quality reads and adapter sequences, respectively. Subsequently, the cleaned reads were aligned to the reference genome using Bowtie software, allowing precise mapping of miRNA sequences. The known miRNAs were annotated by comparing their aligned sequences with those in the miRBase database, which is a comprehensive repository of miRNA sequences. The miRDeep2 software was used to identify these known miRNAs and predict novel miRNAs by assessing the secondary structure of the precursor miRNAs and their alignment to the reference genome. The prediction of novel miRNAs involves the evaluation of the presence of a stable hairpin structure and the production of a mature miRNA sequence from the precursor.

DE-miRNAs were selected based on stringent criteria of P value < 0.05 and |log2 fold change| ≥ 1, ensuring the identification of miRNAs with substantial expression changes. Furthermore, ten differentially expressed miRNAs (DE-miRNAs) were carefully selected from both the upregulated and downregulated groups while considering the relevant literature pertaining to neuroinflammation. Five differentially regulated miRNAs from each group were selected for reverse transcription-polymerase chain reaction (RT-PCR) and quantitative PCR (qPCR) validation.

Exosome uptake assay

According to the manufacturer's agreement, the PKH67 green fluorescent labeling kit (Umibio, Shanghai, China) was utilized for labeling the isolated exosomes from normal and epileptic mouse BMSCs. Briefly, exosomes were incubated with PKH67 dye for 10 minutes, followed by three washes to remove excess dye using OptimaMAX-XP (Backman, UT, United States). Subsequently, these cells were co-cultured with HT22 cells for 24 hours. After three additional washes with PBS, red CellLINK555 dye (Tianjiu Regeneration, Tianjin, China) was added and the cells were incubated for 30 minutes. After another round of washing with PBS, fixation was performed at room temperature with 4% paraformaldehyde for 30 minutes. The cells were then washed three times with PBS and stained with the nuclear stain DAPI for 10 minutes. The uptake of exosomes derived from normal and epileptic mouse BMSCs by HT22 cells was visualized through confocal microscopy analysis. The negative control group consisted of HT22 cells treated similarly to the other groups, but without the addition of PKH67 dye during co-incubation.

Functional experiments of exosome

This study investigated the functional effects of exosomal miR-203 on neuroinflammation in a cellular TLE model. HT22 cells were co-cultured with exosomes isolated from control group or TLE group BMSCs at a concentration of 10 μg/mL. Following 24-hour incubation, the expression levels of the target genes *SOCS3* and *miR-203-3p* were quantified using qPCR. Moreover, changes in inflammatory factors (TNF-α, IL-6) in the cell supernatant were determined by enzyme-linked immunosorbent assay (ELISA). The extent of cellular apoptosis was evaluated using flow cytometry, and cell proliferation was assessed using the CCK8 assay.

Dual luciferase reporter assay

To validate the regulatory association between *miR-203-3p* and its target gene, *SOCS3*, we transfected HEK-293T cells with pmirGLO plasmids harboring wild-type and mutant SOCS3 promoter regions in conjunction with the overexpression of either miR-203-3p mimic (NC) or miR-203-3p. Following a 48-hour transfection period, the luminescence intensity of the firefly luciferase protein was quantified.

NF-κB pathway modulation study

To investigate the regulatory role of miR-203/SOCS3 in neuroinflammation through the NF-κB pathway in mice, we established an epilepsy cell model using HT22 cells. First, we determined the glutamate concentration required to induce HT22 epilepsy using a CCK8 assay. Subsequently, in the HT22 epilepsy cell model, we separately added miR-203-3p mimic or inhibitor, miR-203-3p inhibitor alone, and si-SOCS3/NC along with an NF-κB inhibitor (100 μmol/L)[28,29]. The RNA expression levels of miR-203-3p and its target gene, *SOCS3*, were assessed using qPCR. Additionally, western blotting technique was employed to detect the miRNA target gene (*SOCS3*, 1:2000, Proteintech, IL, United States) as well as markers of the NF-κB pathway: Inhibitor of kappa B kinase alpha/beta (1:1000, ZenBio, NC, United States), phospho-inhibitor of kappa B kinase alpha/beta (1:1000, ZenBio, NC, United States), NF-κB inhibitor alpha (1:10000, Proteintech, IL, United States), phospho-NF-κB inhibitor alpha (1:1000, ZenBio, NC, United States), p65 (1:10000, Proteintech, IL, United States) and p-p65 (1:1000, ZenBio, NC, United States). The secondary antibody was goat anti-rabbit horseradish peroxidase (Bioss, MA, United States) at a dilution of 1:5000. Cell apoptosis was evaluated, and cell proliferation was assessed using the CCK8 assay. Furthermore, inflammatory factors (TNF-α and IL-6) in the cell supernatant were quantified using ELISA.

Statistical analysis

Data were analyzed using GraphPad Prism 9 (Version 9.4.0) and presented as means ± SD. Statistical differences between groups were evaluated using the *t*-test or one-way ANOVA, with P < 0.05 considered statistically significant.

Table 1 Twenty DE-miRNA associated with neuroinflammation

MiRNA	Log2FC	*P* value	*Padj* value
mmu-miR-193a-5p	7.255065725	1.63E-10	1.44E-09
mmu-miR-205-5p	6.611947124	5.89E-33	1.63E-31
mmu-miR-203-3p	6.322996495	6.36E-07	4.34E-06
mmu-miR-200a-5p	5.553009313	0.004701826	0.020589048
mmu-miR-200a-3p	5.551982625	0.00094398	0.004619947
mmu-miR-182-5p	3.510594588	0.000514058	0.0026731
mmu-miR-200c-3p	3.372596465	3.08E-41	1.16E-39
mmu-miR-196a-5p	3.326742762	4.44E-13	4.62E-12
mmu-miR-196a-5p	3.291829303	8.00E-11	7.23E-10
mmu-miR-144-3p	3.077271591	1.10E-22	2.08E-21
mmu-miR-3473h-5p	-2.501671763	0.009780829	0.039890438
mmu-miR-700-3p	-2.477319455	0.000489188	0.002575975
mmu-miR-484	-2.343847305	7.95E-14	8.94E-13
mmu-miR-339-5p	-2.257736292	1.86E-19	3.23E-18
mmu-miR-328-3p	-2.212306543	5.48E-30	1.27E-28
mmu-miR-30b-5p	-2.151354017	0.000281059	0.00153843
mmu-miR-23a-3p	-2.129117956	4.09E-67	1.89E-65
mmu-miR-128-3p	-2.122702882	5.11E-20	9.25E-19
mmu-miR-181c-5p	-2.02817	7.15E-06	4.65E-05
mmu-miR-221-3p	-1.25811	0.007661	0.031871

MiRNA: MicroRNA; FC: Fold change.

RESULTS

Examination of exosomes derived from mouse BMSCs

Transmission electron microscopy imaging revealed that exosomes from both the epilepsy and normal groups displayed the characteristic "cup-shape" morphology, with a clear membrane structure (Figure 1A). The average particle size and concentration were determined to be 85.31 nm and 1.62E+10 particles/mL for the epilepsy group, and 84.64 nm and 3.29E+10 particles/mL for the normal group, respectively (Figure 1B). Exosomes from both groups showed positive expression of the protein markers CD9 and CD63, with the epilepsy group showing a slightly higher positivity rate for CD9 (2.7%) than the normal group (2.1%). The expression of CD63 was minimal in both groups, with 0.6% and 0.3% positivity in the epilepsy and control groups, respectively (Figure 1C).

Identification and validation of differentially expressed miRNAs in epileptic mouse BMSCs

Table 1 presents the 20 miRNAs with the most significantly differential expression related to neuroinflammation, selected based on the degree of difference. This includes 10 miRNAs with upregulated expression and 10 with downregulated expression. A total of 10 differentially expressed miRNAs were selected for experimental validation by RT-qPCR, including five upregulated miRNAs (*miR-144-3p*, *miR-193a-5p*, *miR-205-5p*, *miR-200a-3p*, and *miR-203-3p*) and five downregulated miRNAs (*miR-128-3p*, *miR-181c-5p*, *miR-23a-3p*, *miR-30b-3p*, and *miR-221-3p*). Compared to extracellular vesicles from normal mouse BMSCs, the levels of extracellular vesicles in epileptic mouse BMSCs were significantly increased ($P < 0.05$), including an increase in the aforementioned upregulated miRNAs: *MiR-144-3P*, *miR-193a-5P*, *miR-200a-3P*, and *miR-203–3P*, whereas the levels of certain downregulated miRNAs decreased: *MiR-181c-5P*, *miR-23a-3P*, and *miR-30b-3P* ($P < 0.05$, Figure 2). However, no significant differences were observed between extracellular vesicles isolated from epileptic and normal mice for *miR-205-5P*, *miR-128-3P*, and *miR-221-3P* ($P > 0.05$, Figure 2). The consistency rate between the sequencing analysis results and RT-qPCR results was approximately 70%, indicating the high reliability of the sequencing results. Furthermore, owing to its more pronounced upregulation compared to *miR-144-3p* and *miR-200a–3p*, the focus of subsequent experiments was on *miR-203-3p*. qPCR validation of ten differentially expressed miRNAs associated with neuroinflammation is presented.

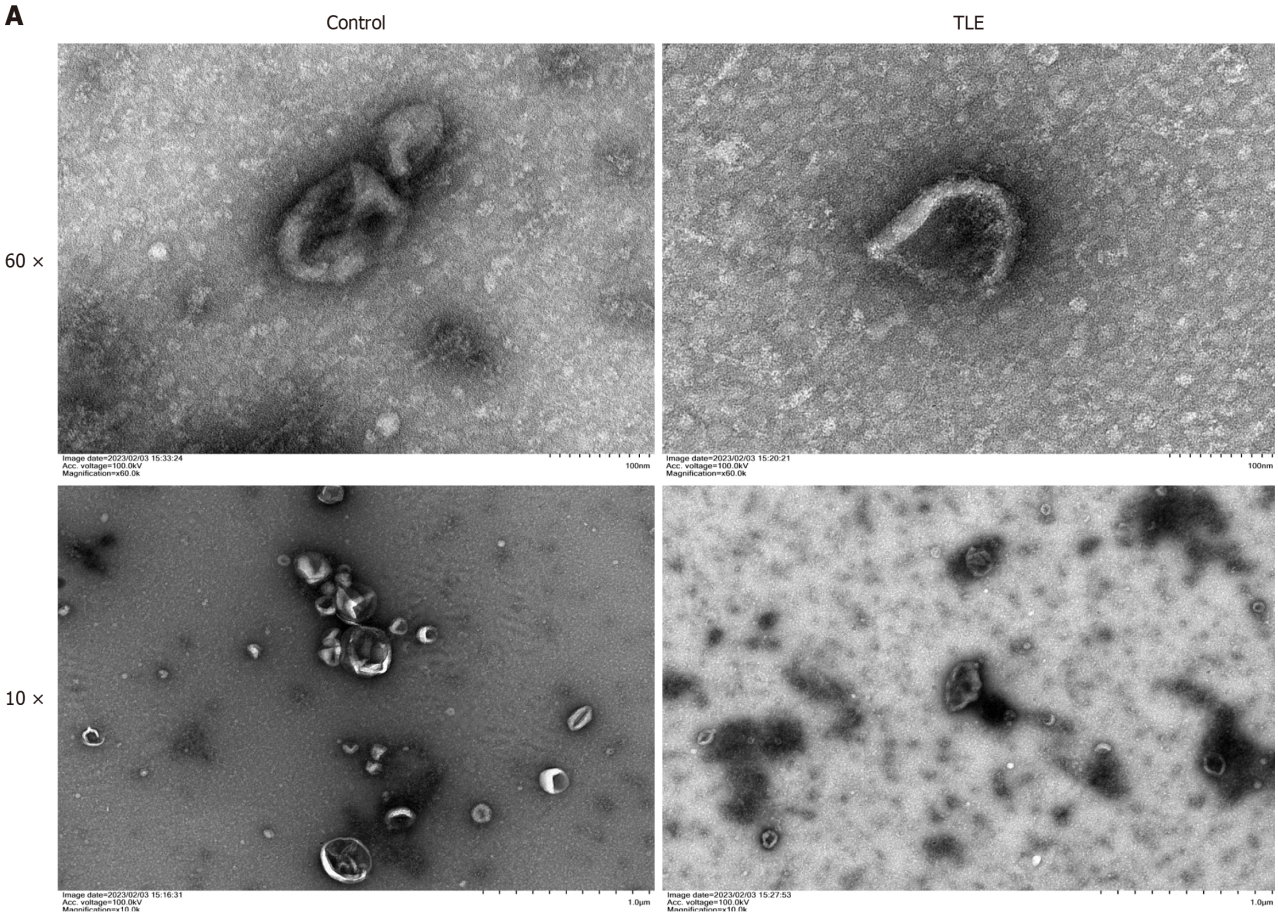
A
Control
TLE
60 ×
10 ×

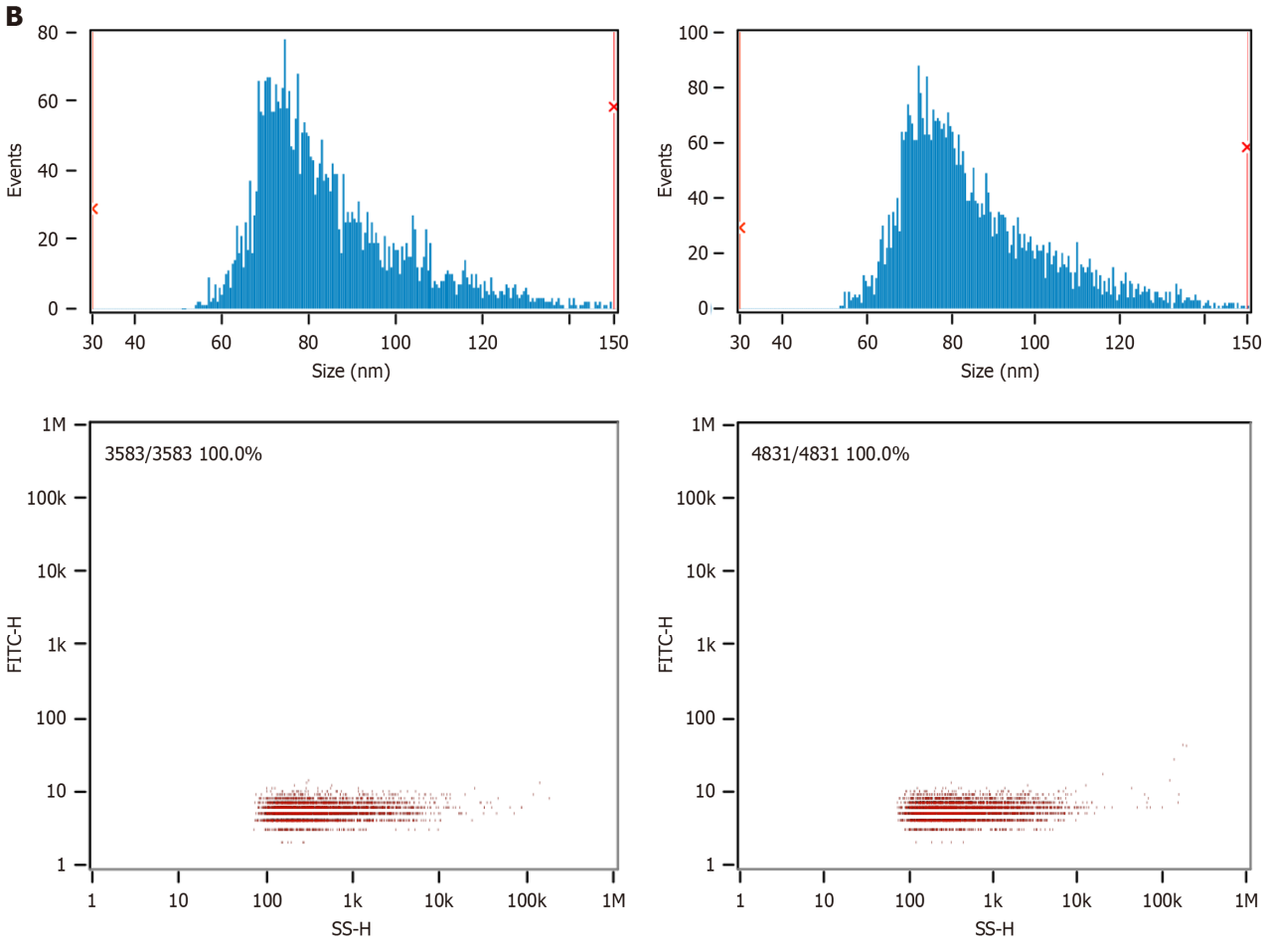
B
Events
Size (nm)
3583/3583 100.0%
4831/4831 100.0%
FITC-H
SS-H

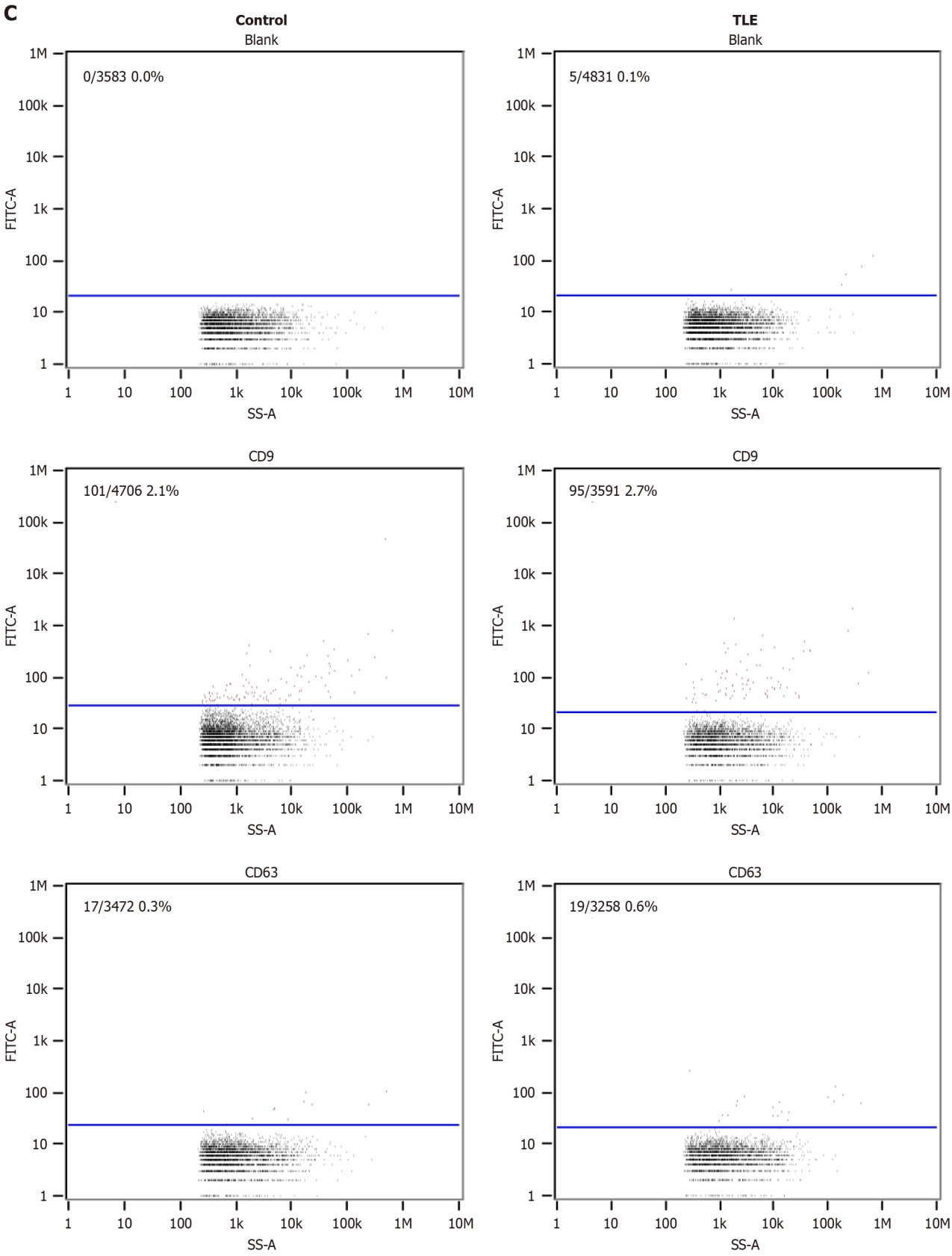

Figure 1 Characteristic of exosomes from bone marrow mesenchymal stem cells. A: Transmission electron microscopy images reveal the characteristic "cup-shaped" morphology and clear membrane structure of exosomes from both the epilepsy and normal groups of mice; B: Nanoparticle tracking analysis shows the average particle size and concentration to be 8531 nm and 1.62E+10 particles/mL for the epilepsy group, and 84.64 nm and 3.29E+10 particles/mL for the normal group, respectively; C: Flow cytometry analysis demonstrates positive expression of the protein markers CD9 and CD63 in exosomes from both groups, with a slightly higher positive rate for CD9 in the epilepsy group than in the normal group and minimal expression of CD63 in both groups. TLE: Temporal lobe epilepsy.

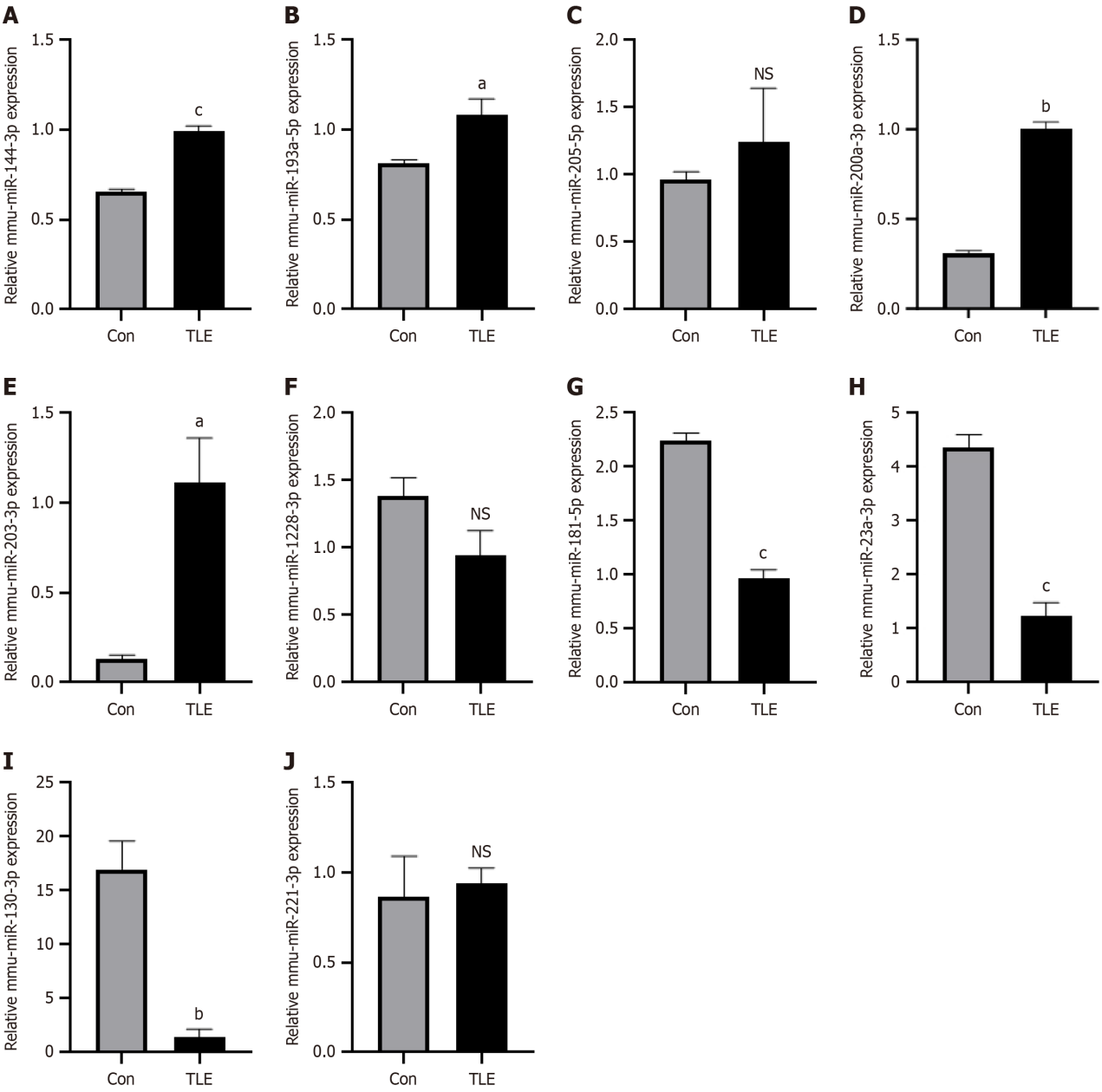

Figure 2 Quantitative polymerase chain reaction validation of DE-miRNAs. A-J: Expression miRNAs in epileptic mouse bone marrow mesenchymal stem cells. [a]*P* < 0.05, [b]*P* < 0.01, [c]*P* < 0.001, NS: No significance. TLE: Temporal lobe epilepsy.

Exosomes secreted by BMSCs enhance the secretion of inflammatory mediators in hippocampal neurons

After incubation with PKH67-labeled exosomes, HT22 cells showed significant fluorescence, indicating the efficient uptake of exosomes by the cells (Figure 3A). HT22 cells also showed significant fluorescence (Figure 3B), and incubation with FAM-labeled miR-203-3p from BMSCs (Figure 3C and D). This indicates the efficient uptake of miR-203-3p from exosomes by cells. The qPCR results revealed a significant increase in miR-203-3p levels ($P = 0.0497$, $P < 0.05$; Figure 3E) and a significant decrease in *SOCS3* mRNA expression ($P = 0.0217$, $P < 0.05$; Figure 3F) in the TLE group. Flow cytometry analysis demonstrated an elevated apoptosis rate ($P = 0.0005$, $P < 0.05$, Figure 3G-K), while the CCK8 assay indicated a reduced cell proliferation ability ($P = 0.00334$, $P < 0.05$, Figure 3L). Furthermore, ELISA detection showed upregulated levels of inflammatory factors such as TNF-α and IL-6 in the TLE group (TNF-α: $P = 0.0005$, $P < 0.05$, Figure 3M; $P = 0.0004$, $P < 0.05$, Figure 3N).

MiR-203-3p/SOCS3 regulates neuroinflammation of hippocampal neurons in epileptic mice through the NF-κB pathway

In the presence of wild-type plasmid SOCS3 co-expressed with miR-203-3p or mimic NC, overexpression of miR-203-3p led to a significant reduction in firefly luciferase intensity ($P = 0.0002$, $P < 0.05$, Figure 4A). However, mutation of the binding site of SOCS3 restored firefly luciferase intensity. The IC_{50} of glutamate in HT22 cells was determined to be 25.01 mmol/L using CCK8 assay (Figure 4B). In subsequent experiments, when this concentration was used as the induction dose for an epilepsy model, the expression level of miR-203-3p remained consistently higher than that in the untreated group, regardless of whether it was overexpressed by miR-203-3p mimics or suppressed by inhibitor treatment. Notably,

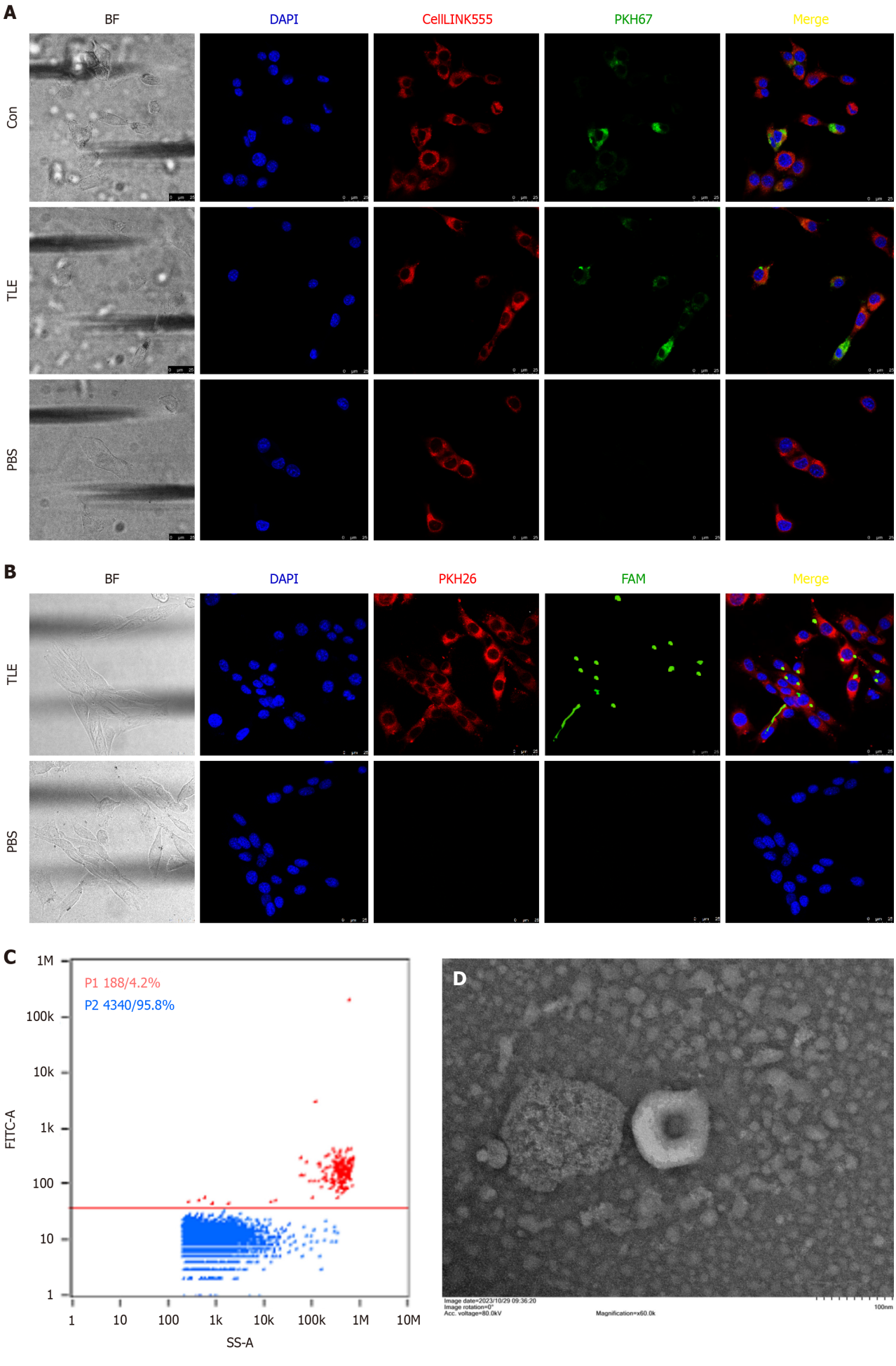
A
BF
DAPI
CellLINK555
PKH67
Merge
Con
TLE
PBS
B
BF
DAPI
PKH26
FAM
Merge
TLE
PBS
C
P1 188/4.2%
P2 4340/95.8%
FITC-A
SS-A
1M
100k
10k
1k
100
10
1
1
10
100
1k
10k
100k
1M
10M
D

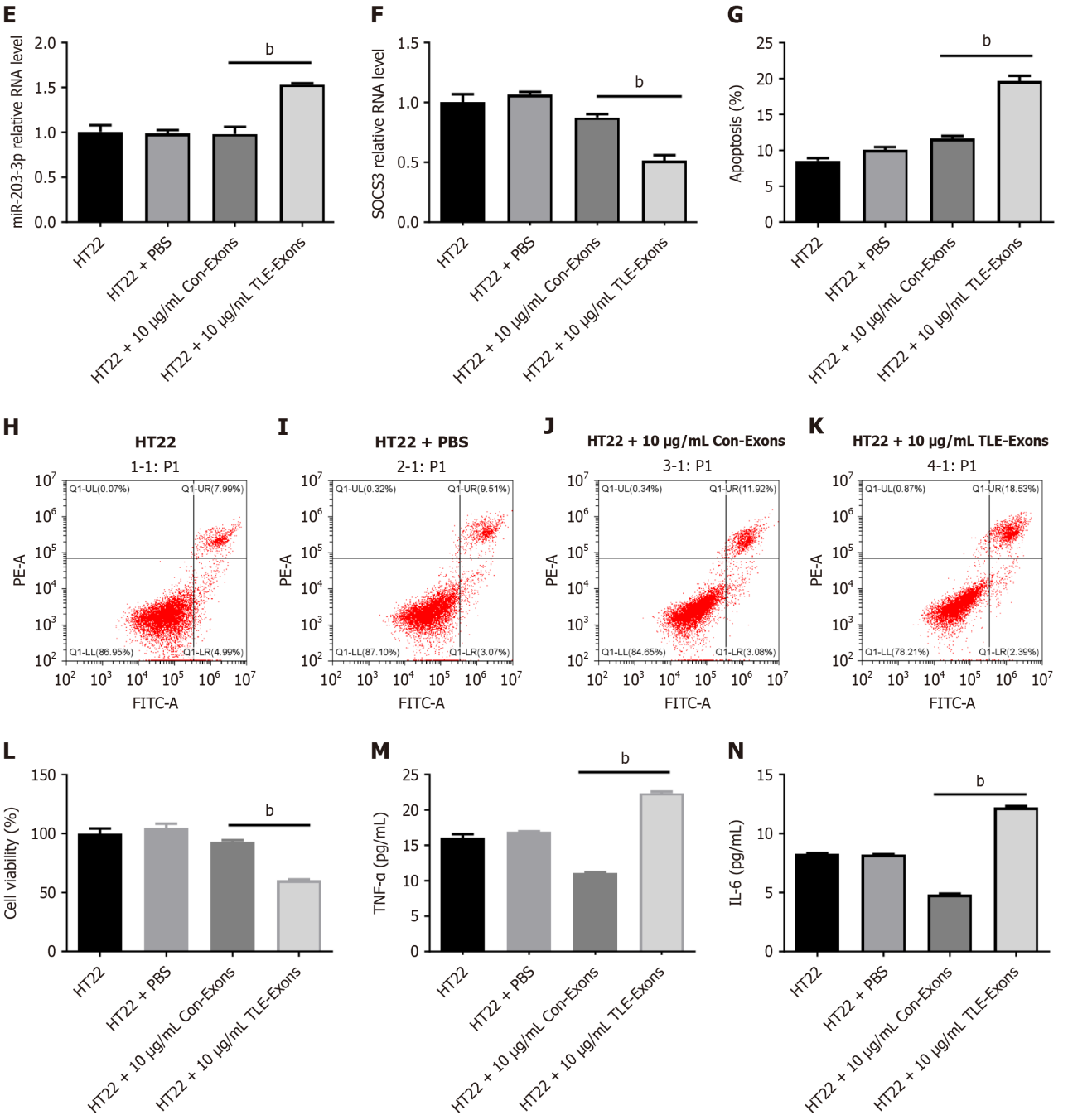

Figure 3 Exosomes secreted by bone marrow mesenchymal stem cells enhance the secretion of inflammatory mediators in hippocampal neurons. A: Confocal microscopy images of HT22 cells co-cultured with bone marrow mesenchymal stem cell-derived exosomes. Cell nuclei were stained with DAPI, cell membranes were stained with CellLINK555, and exosomes were labeled with PKH67. The scale is 25 μm; B: Confocal microscopy imaging was performed after co-culturing HT22 cells with extracellular vesicles from bone marrow mesenchymal stem cells. DAPI staining visualized the cell nuclei, PKH26 staining labeled the cell membrane, and FAM labeling detected miR-203-3p within the extracellular vesicles. The scale bar represents 25 μm; C: Flow cytometry analysis of extracellular vesicles in the supernatant after HT22 cell transfection with FAM-miR-203-3p; D: Electron microscopic examination of extracellular vesicles in the supernatant after HT22 cell transfection with FAM-miR-203-3p; E: Quantitative polymerase chain reaction results reveal a significant increase in miR-203-3p levels in the temporal lobe epilepsy (TLE) group; F: Significant decrease in suppression of cytokine signaling 3 mRNA expression was observed in the TLE group; G-K: Flow cytometric analysis demonstrated an elevated apoptosis rate in the TLE group; L: CCK8 assay indicated reduced cell proliferation in the TLE group; M and N: Enzyme-linked immunosorbent assay detection shows upregulated levels of inflammatory factors such as tumor necrosis factor-α and interleukin-6 in the TLE group. $^{b}P < 0.01$. TLE: Temporal lobe epilepsy; PBS: Phosphate-buffered saline; TNF-α: Tumor necrosis factor-α; IL-6: Interleukin-6.

miR-203-3p expression was significantly higher in the miR-203-3p mimic overexpression group than in the inhibitor group (Figure 4C). Although minimal changes were observed at the RNA level for the *SOCS3* gene (Figure 4D), its protein level showed an overall decrease and was lower in the miR2033p mimics group than in the inhibitor group. Additionally, activation of NF-κB pathway markers along with increased levels of inflammation (IL-6 and TNF-α) were observed in the miR-203-3p mimics group (Figure 4E-N).

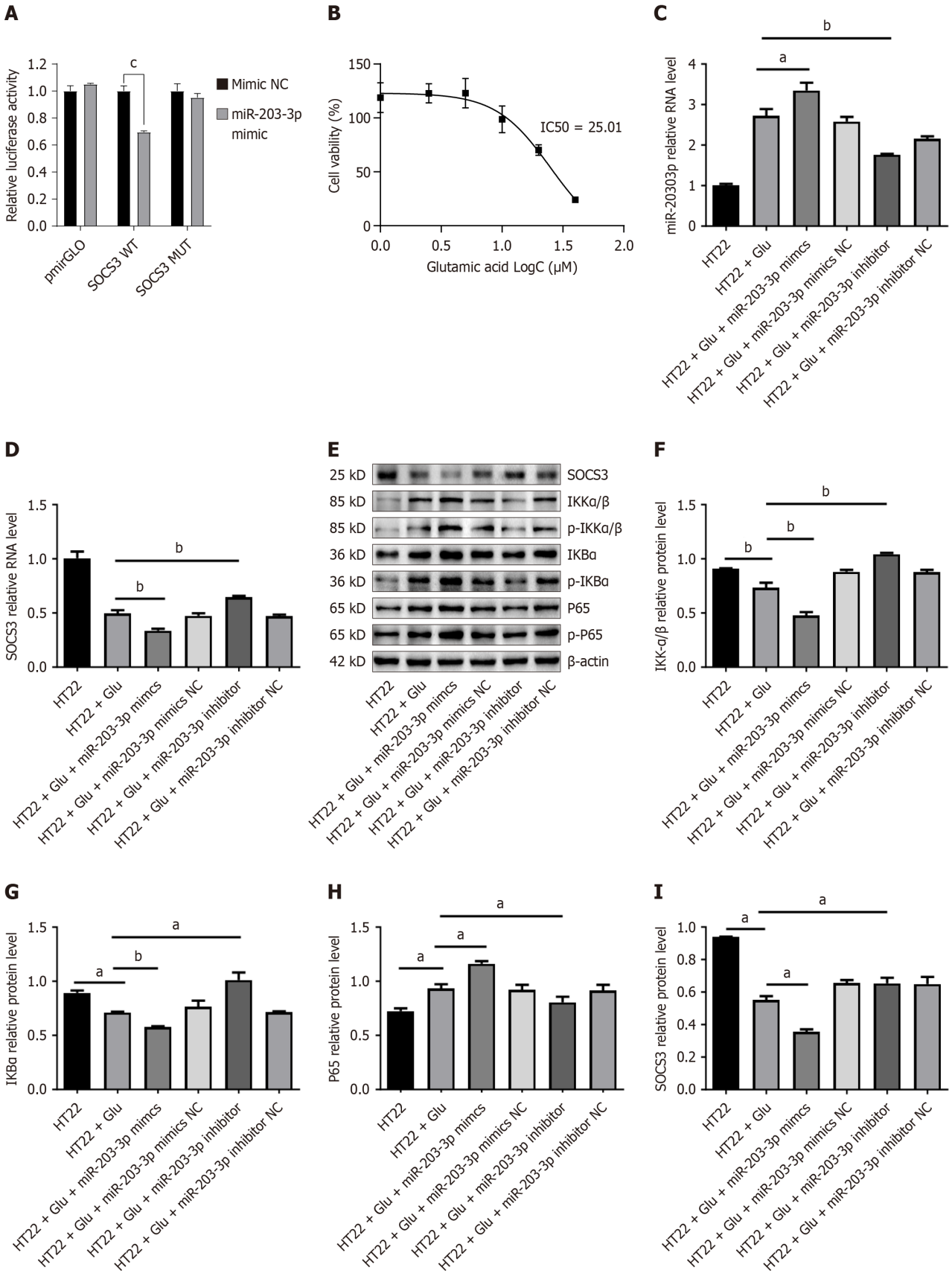
A
Relative luciferase activity
Mimic NC
miR-203-3p mimic
pmirGLO
SOCS3 WT
SOCS3 MUT
B
Cell vability (%)
IC50 = 25.01
Glutamic acid LogC (μM)
C
miR-20303p relative RNA level
D
SOCS3 relative RNA level
E
25 kD SOCS3
85 kD IKKα/β
85 kD p-IKKα/β
36 kD IKBα
36 kD p-IKBα
65 kD P65
65 kD p-P65
42 kD β-actin
F
IKK-α/β relative protein level
G
IKBα relative protein level
H
P65 relative protein level
I
SOCS3 relative protein level
HT22
HT22 + Glu
HT22 + Glu + miR-203-3p mimcs
HT22 + Glu + miR-203-3p mimics NC
HT22 + Glu + miR-203-3p inhibitor
HT22 + Glu + miR-203-3p inhibitor NC

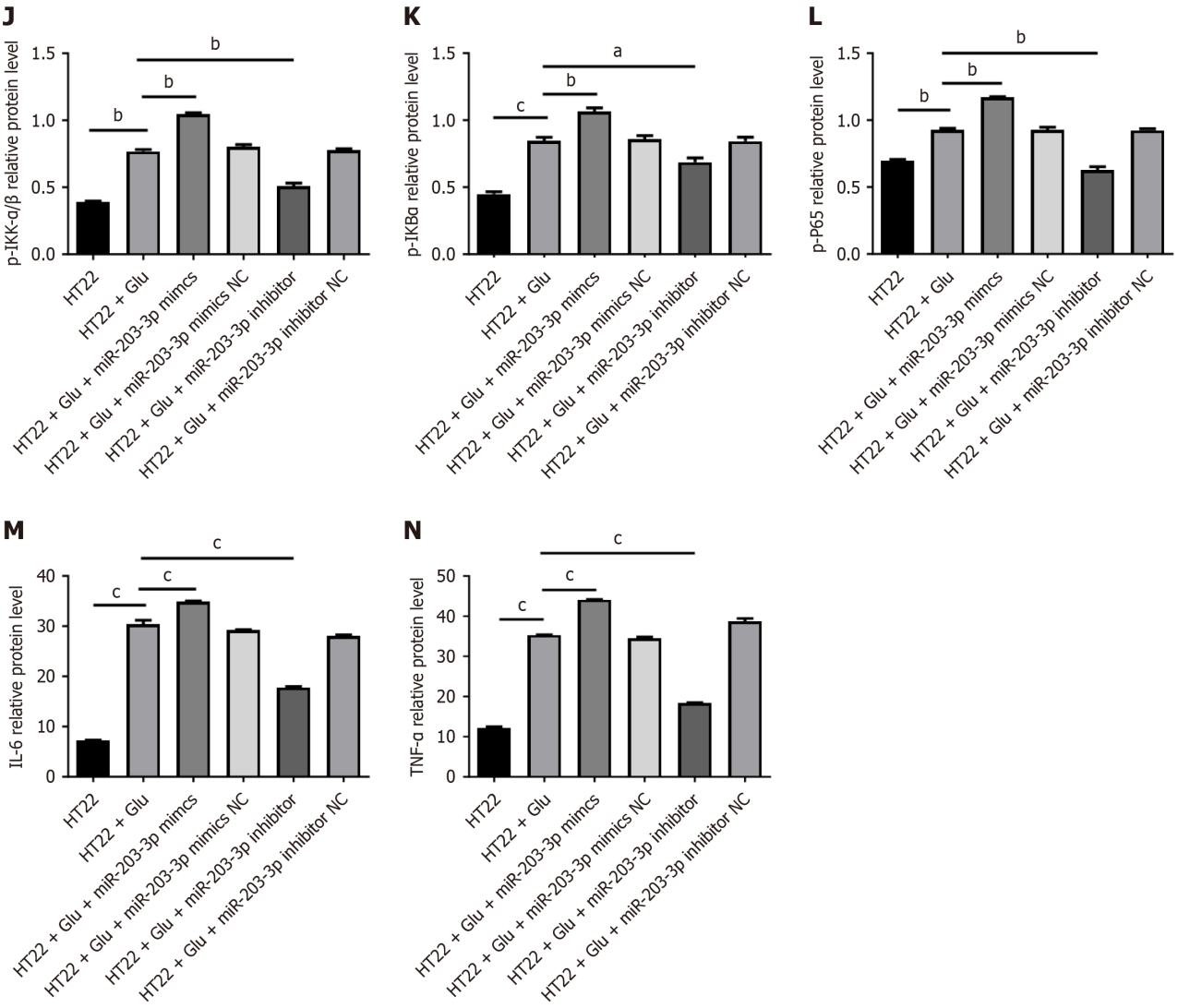

Figure 4 MiR-203-3p regulates inflammation by targeting the suppression of cytokine signaling 3-mediated nuclear factor kappaB pathway. A: Luciferase reporter assay showing the relative firefly luciferase activity in HEK-293T cells co-transfected with wild-type or mutant suppression of cytokine signaling 3 3' untranslated region reporter plasmids and miR-203-3p mimic or miR-203-3p; B: CCK8 assay to determine the IC_{50} concentration of glutamate required to induce HT22 epilepsy; C: Quantitative polymerase chain reaction analysis of miR-203-3p expression in HT22 cells after treatment with miR-203-3p mimic or inhibitor; D: Quantitative polymerase chain reaction analysis of suppression of cytokine signaling 3 mRNA expression in HT22 cells under the conditions described in Figure 3C; E-L: Western blot analysis of key proteins involved in the nuclear factor kappaB pathway, including total and phosphorylated forms of inhibitor of kappa B kinase alpha/beta, nuclear factor kappaB inhibitor alpha, and p65, in HT22 cells treated with miR-203-3p mimics or inhibitors; M and N: Enzyme-linked immunosorbent assay measurements of the inflammatory cytokines interleukin-6 and tumor necrosis factor-α in the supernatant of HT22 cells treated as in Figure 3C. Data are presented as mean ± SEM of three independent experiments. $^{a}P < 0.05$, $^{b}P < 0.01$, $^{c}P < 0.001$. SOCS3: Suppression of cytokine signaling 3; IKKα/β: Inhibitor of kappa B kinase alpha/beta; p-IKKα/β: Phospho-inhibitor of kappa B kinase alpha/beta; IKBα: Nuclear factor kappaB inhibitor alpha; p-IKBα: Phospho-nuclear factor kappaB inhibitor alpha; TNF-α: Tumor necrosis factor-α; IL-6: Interleukin-6.

Compared with the single knockout of miR-203 3p in the HT22 epileptic cell model, the double-knockout group of miR-203-3p and SOCS3 showed no difference in miR-203-3p expression (Figure 5A), while the expression levels of SOCS3 RNA (Figure 5B) and protein (Figure 5C and D) decreased. Furthermore, the double knockout group also demonstrated restoration of NF-κB pathway markers (Figure 5E-J), as well as IL-6 (Figure 5K) and TNF-α levels (Figure 5L). Additionally, after knocking out SOCS3 in the HT22 epileptic cell model, no significant difference was observed in the expression of miR-203-3p (Figure 6A), while the expression of SOCS3 RNA and protein was significantly reduced (Figure 6B-D). Moreover, an up-regulation of markers related to the NF-κB pathway was observed. However, upon administration of an inhibitor targeting the NF-κB pathway, although markers associated with the NF-κB pathway still exhibited upregulation (Figure 6E-J), a concomitant reduction in IL-6 and TNF-α levels was observed (Figure 6K and L).

Exosomes regulate the expression of SOCS3 in the hippocampus through miR-203, affecting epileptic seizures

In kainic acid-induced TLE mice, both plasma and hippocampal levels of miR-203-3p were significantly upregulated (Figure 7A and B), while only the hippocampal expression of SOCS3 was decreased (Figure 7C). Importantly, no significant difference was observed in the plasma levels of SOCS3 compared to those in the control group (Figure 7D).

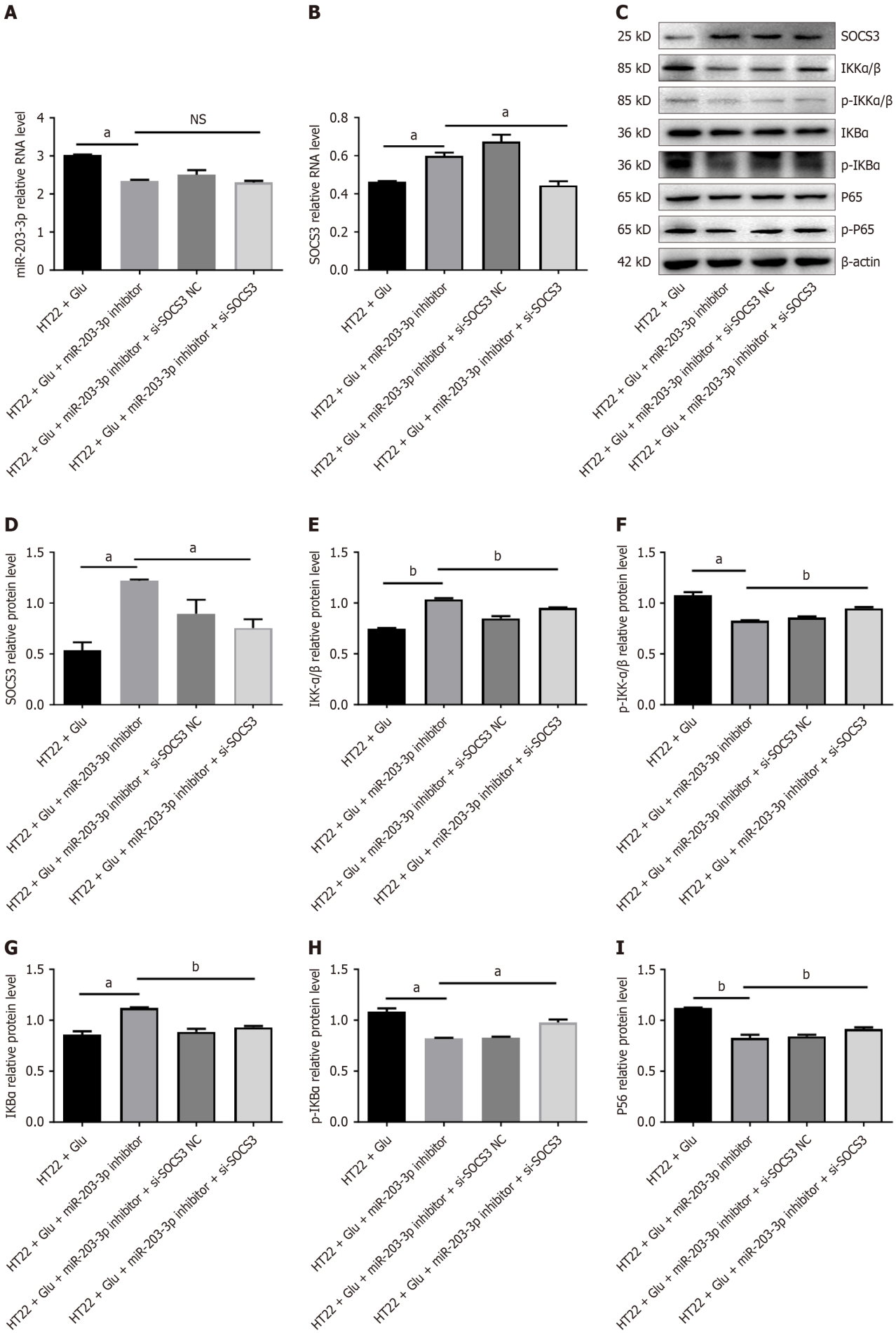
A
miR-203-3p relative RNA level
a
NS
B
SOCS3 relative RNA level
a
a
C
25 kD
SOCS3
85 kD
IKKα/β
85 kD
p-IKKα/β
36 kD
IKBα
36 kD
p-IKBα
65 kD
P65
65 kD
p-P65
42 kD
β-actin
D
SOCS3 relative protein level
a
a
E
IKK-α/β relative protein level
b
b
F
p-IKK-α/β relative protein level
a
b
G
IKBα relative protein level
a
b
H
p-IKBα relative protein level
a
a
I
P56 relative protein level
b
b
HT22 + Glu
HT22 + Glu + miR-203-3p inhibitor
HT22 + Glu + miR-203-3p inhibitor + si-SOCS3 NC
HT22 + Glu + miR-203-3p inhibitor + si-SOCS3

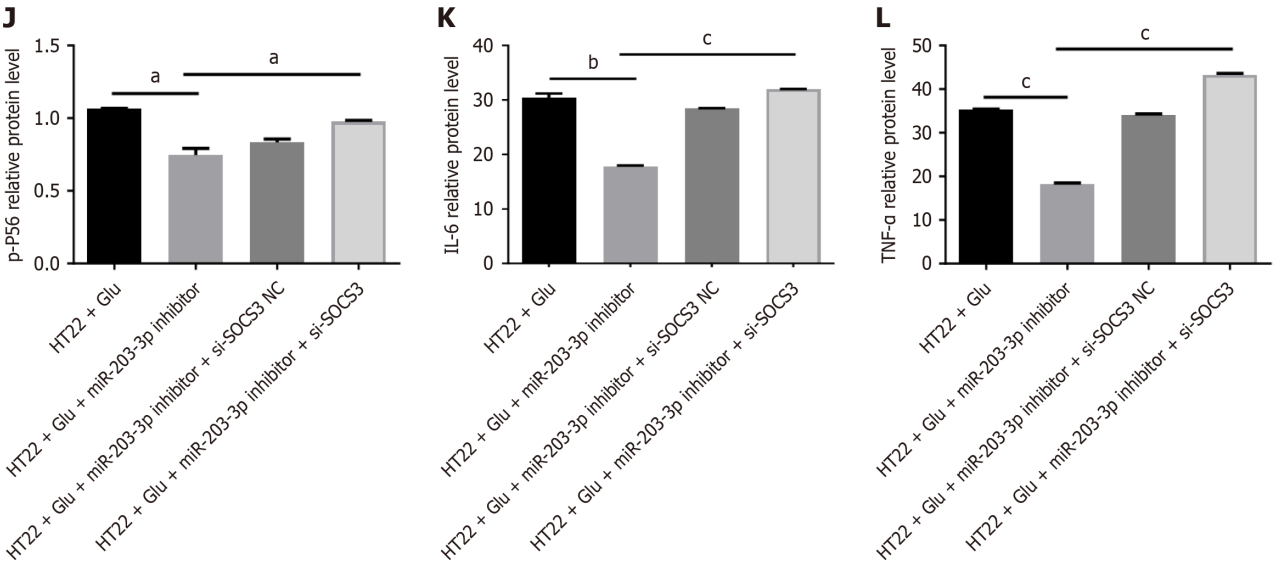

Figure 5 Downregulation of miR-203-3p and suppression of cytokine signaling 3 can reinstate an inflammatory phenotype. A: Schematic representation of the experimental design of HT22 cells co-transfected with the miR-203-3p inhibitor and si-suppression of cytokine signaling 3 (SOCS3) or si-NC; B: Quantitative polymerase chain reaction analysis of *SOCS3* mRNA expression in HT22 cells following co-transfection; C and D: Western blot analysis of SOCS3 protein levels in HT22 cells under the same conditions as Figure 5C; E-J: Western blot analysis of nuclear factor kappaB pathway markers in HT22 cells co-transfected with miR-203-3p inhibitor and si-SOCS3 or si-NC; K and L: Enzyme-linked immunosorbent assay measurements of interleukin-6 and tumor necrosis factor-α levels in the supernatant of HT22 cells co-transfected as in Figure 5C. Data are presented as mean ± SEM of three independent experiments. $^{a}P < 0.05$, $^{b}P < 0.01$, $^{c}P < 0.001$, NS: No significance. SOCS3: Suppression of cytokine signaling 3; IKKα/β: Inhibitor of kappa B kinase alpha/beta; p-IKKα/β: Phospho-inhibitor of kappa B kinase alpha/beta; IKBα: Nuclear factor kappaB inhibitor alpha; p-IKBα: Phospho-nuclear factor kappaB inhibitor alpha; TNF-α: Tumor necrosis factor-α; IL-6: Interleukin-6.

DISCUSSION

Our study revealed significant upregulation of exosomal miR-203 in BMSCs derived from epileptic mice. This finding suggests a potential role for miR-203 in the pathogenesis of TLE. The increased levels of miR-203 in exosomes from epileptic mice may be a response to ongoing neuroinflammatory processes in the brain. However, the role of miR-203 in epilepsy is poorly understood. Our findings indicated that miR-203 may serve as a critical regulator of the neuroinflammatory response associated with TLE. Similar to the work of Wang *et al*[15], circulating exosomal miRNAs have been identified as potential biomarkers in the diagnosis and treatment of DRE. The differential expression of miR-203 in BMSC-derived exosomes from epileptic mice compared to controls highlights its potential as a novel biomarker for epilepsy, a concept also supported by García-Gracia *et al*[14] and Jeppesen *et al*[30].

Our data demonstrate that exosomal miR-203 from BMSCs can be internalized by hippocampal neurons, leading to the downregulation of SOCS3 and subsequent activation of the NF-κB pathway. This pathway is well-known for its pro-inflammatory effects, which can exacerbate the neuroinflammatory state in TLE. This is in line with the findings of Xian *et al*[31], who showed that NF-κB activation is a key mediator of the neuroinflammatory processes of epilepsy. The enhanced secretion of pro-inflammatory cytokines, such as TNF-α and IL-6, following the uptake of exosomal miR-203 by hippocampal neurons, underscores the significant impact of neuroinflammation in the progression of epilepsy. This finding is consistent with the growing body of evidence that implicates neuroinflammation as a key factor in the pathophysiology of epilepsy[32,33].

Exosomes have emerged as important mediators of intercellular communication, particularly in neurodegenerative diseases. Our study adds to this body of knowledge by showing that exosomes can transfer miR-203 from BMSCs to neurons, thereby modulating the neuroinflammatory responses in epilepsy. This is supported by the work of Cui *et al*[34], who demonstrated the transfer of miRNAs *via* exosomes in a mouse model of Alzheimer's disease. The modulate expression of miR-203 is a promising therapeutic strategy for epilepsy treatment. Targeting miR-203 could reduce the neuroinflammatory response and improve outcomes in patients with DRE, as suggested by the therapeutic potential of miRNAs discussed by Dixit *et al*[35] and Boileau *et al*[36].

Although previous studies have explored the role of miRNAs in epilepsy, the focus on miR-203 and its specific role in modulating the SOCS3/NF-κB pathway is novel. Our findings expand the current understanding of the miRNA-mediated regulation of epilepsy and highlight the potential of exosome-based therapies. This aligns with the innovative approach adopted by Wang *et al*[37] in their study of exosomal miRNAs in a stroke model. One limitation of our study is the use of a single animal model and the need for further validation in human studies. Future research should investigate the long-term effects of miR-203 modulation and explore the potential of exosomal miR-203 as a therapeutic agent in clinical trials, as recommended by Batrakova and Kim[38] in their review on the translational potential of exosome research. Another limitation is the lack of additional experiments to comprehensively analyze potential treatments and their safety. Although our study provides preliminary evidence of miR-203's involvement in neuroinflammation, it does not fully explore the therapeutic effects of targeting miR-203. Future studies should include *in vivo* experiments to assess

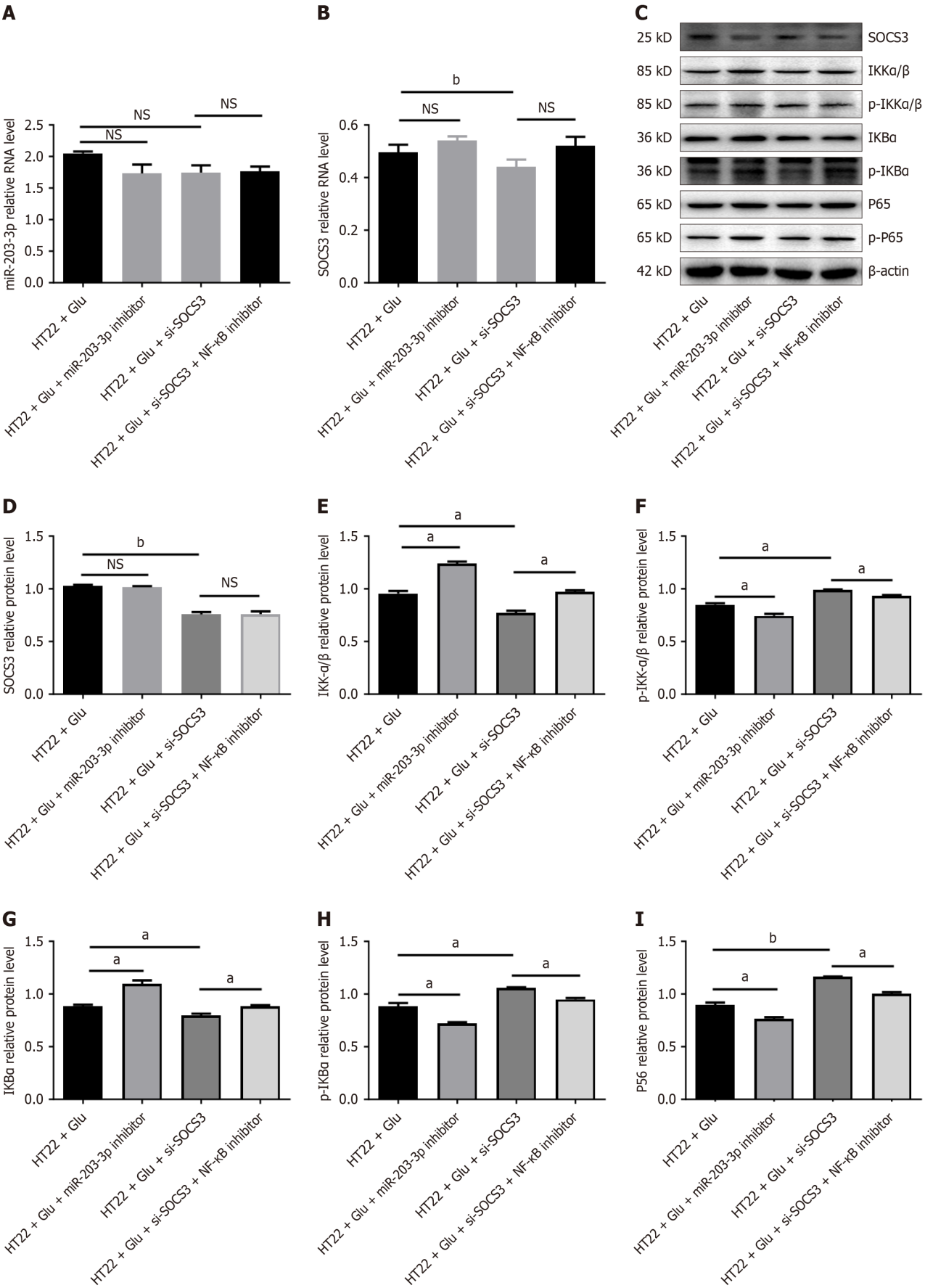
A
miR-203-3p relative RNA level
NS
NS
NS
B
SOCS3 relative RNA level
b
NS
NS
C
25 kD
85 kD
85 kD
36 kD
36 kD
65 kD
65 kD
42 kD
SOCS3
IKKα/β
p-IKKα/β
IKBα
p-IKBα
P65
p-P65
β-actin
D
SOCS3 relative protein level
b
NS
NS
E
IKK-α/β relative protein level
a
a
a
F
p-IKK-α/β relative protein level
a
a
a
G
IKBα relative protein level
a
a
a
H
p-IKBα relative protein level
a
a
a
I
P56 relative protein level
b
a
a
HT22 + Glu
HT22 + Glu + miR-203-3p inhibitor
HT22 + Glu + si-SOCS3
HT22 + Glu + si-SOCS3 + NF-κB inhibitor

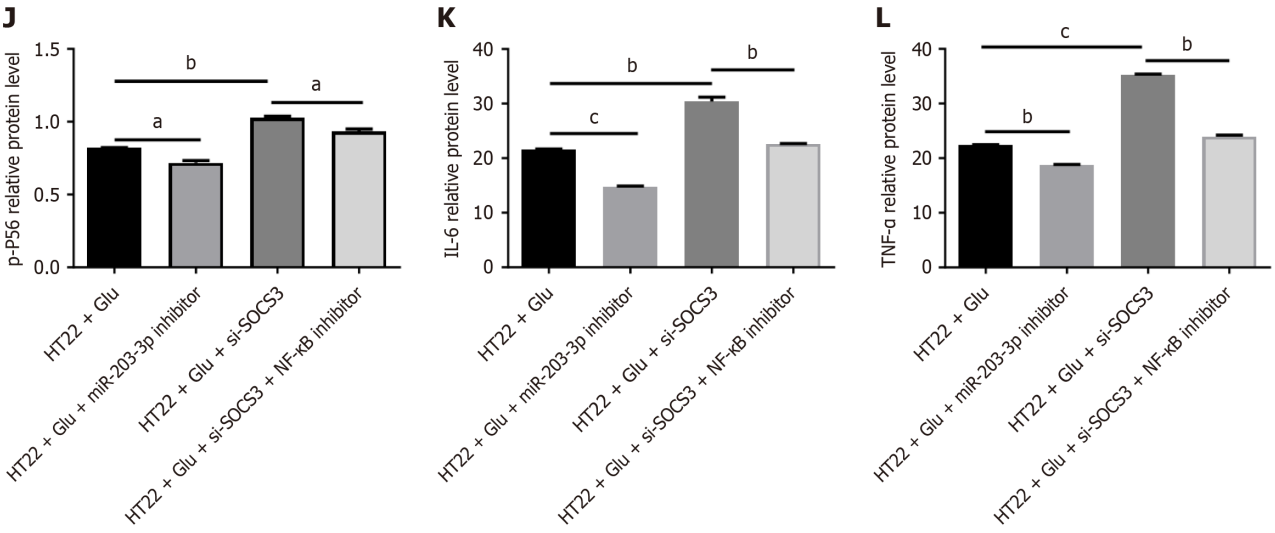

Figure 6 Inhibition of the target gene suppression of cytokine signaling 3 can activate the nuclear factor kappaB pathway and promote neuroinflammation. A: Schematic representation of the experimental design for HT22 cells transfected with si-suppression of cytokine signaling 3 (SOCS3) or si-NC, with or without nuclear factor kappaB pathway inhibitor treatment; B: Quantitative polymerase chain reaction analysis of *SOCS3* mRNA expression in HT22 cells after transfection; C-J: Western blot analysis of SOCS3 protein levels and nuclear factor kappaB pathway markers in HT22 cells under the same conditions as Figure 6C; K and L: Enzyme-linked immunosorbent assay measurements of interleukin-6 and tumor necrosis factor-α levels in the supernatant of HT22 cells treated as in Figure 6C. Data are presented as mean ± SEM of three independent experiments. $^{a}P < 0.05$, $^{b}P < 0.01$, $^{c}P < 0.001$, NS: No significance. SOCS3: Suppression of cytokine signaling 3; NF-κB: Nuclear factor kappaB; IKKα/β: Inhibitor of kappa B kinase alpha/beta; p-IKKα/β: Phospho-inhibitor of kappa B kinase alpha/beta; IKBα: Nuclear factor kappaB inhibitor alpha; p-IKBα: Phospho-nuclear factor kappaB inhibitor alpha; TNF-α: Tumor necrosis factor-α; IL-6: Interleukin-6.

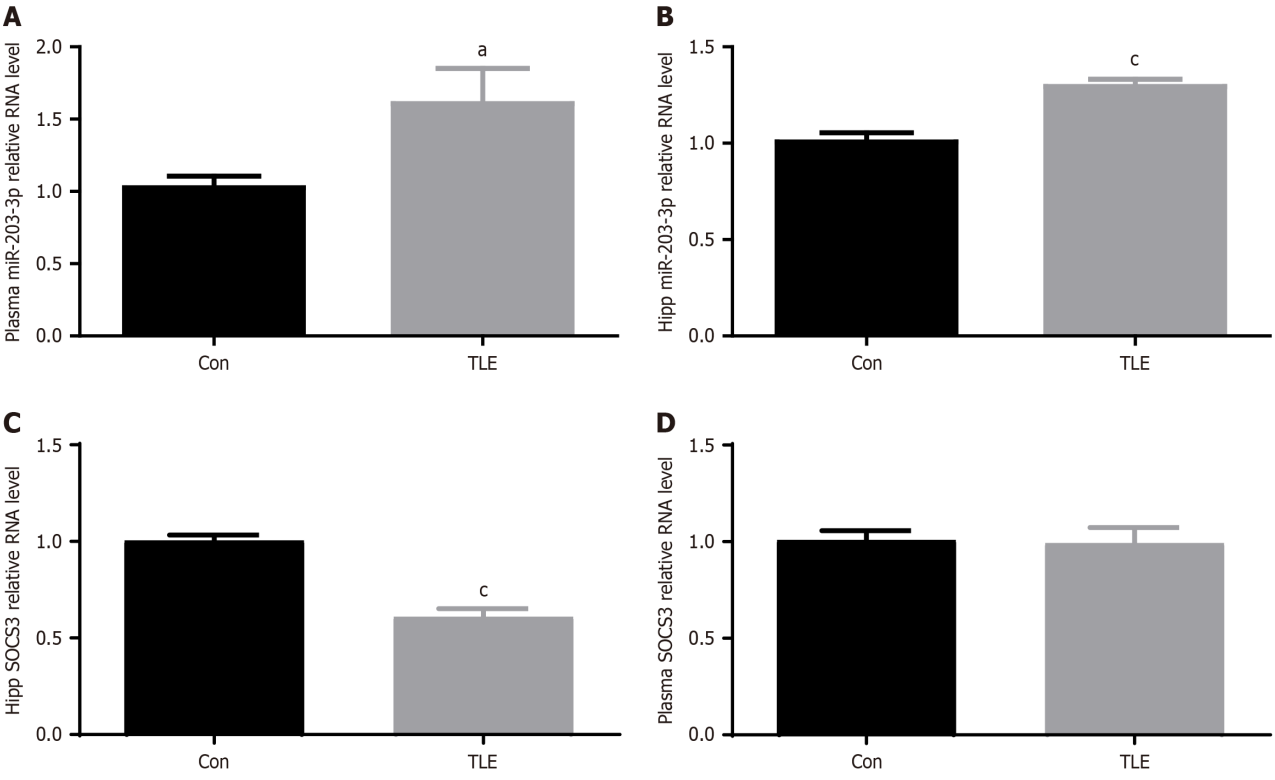

Figure 7 Differences between temporal lobe epilepsy mouse plasma and the expression of miR-203-3p and suppression of cytokine signaling 3 in the hippocampal region. A-D: Quantitative polymerase chain reaction analysis of miR-203-3p and suppression of cytokine signaling 3 mRNA expression in the plasma and hippocampal regions of the temporal lobe epilepsy model. $^{a}P < 0.05$, $^{c}P < 0.001$. TLE: Temporal lobe epilepsy.

the efficacy and safety of miR-203-targeting therapies in TLE models. This could involve the administration of miR-203 inhibitors or the delivery of exosomes engineered to modulate miR-203 levels, followed by monitoring of seizure frequency, severity, and duration, as well as evaluating any potential side effects on cognitive and behavioral functions.

CONCLUSION

The clinical implications of our findings are significant as they provide a basis for developing new therapeutic strategies for epilepsy. Targeting exosomal miR-203 could offer a noninvasive approach to modulate neuroinflammation and improve patient outcomes, particularly in patients with DRE. This is supported by the clinical studies by Gonçalves *et al* [39], who highlighted the importance of non-invasive biomarkers in epilepsy management. In conclusion, our study identifies exosomal miR-203 as a key regulator of neuroinflammation in a mouse model of epilepsy. Targeting miR-203 may offer a novel therapeutic strategy for epilepsy by modulating the SOCS3/NF-κB pathway, thus providing a potential avenue for the development of cell-free therapeutics.

FOOTNOTES

Author contributions: Wang W and Yin J conceived the project and jointly wrote the initial draft of the manuscript; Yin J collected and analyzed the data, and provided expert advice and revised the manuscript. All the authors contributed to this study and approved the submitted version.

Institutional animal care and use committee statement: All procedures involving animals were reviewed and approved by the Institutional Animal Care and Use Committee of the Second Affiliated Hospital of Dalian Medical University, IACUC protocol number: Protocol No. JL-WW2022120601.

Conflict-of-interest statement: All the authors report no relevant conflicts of interest for this article.

Data sharing statement: The original contributions presented in the study are included in the article. Further inquiries can be directed to the corresponding authors.

ARRIVE guidelines statement: The authors have read the ARRIVE Guidelines, and the manuscript was prepared and revised according to the ARRIVE Guidelines.

Country of origin: China

ORCID number: Wei Wang 0009-0002-9464-938X; Jian Yin 0009-0005-8426-957X.

S-Editor: Wang JJ
L-Editor: A
P-Editor: Zheng XM

REFERENCES

1 **Guekht A**, Brodie M, Secco M, Li S, Volkers N, Wiebe S. The road to a World Health Organization global action plan on epilepsy and other neurological disorders. *Epilepsia* 2021; **62**: 1057-1063 [PMID: 33675058 DOI: 10.1111/epi.16856]
2 **Moshé SL**, Perucca E, Ryvlin P, Tomson T. Epilepsy: new advances. *Lancet* 2015; **385**: 884-898 [PMID: 25260236 DOI: 10.1016/S0140-6736(14)60456-6]
3 **Tamula G**, Katyal R, Beniczky S, Nascimento FA. Focal cortical dysplasias: New advances for curing epilepsy. *Epileptic Disord* 2023; **25**: 284 [PMID: 37013259 DOI: 10.1002/epd2.20013]
4 **Karakis I**. Focal Cortical Dysplasias: New Advances for Curing Epilepsy. *J Clin Neurophysiol* 2023; **40**: e15-e16 [PMID: 38787749 DOI: 10.1097/WNP.0000000000000984]
5 **Kwan P**, Brodie MJ. Early identification of refractory epilepsy. *N Engl J Med* 2000; **342**: 314-319 [PMID: 10660394 DOI: 10.1056/NEJM200002033420503]
6 **Dwivedi R**, Ramanujam B, Chandra PS, Sapra S, Gulati S, Kalaivani M, Garg A, Bal CS, Tripathi M, Dwivedi SN, Sagar R, Sarkar C, Tripathi M. Surgery for Drug-Resistant Epilepsy in Children. *N Engl J Med* 2017; **377**: 1639-1647 [PMID: 29069568 DOI: 10.1056/NEJMoa1615335]
7 **O'Shea JJ**, Plenge R. JAK and STAT signaling molecules in immunoregulation and immune-mediated disease. *Immunity* 2012; **36**: 542-550 [PMID: 22520847 DOI: 10.1016/j.immuni.2012.03.014]
8 **Vezzani A**, French J, Bartfai T, Baram TZ. The role of inflammation in epilepsy. *Nat Rev Neurol* 2011; **7**: 31-40 [PMID: 21135885 DOI: 10.1038/nrneurol.2010.178]

9 **Tiwari D**, Peariso K, Gross C. MicroRNA-induced silencing in epilepsy: Opportunities and challenges for clinical application. *Dev Dyn* 2018; **247**: 94-110 [PMID: 28850760 DOI: 10.1002/dvdy.24582]

10 **Bohosova J**, Vajcner J, Jabandziev P, Oslejskova H, Slaby O, Aulicka S. MicroRNAs in the development of resistance to antiseizure drugs and their potential as biomarkers in pharmacoresistant epilepsy. *Epilepsia* 2021; **62**: 2573-2588 [PMID: 34486106 DOI: 10.1111/epi.17063]

11 **Ghafouri-Fard S**, Hussen BM, Abak A, Taheri M, Jalili Khoshnoud R. Aberrant expression of miRNAs in epilepsy. *Mol Biol Rep* 2022; **49**: 5057-5074 [PMID: 35088379 DOI: 10.1007/s11033-022-07188-5]

12 **Wang J**, Zhao J. MicroRNA Dysregulation in Epilepsy: From Pathogenetic Involvement to Diagnostic Biomarker and Therapeutic Agent Development. *Front Mol Neurosci* 2021; **14**: 650372 [PMID: 33776649 DOI: 10.3389/fnmol.2021.650372]

13 **Pusic AD**, Pusic KM, Clayton BL, Kraig RP. IFNγ-stimulated dendritic cell exosomes as a potential therapeutic for remyelination. *J Neuroimmunol* 2014; **266**: 12-23 [PMID: 24275061 DOI: 10.1016/j.jneuroim.2013.10.014]

14 **García-Gracia M**, Moreno-Martinez L, Hernaiz A, Usón S, Moral J, Sanz-Rubio D, Zaragoza P, Palacio J, Rosado B, Osta R, García-Belenguer S, Martín Burriel I. Analysis of Plasma-Derived Exosomal MicroRNAs as Potential Biomarkers for Canine Idiopathic Epilepsy. *Animals (Basel)* 2024; **14**: 252 [PMID: 38254420 DOI: 10.3390/ani14020252]

15 **Wang J**, Tan L, Tan L, Tian Y, Ma J, Tan CC, Wang HF, Liu Y, Tan MS, Jiang T, Yu JT. Circulating microRNAs are promising novel biomarkers for drug-resistant epilepsy. *Sci Rep* 2015; **5**: 10201 [PMID: 25984652 DOI: 10.1038/srep10201]

16 **Wang ZY**, Wen ZJ, Xu HM, Zhang Y, Zhang YF. Exosomal noncoding RNAs in central nervous system diseases: biological functions and potential clinical applications. *Front Mol Neurosci* 2022; **15**: 1004221 [PMID: 36438184 DOI: 10.3389/fnmol.2022.1004221]

17 **Moffatt CE**, Lamont RJ. Porphyromonas gingivalis induction of microRNA-203 expression controls suppressor of cytokine signaling 3 in gingival epithelial cells. *Infect Immun* 2011; **79**: 2632-2637 [PMID: 21536793 DOI: 10.1128/IAI.00082-11]

18 **Sawoo R**, Bishayi B. TLR4/TNFR1 blockade suppresses STAT1/STAT3 expression and increases SOCS3 expression in modulation of LPS-induced macrophage responses. *Immunobiology* 2024; **229**: 152840 [PMID: 39126792 DOI: 10.1016/j.imbio.2024.152840]

19 **Hebenstreit D**, Horejs-Hoeck J, Duschl A. JAK/STAT-dependent gene regulation by cytokines. *Drug News Perspect* 2005; **18**: 243-249 [PMID: 16034480 DOI: 10.1358/dnp.2005.18.4.908658]

20 **Navarro A**, Pairet S, Álvarez-Larrán A, Pons A, Ferrer G, Longarón R, Fernández-Rodríguez C, Camacho L, Monzó M, Besses C, Bellosillo B. miR-203 and miR-221 regulate SOCS1 and SOCS3 in essential thrombocythemia. *Blood Cancer J* 2016; **6**: e406 [PMID: 26990535 DOI: 10.1038/bcj.2016.10]

21 **Liu HP**, Zhang Y, Liu ZT, Qi H, Zheng XM, Qi LH, Wang JY. MiR-203 regulates proliferation and apoptosis of ovarian cancer cells by targeting SOCS3. *Eur Rev Med Pharmacol Sci* 2020; **24**: 7914 [PMID: 32767307 DOI: 10.26355/eurrev_202008_22448]

22 **Lin XM**, Chen H, Zhan XL. MiR-203 regulates JAK-STAT pathway in affecting pancreatic cancer cells proliferation and apoptosis by targeting SOCS3. *Eur Rev Med Pharmacol Sci* 2019; **23**: 6906-6913 [PMID: 31486490 DOI: 10.26355/eurrev_201908_18730]

23 **Pegtel DM**, Gould SJ. Exosomes. *Annu Rev Biochem* 2019; **88**: 487-514 [PMID: 31220978 DOI: 10.1146/annurev-biochem-013118-111902]

24 **Zhao S**, Mi Y, Guan B, Zheng B, Wei P, Gu Y, Zhang Z, Cai S, Xu Y, Li X, He X, Zhong X, Li G, Chen Z, Li D. Tumor-derived exosomal miR-934 induces macrophage M2 polarization to promote liver metastasis of colorectal cancer. *J Hematol Oncol* 2020; **13**: 156 [PMID: 33213490 DOI: 10.1186/s13045-020-00991-2]

25 **Terstappen GC**, Meyer AH, Bell RD, Zhang W. Strategies for delivering therapeutics across the blood-brain barrier. *Nat Rev Drug Discov* 2021; **20**: 362-383 [PMID: 33649582 DOI: 10.1038/s41573-021-00139-y]

26 **Rehman FU**, Liu Y, Zheng M, Shi B. Exosomes based strategies for brain drug delivery. *Biomaterials* 2023; **293**: 121949 [PMID: 36525706 DOI: 10.1016/j.biomaterials.2022.121949]

27 **Broekman ML**, Maas SLN, Abels ER, Mempel TR, Krichevsky AM, Breakefield XO. Multidimensional communication in the microenvirons of glioblastoma. *Nat Rev Neurol* 2018; **14**: 482-495 [PMID: 29985475 DOI: 10.1038/s41582-018-0025-8]

28 **Minghua W**, Zhijian G, Chahua H, Qiang L, Minxuan X, Luqiao W, Weifang Z, Peng L, Biming Z, Lingling Y, Zhenzhen W, Jianqing X, Huihui B, Xiaozhong W, Xiaoshu C. Plasma exosomes induced by remote ischaemic preconditioning attenuate myocardial ischaemia/reperfusion injury by transferring miR-24. *Cell Death Dis* 2018; **9**: 320 [PMID: 29476052 DOI: 10.1038/s41419-018-0274-x]

29 **Lu Q**, Qin H, Tan H, Wei C, Yang X, He J, Liang W, Li J. Senescence Osteoblast-Derived Exosome-Mediated miR-139-5p Regulates Endothelial Cell Functions. *Biomed Res Int* 2021; **2021**: 5576023 [PMID: 33954179 DOI: 10.1155/2021/5576023]

30 **Jeppesen DK**, Fenix AM, Franklin JL, Higginbotham JN, Zhang Q, Zimmerman LJ, Liebler DC, Ping J, Liu Q, Evans R, Fissell WH, Patton JG, Rome LH, Burnette DT, Coffey RJ. Reassessment of Exosome Composition. *Cell* 2019; **177**: 428-445.e18 [PMID: 30951670 DOI: 10.1016/j.cell.2019.02.029]

31 **Xian P**, Hei Y, Wang R, Wang T, Yang J, Li J, Di Z, Liu Z, Baskys A, Liu W, Wu S, Long Q. Mesenchymal stem cell-derived exosomes as a nanotherapeutic agent for amelioration of inflammation-induced astrocyte alterations in mice. *Theranostics* 2019; **9**: 5956-5975 [PMID: 31534531 DOI: 10.7150/thno.33872]

32 **Umpierre AD**, Li B, Ayasoufi K, Zhao S, Xie M, Thyen G, Hur B, Zheng J, Liang Y, Wu Z, Yu X, Sung J, Johnson AJ, Li Y, Wu LJ. Microglial P2Y(6) calcium signaling promotes phagocytosis and shapes neuroimmune responses in epileptogenesis. *bioRxiv* 2023 [PMID: 37398001 DOI: 10.1101/2023.06.12.544691]

33 **Liu C**, Zhao XM, Wang Q, Du TT, Zhang MX, Wang HZ, Li RP, Liang K, Gao Y, Zhou SY, Xue T, Zhang JG, Han CL, Shi L, Zhang LW, Meng FG. Astrocyte-derived SerpinA3N promotes neuroinflammation and epileptic seizures by activating the NF-κB signaling pathway in mice with temporal lobe epilepsy. *J Neuroinflammation* 2023; **20**: 161 [PMID: 37422673 DOI: 10.1186/s12974-023-02840-8]

34 **Cui GH**, Guo HD, Li H, Zhai Y, Gong ZB, Wu J, Liu JS, Dong YR, Hou SX, Liu JR. RVG-modified exosomes derived from mesenchymal stem cells rescue memory deficits by regulating inflammatory responses in a mouse model of Alzheimer's disease. *Immun Ageing* 2019; **16**: 10 [PMID: 31114624 DOI: 10.1186/s12979-019-0150-2]

35 **Dixit AB**, Tripathi M, Chandra PS, Banerjee J. Molecular biomarkers in drug-resistant epilepsy: Facts & possibilities. *Int J Surg* 2016; **36**: 483-491 [PMID: 26306771 DOI: 10.1016/j.ijsu.2015.08.029]

36 **Boileau C**, Deforges S, Peret A, Scavarda D, Bartolomei F, Giles A, Partouche N, Gautron J, Viotti J, Janowitz H, Penchet G, Marchal C, Lagarde S, Trebuchon A, Villeneuve N, Rumi J, Marissal T, Khazipov R, Khalilov I, Martineau F, Maréchal M, Lepine A, Milh M, Figarella-Branger D, Dougy E, Tong S, Appay R, Baudouin S, Mercer A, Smith JB, Danos O, Porter R, Mulle C, Crépel V. GluK2 Is a Target for Gene Therapy in Drug-Resistant Temporal Lobe Epilepsy. *Ann Neurol* 2023; **94**: 745-761 [PMID: 37341588 DOI: 10.1002/ana.26723]

37 **Wang Y**, Niu H, Li L, Han J, Liu Z, Chu M, Sha X, Zhao J. Anti-CHAC1 exosomes for nose-to-brain delivery of miR-760-3p in cerebral ischemia/reperfusion injury mice inhibiting neuron ferroptosis. *J Nanobiotechnology* 2023; **21**: 109 [PMID: 36967397 DOI:

10.1186/s12951-023-01862-x]

38 **Batrakova EV**, Kim MS. Using exosomes, naturally-equipped nanocarriers, for drug delivery. *J Control Release* 2015; **219**: 396-405 [PMID: 26241750 DOI: 10.1016/j.jconrel.2015.07.030]

39 **Gonçalves R**, Anderson TJ, Innocent G, Penderis J. Effect of seizures on cerebrospinal fluid analysis in dogs with idiopathic epilepsy. *Vet Rec* 2010; **166**: 497-498 [PMID: 20400742 DOI: 10.1136/vr.b4812]

World Journal of Stem Cells

Submit a Manuscript: https://www.f6publishing.com

World J Stem Cells 2025 February 26; 17(2): 102091

DOI: 10.4252/wjsc.v17.i2.102091

ISSN 1948-0210 (online)

ORIGINAL ARTICLE

Basic Study

Effect of adipose-derived stem cells exosomes cross-linked chitosan-αβ-glycerophosphate thermosensitive hydrogel on deep burn wounds

Lei Xu, Dan Liu, Hai-Long Yun, Wei Zhang, Li Ren, Wen-Wen Li, Chuan Han

Specialty type: Cell and tissue engineering

Provenance and peer review: Unsolicited article; Externally peer reviewed.

Peer-review model: Single blind

Peer-review report's classification

Scientific Quality: Grade C, Grade C

Novelty: Grade B, Grade B

Creativity or Innovation: Grade B, Grade B

Scientific Significance: Grade B, Grade B

P-Reviewer: Zhang ZY

Received: October 8, 2024

Revised: December 16, 2024

Accepted: February 7, 2025

Published online: February 26, 2025

Processing time: 138 Days and 16.9 Hours

Lei Xu, Hai-Long Yun, Department of Pathology, General Hospital of the Western Theater Command, Chengdu 610038, Sichuan Province, China

Dan Liu, Wei Zhang, Li Ren, Wen-Wen Li, Chuan Han, Department of Endocrinology, General Hospital of the Western Theater Command, Chengdu 610038, Sichuan Province, China

Co-first authors: Lei Xu and Dan Liu.

Corresponding author: Chuan Han, MD, Associate Chief Physician, Department of Endocrinology, General Hospital of the Western Theater Command, No. 270 Tianhui Road, Chengdu 610038, Sichuan Province, China. hanchuan3012005173@126.com

Abstract

BACKGROUND

Burn wound management is challenging, and while mesenchymal stem cell-derived exosomes show therapeutic potential, optimal delivery methods are unclear.

AIM

To study chitosan (CS)-αβ-glycerophosphate (CS-αβ-GP) hydrogel crosslinked with adipose-derived stem cell exosomes (ASC-Exos) for healing deep burn injuries.

METHODS

Rats with deep burn injuries were divided into the CS + ASCs-Exos group, the ASCs-Exos group, the CS group, and the control group. The healing rates on days 4, 7, and 14 after treatment were analyzed using ImageJ software. On day 14, the tissues were stained with hematoxylin and eosin staining, Masson's trichrome staining, and immunohistochemical analysis to evaluate tumor necrosis factor α, interleukin-6 (IL-6), IL-1α, IL-10, transforming growth factor β, and epidermal growth factor. The mRNA levels of IL-1α, CD86, C-C motif chemokine ligand 22, and CD163 were evaluated through quantitative polymerase chain reaction.

RESULTS

The CS + ASC-Exos group exhibited enhanced healing, reduced lymphocyte infiltration, blood vessels, and muscle fiber distribution. Increased IL-10, transforming

growth factor β, and epidermal growth factor and decreased tumor necrosis factor α, IL-1α, and IL-6 expression were observed. Quantitative polymerase chain reaction revealed reduced IL-1α and CD86 and increased C-C motif chemokine ligand 22 and CD163 expression. Protein analysis showed downregulation of phosphorylated inhibitor of kappa Balpha and P65 in the nuclear factor κB (NF-κB) pathway. ASC-Exos crosslinked with CS-αβ-GP hydrogel demonstrates superior effects in anti-inflammation, wound healing promotion, and promotion of M1 macrophage transformation to M2 macrophage by blocking the NF-κB pathway compared to ASC-Exos alone.

CONCLUSION

Our research demonstrates that the ASC-Exos cross-linked CS-αβ-GP hydrogel represents an advanced therapeutic approach for treating deep burn wounds. It has anti-inflammatory effects, promotes wound healing, and facilitates the transition of M1 macrophages to M2 macrophages by blocking the NF-κB pathway.

Key Words: Adipose-derived stem cells; Exosomes; Hydrogel; Burn; Wound healing

Core Tip: Studies indicate that the exosome hydrogel composite demonstrates exceptional efficacy in facilitating the healing of deep burn wounds and managing infection. It has anti-inflammatory effects, promotes wound healing, and facilitates the transition of M1 macrophages to M2 macrophages by blocking the nuclear factor κB pathway, thereby offering a novel strategy for the clinical utilization of mesenchymal stem cell-derived exosomes.

Citation: Xu L, Liu D, Yun HL, Zhang W, Ren L, Li WW, Han C. Effect of adipose-derived stem cells exosomes cross-linked chitosan-αβ-glycerophosphate thermosensitive hydrogel on deep burn wounds. *World J Stem Cells* 2025; 17(2): 102091
URL: https://www.wjgnet.com/1948-0210/full/v17/i2/102091.htm
DOI: https://dx.doi.org/10.4252/wjsc.v17.i2.102091

INTRODUCTION

In clinical practice, improving burn wound management remains a critical issue due to the increasing incidence of burns resulting from both natural disasters and human activities. Mesenchymal stem cell (MSC) derived exosomes (MSC-Exos), referred to as MSC-Exos, have emerged as a highly promising therapeutic modality for the management of chronic wounds, as revealed by recent developments in regenerative medicine and tissue engineering.

Extensive research has demonstrated that MSC-Exos can significantly enhance the healing of burn wounds, offering several advantages compared to MSCs alone. These benefits encompass superior safety profiles, increased storage stability, and simplified collection operations[1-3]. The present applications of MSC-Exos in wound repair predominantly depend on subcutaneous or intravenous delivery. But these methods have significant limitations due to rapid clearance and burst release patterns, which could potentially compromise their therapeutic efficacy across the complex stages of wound healing.

Several different delivery technologies, such as patches, injectable microcarriers, and hydrogels, are being investigated by researchers in order to solve these constraints. The goal of these systems is to preserve Exos function at wound sites while simultaneously enhancing both efficiency and safety[4-6]. Chitosan (CS) has demonstrated a great deal of promise among the many artificial injectable hydrogels that promote sustained Exo release and enhance local retention. This is mostly owing to the fact that it possesses natural antibacterial qualities and the capacity to maintain appropriate wound moisture[7]. This study seeks to evaluate if this approach serves as an optimal vehicle for MSC-Exos in burn wound healing applications.

MATERIALS AND METHODS

Isolation and culture of adipose-derived stem cells exosomes

Sprague Dawley rat adipose-derived stem cells (ASC) (product code: RASMD-01001) were obtained from OriCell with approval from the Ethics Committee (approval number: XBZQZYY2021-046). Cell culture was initiated by diluting 1 mL of cells in 9 mL basic medium, followed by centrifugation at 1000 rpm for 5 minutes. Following the removal of the supernatant, the cells were resuspended in 4 mL of medium supplemented with 10% serum and subsequently transferred to a 25T culture flask.

Cultures were maintained at 37 °C with 5% CO_2, with initial media change after 24 hours following confirmation of cell adherence. Cells were passaged at 90%-100% confluence using standard protocols. For passaging, cells were rinsed with phosphate buffered saline (PBS), detached, and split between new culture flasks supplemented with complete medium. For cryopreservation, cells showing optimal viability (approximately 70% density) were collected, centrifuged, and

resuspended in cryopreservation solution at a density of 5 × 10^6 cells/mL to 1 × 10^7 cells/mL. The cell suspension was divided between cryopreservation tubes, gradually frozen at -80 °C overnight, and transferred to liquid nitrogen for long-term storage.

Identification of ASC-Exos

Electron microscopy observation: The morphology of Exos was carefully analyzed using transmission electron microscopy, a powerful tool for examining nanoscale structures. Exo suspensions were first prepared by dissolving the Exos at a concentration of 0.5 g/L in PBS. To preserve the structural integrity of the Exos, the suspension was fixed with 2.5% glutaraldehyde, which stabilizes the particles by crosslinking proteins and other biomolecules. A 20-30 μL aliquot of the fixed Exo suspension was then applied to carbon-coated copper grids, which serve as a stable substrate for the Exos during imaging. These grids were briefly dried under an infrared lamp for 5 minutes to remove excess solution, ensuring that the sample adhered well to the surface.

The Exo samples were subsequently stained with 1% phosphotungstic acid at room temperature for 5 minutes. Phosphotungstic acid is commonly used as a negative stain to enhance contrast in electron microscopy, as it binds to the surface of the Exos and helps to highlight their structure. After staining, the samples were dried again for 10 minutes to remove any excess staining solution. The final samples were then carefully examined under a transmission electron microscope, which allowed for detailed observation of the Exo size, shape, and surface characteristics.

Western blot detection of protein expression level: Protein expression levels were assessed using western blotting, a widely used technique for detecting specific proteins within a complex mixture. The first step in the process involved lysing the samples in a buffer containing phenylmethylsulfonyl fluoride, a protease inhibitor, at a ratio of 100:1. The mixture was incubated on ice for 10-15 minutes to ensure complete lysis of the cells or Exos, followed by centrifugation at 12000 rpm for 10 minutes at 4 °C. This step allowed for the separation of cellular debris from the soluble proteins, with the supernatant containing the proteins of interest.

The protein solution was then heat-treated at 100 °C for 20 minutes with loading buffer to denature the proteins and break down any secondary structures, ensuring they were in their linear forms for electrophoresis. The samples were stored at -20 °C until further analysis. After electrophoresis, proteins were transferred to a membrane for immunostaining, where primary antibodies specific to the target proteins were used to bind to the proteins of interest. Secondary antibodies conjugated with an enzyme were then applied to facilitate detection. The results were quantified using ImageJ software, which allowed for precise measurement of the intensity of protein bands, enabling comparison of protein expression levels across different samples and treatment conditions.

Preparation of cross-linked ASC-Exos with CS-αβ-glycerophosphate hydrogel

The preparation of the cross-linked ASC-Exos hydrogel involved a careful synthesis process to ensure the successful incorporation of Exos into the hydrogel matrix. CS, a biopolymer with excellent biocompatibility and gelation properties, was first dissolved at a concentration of 2 g in 100 mL of acetic acid/sodium acetate buffer, adjusted to a pH of 4.6. CS has a degree of deacetylation of 75%, which contributes to its ability to form gels in specific conditions. The solution was filtered to remove any particulates and sterilized to ensure that the hydrogel would be safe for use in biological applications.

Next, the CS solution was cooled in an ice bath to prepare it for the addition of αβ-glycerophosphate (αβ-GP) (a gel-forming agent). A 50% weight/volume (W/V) αβ-GP solution was prepared separately and added dropwise to the chilled CS solution. The CS/αβ-GP ratio was carefully controlled at 8.8/1.2 to achieve the desired gel strength and thermosensitive properties. The mixture was kept in the ice bath for 20 minutes to promote the crosslinking process and to ensure a homogenous blend. The resulting hydrogel was then stored at 4 °C for further use.

To incorporate Exos into the hydrogel, ASC-Exos were added at a concentration of 1 g/L. This allowed for the controlled release of Exos upon application, providing sustained therapeutic effects at the wound site. The incorporation of Exos into the hydrogel matrix enhances the overall functionality of the system, allowing for both localized delivery and prolonged release of therapeutic Exos. The final formulation of the CS-αβ-GP hydrogel loaded with ASC-Exos is expected to offer a promising therapeutic strategy for wound healing, combining the advantages of biocompatible materials and bioactive molecules.

Characterization of CS-αβ-GP hydrogel

Porosity of the CS-αβ-GP hydrogel: The porosity of the hydrogel was calculated using the anhydrous ethanol displacement method by measuring the change in ethanol volume. Anhydrous ethanol was poured into a 50 mL volumetric flask, and the initial volume of ethanol (V0) was recorded. The dried hydrogel sample was immersed in anhydrous ethanol, and the volume of ethanol at this point was measured as V1. After removing the hydrogel sample from the ethanol, the remaining volume of ethanol was recorded as V2. Each sample was subjected to at least three replicate experiments, and the average was taken as the final porosity, as per the equation: Porosity = (V0 - V2)/(V1 - V2) × 100%.

The cumulative release rate of Exos after crosslinking the CS-αβ-GP hydrogel with ASC-Exos: A 200 μL hydrogel-Exos complex containing 200 μg of Exos was immersed in PBS solution at 37 °C. The supernatant was analyzed at 1, 2, 3, 4, 6, 8, 10, 12, 24, 36, and 72 hours using a BCA protein assay kit (Pierce, Rockford, IL, United States). The cumulative release rate of Exos = (amount in supernatant/initial amount in hydrogel) × 100%.

Rheological testing of CS-αβ-GP hydrogel: The elastic modulus (G') and viscous modulus (G'') of the samples were assessed utilizing a rotational rheometer (Physician MCR301, Anton Paar, Austria) across a temperature range of 10 °C to 50 °C to analyze their rheological characteristics.

Degradation rate of CS-αβ-GP hydrogel: The initial quantity of hydrogel, W0, was documented. The hydrogel was incubated in PBS solution for 72 hours, with its weight measured at 1, 2, 3, 4, 6, 8, 10, 12, 24, 36, and 72 hours, recorded as Wt. The degradation of the hydrogels in PBS was assessed over a period of 72 hours, as the equation: Degradation rate = (W0 - Wt)/W0 × 100%.

Establishment of deep second-degree burn model in rats

Based on previous literature and experience with animal sample sizes, 40 rats were purchased and divided into four groups with ten rats in each group[8]. The procedure began with anesthesia using intravenous thiopental sodium (40 mg/kg), administered through the tail vein to ensure the rats were fully sedated. The fur on the rats' backs was then shaved to expose the skin for the burn induction. To create the burn, 80 °C water was applied to the skin for 8 seconds, resulting in a burn wound with a diameter of 16 mm. After the burn was induced, sterile saline-soaked gauze was placed over the wound for 6 minutes to control immediate post-burn effects and minimize thermal damage. Once the burn was established, the rats were assigned to one of four groups for further treatment: Group A (CS + ASC-Exos), which received the application of a cross-linked hydrogel containing 200 μg of Exos; group B (ASC-Exos), which received 200 μg of Exos in 200 μL of PBS; group C (CS), which received the equivalent volume of the hydrogel without Exos; and group D (control), which received only a standard transparent dressing. All groups had their dressings changed every two days during the study period to maintain a controlled healing environment.

Assessment of wound healing

Wound healing progression was evaluated using standardized digital photography and quantitative analysis. Images were captured immediately post-injury and at designated timepoints (4, 7, and 14 days) across all treatment groups. Wound areas were precisely measured using ImageJ software calibrated with a standardized scale marker in each image. The healing rate was calculated using the formula: Wound healing rate = (1 - unhealed wound area/original wound area) × 100%.

Pathological assessment of wound healing

After the 14-day treatment period, full-thickness tissue samples were collected from both the wound sites and corresponding uninjured areas, which served as internal controls. The tissue specimens were processed by first fixing them in 40 g/L paraformaldehyde solution at room temperature for 24 hours. Subsequent to fixation, the samples were subjected to a dehydration procedure utilising graded alcohols, after which they were embedded in paraffin. Subsequent to this, serial sections with a thickness of 4 μm were generated utilising a rotary microtome.

The histological analysis involved staining protocols to evaluate tissue characteristics. Hematoxylin and eosin staining was used to assess the cellular architecture and inflammatory infiltrate, while Masson's Trichrome staining allowed for the evaluation of collagen deposition and organization. To ensure quantitative analysis, inflammatory cell infiltration was assessed by counting the lymphocytes per high-power field using ImageJ software. Additionally, the collagen volume fraction (CVF) was calculated by digitally analyzing Masson's stained sections using standardized thresholding methods.

Immunohistochemical assessment of wound

Immunohistochemical analysis was employed to evaluate the expression of pro-inflammatory markers at the wound site. Specific markers such as tumor necrosis factor α (TNF-α), interleukin-6 (IL-6), and other cytokines were assessed to determine the inflammatory status of the wound. These markers are crucial for understanding the immune response and inflammation dynamics during the healing process, as they play significant roles in the regulation of tissue repair and regeneration. By quantifying these markers, the study aimed to assess the effect of the different treatments on modulating inflammation and promoting tissue regeneration.

Gene expression detection by quantitative polymerase chain reaction

Macrophage polarization was assessed by analyzing the mRNA expression of key markers for M1 and M2 macrophages from wound tissues collected on day 14. To evaluate the polarization of macrophages, we focused on pro-inflammatory M1 markers, such as IL-1α and CD86, which are associated with the promotion of inflammation and tissue damage, and anti-inflammatory M2 markers, including C-C motif chemokine ligand 22 (CCL22) and CD163, which play a role in tissue repair and resolution of inflammation. RNA was extracted from the wound tissues of rats in the different treatment groups and analyzed using quantitative polymerase chain reaction. The expression levels of the selected markers were normalized to GAPDH as a housekeeping gene to account for any variations in RNA quantity and quality across the samples. This normalization allowed for a precise comparison of M1 and M2 polarization between the treatment groups.

Statistical analysis

Statistical analyses were conducted utilising SPSS Statistics (version 22.0; IBM, Armonk, NY, United States) and GraphPad Prism (version 8.0, San Diego, CA, United States). One-way analysis of variance (ANOVA) accompanied by Bonferroni's test was employed to assess the differences among groups. All experimental outcomes are shown as mean ± SD. Statistical significance was established at $P < 0.05$.

RESULTS

Characterization of ASC-Exos and the CS-αβ-GP hydrogel

Comprehensive biophysical characterization confirmed the successful isolation and purification of ASC-Exos. Transmission electron microscopy analysis revealed distinctive nanostructures exhibiting characteristic morphology of extracellular vesicles. These vesicular structures displayed the expected double-membrane architecture with diameters consistently falling within the 30-150 nm range typical of Exos (Figure 1A). Molecular analysis through western blotting confirmed the presence of canonical Exo surface markers, including strong expression of CD9, CD63, and CD81 proteins, validating the identity and purity of the isolated vesicles (Figure 1B).

The physical and mechanical properties of the CS-αβ-GP hydrogel were comprehensively evaluated through various characterization methods. As shown in Figure 1C, the porosity of the CS-αβ-GP thermosensitive hydrogel is significantly higher than that of the CS hydrogel, suggesting that the CS-αβ-GP thermosensitive hydrogel is more suitable for cell adhesion and growth compared to the CS hydrogel. As illustrated in Figure 1D, after crosslinking ASCs-Exos with the CS-αβ-GP thermosensitive hydrogel, the cumulative release rate of exosomes reached only about 70% after 24 hours, indicating that this material is suitable for the sustained release of ASCs-Exos. As shown in Figure 1E, the G′ and G′′ values of the CS-αβ-GP thermosensitive hydrogel rapidly increased at temperatures 30 °C and 40 °C, completing the sol-gel transition process at 37 °C. The results indicate that the CS-αβ-GP thermosensitive hydrogel possesses a phase transition temperature that is well-suited for wound administration. An effective wound dressing needs to have a certain degree of degradability. As depicted in Figure 1F, the weight of the CS-αβ-GP thermosensitive hydrogel decreased to about 40% after 72 hours, demonstrating its degradability.

Enhancing wound healing in deep burn injuries in rats through the cross-linking of ASC-Exos with the CS-αβ-GP hydrogel

To establish therapeutic efficacy, we evaluated the Exos hydrogel composite in a rat burn model. As depicted in Figure 2, the CS + ASC-Exos group demonstrated superior healing kinetics, with significant acceleration beginning on day 4 and continuing to show improved outcomes through day 14 compared to other groups. This enhanced performance validates the Exos hydrogel composite's therapeutic potential.

Mitigating inflammation of wound following cross-linking of ASC-Exos with CS-αβ-GP hydrogel

Histological analysis was conducted on full-thickness skin samples obtained after 14 days of treatment, with normal tissue used as a control for comparison. As depicted in Figure 3A, hematoxylin and eosin staining revealed significant differences between the treatment groups. The CS + ASC-Exos group demonstrated notably reduced lymphocyte infiltration and blood vessel density in the wound area compared to the other groups. This indicates that the Exo-loaded hydrogel effectively controlled inflammation, reducing the cellular inflammatory response and promoting a more favorable wound healing environment.

As shown in Figure 3B, Masson's Trichrome staining revealed that, in the CS + ASC-Exos group, after 14 days, normal tissue exhibited a small amount of collagen fibers interspersed between the abundant muscle fibers. In the wound tissue, the amount and distribution of collagen and muscle fibers were consistent with those in the normal tissues under a microscope. This suggests that the Exo-loaded hydrogel facilitated tissue regeneration by promoting a well-organized matrix that resembled the natural tissue structure. The collagen deposition was well-structured, contributing to improved tissue integrity and function. The lower CVF observed in the CS + ASC-Exos group suggests that the treatment promoted better wound healing with reduced scar formation.

Immunohistochemical analysis of important inflammatory markers confirmed that CS + ASC-Exos treatment affects wound healing. In the CS + ASC-Exos group, anti-inflammatory and growth factors including IL-10, transforming growth factor β, and epidermal growth factor were upregulated, whereas pro-inflammatory cytokines like TNF-α, IL-1α, and IL-6 were considerably decreased. These data suggest that CS + ASC-Exos treatment promotes tissue regeneration and regulates inflammation to improve wound healing (Figure 3C).

After crosslinking with CS-αβ-GP hydrogel, ASC-Exos facilitate the conversion of M1 to M2 macrophages by blocking the nuclear factor κB pathway

The CS + ASC-Exos therapy drastically affected macrophage polarization, as indicated by alterations in the expression of essential macrophage markers. As depicted in Figure 4A, the therapy group exhibited a significant reduction in the pro-inflammatory M1 markers IL-1α and CD86, which are commonly linked to inflammation and tissue damage. Concurrently, M2 macrophage markers CCL22 and CD163 were increased, signifying a transition towards an anti-inflammatory phenotype that facilitates tissue repair and regeneration. This shift in macrophage polarization indicates that CS + ASC-Exos therapy not only diminishes inflammation but also promotes a more conducive wound healing environment by facilitating macrophage polarization towards the M2 phenotype.

To investigate the immunomodulatory effect of Exos hydrogel composite, nuclear factor κB (NF-κB) inflammatory pathway protein levels were assessed. Figure 4B and C demonstrate that the CS + ASC-Exos group had considerably lower p-inhibitor of kappa Balpha (p-IκBα) protein expression relative to other treatment groups. A significant decrease in p-P65 protein levels in the inflammatory NF-κB pathway was seen in the CS + ASC-Exos group. The study found that CS + ASC-Exos can modulate macrophage polarisation from M1 to M2 by blocking the NF-κB pathway.

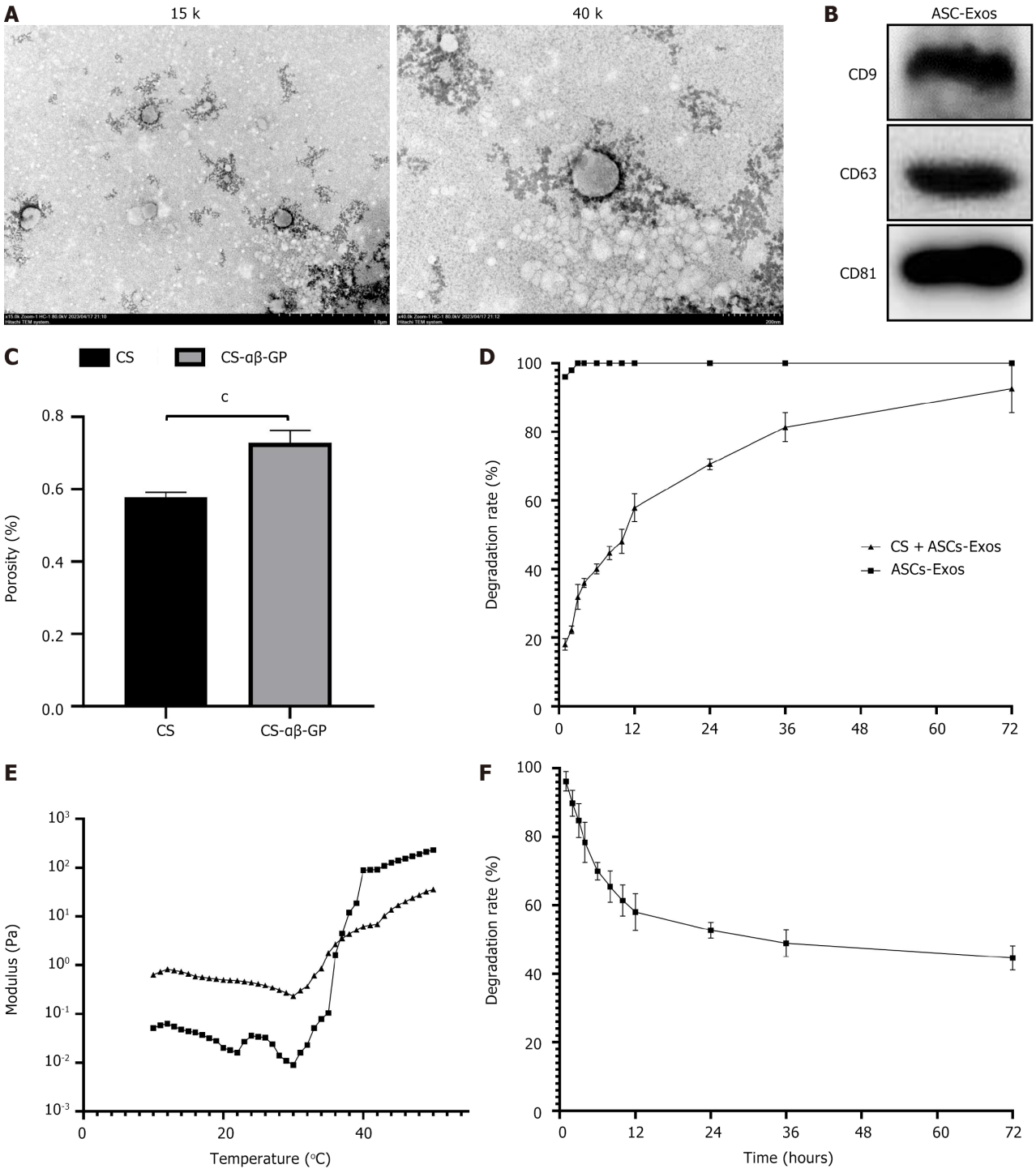

Figure 1 Physical characterization of adipose-derived stem cell exosomes and chitosan-αβ-glycerophosphate hydrogel. A: Electron microscopy showing vesicle-like structures (30-150 nm) with double-concave bilayer membranes at 15 k and 40 k magnification; B: Western blot confirmation of exosome markers CD9, CD63, and CD81; C: Enhanced porosity of chitosan-αβ-glycerophosphate hydrogel *vs* chitosan hydrogel; D: Temporal release profile of cross-linked *vs* non-cross-linked adipose-derived stem cell exosomes; E: Temperature-dependent storage (G') and loss (G'') moduli; F: *In vitro* degradation profile. $^{c}P < 0.001$. ASC-Exos: Adipose-derived stem cell exosomes; CS: Chitosan; CS-αβ-GP: Chitosan-αβ-glycerophosphate.

DISCUSSION

MSCs are multipotent progenitor cells capable of differentiating into many cell types under specific conditions. Approximately 5000 ASCs can be obtained from one gramme of adipose tissue. Despite the existence of various sources of MSCs, ASCs have attracted significant interest due to their availability and yield[8]. Research has shown that MSCs respond to tissue damage by migrating to affected regions and engaging with the immune and inflammatory systems throughout their presence there[9]. MSCs release beneficial chemicals *via* paracrine pathways, facilitating wound repair and tissue regeneration in response to inflammatory conditions[9].

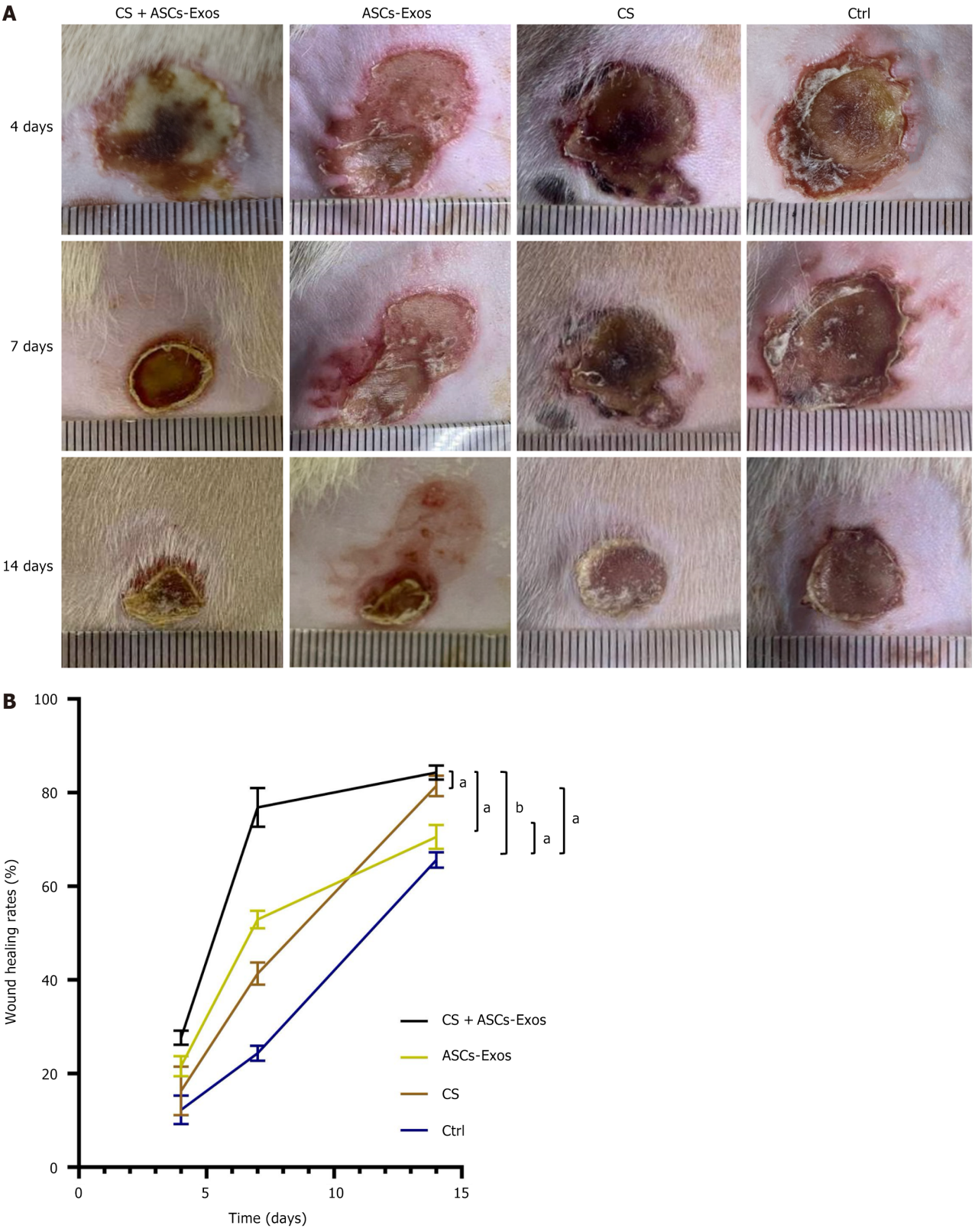

Figure 2 The effect of chitosan-αβ-glycerophosphate hydrogel crosslinked with adipose-derived stem cell exosomes on the healing rate of deep burn wounds in rats. A: Wound healing images of the four groups at 4, 7, and 14 days after wound treatment; B: Wound healing rates (%) of the four groups at 4, 7, and 14 days after wound treatment. $^{a}P < 0.05$, $^{b}P < 0.01$. ASC-Exos: Adipose-derived stem cell exosomes; CS: Chitosan.

When it comes to therapeutic applications, however, MSCs encounter a number of hurdles, such as the potential for tumorigenicity, concerns over immunological rejection, and complex storage needs. MSC-Exos have a number of advantages over their parent cells, including the following: (1) High stability: Despite being approximately one millionth the size of Exos are able to sustain their activity even when stored for an extended period of time at a temperature of -80 degrees Celsius[1]; (2) Efficient production: Each MSC has the ability to generate thousands of Exos, which can be

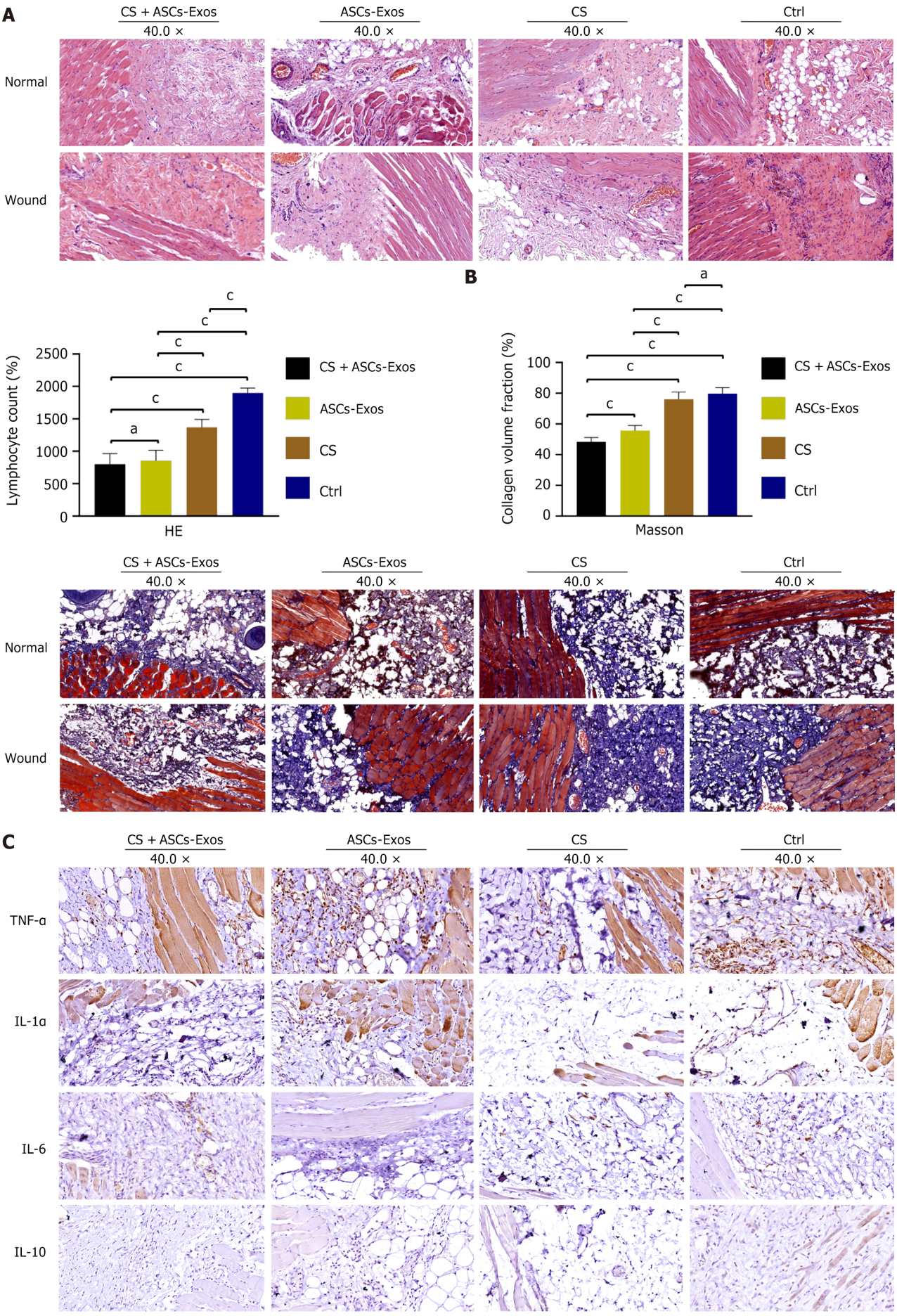
A
CS + ASCs-Exos
ASCs-Exos
CS
Ctrl
40.0 ×
Normal
Wound
B
Lymphocyte count (%)
HE
Collagen volume fraction (%)
Masson
CS + ASCs-Exos
ASCs-Exos
CS
Ctrl
C
TNF-α
IL-1α
IL-6
IL-10

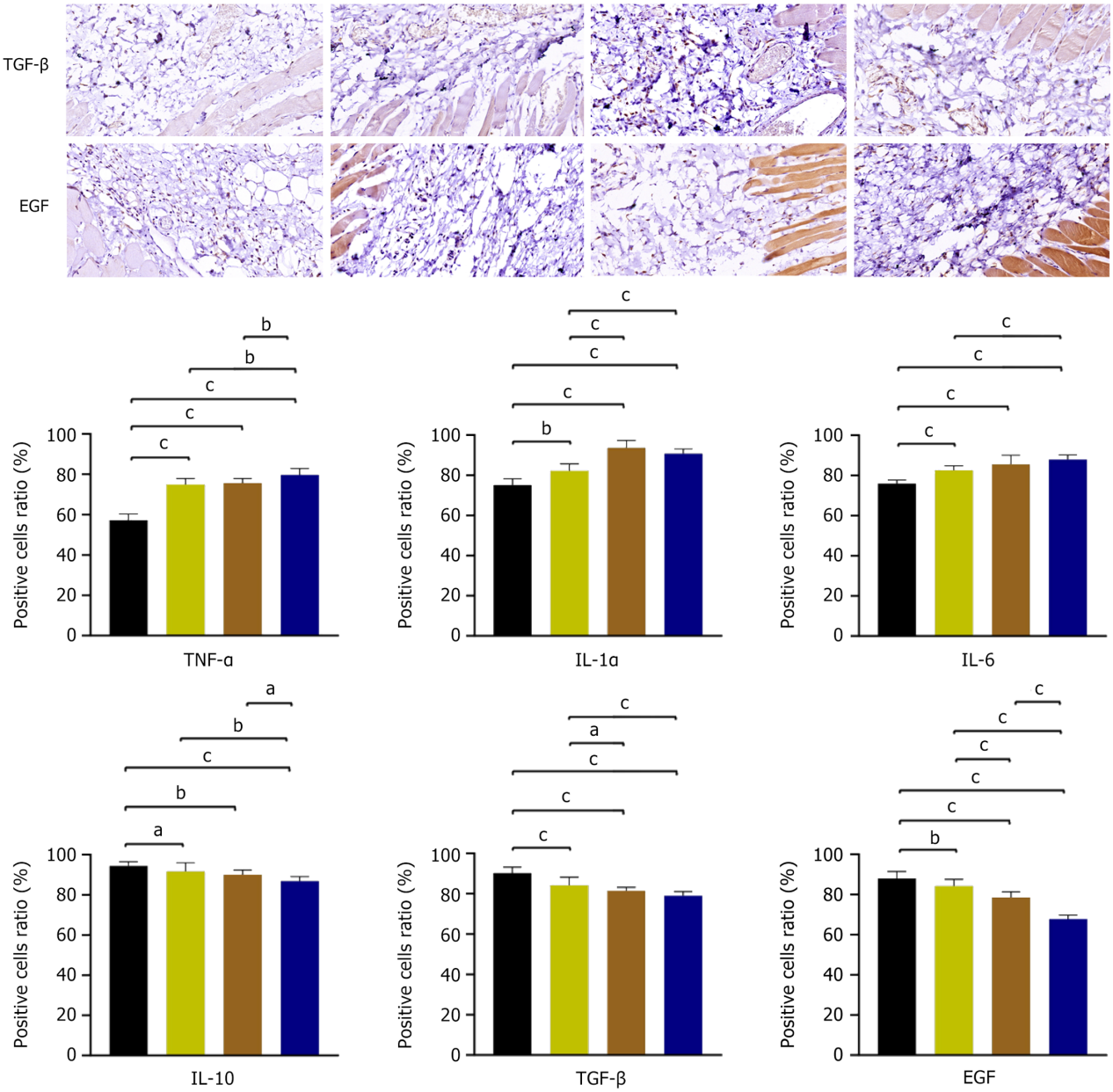

Figure 3 Histological and immunohistochemical analysis of wound healing. A: Hematoxylin and eosin: Chitosan (CS) + adipose-derived stem cell exosomes (ASC-Exos) treatment reduced lymphocyte infiltration and vascular density compared to normal tissue. ASC-Exos alone showed similar effects but with prominent glands. CS group displayed increased smooth muscle, fibroblasts, and vascular structures. Control group exhibited extensive fibroblast presence, disorganized vasculature, and marked lymphocyte infiltration; B: Masson: CS+ASC-Exos: In the wound, numerous muscle fibers are interspersed with a small amount of collagen fibers, and the quantity and distribution of collagen fibers and muscle fibers are consistent with those in normal tissue. ASC-Exos group showed mild collagen increase. CS and control groups demonstrated excessive collagen deposition and muscle fiber formation. Collagen volume fraction was significantly lower in CS + ASC-Exos group; C: Immunohistochemical: CS + ASC-Exos group showed elevated interleukin (IL)-10, transforming growth factor-β, and epidermal growth factor expression, with reduced tumor necrosis factor-α, IL-1α, and IL-6 levels compared to other groups. $^{a}P < 0.05$, $^{b}P < 0.01$, $^{c}P < 0.001$. ASC-Exos: Adipose-derived stem cell exosomes; CS: Chitosan; TNF: Tumor necrosis factor; IL: Interleukin; TGF: Transforming growth factor; EGF: Epidermal growth factor.

recovered using conventional techniques such as ultracentrifugation[2]; and (3) Safety: Exos have a low membrane-bound protein content and are non-proliferative, which means that they have small risk of immune rejection or tumour formation[3]. This is one of the reasons why their safety profile has been enhanced.

According to the findings of a number of studies, MSC-Exos are effective in the process of wound healing. Zhang *et al* [10] demonstrated that induced pluripotent stem cell-MSC-Exos sped up the process of epithelial reconstruction, decreased the width of scars, and enhanced collagen maturation while simultaneously stimulating angiogenesis. Similarly, research conducted using umbilical cord-MSC-Exos showed their capacity to stimulate wound re-epithelial by activating the Wnt/β-catenin pathway[11]. Li *et al*[12] established that umbilical cord-MSC-Exos containing miR-181c could control inflammation by the Toll-like receptor 4 signaling pathway. Several studies explicitly focused on ASC-Exos have produced encouraging findings. In their study, Hu *et al*[13] proved that the treatment with ASC-Exos, either locally or systemically, enhanced fibroblast function and maximized collagen production. Using Wnt/β-catenin signaling, Ma *et al*[14] demonstrated that ASC-Exos could promote keratinocyte proliferation and migration while simultaneously

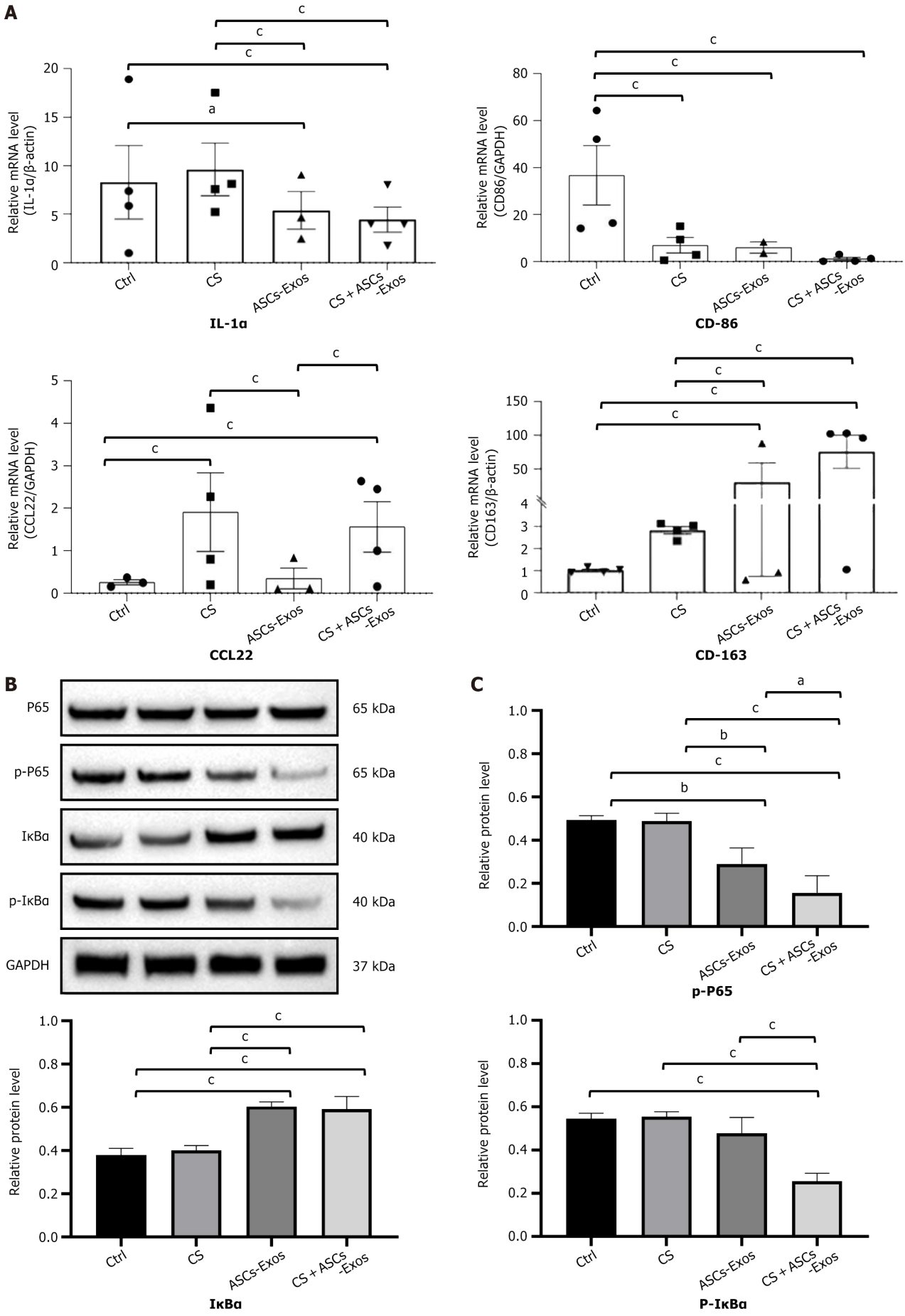

Figure 4 Impact of chitosan-αβ-glycerophosphate hydrogel cross-linked with adipose-derived stem cell exosome on wound macro-

phages. A: The expression of interleukin-1α and CD86 in the chitosan + adipose-derived stem cell exosomes group is lower compared to the control group, while the expression of C-C motif chemokine ligand 22 and CD163 is higher; B: Western blotting analysis of nuclear factor κB pathway-related protein expression; C: Quantification of nuclear factor κB pathway-related proteins. $^{a}P < 0.05$, $^{b}P < 0.01$, $^{c}P < 0.001$. ASC-Exos: Adipose-derived stem cell exosomes; CS: Chitosan; IL: Interleukin; CCL22: C-C motif chemokine ligand 22; IκBα: Inhibitor of kappa Balpha.

suppressing. It has also been widely examined how macrophage polarization plays a role, with M1 macrophages responsible for producing pro molecules and M2 macrophages responsible for secreting anti-inflammatory mediators [15]. By focusing on pknox1, He *et al*[16] demonstrated that bone marrow-MSC-Exos containing miR-223 could enhance M2 polarization.

MSC-Exos have shown significant potential in promoting burn wound healing, yet traditional delivery methods often face challenges, such as rapid clearance and burst release, which limit their effectiveness[17]. Recent advancements in injectable hydrogels have addressed these issues, offering a more controlled and sustained release, thereby enhancing the local retention of Exos and improving therapeutic outcomes. Among various hydrogel systems, CS-based hydrogels have garnered particular attention due to their intrinsic antibacterial properties, biocompatibility, and ability to maintain optimal moisture levels at wound sites, which are crucial for healing[7]. The CS-αβ-GP hydrogel, which exhibits temperature-dependent gelation and long-term stability at 4 °C, stands out as an excellent candidate for Exo delivery, providing a favorable environment for burn wound regeneration[18].

In our study, the CS + ASC-Exos hydrogel system demonstrated superior therapeutic efficacy. Notably, the system accelerated the healing process starting from day 4, with significantly better final healing rates at day 14 compared to the control groups. Histological analysis revealed that the CS + ASC-Exos treatment reduced inflammatory cell infiltration and vascularization, which suggests effective modulation of the inflammatory response. Moreover, the collagen and muscle fiber distribution in the wound area showed remarkable normalization, with the CVF notably lower in the CS + ASC-Exos group, indicating improved tissue regeneration and better scar formation outcomes.

The immunomodulatory effects of the CS + ASC-Exos system were also evident, as demonstrated by the increased expression of anti-inflammatory and growth factors, such as IL-10, transforming growth factor β, and epidermal growth factor. In contrast, pro-inflammatory markers, including TNF-α, IL-6, and IL-1α, were significantly reduced. Additionally, the treatment promoted macrophage polarization toward the anti-inflammatory M2 phenotype, evidenced by higher levels of M2 markers like CCL22 and CD163, while M1 markers such as IL-1α and CD86 were reduced. This shift in macrophage polarization suggests that the CS + ASC-Exos system not only accelerates wound healing but also plays a key role in regulating the inflammatory environment to favor tissue repair.

It has been reported that MSC-derived Exos contain a large number of active molecules, such as lipids, proteins, and microRNAs, especially miR-199a, which regulates the innate immune system by blocking factors in the NF-κB pathway [19-22]. Phosphorylated IκBα, a key regulatory factor in the NF-κB signaling pathway, positively regulates the expression of pro-inflammatory molecules[21,22]. Our study found that, compared to other treatment groups, the protein expression of p-IκBα was significantly downregulated in the CS + ASC-Exos group. Consistently, the protein level of the downstream molecule p-P65 in the inflammatory NF-κB pathway was significantly inhibited in the CS + ASC-Exos group. These findings confirm that the CS + ASC-Exos system can regulate the polarization of macrophages from M1 to M2 by blocking the NF-κB pathway, thereby promoting wound healing through enhanced anti-inflammatory effects.

However, while this study presents promising results, several aspects require further investigation to fully understand and optimize the therapeutic potential of this composite system. One key area for future research is the detailed examination of additional signaling pathways involved in wound healing and tissue regeneration. Identifying and targeting other relevant pathways could further enhance the effectiveness of the treatment. Another important area of exploration is the comprehensive analysis of the molecular components enriched in the ASC-Exos and their specific roles in tissue repair. Understanding which proteins, RNAs, and lipids contribute to the observed therapeutic effects will help refine Exo-based treatments and improve their clinical efficacy. Finally, clinical validation studies are essential to translate these promising results into real-world applications. These studies will provide critical insights into the safety, feasibility, and efficacy of the ASC-Exos-loaded hydrogel in human patients.

CONCLUSION

Our research demonstrates that the ASC-Exos cross-linked CS-αβ-GP hydrogel represents an advanced therapeutic approach for treating deep burn wounds. It has anti-inflammatory effects, promotes wound healing, and facilitates the transition of M1 macrophages to M2 macrophages by blocking the NF-κB pathway.

ACKNOWLEDGEMENTS

We thank Dr. Xian-Hui Li from the Department of Burns at the General Hospital of the Western Theater Command and Dr. Hao Yao from the Department of Hematology at the General Hospital of the Western Theater Command for their contributions to the study.

FOOTNOTES

Author contributions: Xu L and Liu D contributed equally to this study and as co-first authors. Xu L, Liu D, Zhang W, Ren L, Li WW, and Han C contributed to manuscript writing; Xu L and Yun HL were responsible for the preparation of figures; and all authors participated in the manuscript review.

Supported by the Incubation Program of the General Hospital of the Western Theater Command, No. 2021-XZYG-C29 and No. 2021-XZYG-B32.

Institutional animal care and use committee statement: The animal care and experimental protocols were approved by the Institutional Animal Care and Use Committee of the General Hospital of the Western Theater Command (Approval Number: XBZQZYY2021-046). The study was designed to minimize animal distress, and all rats were humanely euthanized using an overdose of barbiturate through intravenous injection of 150 mg/kg pentobarbital sodium for tissue collection, aligning with the committee's guidelines for ethical animal research. The committee ensures that all research involving animals adheres to the principles of the 3Rs (replacement, reduction, refinement) to minimize pain or discomfort. All efforts were made to ensure the welfare of the animals throughout the study, and the methods used for euthanasia were in strict accordance with the guidelines for humane endpoints.

Conflict-of-interest statement: All the authors report no relevant conflicts of interest for this article.

Data sharing statement: The datasets used and analyzed during the current study are available from the corresponding author upon reasonable request.

ARRIVE guidelines statement: The authors have read the ARRIVE guidelines, and the manuscript was prepared and revised according to the ARRIVE guidelines.

Country of origin: China

ORCID number: Chuan Han 0000-0002-0330-1082.

S-Editor: Wang JJ
L-Editor: A
P-Editor: Zhang XD

REFERENCES

1 **Yu B**, Zhang X, Li X. Exosomes derived from mesenchymal stem cells. *Int J Mol Sci* 2014; **15**: 4142-4157 [PMID: 24608926 DOI: 10.3390/ijms15034142]
2 **Mendt M**, Kamerkar S, Sugimoto H, McAndrews KM, Wu CC, Gagea M, Yang S, Blanko EVR, Peng Q, Ma X, Marszalek JR, Maitra A, Yee C, Rezvani K, Shpall E, LeBleu VS, Kalluri R. Generation and testing of clinical-grade exosomes for pancreatic cancer. *JCI Insight* 2018; **3**: e99263 [PMID: 29669940 DOI: 10.1172/jci.insight.99263]
3 **Marote A**, Teixeira FG, Mendes-Pinheiro B, Salgado AJ. MSCs-Derived Exosomes: Cell-Secreted Nanovesicles with Regenerative Potential. *Front Pharmacol* 2016; **7**: 231 [PMID: 27536241 DOI: 10.3389/fphar.2016.00231]
4 **Shi Q**, Qian Z, Liu D, Sun J, Wang X, Liu H, Xu J, Guo X. GMSC-Derived Exosomes Combined with a Chitosan/Silk Hydrogel Sponge Accelerates Wound Healing in a Diabetic Rat Skin Defect Model. *Front Physiol* 2017; **8**: 904 [PMID: 29163228 DOI: 10.3389/fphys.2017.00904]
5 **Shafei S**, Khanmohammadi M, Heidari R, Ghanbari H, Taghdiri Nooshabadi V, Farzamfar S, Akbariqomi M, Sanikhani NS, Absalan M, Tavoosidana G. Exosome loaded alginate hydrogel promotes tissue regeneration in full-thickness skin wounds: An in vivo study. *J Biomed Mater Res A* 2020; **108**: 545-556 [PMID: 31702867 DOI: 10.1002/jbm.a.36835]
6 **Mol EA**, Lei Z, Roefs MT, Bakker MH, Goumans MJ, Doevendans PA, Dankers PYW, Vader P, Sluijter JPG. Injectable Supramolecular Ureidopyrimidinone Hydrogels Provide Sustained Release of Extracellular Vesicle Therapeutics. *Adv Healthc Mater* 2019; **8**: e1900847 [PMID: 31559704 DOI: 10.1002/adhm.201900847]
7 **Goy RC**, Morais ST, Assis OB. Evaluation of the antimicrobial activity of chitosan and its quaternized derivative on E. coli and S. aureus growth. *Rev Bras Farmacogn* 2016; **26**: 122-127 [DOI: 10.1016/j.bjp.2015.09.010]
8 **Rangatchew F**, Vester-Glowinski P, Rasmussen BS, Haastrup E, Munthe-Fog L, Talman ML, Bonde C, Drzewiecki KT, Fischer-Nielsen A, Holmgaard R. Mesenchymal stem cell therapy of acute thermal burns: A systematic review of the effect on inflammation and wound healing. *Burns* 2021; **47**: 270-294 [PMID: 33218945 DOI: 10.1016/j.burns.2020.04.012]
9 **Tamama K**, Kerpedjieva SS. Acceleration of Wound Healing by Multiple Growth Factors and Cytokines Secreted from Multipotential Stromal Cells/Mesenchymal Stem Cells. *Adv Wound Care (New Rochelle)* 2012; **1**: 177-182 [PMID: 24527301 DOI: 10.1089/wound.2011.0296]
10 **Zhang J**, Guan J, Niu X, Hu G, Guo S, Li Q, Xie Z, Zhang C, Wang Y. Exosomes released from human induced pluripotent stem cells-derived MSCs facilitate cutaneous wound healing by promoting collagen synthesis and angiogenesis. *J Transl Med* 2015; **13**: 49 [PMID: 25638205 DOI: 10.1186/s12967-015-0417-0]

11 **Zhang B**, Wang M, Gong A, Zhang X, Wu X, Zhu Y, Shi H, Wu L, Zhu W, Qian H, Xu W. HucMSC-Exosome Mediated-Wnt4 Signaling Is Required for Cutaneous Wound Healing. *Stem Cells* 2015; **33**: 2158-2168 [PMID: 24964196 DOI: 10.1002/stem.1771]

12 **Li X**, Liu L, Yang J, Yu Y, Chai J, Wang L, Ma L, Yin H. Exosome Derived From Human Umbilical Cord Mesenchymal Stem Cell Mediates MiR-181c Attenuating Burn-induced Excessive Inflammation. *EBioMedicine* 2016; **8**: 72-82 [PMID: 27428420 DOI: 10.1016/j.ebiom.2016.04.030]

13 **Hu L**, Wang J, Zhou X, Xiong Z, Zhao J, Yu R, Huang F, Zhang H, Chen L. Exosomes derived from human adipose mensenchymal stem cells accelerates cutaneous wound healing *via* optimizing the characteristics of fibroblasts. *Sci Rep* 2016; **6**: 32993 [PMID: 27615560 DOI: 10.1038/srep32993]

14 **Ma T**, Fu B, Yang X, Xiao Y, Pan M. Adipose mesenchymal stem cell-derived exosomes promote cell proliferation, migration, and inhibit cell apoptosis *via* Wnt/β-catenin signaling in cutaneous wound healing. *J Cell Biochem* 2019; **120**: 10847-10854 [PMID: 30681184 DOI: 10.1002/jcb.28376]

15 **Xiu C**, Zheng H, Jiang M, Li J, Zhou Y, Mu L, Liu W. MSCs-Derived miR-150-5p-Expressing Exosomes Promote Skin Wound Healing by Activating PI3K/AKT Pathway through PTEN. *Int J Stem Cells* 2022; **15**: 359-371 [PMID: 35769052 DOI: 10.15283/ijsc21135]

16 **He X**, Dong Z, Cao Y, Wang H, Liu S, Liao L, Jin Y, Yuan L, Li B. MSC-Derived Exosome Promotes M2 Polarization and Enhances Cutaneous Wound Healing. *Stem Cells Int* 2019; **2019**: 7132708 [PMID: 31582986 DOI: 10.1155/2019/7132708]

17 **Yi H**, Wang Y, Yang Z, Xie Z. Efficacy assessment of mesenchymal stem cell transplantation for burn wounds in animals: a systematic review. *Stem Cell Res Ther* 2020; **11**: 372 [PMID: 32859266 DOI: 10.1186/s13287-020-01879-1]

18 **Zhou HY**, Chen XG, Kong M, Liu CS. Preparation of chitosan-based thermosensitive hydrogels for drug delivery. *J Appl Polym Sci* 2009; **112**: 1509-1515 [DOI: 10.1002/app.29721]

19 **Guan P**, Liu C, Xie D, Mao S, Ji Y, Lin Y, Chen Z, Wang Q, Fan L, Sun Y. Exosome-loaded extracellular matrix-mimic hydrogel with anti-inflammatory property Facilitates/promotes growth plate injury repair. *Bioact Mater* 2022; **10**: 145-158 [PMID: 34901536 DOI: 10.1016/j.bioactmat.2021.09.010]

20 **Fan L**, Liu C, Chen X, Zheng L, Zou Y, Wen H, Guan P, Lu F, Luo Y, Tan G, Yu P, Chen D, Deng C, Sun Y, Zhou L, Ning C. Exosomes-Loaded Electroconductive Hydrogel Synergistically Promotes Tissue Repair after Spinal Cord Injury *via* Immunoregulation and Enhancement of Myelinated Axon Growth. *Adv Sci (Weinh)* 2022; **9**: e2105586 [PMID: 35253394 DOI: 10.1002/advs.202105586]

21 **Yang Q**, Su S, Liu S, Yang S, Xu J, Zhong Y, Yang Y, Tian L, Tan Z, Wang J, Yu Z, Shi Z, Liang F. Exosomes-loaded electroconductive nerve dressing for nerve regeneration and pain relief against diabetic peripheral nerve injury. *Bioact Mater* 2023; **26**: 194-215 [PMID: 36923267 DOI: 10.1016/j.bioactmat.2023.02.024]

22 **Fan L**, Guan P, Xiao C, Wen H, Wang Q, Liu C, Luo Y, Ma L, Tan G, Yu P, Zhou L, Ning C. Exosome-functionalized polyetheretherketone-based implant with immunomodulatory property for enhancing osseointegration. *Bioact Mater* 2021; **6**: 2754-2766 [PMID: 33665507 DOI: 10.1016/j.bioactmat.2021.02.005]

World Journal of Stem Cells

Submit a Manuscript: https://www.f6publishing.com

World J Stem Cells 2025 February 26; 17(2): 102404

DOI: 10.4252/wjsc.v17.i2.102404

ISSN 1948-0210 (online)

LETTER TO THE EDITOR

Impact of miR-214-5p and miR-21-5p from hypoxic endometrial exosomes on human umbilical cord mesen-chymal stem cell function

Jin-Wei Zhang

Specialty type: Cell and tissue engineering

Provenance and peer review: Invited article; Externally peer reviewed.

Peer-review model: Single blind

Peer-review report's classification

Scientific Quality: Grade B, Grade B, Grade C, Grade C, Grade D

Novelty: Grade B, Grade B, Grade C, Grade C, Grade C

Creativity or Innovation: Grade B, Grade B, Grade B, Grade C, Grade C

Scientific Significance: Grade B, Grade B, Grade B, Grade C, Grade C

P-Reviewer: Li J; Wang KY; Ying W

Received: October 16, 2024

Revised: December 21, 2024

Accepted: January 16, 2025

Published online: February 26, 2025

Processing time: 130 Days and 20.8 Hours

Jin-Wei Zhang, State Key Laboratory of Chemical Biology, Shanghai Institute of Organic Chemistry, Chinese Academy of Sciences, Shanghai 200032, China

Jin-Wei Zhang, Institute of Biomedical and Clinical Sciences, Medical School, Faculty of Health and Life Sciences, University of Exeter, Exeter EX4 4PS, United Kingdom

Corresponding author: Jin-Wei Zhang, State Key Laboratory of Chemical Biology, Shanghai Institute of Organic Chemistry, Chinese Academy of Sciences, No. 345 Lingling Road, Shanghai 200032, China. jinweizhang@sioc.ac.cn

Abstract

Exosomes derived from hypoxic endometrial epithelial cells are pivotal in cellular communication and tissue repair, offering new perspectives on reproductive health. This manuscript highlights the study by Zhang *et al*, which investigates the effects of miR-214-5p and miR-21-5p in hypoxic cell-derived exosomes on human umbilical cord mesenchymal stem cells. The study reveals that low levels of these microRNAs activate the signal transducer and activator of transcription 3 signaling pathway, enhancing human umbilical cord mesenchymal stem cell migration and differentiation. These findings provide novel insights into therapeutic strategies for improving endometrial health and addressing infertility linked to thin endometrium.

Key Words: MiR-214-5p; MiR-21-5p; Hypoxic endometrial epithelial cells; Exosomes; Human umbilical cord mesenchymal stem cells; Signal transducer and activator of transcription 3 signaling; Thin endometrium; Infertility

Core Tip: This manuscript examines the study by Zhang *et al* on the effects of miR-214-5p and miR-21-5p in hypoxic endometrial epithelial-cell-derived exosomes on human umbilical cord mesenchymal stem cells. The study highlights how low expression levels of these microRNAs activate the signal transducer and activator of transcription 3 signaling pathway, promoting human umbilical cord mesenchymal stem cell migration and differentiation - key processes in tissue repair and regeneration. These findings offer new insights into addressing thin endometrium, a common cause of infertility, by leveraging exosome-based therapies or targeted microRNA modulation. This article underscores the potential of miR-214-5p and miR-21-5p as therapeutic targets for improving endometrial health and reproductive outcomes.

Citation: Zhang JW. Impact of miR-214-5p and miR-21-5p from hypoxic endometrial exosomes on human umbilical cord mesenchymal stem cell function. *World J Stem Cells* 2025; 17(2): 102404
URL: https://www.wjgnet.com/1948-0210/full/v17/i2/102404.htm
DOI: https://dx.doi.org/10.4252/wjsc.v17.i2.102404

TO THE EDITOR

Thin endometrium is a significant barrier to successful embryo implantation and a primary cause of repeated implantation failure and infertility, posing challenges in assisted reproductive technologies[1]. In the recent issue of the *World Journal of Stem Cells*, a study by Zhang *et al*[2] investigates the potential of exosomes derived from hypoxic endometrial epithelial cells (EECs) to modulate the function of human umbilical cord mesenchymal stem cells (HucMSCs), which are known for their regenerative capabilities[3]. Hypoxic EECs are those subjected to low oxygen conditions, leading to cellular stress and compromised tissue repair, which is relevant in conditions like thin endometrium.

Exosomes are nanosized vesicles released by cells that carry bioactive molecules such as nucleic acids, lipids, and proteins[4]. They play a crucial role in intercellular communication and can influence various cellular processes, including proliferation, differentiation, and migration[4]. In the context of endometrial health, exosomes derived from EECs can modulate the function of other cells, such as HucMSCs[5]. The study highlights the role of the signal transducer and activator of transcription 3 (STAT3) signaling pathway, a critical mediator of cellular responses to cytokines and growth factors, involved in processes such as cell growth, survival, and differentiation[6].

The authors focus on the microRNAs (miRNAs) miR-21-5p and miR-214-5p, which are small non-coding RNAs that regulate gene expression by binding to target mRNAs. These miRNAs have been implicated in various cellular processes, including proliferation and differentiation[7-10]. In the context of thin endometrium, miR-21-5p and miR-214-5p are involved in modulating the migration and differentiation of HucMSCs. By targeting the STAT3 signaling pathway, these miRNAs can enhance the regenerative potential of HucMSCs, promoting tissue repair and improving endometrial receptivity. This makes them promising therapeutic targets for addressing infertility issues related to thin endometrium.

Methods

The researchers isolated exosomes from both normal and hypoxia-damaged EECs and characterized them using techniques such as western blotting and nanoparticle-tracking analysis. HucMSCs were cocultured with these exosomes, and the expression of miR-21-5p and miR-214-5p was analyzed through sequencing and reverse transcription quantitative polymerase chain reaction. The effects of inhibiting or overexpressing these miRNAs on HucMSC migration and differentiation were assessed using transwell and wound healing assays.

Key findings

The expression levels of miR-21-5p and miR-214-5p in HucMSCs treated with hypoxic EEC-derived exosomes were found to be significantly lower compared to those treated with exosomes from normal EECs. The low expression levels of miR-21-5p and miR-214-5p in EEC-derived exosomes-pretreated HucMSCs were associated with enhanced migratory and differentiative potentials of the HucMSCs, as these miRNAs negatively regulate the STAT3 signaling pathway. The inhibition of miR-21-5p and miR-214-5p led to increased phosphorylation of STAT3, promoting HucMSC migration and differentiation into EECs. These findings suggest that miR-21-5p and miR-214-5p play a crucial role in modulating the regenerative capabilities of HucMSCs through the STAT3 pathway, offering potential therapeutic targets for improving endometrial health.

Critical appraisal

The findings of this study align with previous research indicating that exosomes play a vital role in cell communication and tissue repair. For instance, Liang *et al*[5] demonstrated that exosomes from HucMSCs could repair injured EECs, highlighting the therapeutic potential of stem cell-derived exosomes in reproductive health. However, the current study adds a novel dimension by specifically identifying the roles of miR-21-5p and miR-214-5p in this context, which had not been previously elucidated.

Future perspectives

The study by Zhang *et al*[2] provides a foundational understanding of how miR-214-5p and miR-21-5p in hypoxic en-

dometrial epithelial-cell-derived exosomes can modulate the function of HucMSCs. This research opens several avenues for future exploration and clinical application, particularly in the field of gynecology and beyond.

Recent advances in clinical applications

In gynecology, exosome-based therapies are gaining traction as potential treatments for conditions like thin endometrium, which is a significant barrier to successful embryo implantation and pregnancy[11]. Recent studies have demonstrated the efficacy of exosome-hydrogel systems in promoting endometrial regeneration and improving fertility outcomes[1,12]. These systems protect and deliver exosomes to the target tissue, enhancing their therapeutic potential. The findings from Zhang *et al*[2] suggest that manipulating miR-214-5p and miR-21-5p levels could further optimize these therapies, offering a targeted approach to improve endometrial receptivity and address infertility issues.

Implications for stem cell, cancer, and immune therapies

Beyond gynecology, the modulation of miRNAs in exosomes holds promise for stem cell therapy, cancer treatment, and immune-related therapies. In stem cell therapy, miRNA manipulation can enhance the regenerative capabilities of stem cells, potentially improving outcomes in tissue repair and regeneration[13]. In cancer therapy, targeting specific miRNAs could inhibit tumor growth and metastasis by modulating key signaling pathways[14]. For immune-related therapies, exosomes can be engineered to deliver miRNAs that modulate immune responses, offering new strategies for treating autoimmune diseases and enhancing vaccine efficacy[15].

Exosome-based therapies

Exosome-based therapies offer a novel approach to delivering therapeutic agents directly to target tissues. Exosomes can be engineered to carry specific miRNAs, such as miR-214-5p and miR-21-5p, to modulate cellular functions[2]. This method leverages the natural ability of exosomes to facilitate intercellular communication and deliver bioactive molecules. However, challenges in clinical implementation include developing efficient and scalable exosome isolation and purification methods, ensuring the stability and bioavailability of exosome preparations, and addressing potential immunogenicity.

MiRNA mimics/inhibitors

The use of miRNA mimics or inhibitors represents another promising strategy. MiRNA mimics can be used to restore the function of downregulated miRNAs, while inhibitors can suppress the activity of overexpressed miRNAs[16]. These interventions can be tailored to modulate the STAT3 signaling pathway, which is crucial for HucMSC function and endometrial repair. The primary challenges in this approach include developing safe and effective delivery systems that can target specific tissues without off-target effects, as well as ensuring the stability and controlled release of miRNA therapeutics.

Challenges in clinical implementation

One of the main challenges in translating these strategies to clinical practice is the development of delivery systems that can efficiently and specifically deliver miRNA-based therapeutics to the endometrium. Nanoparticle-based delivery systems, liposomes, and viral vectors are being explored to enhance delivery efficiency and specificity. Safety considerations are paramount, as miRNA-based therapies must be carefully evaluated for potential off-target effects and long-term safety. Regulatory hurdles and the need for robust manufacturing processes also pose significant challenges.

Future research directions

Future research should focus on optimizing miRNA manipulation strategies for therapeutic use. This includes developing more efficient delivery systems for miRNA mimics and inhibitors, as well as exploring the use of CRISPR/Cas9 technology for precise miRNA editing. Preclinical studies should be conducted to assess the therapeutic potential of miRNA-based interventions in animal models of thin endometrium, providing critical data on efficacy, safety, and pharmacokinetics. Following successful preclinical evaluation, clinical trials will be necessary to determine the safety and efficacy of these interventions in humans. These trials should aim to establish optimal dosing regimens, evaluate long-term outcomes, and identify any potential adverse effects. Additionally, research should investigate the long-term effects of miRNA modulation on tissue health and function, as well as potential off-target effects.

Conclusions

The study by Zhang *et al*[2] provides valuable insights into the role of exosomal miRNAs in enhancing the regenerative potential of HucMSCs in the context of thin endometrium. Targeting miR-21-5p and miR-214-5p may offer a promising therapeutic strategy for improving endometrial receptivity and addressing infertility issues related to thin endometrium.

FOOTNOTES

Author contributions: Zhang JW designed the overall concept and outline of the manuscript, contributed to the discussion and design of the manuscript, and contributed to the writing and editing of the manuscript, illustrations, and review of the literature.

Supported by the National Natural Science Foundation of China, No. 82170406 and No. 81970238; and the Royal Society United

Kingdom, No. IEC\NSFC\201094.

Conflict-of-interest statement: The author reports no relevant conflicts of interest for this article.

Country of origin: China

ORCID number: Jin-Wei Zhang 0000-0001-8683-509X.

S-Editor: Wang JJ
L-Editor: A
P-Editor: Xu ZH

REFERENCES

1 **Lin J**, Wang Z, Huang J, Tang S, Saiding Q, Zhu Q, Cui W. Microenvironment-Protected Exosome-Hydrogel for Facilitating Endometrial Regeneration, Fertility Restoration, and Live Birth of Offspring. *Small* 2021; **17**: e2007235 [PMID: 33590681 DOI: 10.1002/smll.202007235]
2 **Zhang WY**, Wang HB, Deng CY. Effects of miR-214-5p and miR-21-5p in hypoxic endometrial epithelial-cell-derived exosomes on human umbilical cord mesenchymal stem cells. *World J Stem Cells* 2024; **16**: 906-925 [PMID: 39619875 DOI: 10.4252/wjsc.v16.i11.906]
3 **Zhou S**, Lei Y, Wang P, Chen J, Zeng L, Qu T, Maldonado M, Huang J, Han T, Wen Z, Tian E, Meng X, Zhong Y, Gu J. Human Umbilical Cord Mesenchymal Stem Cells Encapsulated with Pluronic F-127 Enhance the Regeneration and Angiogenesis of Thin Endometrium in Rat *via* Local IL-1β Stimulation. *Stem Cells Int* 2022; **2022**: 7819234 [PMID: 35761831 DOI: 10.1155/2022/7819234]
4 **Kalluri R**, LeBleu VS. The biology, function, and biomedical applications of exosomes. *Science* 2020; **367**: eaau6977 [PMID: 32029601 DOI: 10.1126/science.aau6977]
5 **Liang L**, Wang L, Zhou S, Li J, Meng L, Zhang H, Cui C, Zhang C. Exosomes derived from human umbilical cord mesenchymal stem cells repair injured endometrial epithelial cells. *J Assist Reprod Genet* 2020; **37**: 395-403 [PMID: 31938932 DOI: 10.1007/s10815-019-01687-4]
6 **Zou S**, Tong Q, Liu B, Huang W, Tian Y, Fu X. Targeting STAT3 in Cancer Immunotherapy. *Mol Cancer* 2020; **19**: 145 [PMID: 32972405 DOI: 10.1186/s12943-020-01258-7]
7 **Hua R**, Zhang X, Li W, Lian W, Liu Q, Gao D, Wang Y, Lei M. Ssc-miR-21-5p regulates endometrial epithelial cell proliferation, apoptosis and migration *via* the PDCD4/AKT pathway. *J Cell Sci* 2020; **133**: jcs248898 [PMID: 33097608 DOI: 10.1242/jcs.248898]
8 **Valenti MT**, Deiana M, Cheri S, Dotta M, Zamboni F, Gabbiani D, Schena F, Dalle Carbonare L, Mottes M. Physical Exercise Modulates miR-21-5p, miR-129-5p, miR-378-5p, and miR-188-5p Expression in Progenitor Cells Promoting Osteogenesis. *Cells* 2019; **8**: 742 [PMID: 31330975 DOI: 10.3390/cells8070742]
9 **Sikora M**, Śmieszek A, Pielok A, Marycz K. MiR-21-5p regulates the dynamic of mitochondria network and rejuvenates the senile phenotype of bone marrow stromal cells (BMSCs) isolated from osteoporotic SAM/P6 mice. *Stem Cell Res Ther* 2023; **14**: 54 [PMID: 36978118 DOI: 10.1186/s13287-023-03271-1]
10 **He Q**, Li R, Hu B, Li X, Wu Y, Sun P, Jia Y, Guo Y. Stromal cell-derived factor-1 promotes osteoblastic differentiation of human bone marrow mesenchymal stem cells *via* the lncRNA-H19/miR-214-5p/BMP2 axis. *J Gene Med* 2021; **23**: e3366 [PMID: 34032330 DOI: 10.1002/jgm.3366]
11 **Wang Y**, Tang Z, Teng X. New advances in the treatment of thin endometrium. *Front Endocrinol (Lausanne)* 2024; **15**: 1269382 [PMID: 38745960 DOI: 10.3389/fendo.2024.1269382]
12 **Sun J**, Yin Z, Wang X, Su J. Exosome-Laden Hydrogels: A Novel Cell-free Strategy for In-situ Bone Tissue Regeneration. *Front Bioeng Biotechnol* 2022; **10**: 866208 [PMID: 35433664 DOI: 10.3389/fbioe.2022.866208]
13 **Sen CK**, Ghatak S. miRNA control of tissue repair and regeneration. *Am J Pathol* 2015; **185**: 2629-2640 [PMID: 26056933 DOI: 10.1016/j.ajpath.2015.04.001]
14 **Arghiani N**, Shah K. Modulating microRNAs in cancer: Next-generation therapies. *Cancer Biol Med* 2021; **19**: 289-304 [PMID: 34846108 DOI: 10.20892/j.issn.2095-3941.2021.0294]
15 **Cao J**, Lv G, Wei F. Engineering exosomes to reshape the immune microenvironment in breast cancer: Molecular insights and therapeutic opportunities. *Clin Transl Med* 2024; **14**: e1645 [PMID: 38572668 DOI: 10.1002/ctm2.1645]
16 **Fu Z**, Wang L, Li S, Chen F, Au-Yeung KK, Shi C. MicroRNA as an Important Target for Anticancer Drug Development. *Front Pharmacol* 2021; **12**: 736323 [PMID: 34512363 DOI: 10.3389/fphar.2021.736323]

World Journal of Stem Cells

Submit a Manuscript: https://www.f6publishing.com

World J Stem Cells 2025 February 26; 17(2): 102702

DOI: 10.4252/wjsc.v17.i2.102702

ISSN 1948-0210 (online)

LETTER TO THE EDITOR

Perspectives on Schwann-like cells derived from bone marrow-mesenchymal stem cells: Advancing peripheral nerve injury therapies

Lucas Vinícius de Oliveira Ferreira, Rogério Martins Amorim

Specialty type: Cell and tissue engineering

Provenance and peer review: Unsolicited article; Externally peer reviewed.

Peer-review model: Single blind

Peer-review report's classification
Scientific Quality: Grade B
Novelty: Grade B
Creativity or Innovation: Grade C
Scientific Significance: Grade B

P-Reviewer: Kumar R

Received: October 28, 2024
Revised: December 18, 2024
Accepted: January 18, 2025
Published online: February 26, 2025
Processing time: 121 Days and 10.7 Hours

Lucas Vinícius de Oliveira Ferreira, Rogério Martins Amorim, Department of Veterinary Clinic, School of Veterinary Medicine and Animal Science, São Paulo State University (UNESP), Botucatu 18618-681, São Paulo, Brazil

Corresponding author: Lucas Vinícius de Oliveira Ferreira, Department of Veterinary Clinic, School of Veterinary Medicine and Animal Science, São Paulo State University (UNESP), Prof. Dr. Walter Maurício Corrêa Street, s/n, Botucatu 18618-681, São Paulo, Brazil.
lv.ferreira@unesp.br

Abstract

Peripheral nerve injuries are clinical conditions that often result in functional deficits, compromising patient quality of life. Given the relevance of these injuries, new treatment strategies are constantly being investigated. Although mesenchymal stem cells already demonstrate therapeutic potential due to their paracrine action, the transdifferentiation of these cells into Schwann-like cells (SLCs) represents a significant advancement in nerve injury therapy. Recent studies indicate that SLCs can mimic the functions of Schwann cells, with promising results in animal models. However, challenges remain, such as the diversity of transdifferentiation protocols and the scalability of these therapies for clinical applications. A recent study by Zou *et al* provided a comprehensive overview of the role of bone marrow-derived mesenchymal stem cells in the treatment of peripheral nerve injuries. Therefore, we would like to discuss and explore the use of SLCs derived from bone marrow-derived mesenchymal stem cells in more detail as a promising alternative in the field of nerve regeneration.

Key Words: Cell therapy; Nerve repair; Peripheral nervous system; Transdifferentiation; Transplantation

Core Tip: Schwann-like cells (SLCs) derived from bone marrow-mesenchymal stem cells have emerged as a promising therapeutic approach for peripheral nerve regeneration. However, further *in vitro* and *in vivo* studies are needed to optimize transdifferentiation and transplantation methodologies, as well as to explore the efficacy of SLCs in different injury models. The development of strategies that integrate SLCs could enhance neuroregeneration, promoting cell survival and therapeutic success.

Citation: Ferreira LVO, Amorim RM. Perspectives on Schwann-like cells derived from bone marrow-mesenchymal stem cells: Advancing peripheral nerve injury therapies. *World J Stem Cells* 2025; 17(2): 102702
URL: https://www.wjgnet.com/1948-0210/full/v17/i2/102702.htm
DOI: https://dx.doi.org/10.4252/wjsc.v17.i2.102702

TO THE EDITOR

We would like to express our sincere appreciation for the publication of the review entitled "Bone marrow-mesenchymal stem cells in treatment of peripheral nerve injury" by Zou *et al*[1], which provides a comprehensive overview of the role of bone marrow-derived mesenchymal stem cells (BM-MSCs) in the treatment of peripheral nerve injuries (PNI). In addition to highlighting the relevance of BM-MSCs, we would like to commend the authors and offer a more in-depth perspective on the use of Schwann-like cells (SLCs) derived from BM-MSCs as a promising alternative in the field of nerve regeneration.

PNI represents a significant clinical challenge in both humans and animals[2,3], due to the complexity of the neural microenvironment and the limited regenerative capacity, especially in severe injuries[4-6]. In long-gap injury, autograft is the gold standard treatment; however, it presents several limitations, including incomplete functional recovery, donor nerve morbidity, scar tissue formation, and the risk of neuroma formation[7,8]. Given these challenges, new therapeutic strategies are constantly being investigated.

Mesenchymal stem cells (MSCs) have attracted considerable attention for peripheral nerve regeneration[9]. Their ease of expansion in culture, the ability to differentiate into various cell types[10], and their neuroprotective, anti-inflammatory, immunomodulatory, and pro-angiogenic properties highlight MSCs as a strategy with great therapeutic potential, as reported by Zou *et al*[1]. The transplantation of BM-MSCs in PNI has been investigated in small and large animal models, such as rats[11], dogs[12], rabbits[13], sheep[14], and horses[15]. Furthermore, studies have demonstrated the potential for the transdifferentiation of BM-MSCs into SLCs, as highlighted by Zou *et al*[1].

Different protocols are described for performing transdifferentiation and exploring the potential of the transplantation of SLCs derived from BM-MSCs into animal models (Figure 1). In this manuscript, we also present *in vitro* approaches that utilize exosomes derived from different cell sources[16] and conditioned medium containing secreted factors from the peripheral nerves of both rats[17] and horses[18]. The method using conditioned medium enhances the gene expression of neurotrophic factors following transdifferentiation[18]. This recent approach still needs to be further explored to determine which factors specifically trigger the transdifferentiation process, which could open new avenues for research and experimental methodologies.

Schwann cells (SCs) are the main glial cells in the peripheral nervous system and play a crucial role in neuroregeneration through proliferation, formation of Büngner bands, secretion of neurotrophic factors, phagocytosis of myelin debris, and recruitment of macrophages[19]. While protocols for SCs isolation are well-established and their transplantation has shown benefits in treating PNI[20,21], this approach has limitations. These include the need to sacrifice a functional nerve for cell harvesting and the extended time required for cell expansion, which can delay treatment[22]. In this context, SLCs have emerged as a promising alternative to mimic SCs. The generation of SLCs from MSCs reduces complications associated with donor nerve harvesting. However, potential challenges in translating SLC therapies to clinical applications must be addressed. Issues related to cell quality, phenotypic instability, immune compatibility, and long-term safety remain significant concerns. Moving forward, it will be essential to reach a consensus on the criteria to characterize these cells, ensuring reproducibility and reliability across different studies. Although various methodologies and protocols have been developed, offering promising strategies for nerve regeneration, further investigations are necessary. Studies focusing on BM-MSC-derived SLCs and comparative analyses of different approaches are crucial to optimize and enhance the therapeutic potential of SLCs.

SLCS TRANSPLANTATION

Studies evaluating the transplantation of SLCs derived from BM-MSCs in PNI have demonstrated significant therapeutic benefits (Table 1). There is considerable evidence that the use of these cells can assist in nerve regeneration, underscoring their therapeutic potential. However, further investigations are still needed to establish effective protocols for clinical application. Although MSCs are considered immune evasive[23], the use of immunosuppressants such as tacrolimus and cyclosporine has been adopted in some studies to prevent immune rejection in xenogeneic transplants[24,25]. In addition, many studies have combined cell transplantation with biomaterials, optimizing treatment efficacy by creating a favorable microenvironment for regeneration[26,27].

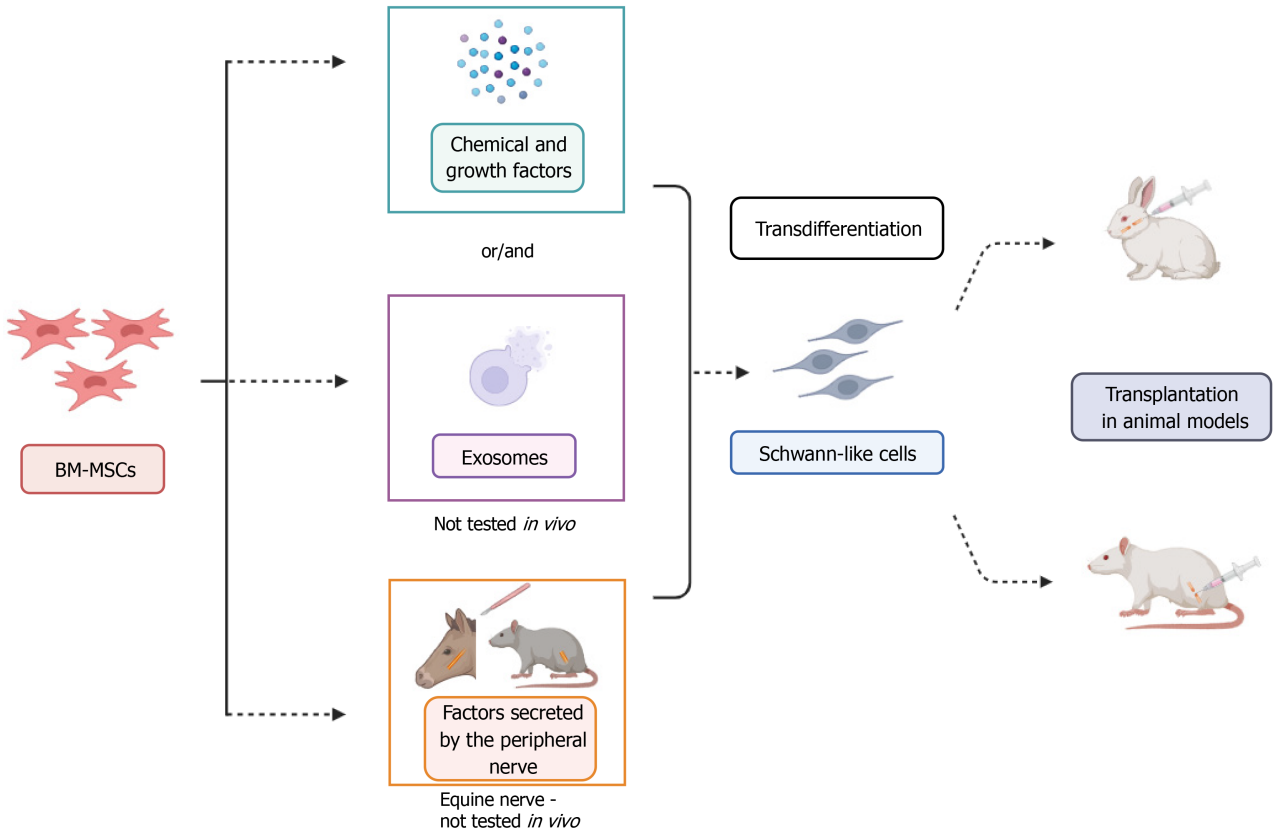

Figure 1 Schematic representation of the transdifferentiation of bone marrow-derived mesenchymal stem cells into Schwann-like cells using different protocols and their potential *in vivo* application. Protocols involving chemical agents, growth factors, exosomes derived from various cell sources, and secreted factors from equine and rat peripheral nerves are used for the *in vitro* transdifferentiation of bone marrow-derived mesenchymal stem cells into Schwann-like cells. Studies involving the transplantation of Schwann-like cells into animal models generally use chemical agents and growth factors to induce transdifferentiation. Created with Biorender (https://BioRender.com/p72z610). BM-MSCs: Bone marrow-derived mesenchymal stem cells.

Biomaterials have been widely studied for the construction of nerve guidance conduits (NGCs), which may be natural or synthetic, exhibiting a wide range of characteristics that play crucial roles in nerve regeneration[28]. NGCs are designed to provide structural support and create a favorable microenvironment for axonal growth[3]. Physical properties, such as porosity, stiffness, and biocompatibility, as well as incorporated bioactive components, are key determinants for successful neural regeneration[29,30]. The use of 3D printing has revolutionized the design and fabrication of NGCs, enabling customization with complex architectures[31]. This technology allows the creation of NGCs with geometries tailored to different types of nerve injuries, while precisely controlling features such as pore size, fiber orientation, and material composition[32,33]. In this context, the combination of SLCs with 3D-printed personalized NGCs represents a promising approach for the treatment of PNI, enhancing functional recovery and opening new perspectives for nerve tissue engineering. These findings highlight the importance of continuing to explore the transdifferentiation capacity of BM-MSCs and conducting new studies in combination with different approaches aimed at improving the efficacy of cell-based therapy in neuroregeneration.

CONCLUSIONS AND PERSPECTIVES

Despite evidence suggesting that SLCs are a promising alternative for nerve regeneration, several challenges remain to be addressed. Issues such as the quantity of cells to be used, the most efficient methodology for transdifferentiation, the application frequency, long-term safety, potential immune responses, dedifferentiation after the removal of the inducing medium, and efficacy in different types of injuries require further investigation.

To advance in this field, it is essential to standardize transdifferentiation protocols and establish a consensus on the characterization of SLCs. This will assist in ensuring reproducibility and clinical applicability. Preclinical studies utilizing large animal models to evaluate the safety and effectiveness of SLC-based therapies, followed by clinical trials, are also crucial to translate these findings into clinical practice. The combination of cellular therapy with biomaterials and other technologies has the potential to further enhance neuroregeneration. In this context, future studies should investigate the 3D bioprinting of NGCs incorporated with BM-MSCs, as demonstrated by Liu *et al*[34], or with SLCs, aiming to develop better therapeutic approaches for PNI. It is vital to create an optimal microenvironment that promotes cell survival and integration after transplantation. Moreover, incorporating and distributing stimulating factors that influence the phenotype of SLCs will be crucial for the therapeutic success of these approaches. Thus, we would like to highlight future

Table 1 Transplantation of Schwann-like cells derived from bone marrow-mesenchymal stem cells in peripheral nerve injuries

Model	Cells/grafts	Method of transdifferentiation	Outcome	Limitations	Ref.
Rat sciatic nerve (12 mm gap)	SLCs (rats). Hollow fiber	Chemical and growth factors	Improvements in motor conduction, sciatic nerve function index, regeneration of the nodes of Ranvier, and remyelination. No tumor formation was detected 6 months post-transplantation	Lack of detailed sensory functional analysis and gene expression evaluation of SLCs and nerve regeneration markers	[35]
Rat sciatic nerve (10 mm gap)	SLCs (humans). Transpermeable tube. Immunosuppressants used	Chemical and growth factors	Improvements in nerve regeneration and functional recovery	Lack of detailed sensory functional analysis, gene expression evaluation of SLCs and nerve regeneration markers, no electroneuromyography, assessed for three weeks	[25]
Rat sciatic nerve (12 mm gap)	SLCs (rats). Chitosan conduits	Neurosphere induction, incubation with growth factors and co-culture	Improvements in remyelination and axonal growth. No significant difference was observed compared to the transplantation of Schwann cells derived from the sciatic nerve	No undifferentiated BM-MSC transplantation group, lack of detailed sensory functional analysis and gene expression evaluation of SLCs and nerve regeneration markers	[26]
Buccal branch of the facial nerve in rabbits (1 cm gap)	SLCs (rabbits). Vein graft	Chemical and growth factors	Acceleration of axonal regeneration and improvement in remyelination	Lack of detailed sensory functional analysis of the facial nerve and gene expression evaluation of SLCs markers	[27]
Rat sciatic nerve (12 mm gap)	SLCs (humans). Chitosan conduits. Immunosuppressants used	Neurosphere induction, incubation with growth factors and co-culture	Improvements in axonal regeneration and myelination	No undifferentiated BM-MSC transplantation group, lack of detailed motor and sensory functional analysis, electroneuromyography, and gene expression evaluation of SLCs and nerve regeneration markers	[24]

The studies are predominantly conducted using laboratory animal models, while there is a lack of research evaluating the regenerative potential of Schwann-like cells derived from bone marrow-derived mesenchymal stem cells in large animal models. These larger models are particularly relevant for translational studies, as the size of the peripheral nerve in these animals allows for larger lesions, providing more realistic data on the nerve regeneration process, which can be applied to human treatments[4]. SLCs: Schwann-like cells; BM-MSC: Bone marrow-derived mesenchymal stem cell.

perspectives toward therapies based on SLCs derived from BM-MSCs, which have great potential for the treatment of PNI.

FOOTNOTES

Author contributions: Ferreira LVO and Amorim RM made equal contributions to this study. Ferreira LVO and Amorim RM prepared and wrote the manuscript; and all authors have read and approved the final manuscript.

Conflict-of-interest statement: All the authors report no relevant conflicts of interest for this article.

Country of origin: Brazil

ORCID number: Lucas Vinícius de Oliveira Ferreira 0000-0001-8835-9736; Rogério Martins Amorim 0000-0003-3750-5857.

S-Editor: Wang JJ
L-Editor: Filipodia
P-Editor: Zheng XM

REFERENCES

1 **Zou XF**, Zhang BZ, Qian WW, Cheng FM. Bone marrow mesenchymal stem cells in treatment of peripheral nerve injury. *World J Stem Cells* 2024; **16**: 799-810 [PMID: 39219723 DOI: 10.4252/wjsc.v16.i8.799]

2 **Gouveia D**, Cardoso A, Carvalho C, Oliveira AC, Almeida A, Gamboa Ó, Lopes B, Coelho A, Alvites R, Varejão AS, Maurício AC, Ferreira A, Martins Â. Early Intensive Neurorehabilitation in Traumatic Peripheral Nerve Injury-State of the Art. *Animals (Basel)* 2024; **14**: 884 [PMID: 38539981 DOI: 10.3390/ani14060884]

3 **Lopes B**, Sousa P, Alvites R, Branquinho M, Sousa AC, Mendonça C, Atayde LM, Luís AL, Varejão ASP, Maurício AC. Peripheral Nerve Injury Treatments and Advances: One Health Perspective. *Int J Mol Sci* 2022; **23**: 918 [PMID: 35055104 DOI: 10.3390/ijms23020918]

4 **Alvites R**, Lopes B, Coelho A, Maurício AC. Peripheral nerve regeneration: a challenge far from being overcome. *Regen Med* 2024; **19**: 155-159 [PMID: 37786972 DOI: 10.2217/rme-2023-0072]

5 **Klimovich P**, Rubina K, Sysoeva V, Semina E. New Frontiers in Peripheral Nerve Regeneration: Concerns and Remedies. *Int J Mol Sci* 2021; **22**: 13380 [PMID: 34948176 DOI: 10.3390/ijms222413380]

6 **Kuffler DP**, Foy C. Restoration of Neurological Function Following Peripheral Nerve Trauma. *Int J Mol Sci* 2020; **21**: 1808 [PMID: 32155716 DOI: 10.3390/ijms21051808]

7 **Bassilios Habre S**, Bond G, Jing XL, Kostopoulos E, Wallace RD, Konofaos P. The Surgical Management of Nerve Gaps: Present and Future. *Ann Plast Surg* 2018; **80**: 252-261 [PMID: 29166306 DOI: 10.1097/SAP.0000000000001252]

8 **Manoukian OS**, Baker JT, Rudraiah S, Arul MR, Vella AT, Domb AJ, Kumbar SG. Functional polymeric nerve guidance conduits and drug delivery strategies for peripheral nerve repair and regeneration. *J Control Release* 2020; **317**: 78-95 [PMID: 31756394 DOI: 10.1016/j.jconrel.2019.11.021]

9 **Martins Amorim R**, Vinícius de Oliveira Ferreira L. Schwann-like cells derived from mesenchymal stem cells: Their potential for peripheral nerve regeneration. In: Stem Cell Transplantation. United Kingdom: IntechOpen, 2024

10 **Barberini DJ**, Freitas NP, Magnoni MS, Maia L, Listoni AJ, Heckler MC, Sudano MJ, Golim MA, da Cruz Landim-Alvarenga F, Amorim RM. Equine mesenchymal stem cells from bone marrow, adipose tissue and umbilical cord: immunophenotypic characterization and differentiation potential. *Stem Cell Res Ther* 2014; **5**: 25 [PMID: 24559797 DOI: 10.1186/scrt414]

11 **Cooney DS**, Wimmers EG, Ibrahim Z, Grahammer J, Christensen JM, Brat GA, Wu LW, Sarhane KA, Lopez J, Wallner C, Furtmüller GJ, Yuan N, Pang J, Sarkar K, Lee WP, Brandacher G. Mesenchymal Stem Cells Enhance Nerve Regeneration in a Rat Sciatic Nerve Repair and Hindlimb Transplant Model. *Sci Rep* 2016; **6**: 31306 [PMID: 27510321 DOI: 10.1038/srep31306]

12 **Daradka MH**, Bani Ismail ZA, Irsheid MA. Peripheral nerve regeneration: A comparative study of the effects of autologous bone marrow-derived mesenchymal stem cells, platelet-rich plasma, and lateral saphenous vein graft as a conduit in a dog model. *Open Vet J* 2021; **11**: 686-694 [PMID: 35070865 DOI: 10.5455/OVJ.2021.v11.i4.20]

13 **Sivanarayanan TB**, Bhat IA, Sharun K, Palakkara S, Singh R, Remya 5th, Parmar MS, Bhardwaj R, Chandra V, Munuswamy P, Kinjavdekar P, Pawde AM, Amarpal, Sharma GT. Allogenic bone marrow-derived mesenchymal stem cells and its conditioned media for repairing acute and sub-acute peripheral nerve injuries in a rabbit model. *Tissue Cell* 2023; **82**: 102053 [PMID: 36907044 DOI: 10.1016/j.tice.2023.102053]

14 **Casañas J**, de la Torre J, Soler F, García F, Rodellar C, Pumarola M, Climent J, Soler R, Orozco L. Peripheral nerve regeneration after experimental section in ovine radial and tibial nerves using synthetic nerve grafts, including expanded bone marrow mesenchymal cells: morphological and neurophysiological results. *Injury* 2014; **45** Suppl 4: S2-S6 [PMID: 25384470 DOI: 10.1016/S0020-1383(14)70003-8]

15 **Cruz Villagrán C**, Schumacher J, Donnell R, Dhar MS. A Novel Model for Acute Peripheral Nerve Injury in the Horse and Evaluation of the Effect of Mesenchymal Stromal Cells Applied In Situ on Nerve Regeneration: A Preliminary Study. *Front Vet Sci* 2016; **3**: 80 [PMID: 27695697 DOI: 10.3389/fvets.2016.00080]

16 **Zhang X**, Zhang W, Sun H, Wang H. The effects of exosomes originating from different cell sources on the differentiation of bone marrow mesenchymal stem cells into schwann cells. *J Nanobiotechnology* 2024; **22**: 220 [PMID: 38698449 DOI: 10.1186/s12951-024-02450-3]

17 **Galhom RA**, Hussein Abd El Raouf HH, Mohammed Ali MH. Role of bone marrow derived mesenchymal stromal cells and Schwann-like cells transplantation on spinal cord injury in adult male albino rats. *Biomed Pharmacother* 2018; **108**: 1365-1375 [PMID: 30372839 DOI: 10.1016/j.biopha.2018.09.131]

18 **Ferreira LVO**, Kamura BDC, Oliveira JPM, Chimenes ND, Carvalho M, Santos LAD, Dias-Melicio LA, Amorim RL, Amorim RM. In Vitro Transdifferentiation Potential of Equine Mesenchymal Stem Cells into Schwann-Like Cells. *Stem Cells Dev* 2023; **32**: 422-432 [PMID: 37071193 DOI: 10.1089/scd.2022.0274]

19 **Jessen KR**, Mirsky R. The Success and Failure of the Schwann Cell Response to Nerve Injury. *Front Cell Neurosci* 2019; **13**: 33 [PMID: 30804758 DOI: 10.3389/fncel.2019.00033]

20 **Han GH**, Peng J, Liu P, Ding X, Wei S, Lu S, Wang Y. Therapeutic strategies for peripheral nerve injury: decellularized nerve conduits and Schwann cell transplantation. *Neural Regen Res* 2019; **14**: 1343-1351 [PMID: 30964052 DOI: 10.4103/1673-5374.253511]

21 **Levi AD**, Burks SS, Anderson KD, Dididze M, Khan A, Dietrich WD. The Use of Autologous Schwann Cells to Supplement Sciatic Nerve Repair With a Large Gap: First in Human Experience. *Cell Transplant* 2016; **25**: 1395-1403 [PMID: 26610173 DOI: 10.3727/096368915X690198]

22 **Piovesana R**, Faroni A, Tata AM, Reid AJ. Schwann-like adipose-derived stem cells as a promising therapeutic tool for peripheral nerve regeneration: effects of cholinergic stimulation. *Neural Regen Res* 2021; **16**: 1218-1220 [PMID: 33269784 DOI: 10.4103/1673-5374.300433]

23 **Ankrum JA**, Ong JF, Karp JM. Mesenchymal stem cells: immune evasive, not immune privileged. *Nat Biotechnol* 2014; **32**: 252-260 [PMID: 24561556 DOI: 10.1038/nbt.2816]

24 **Cai S**, Tsui YP, Tam KW, Shea GK, Chang RS, Ao Q, Shum DK, Chan YS. Directed Differentiation of Human Bone Marrow Stromal Cells to Fate-Committed Schwann Cells. *Stem Cell Reports* 2017; **9**: 1097-1108 [PMID: 28890164 DOI: 10.1016/j.stemcr.2017.08.004]

25 **Shimizu S**, Kitada M, Ishikawa H, Itokazu Y, Wakao S, Dezawa M. Peripheral nerve regeneration by the in vitro differentiated-human bone marrow stromal cells with Schwann cell property. *Biochem Biophys Res Commun* 2007; **359**: 915-920 [PMID: 17573041 DOI: 10.1016/j.bbrc.2007.05.212]

26 **Ao Q**, Fung CK, Tsui AY, Cai S, Zuo HC, Chan YS, Shum DK. The regeneration of transected sciatic nerves of adult rats using chitosan nerve conduits seeded with bone marrow stromal cell-derived Schwann cells. *Biomaterials* 2011; **32**: 787-796 [PMID: 20950852 DOI: 10.1016/j.biomaterials.2010.09.046]

27 **Wang X**, Luo E, Li Y, Hu J. Schwann-like mesenchymal stem cells within vein graft facilitate facial nerve regeneration and remyelination.

Brain Res 2011; **1383**: 71-80 [PMID: 21295556 DOI: 10.1016/j.brainres.2011.01.098]

28 **Mankavi F**, Ibrahim R, Wang H. Advances in Biomimetic Nerve Guidance Conduits for Peripheral Nerve Regeneration. *Nanomaterials (Basel)* 2023; **13**: 2528 [PMID: 37764557 DOI: 10.3390/nano13182528]

29 **Huang Y**, Wu W, Liu H, Chen Y, Li B, Gou Z, Li X, Gou M. 3D printing of functional nerve guide conduits. *Burns Trauma* 2021; **9**: tkab011 [PMID: 34212061 DOI: 10.1093/burnst/tkab011]

30 **Vijayavenkataraman S**. Nerve guide conduits for peripheral nerve injury repair: A review on design, materials and fabrication methods. *Acta Biomater* 2020; **106**: 54-69 [PMID: 32044456 DOI: 10.1016/j.actbio.2020.02.003]

31 **Soman SS**, Vijayavenkataraman S. Perspectives on 3D Bioprinting of Peripheral Nerve Conduits. *Int J Mol Sci* 2020; **21**: 5792 [PMID: 32806758 DOI: 10.3390/ijms21165792]

32 **Pedde RD**, Mirani B, Navaei A, Styan T, Wong S, Mehrali M, Thakur A, Mohtaram NK, Bayati A, Dolatshahi-Pirouz A, Nikkhah M, Willerth SM, Akbari M. Emerging Biofabrication Strategies for Engineering Complex Tissue Constructs. *Adv Mater* 2017; **29** [PMID: 28370405 DOI: 10.1002/adma.201606061]

33 **Zhu W**, Tringale KR, Woller SA, You S, Johnson S, Shen H, Schimelman J, Whitney M, Steinauer J, Xu W, Yaksh TL, Nguyen QT, Chen S. Rapid continuous 3D printing of customizable peripheral nerve guidance conduits. *Mater Today (Kidlington)* 2018; **21**: 951-959 [PMID: 31156331 DOI: 10.1016/j.mattod.2018.04.001]

34 **Liu J**, Zhang B, Li L, Yin J, Fu J. Additive-lathe 3D bioprinting of bilayered nerve conduits incorporated with supportive cells. *Bioact Mater* 2021; **6**: 219-229 [PMID: 32913930 DOI: 10.1016/j.bioactmat.2020.08.010]

35 **Mimura T**, Dezawa M, Kanno H, Sawada H, Yamamoto I. Peripheral nerve regeneration by transplantation of bone marrow stromal cell-derived Schwann cells in adult rats. *J Neurosurg* 2004; **101**: 806-812 [PMID: 15540919 DOI: 10.3171/jns.2004.101.5.0806]

Published by **Baishideng Publishing Group Inc**
7041 Koll Center Parkway, Suite 160, Pleasanton, CA 94566, USA
Telephone: +1-925-3991568
E-mail: office@baishideng.com
Help Desk: https://www.f6publishing.com/helpdesk
https://www.wjgnet.com